Interactions microsporidies-insectes in vivo : dissémination de Nosema bombycis (Microsporidia) dans son hôte Bombyx mori (Lepidoptera) et caractérisation de protéines structurales majeures de N. bombycis impliquées dans l'invasion

Jian-Yang Wang

UNIVERSITE BLAISE PASCAL **UNIVERSITE D'AUVERGNE**
N° D.U.:

Ecole Doctorale
des Sciences de la Vie et de la Santé
N° d'ordre:

THESE

pour l'obtention du grade de

DOCTEUR D'UNIVERSITE

Spécialité: Parasitologie Moléculaire et Cellulaire
Présentée et soutenue publiquement
par

Wang Jian-Yang

le 2 Mars, 2007

Interactions Microsporidies-insectes *in vivo*: dissémination de *Nosema bombycis* (Microsporidia) dans son hôte *Bombyx mori* (Lepidoptera) et caractérisation de protéines structurales majeures de *N. bombycis* impliquées dans l'invasion.

JURY

Président:	**Dr. Bernard Mauchamp, Unité Nationale Séricicole / INRA, Lyon**
Rapporteurs:	**Dr. Gérard Chavancy, Unité Nationale Séricicole / INRA, Lyon**
	Dr. Roger Frutos, UPR 15 CIRAD TA 30/G, Montpellier
	Pr. René Chermette, Ecole Nationale Vétérinaire d'Alfort, Maisons-Alfort
Directeur de thèse:	**Pr. Christian Vivarès, Université Blaise Pascal, Clermont-Ferrand**
Examinateur:	**Dr. Catherine Texier, Université Blaise Pascal, Clermont-Ferrand**

Laboratoire de Biologie des Protistes UMR CNRS 6023, équipeParasitologie Moléculaire et Cellulaire
Université Blaise Pascal, Clermont-Ferrand

ACKNOWLEDGEMENT

I warmly thank Professor Christian Amblard, the director of “Laboratoire de Biologie des Protistes, UMR CNRS 6023” of Université Blaise Pascal, who gave me the opportunity to complete this thesis in his laboratory.

I would like to express my deepest and sincere gratitude to my supervisor, Professor Christian P. VIVARES, Head of “Equipe Parasitologie Moléculaire et Cellulaire, LBP UMR CNRS 6023”, for giving me the most important support throughout this work and helping me achieve this milestone in my life. I am really very glad that I have a chance to get know him and be supervised by him. His overly enthusiasm for and dedication to parasitology science, integral view on research, logical and swift thinking, preeminent leadership have had a remarkable influence on my entire career.

I am deeply and specially indebted to my mentor, Dr. Texier Catherine, who kept an eye on the progress of my work and was always available when I needed her advises. Her guidance, stimulating suggestions and untiring support always accompanied me and greatly encouraged me to go through those difficult moments. Her ideals, concepts, seriousness and earnestness to the scientific researches have also set a perfect example to me and will be of great value in my future academic career. I also owe her the most overwhelming debt of gratitude for her so much sympathetic personal help during these three years.

My most sincere thanks are also due to Professor Gérard Prensier, who also kindly directed me in the host-parasite interactions study and introduced me to the parasite untrastructural realm. It is my great pleasure in my life to be directed by a well-known TEM specialist.

My most warm thanks also go to Dr. Gérard Chavancy, Dr. Bernard Mauchamp, Dr. Roger Frutos and Professor René Chermette who accepted to jury this work. Professor Gérard Chavancy also kindly provided the silkworm eggs and artifical diet powder for this work.

I wish to express my sincere thanks to Emmanuel Cornillot for his constructive suggestions, to Guy Méténier, Frédéric Delbac and Hicham El-Alaoui for their valuble discussions and comments on this thesis. I am also very grateful to Dr. Brosson Damien, who substantially contributed to the development of this work. My specific thanks are due to Jean-Luc Vincenot who always enthusiastically helps me in scanning a large number of SDS-PAGE gels and TEM micrographs.

During these three years, I have been also accompanied and supported by many other members in our laboratory. It is a pleasant aspect that now I have the opportunity to express my gratitude for all of them. I want to thank them for providing me an excellent work environment and all their sympathetic help, support, interest and valuable hints. I am very glad that I had been one of this excellent and harmonious group.

I wish to specially thank my master supervisor Lu Chang-De. He is always paternally concerned about my academic progress and my life. His inexhaustible guidance and encouragement always go with me. He taught me the good things that really matter in life. I am also very grateful to my master supervisor Huang Ke-Wei and other colleages in Institute of Sericultural Research, Chinese Academy of Agricultural Sciences, who not only provided me my pet *Nosema bobmycis* but also always give me unwavering support.

I feel a deep sense of gratitude for the loving support and understanding of my parents, my husband, my two brothers and their families during these years I dedicated to achieving this milestone in my life and career.

The financial supports of the Conseil Régional d’Auvergne and our laboratory are gratefully acknowledged.

Bow my everlasting thanks to my parents!

My deepest and sincere gratitude for inspiring and guiding this humble being.

A journey is easier when you travel together. Interdependence is certainly more valuable than independence.

CONTENTS

Introduction

INTRODUCTION

The unicellular and eukaryotic microsporidian, defined by their formation of small resistant spores, are a large group of obligate and extremely diverse intracellular parasites in the phylum Microsporidia Balbiani 1882, in which currently approximately 150 genera with over 1,200 individual species have been described (Sprague and Becnel, 1999). First considered as early-branching primitive eukaryotes lacking mitochondria, recent molecular phylogenetic analyses have shown that Microsporidia are related to fungi and retain a mitochondrion-derived organelle called mitosome (Katinka *et al*., 2001). Microsporidia can infect nearly the whole invertebrate phyla as well as all five classes of vertebrates including humans. They emerged as opportunistic human pathogens with the onset of AIDS pandemic in the last century (Desportes *et al*., 1985). Nowadays, microsporidian still inflict great economic losses to the breedings of several animals such as the silkworm *Bombyx mori*, honeybees and fishes.

Microsporidian resistant spores are characterized by: 1) a unique extrusion and invasion apparatus, called the polar tube, which is a short or very long cylindrical structure coiled within the spore and plays a very important role in microsporidian life cycle to invade the host cell; 2) the chitinous and proteinous thick spore wall, which allows the spore to survive drastic environments. The spore wall is also the important interface of host-parasite recognition, of parasite sensibility to the suitable stimuli needed for germination and host immune reponse.

Nosema bombycis, the first identified microsporidian, is the causative agent of the silkworm *Bombyx mori* epidemic “pepper disease” or pebrine, which broke out for the first time in the south of France in 1845 and nearly destroyed the silkworm industry of Europe. Pasteur’s landmark studies firstly proved that the pathogen can be transmitted both horizontally and transovarially in *B. mori* and developed an effective practical method of control that essentially saved the silkworm industry. Nowadays, pebrine caused by *N. bombycis* is still the most devastating mulberry silkworm disease and inflicts severe worldwide economic losses in the silkworm rearing industries for lack of efficient and thorough therapy.

Most previous studies have been performed on *N. bombycis* biology, serology, histopathology in addition the sporogonial dimorphism which is a milestone in microsporidian studies and resulted in a proposed *N. bombycis* life cyle model (Kawarabata and Ishihara, 1984;

Iwano and Ishihara, 1989, 1991a, b). But very little is known on *N. bombycis* dissemination mechanism in its natural host *B. mori* silkworm and the cellular or molecular interactions between *N. bombycis* and *B. mori*, which are the preliminary steps towards a future therapy.

This work thus intended to:

1. Characterize the *in vivo* life cycle of *Nosema bombycis* strain ISC-ZJ at the ultrastructural level;

2. Characterize the dissemination route of *Nosema bombycis* ISC-ZJ in *Bombyx mori* Nistari, and in particular to elucidate the role of hemocytes in this dissemination;

3. Identify *Nosema bombycis* proteins involved in host-parasite relationships, in particular those of polar tube and spore wall, using a proteomic-based approach.

This work has given rise to different publications:

Article:

Jian-Yang Wang, Christophe Chambon, Chang-De Lu, Ke-Wei Huang, Christian P. Vivarès, Catherine Texier. A proteomic-based approach for the characterization of major structural proteins involved in host-parasite relationships from the silkworm parasite *Nosema bombycis*. ***Proteomics,*** accepted

Poster communications:

1. The 44th Congress of the French Language Protistologue Group. Université Cheikh Anta DIOP de Dakar, Senegal, May, 22~26, 2006

Jian-Yang Wang, Gérard Prensier, Christian P. Vivarès, Catherine Texier. Characterization of *Nosema bombycis* (Microsporidia) spore proteome and identification of its polar tube proteins

Abstract in ***J. Eukaryot. Microbiol.,*** 2007, in press

2. Ph.D Scientific School journey. Clermont-Ferrand, France, March, 30-31, 2006

Jian-Yang Wang, Gérard Prensier, Emmanuel Cornillot, Christian P. Vivarès, Catherine Texier. Identification of the major structural proteins of microsporidia *Nosema bombycis*, a parasite of *Bombyx mori* and the interactions with its host *in vivo*

Scientific Context

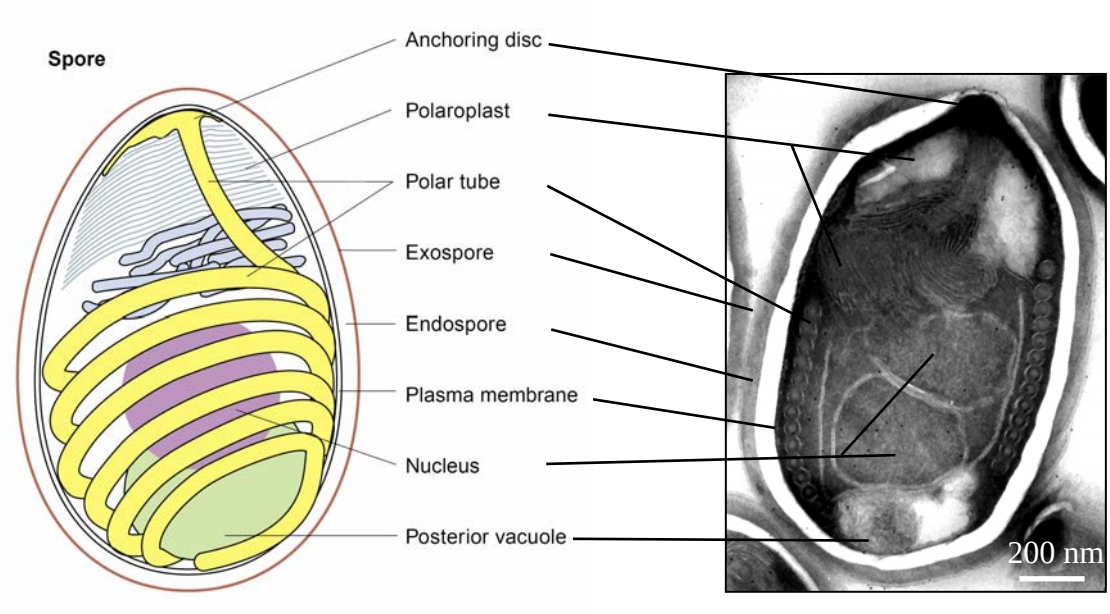

Figure 1. The microsporidian mature spore model (left) and transmission electronic micrograph of *Nosema bombycis* diplokaryotic mature spore (right).

1. *Nosema bombycis*: a silkworm parasite belonging to the Microsporidia phylum

The first microsporidian was described in the middle of the nineteenth century when pebrine, or "pepper disease" was ravaging silkworms in southern Europe and threatening to destroy the European silk industry. From 1863, Pasteur worked several years proving that a protozoan parasite was the etiological agent of the pebrine. In his landmark studies, he also proved that this parasite can be transmitted both horizontally and transovarially. He developped the effective practical control method that essentially saved the silkworm industry (Pasteur, 1870). This pebrine agent was named *Nosema bombycis* by Nägeli in 1857 (Nägeli, 1857). Nägeli considered *Nosema* to be a member of the schizomycete fungi, although classification at that time did not reflect the true diversity of microbial life, and schizomycetes were a grab bag of yeasts and bacteria. The microsporidia have been recognized as a distinct group of unicellular organisms since 1882 when Balbiani accordingly created the order Microsporida to accommodate *Nosema bombycis* after further study (Balbiani, 1882). In 1976, Sprague created the phylum "Microspora" and this phylum name was updated in 1998 to "Microsporidia Balbiani, 1882" (Sprague and Becnel, 1998). With the onset of AIDS pandemic in the last century, microsporidia emerged as opportunistic human pathogens (Desportes *et al*., 1985). As a result of their medical significance, research on microsporidia has been intensified in a variety of disciplines during the past decades. Nowadays, microsporidia still inflict great economic losses to the breedings of several animals such as the silkworm *Bombyx mori*, honeybees and fishes.

1.1. Microsporidia constitute a highly diversified phylum with a controversial phylogeny

Today, the unicellular eukaryotic microsporidia are known to be a large and extremely diverse group of obligate intracellular parasites. There are currently approximately 150 described genera of microsporidia with over 1,200 individual species (Sprague *et al.*, 1992; Sprague and Becnel, 1999).

Table 1. Microsporidian diversities (data from Vávra and Larsson, 1999; Wittner and Weiss, 1999)

Characteristics	Diversity
spore size	1 μm (*Enterocytozoon bieneusi)* ~40 μm (*Bacillidium filiferum)*
spore shape	generally ovoid, also spherical, rod-shaped, or crescent-shaped
exospore	thickness: 10 nm~200 nm
	appendages: absence or presence of tails, fibres, mucous layers, tubular projections
polar filament	isofilar filament* and anisofilar or heterofilar filament*; the thickness, the number and arrangement of coils and the angle of helical polar filament tilt can be diverse
polar tube (PT)*	length: 0.1 μm~0.25 μm; diameter: 50 μm~500 μm;
nucleus configuration	monokaryon or diplokaryon
host-parasite interface	Parasite is in direct contact of the parasite plasmalemma with the host cell cytoplasm (*Nosema bombycis*) or parasite is isolated from host cell cytoplasm by parasitophorous vacuole (PV) (PV: produced by parasite and/or host)
life cycle and host involved	simple life cycle and only one host involved; extremely complex life cycle and two or more host invovled
sporulation sequence	one sporulation sequence such as *Endoreticulatus fidelis*; two sporulation sequences such as *Nosema bombycis* or more
spore types in one life cycle	one spore type and two or more spore types as a result of two or more sporulation sequences
reproduction mode	asexual: merogony and sporogony sexual: karyogamy, gametogenesis, and plasmogamy
number of sporoblast	two sporoblasts (bisporous) and many sporoblasts (polysporous)
genome size	2.3 Mbp (*Encephalitozoon intestinalis*)~19.5 Mbp (*Glugea atherinae*)

* Isofilar filament, the polar filament with the same thickness along its entire length; * anisofilar or heterofilar filament, the polar filament with different thickness along its entire length, often with the anterior part thicker. * polar tube (PT), after microsporidia germinate, the external form of “polar filament” is called “polar tube”

Microsporidia have a number of important, unique features (**Figure 1**): no typical Golgi apparatus, which is the accumulation of small and opaque vesicles enclosed by a single membrane, comparing to the classical Golgi apparatus composed of stacked lamellar cisternae; no peroxisome and hydrogenosome; mitochondrial remnants called "mitosomes" instead of typical mitochondria; ribosomes of prokaryotic type. Further, the microsporidian spore is equipped with a unique infection apparatus in the living world (polar filament, polaroplast, posterior vacuole). Upon the appropriate stimulus, the polar filament everts from the spore and expels the infectious sporoplasm into a host cell. In fact, the polar filament is the definitive characteristic of microsporidia (Wittner and Weiss, 1999; Vávra and Larsson, 1999). While these common features, the microsporidia exhibit a large diversity in many aspects. The most obvious diversity is their great morphologic and cytologic differences which are summarized in **Table 1**. Nevertheless new microsporidian species are still being described and sometimes new genera are created to accommodate them (Sokolova *et al*., 2003; Johny *et al*., 2006).

Because of the lack of typical mitochondria and Golgi apparatus or peroxisomes and because of their several seemingly "prokaryotic" characteristics, such as 70S ribosomes (Ishihara and Hayashi, 1968) and a fused 5.8 S and 28 S rRNA (Vossbrinck and Woese, 1986; Vossbrinck *et al*., 1987), microsporidia were long thought to be a primitive or ancestral eukaryotic lineage, that diverged from the universal eukaryotic ancestor before the gain of the α-proteobacterial endosymbiont, which eventually became the mitochondrion. This hypothesis placed microsporidia into the Kingdom Archezoa, a group of organisms defined by their primitive lack of mitochondria (Cavalier-Smith, 1991) which was supported by the analyses of ribosomal RNA (Vossbrinck *et al*., 1987), elongation factor 1-alpha (EF-1α), isoleucyl-tRNA synthetase (Brown and Doolittle, 1995) and elongation factor 2 (EF-2) sequences (Kamaishi *et al*., 1996a, b).

However on one hand, 22 and 14 mitochondrial protein CDS were shown to be present in *Encephalitozoon cuniculi* and *Antonospora locustae* genomes respectively (Katinka *et al*., 2001; Williams and Keeling, 2005). Mitochondrial PDH E1 alpha and glycerol-3-phosphate dehydrogenase (mtG3PDH) proteins were also shown to be present in spores of *A. locustae* and *E. cuniculi* respectively (Fast and Keeling, 2001; Williams and Keeling, 2005). The expression of mitochondrial inner membrane peptidase 2 (IMP-2) was detected in *A. locustae* spores

Table 2. Pathogenicity of microsporidia isolated from *Bombyx mori*
(Kawarabata, 2003)

Microsporidian isolate	Infection							Transmission	
	Systemic infection	midgut epithelium	muscles	fat body	silk gland	Malpighian tubules	gonadotropic	peroral	transovarial
Nosema bombycis	√	√	√	√	√	√	highly	√	√
Nosema sp. NIS-M11	√		√	√	√	√	moderately	√	rarely
Nosema sp. NIS-M14	√		√	√	√	√		√	possible
Vairimorpha sp. NIS-M12	√							√	
Pleistophora sp. NIS-M27		√						√	
Thelohania sp. NIS-M32			√					√	
Microsporidium sp. NIS-M25	√		√	√	√	√		√	

(Williams and Keeling, 2005). N-terminal sequence analysis of a 68 kDa protein in *N. bombycis* showed similarity to all classes of mitochondrial heat shock proteins (Sironmani, 1999). In line with the discovery of micropsoridian mitochondrion-derived CDS and the mitosome hypothesis (Katinka *et al*., 2001), Williams *et al* (2002) identified a cryptic mitochondrion (~50×90 nm) in the microsporidian *Trachipleistophora hominis*, by immunolocalization of Hsp70. The polar vesicles specifically assembled near the spindle microtubular organizing centre of microsporidia are considered to be mitochondrial remnants 'mitosomes' (Vávra, 2005).

On the other hand, α- and β-tubulin phylogenies (Edlind *et al*., 1996; Keeling and Doolittle, 1996; Keeling *et al*., 2000) indicated a close relationship to fungi, in stark contradiction to the previous data. Additional analyses conducted on mitochondrial Hsp70 (Germot *et al*., 1997; Hirt *et al*., 1997; Peyretaillade *et al*., 1998), TATA-box binding protein (Fast *et al*., 1999), the largest subunit of RNA polymerase II (RPB1) (Hirt *et al*., 1999), glutamyl-tRNA synthetase (Brown and Doolittle, 1999) and pyruvate dehydrogenase (PDH) subunits E1α and β (Fast and Keeling, 2001) strengthened the proposed microsporidia-fungi relationship. Another analysis which combined molecular data from four genes further supported the fungal origin of microsporidia (Baldauf *et al*., 2000). The genome of *Encephalitozoon cuniculi* also yielded a number of proteins with strong fungal affinities (Katinka *et al*., 2001). Phylogenetic analysis of 99 *E. cuniculi* proteins indicated that microsporidia are evolutionarily related to fungi (Thomarat *et al*., 2004). A phylogenetic study performed by Keeling not only strongly supported a relationship between microsporidia and fungi, but also proposed that microsporidia evolved from a zygomycete ancestor (Keeling, 2003). Finally, the four different phylogenetic analyses of eight genes and sequence data from representatives of four fungal phyla place the phylum microsporidia within the fungal clade, as a sister of a combined ascomycete + basidiomycete clade (Gill and Fast, 2006).

While the exact relationship between microsporidia and fungi remains to be clarified, nearly all current evidence does support one major conclusion: microsporidia are not ancient eukaryotes, but are instead highly evolved fungi. This conclusion colors nearly all other aspects of microsporidia in a new light. No longer are they primitive in lacking typical mitochondria and Golgi apparatus or peroxisomes. On the contrary, these features result from reductive evolution,

Table 3. Diversified pathogenicity of microsporidian described in humans (Didier, 2005)

Genus	Species	Tissue specificity	Host range
Encephalitozoon	*Encephalitozoon cuniculi*	disseminated infection	wide host range among mammals: human, rats, guineapigs, hamsters, horses, cows, mink, nonhuman primates
	Encephalitozoon hellem	disseminated infection	humans, Parrots, birds
	Encephalitozoon intestinalis	disseminated infection	humans, dogs, pigs, cows, donkies, goats
Enterocytozoon	*Enterocytozoon bieneusi*	small intestine, biliary tract	humans, pigs, cats, dogs, primates (macaques)
Trachipleistophora	*Trachipleistophora hominis*	skeletal muscle, nasal sinuses	humans
	Trachipleistophora anthropopthera	disseminated infection	humans
Pleistophora	*Pleistophora species*	skeletal muscle	humans, fishes
Vittaforma	*Vittaforma (Nosema) corneae*	corneal stroma, urinary tract	humans
Nosema	*Nosema ocularum*	corneal stroma	humans
Brachiola	*Brachiola (Nosema) connori*	disseminated infection	humans
	Brachiola vesiculatum	corneal stroma, skeletal muscle	humans
	Brachiola (Nosema) algerae	cornea	humans, mosquitoes
Microsporidium	*Microsporidium africanum*	cornea	humans
	Microsporidium celonensis	cornea	humans

probably in response to their growing adaptation to intracellular parasitism. Similarly, microsporidian biochemistry is not primitive, it is reduced. Even at the molecular level, the tiny genomes of microsporidia evolved from larger genomes by gene loss and compaction, and the unusual genes and gene sequences are highly derived, not ancient (Keeling and Fast, 2002).

It is ironic that when Nägeli first named *N. bombycis* in 1857, he placed it among the fungi. With the completion of more and more microsporidian genome sequencing projects and the increasing post-genomics studies, it is possible to shed light on the exact relationship between microsporidia and fungi. Nägeli's prescience that microsporidia were fungi appears to be borne out.

1.2. A wide host spectrum with diversified pathogenicities

Microsporidia have been reported to infect nearly the whole invertebrate phylum, including ciliates, gregarines, myxozoans, cnidarians, plathelminths, nematodes, rotifers, annelids, mollusks, bryozoans and arthropods, as well as all five classes of vertebrates (Wittner and Weiss, 1999). The wide prevalence in arthropods results in the use of some microsporidian species as biological control agents against insect pests, while at the same time the infection of important economic animals such as honeybees, silkworm *Bombyx mori*, fishes and some crustacea can inflict great losses to sericulture, apiculture, fishery and aquaculture (Becnel and Andreadis, 1999; Shaw and Kent, 1999). Fifteen species of microsporidia are known to infect mammals. Among them, 14 species have been found to infect AIDS patients and immunocompromised individuals and occasionally healthy immunocompetent humans leading to a long list of human diseases, including chronic diarrhea and wasting syndrome (Weber *et al*., 1999; Didier *et al*., 2000; Didier, 2005). Microsporidian infections which result in various diseases indicate that these pathogens have a diversified pathogenicity: host range, host tissue and cell type specificity, or transmission modes. **Table 2** and **3** summarized the diversified pathogenicities of microsporidia described in *Bombyx mori* and humans respectively.

1.3. *Nosema bombycis* biological features

Table 4. The different major geographical reference *Nosema bombycis* strains in the world
(Wang *et al*., 2001; Kawarabata, 2003; Rao *et al*., 2005)

Isolate	Isolation	Original host	Identification
Nosema bombycis NIS-001	Before 1918, Honshou, Japan	*Bombyx mori*, larva	spore morphology and biological assays,, ELISA, ssu-rRNA
N. bombycis	1985, Gunma, Japan	*Neptis sappho*, adult	fluorescent antibody technique
N. bombycis NB-Prc-SES-H7901	1979, Tokyo, Japan	*Pieris rapae*, adult	spore morphology and biological assays, fluorescent antibody technique
N. bombycis Sd-NU-IW 8401	1984, Kanagawa, Japan	*Spodoptera depravata*, adult	spore morphology and biological assays, latex adhesion test
N. bombycis Y9101	1990, Kumamoto, Japan	*Spodoptera exigua*, larva	spore morphology and biological assays, latex adhension test, ssu-rRNA
N. bombycis Pr-S-19	1990, Okinawa, Japan	*Pieris rapae*, adult	latex adhesion test
Nosema sp. NIS-402	1974, Fukushima, Japan	*B. mori* female	spore morphology and biological assays, ELISA, ssu-rRNA
Nosema sp. NIS-408	1974, Gunma, Japan	*B. mori* female	spore morphology and biological assays, ELISA, ssu-rRNA
Nosema sp. NIS-520	1975, Saitama, Japan	*B. mori* female	spore morphology and biological assays, ELISA, ssu-rRNA
N. bombycis	Ca.1990, Sichuan, China	*B. mori*	*Nosema bombycis* surface-antigen protein P30.4 (AF245278)
N. bombycs and *N. bombycis* CGS, MG	Guangzhou, China	*B. mori*	spore morphology and biological assays, latex adhesion test
N. bombycis	Dongtai, China	*B. mori*	spore morphology and biological assays, ssu-rRNA
***N. bombycis* ISC-ZJ (used in this study)**	**Zhenjiang, China**	***B. mori*, larva**	**spore morphology and biological assays, ssu-rRNA**
N. bombycis	2000, China	*Spodoptera litura*	ssu-rRNA
N. bombycis	China	*B. mori*	ssu-rRNA
N. bombycis	India	*Antheraea mylitta*	ssu-rRNA
N. bombycis	Northern India	*B. mori*	ssu-rRNA
N. bombycis	Southern India	*B. mori*	ssu-rRNA
N. bombycis NIK-2r	Mysore, India	*B. mori*, adult	spore morphology and biological assays;ssu-rRNA
N. bombycis NIK-1s	Mysore, India	*B. mori*, adult	ISSR-PCR and ssu-rRNA
N. bombycis	Before 1954, Europe	*B. mori*	spore morphology and biological assays, fluorescent antibody technique
N. trichoplusiae *Synonym: N. bombycis*	1959, Hawaii, U.S.A.	*Trichoplusiae ni*, larva	spore morphology and biological assays ssu-rRNA

Since Nägeli named the first described microsporidian *Nosema bombycis*, it has been the reference species for the genus *Nosema* in which about 150 species have been described from at least 12 insect orders (Becnel and Andreadis, 1999). The "*Nosema bombycis* Nägeli 1875" belongs to the *Nosema* genus (Nägeli, 1875), *Nosematidae* family, Microsporida order (Balbiani, 1882), Microsporea class and Microsporidia Balbiani, 1882 phylum (Sprague and Becnel, 1998). The type host is *Bombyx mori* but numerous other Lepidoptera are susceptible, for example, five Lepidopteran insects, *Pieris rapae* (Pieridae), *Spodoptera diparvata* (Noctuidae), *Spodoptera exigua*, *Spodoptera litura* and *Trichoplusia ni,* which are known to be natural hosts of *Nosema bombycis* isolates in Eastern Asia (Kawarabata, 2003). These susceptible hosts can be a wild reservoir for *N. bombycis* and increase the possibility of horizontal transmission in sericulture.

So far, there are at least 20 different geographical major reference strains of *N. bombycis* in the world (Wang *et al*., 2001; Kawarabata, 2003; Rao *et al*., 2005) (**Table 4**). In recent years, previously undescribed microsporidia pathogenic to *B. mori* have been isolated from sericultural farms. Some of them have been identified as the type *N. bombycis*, as *N. bombycis* different variants or transferred to other genus based on their molecular phylogeny and life cycle studies (Sato and Watanabe, 1986; Iguchi *et al*., 1997; Rao *et al*., 2004, 2005). In fact many of the early classifications of microsporidia based on life cycle features, spore size, shape, and ultrastructure of spores including number of polar tube coils and host-parasite relationship resulted in the unnecessary creation of new *Nosema* species. With the application of combining molecular evidences with biological features, many of *Nosema* species have been transferred to other genus, for example, *N. corneae* to *Vittaforma corneae* (Silveira and Canning, 1995), *N. connori* to *Brachiola connori* (Cali *et al*., 1998) and *N. algerae* to *Brachiola algerae* (Lowman *et al*., 2000), *N. grylli* to *Paranosema grylli* (Sokolova *et al*., 2003) and *N. locustae* to *Antonospora locustae* (Slamovits *et al*., 2004).

All major reference *N. bombycis* strains have their species essential features: all stages are diplokarytic and in direct contact with host cell cytoplasm; it has two sporulation sequences and produce primary and environmental spores sequencially; it can be transmitted horizontally and transovarially; it infects nearly all tissues of *Bombyx mori* (systemic infection) except the external cuticle, the spire filament of trachea, the inner wall of the foregut and hindgut, the

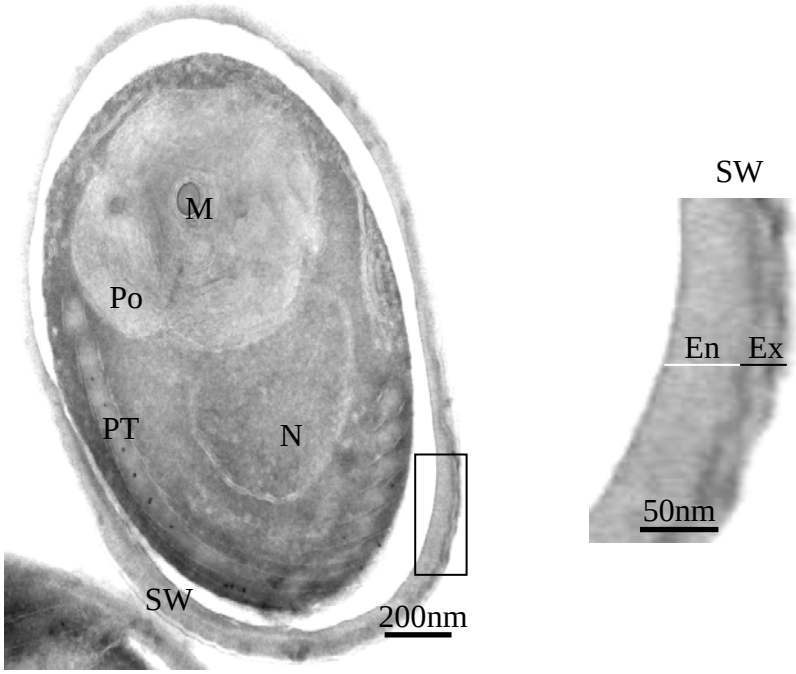

Figure 2. The spore wall (SW) of *Nosema bombycis.* The spore wall of *N. bombycis* is composed of exospore (Ex) and endospore (En). The exospore (20~30 nm) is clearly composed of two electron-dense layers and one middle layer with less electron density. The endospore (40~50 nm) appears as a relatively thick has similar electron density with the middle layer of exospore. The right picture is the enlargement of the rectangle on the left. M, manubrium (anterior part of the polar tube); Po, polaroplast; PT, polar tube; N, nucleus.

cutinized parts like mouthparts (Yu *et al*., 1994; Becnel and Andreadis, 1999).

1.3.1. The spore structure of *Nosema bombycis*

The mature spores of *Nosema bombycis* (**Figure 1**) are oval or oblong in shape and measure 3.1~4.2 μm in length by 1.9~2.6 μm in width (Kawarabata, 2003). *N. bombycis* mature spore is comprised of the spore wall (exospore and endospore), the sporoplasm surrounded by a smooth single plasma membrane and two appressed nuclei or diplokaryon. The cytoplasmic organelles include the invasion apparatus (the polar sac -anchoring disk complex, the isofilar polar filament, the polaroplast, the posterior vacuole of amorphous appearance at the basal end), ribosomes, endoplasmic reticula and atypical Golgi apparatus (Ishihara, 1968; Sato *et al*., 1982; Vávra and Larsson, 1999).

1.3.1.1. *Nosema bombycis* spore wall

The environmental resistant spores of *N. bombycis* possess the typical microsporidia spore wall of two parts: the external spore wall (exospore) and the internal spore wall (endospore).

N. bombycis exospore appeared to be relatively thin (20~30 nm), with three somewhat wavy layers (**Figure 2**) of material with different electron density. The components of its exospore include proteins that may be glycosylated (Vávra, 1965, 1976), as in other micropsoridian species (Vávra, 1965, 1976; Yu *et al*., 1994; Sironmani, 1999).

N. bombycis endospore, which is composed of chitin and proteins (Vávra, 1976), reveals as a single relatively thick layer (40~50 nm) of material of nearly the same electron density as the outer layer of exospore (**Figure 2**).

The anterior end of *N. bombycis* spore, in front of the anchoring disk, has an area where the endospore is less thick (5~10 nm) and more electron-dense (**Figure 1** and **3**). The spore wall, the mechanical properties of which provide resistance to environmental influences and allow the increase in hydrostatic pressure that causes spore discharge, is involved in the initiation of polar filament extrusion and fixation of the everted polar tube by modifications of its architecture (Weidner, 1992; Weidner and Halonen, 1993; Frixione *et al*., 1997).

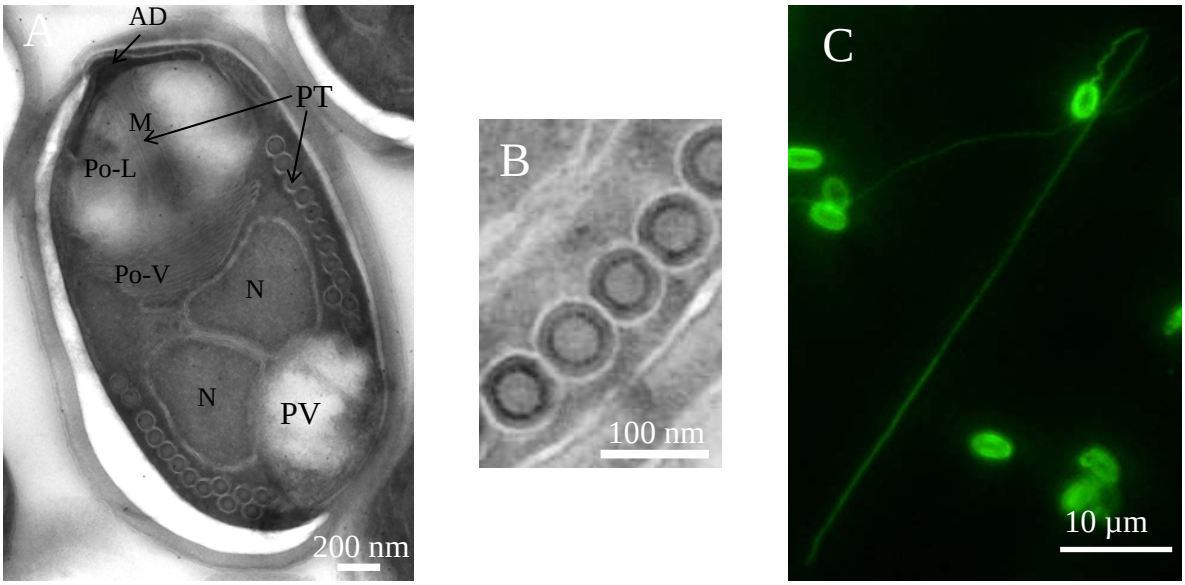

Figure 3. Invasive apparatus of *Nosema bombycis.* The anchoring disk, polar filament, polaroplast and posterior vacuole often function together as the invasive apparatus of microsporidia. A, Transmission electronic micrograph of *Nosema bombycis* spore; B, Fine transverse sections of *N. bombycis* layered polar filament; C, Everted *N. bombycis* polar tube (~65µm) by immunofluorescence technique in photonic microscopy. AD, anchoring disc; PT, polar tube; M, manubrium (anterior part of the polar tube); Po, polaroplast; Po-L, anterior lamellar region of polaroplast; Po-V, posterior vesicular region of polaroplast; PV, posterior vacuole; N, nucleus.

As a typical reference species in the genus *Nosema*, the further characterization of *N. bombycis* spore wall, such as its components and ultrastructure, is very important for the host-parasite interaction study and may also provide the molecular features for species classification.

1.3.1.2. The invasive apparatus

The polar filament, polaroplast, anchoring disk and posterior vacuole often function together as the microsporidia invasive apparatus (**Figure 3**).

As the characteristic structure of microsporidia, the polar filament of *Nosema bombycis* is divided into two regions: the manubrium or straight portion connected to the anchoring disk and the posterior region that forms 12~14 coils around the sporoplasm and has an angle tilt of at least 49° (Ishihara, 1968) (**Figure 3A**). It is composed of concentric layers of different electron density and thickness (Vávra, 1976) (**Figure 3B**). It has been suggested that the polar filament originated from the coalescence of vacuoles of the Golgi complex (Keohane and Weiss, 1999). When the spore germinates, the polar filament inside the spore is everted and its outside form is often called "polar tube". *N. bombycis* polar tubes range from 70~130 μm in length and 0.1~0.25 μm in diameter which can increase to 0.4 μm during sporoplasm passage, and its length shortens by 5~10% after sporoplasm passage (Oshima, 1937) (**Figure 3C**). In addition to its role in protecting the sporoplasm from the harsh external environment during its passage into its host cell, the polar tube can provide a bridge to transfer the sporoplasm directly into the host cell (Xu and Weiss, 2005). The polaroplast is a system of membrane-limited compartments that occupies one-third to one-half of the spore volume. This voluminous structure surrounds the straight-part of the polar tube manubrium and ends at the level of the first filament coils. It is also divided into the anterior closely packed lamellar region and the posterior irregular vesicular region (**Figure 3**). The anchoring disk is a mushroom-shaped, biconvex, layered body at the spore apex where the spore wall is the thinnest and where the rupture occurs during discharges of polar tube. It connects with all layers of polar tube and serves as "hinges" when the polar tube turns inside out (**Figure 3**). As a product of the Golgi vesicles and membrane-lined area, the posterior vacuole has a clear or spongy content and locates in the posterior part of the spore. The swelling of

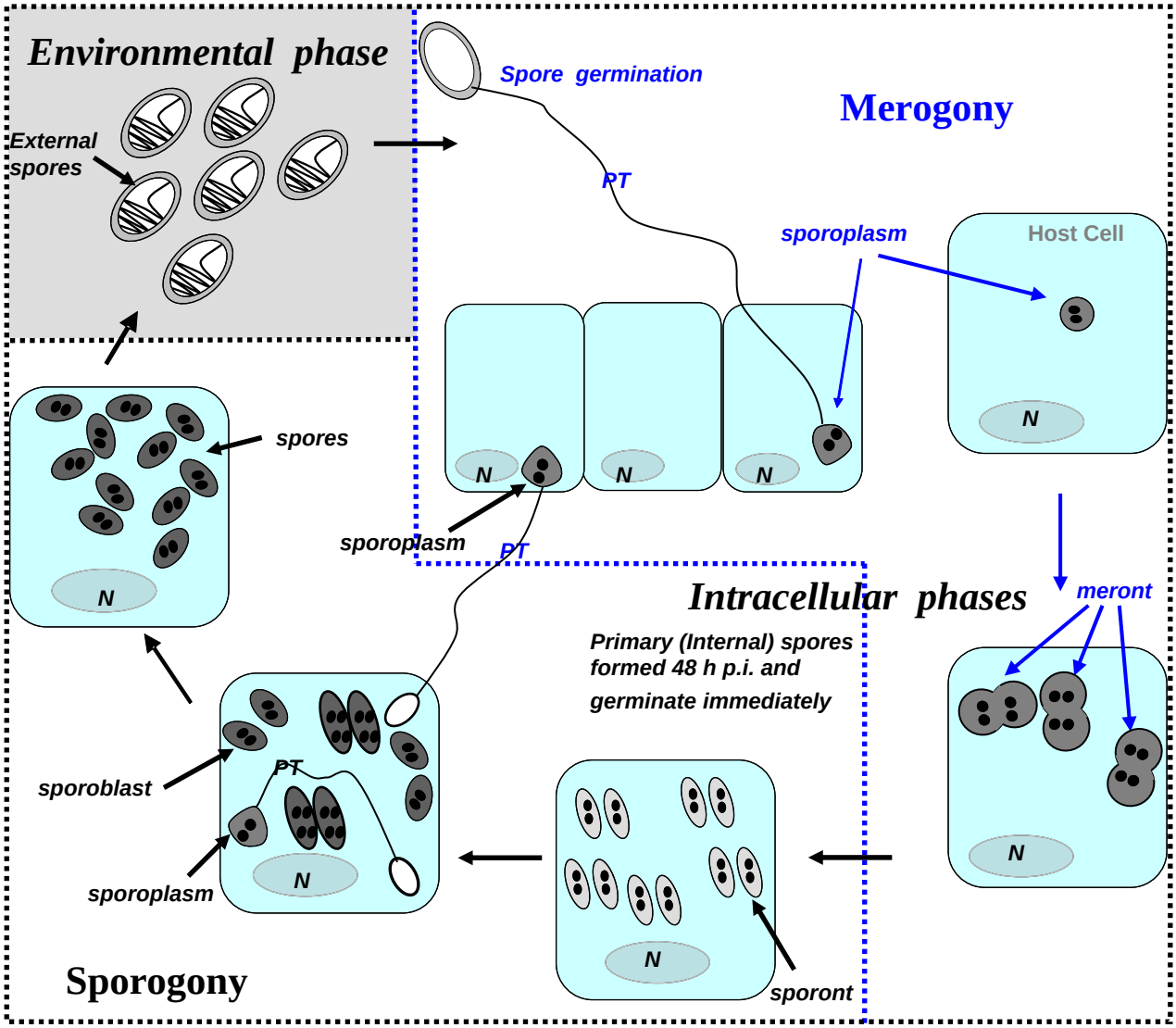

Figure 4. Life cycle model of *Nosema bombycis* (adapted from Cali and Takvorian, 1999). 1. The life cycle of *N. bombycis* is divided into the environmental (infective) phase and intracellular phases (merogony and sporogony). All developmental stages of *N. bombycis* are diplokaryotic. 2. In the environmental infective phase, the proper environmental conditions are required to active mature spores, resulting in polar tube extrusion and sporoplasm deposition into the host cell cytoplasm. 3. In the intracellular phases, *N. bombycis* sporoplasm is in direct contact with the host cell cytoplasm and matures into meront which multiplies by binary fission (merogony). The plasmalemma thickening is the beginning of sporogony stage. Each sporont produces two sporoblasts and each sporoblast produces two mature spores (sporogony). 4. Spore dimorphism: *N. bombycis* completes its relatively simple life cycle with two sporulation sequences forming two types of spore respectively: "primary spore, internal spore or FC (few coils of polar filament) spore" which can germinate quickly after formation (autoinfection) and "environmental spore or external spore". 5. In fact, all *N. bombycis* developmental stages can be present in a given host cell: 1) meront, 2) meront and sporont, 3) meront, sporont and sporoblast, 4) meront, sporont, sporoblast and spore. N, nucleus; PT, polar tube.

posterior vacuole and polaroplast leads to the increase of intrasporal osmotic pressure which can rapidly push the coiled polar filament outside and expel the sporoplasm to pass through its outside form "polar tube" (**Figure 3C**) (Oshima, 1927, 1937).

1.3.1.3. *N. bombycis* sporoplasm

N. bombycis sporoplasm is composed of cytoplasm, cytoplasmic organelles and two nuclei. With the total genetic information inside, the sporoplasm is the real infectious element.

N. bombycis sporoplasm is 0.5~1.5 μm in diameter (Yu *et al*., 1994). The fine structure of sporoplasm discharged into preheated hemolymph of the silkworm *Bombyx mori* was observed by electron micrographs (Ishihara, 1968) *N. bombycis* sporoplasm had a smooth single plasma membrane, two nuclei, ribosome-like particles, vesicles, a vesicular structure having coiled tubules, a concentric ring structure consisting of two or four rings and containing granules. No typical mitochondria, polyribosomic cluster of ribosomes, or endoplasmic reticulum having rough surface were recognized. After the sporoplasm was injected into the host tissue, a new membrane system surrounded the sporoplasm was revealed (Ishihara, 1968). This membrane is obtained from the extrusion apparatus during sproplasm passage through the polar tube (Weidner *et al*., 1984)

1.3.2. *N. bombycis* life cycle model

As the type species of *Nosema* genus, *N. bombycis* development is apansporoblastic and in direct contact with the cytoplasm of host cell. All developmental stages are diplokaryotic with paired abutted nuclei (Cali, 1971). The intracellular cycles of *N. bombycis* include the proliferative merogonic stage (merogony) and sporogonic stage (sporogony) (**Figure 4**). A triggered *N. bombycis* spore injects its diplokaryotic sporoplasm into the host cell cytoplasm. The sporoplasm matures into meront and starts the merogonic stage. During this proliferative stage, *N. bombycis* multiplies by binary fission (karyokinesis linked to cytokinesis) and forms binucleate meronts. The meronts, round or irregular cells surrounded by a unit membrane, often have a large nuclear region including double D-shaped diplokarya and a weakedly developed cytoplasm with relatively sparse dispersed ribosomes and ER. The Golgi complex is generally

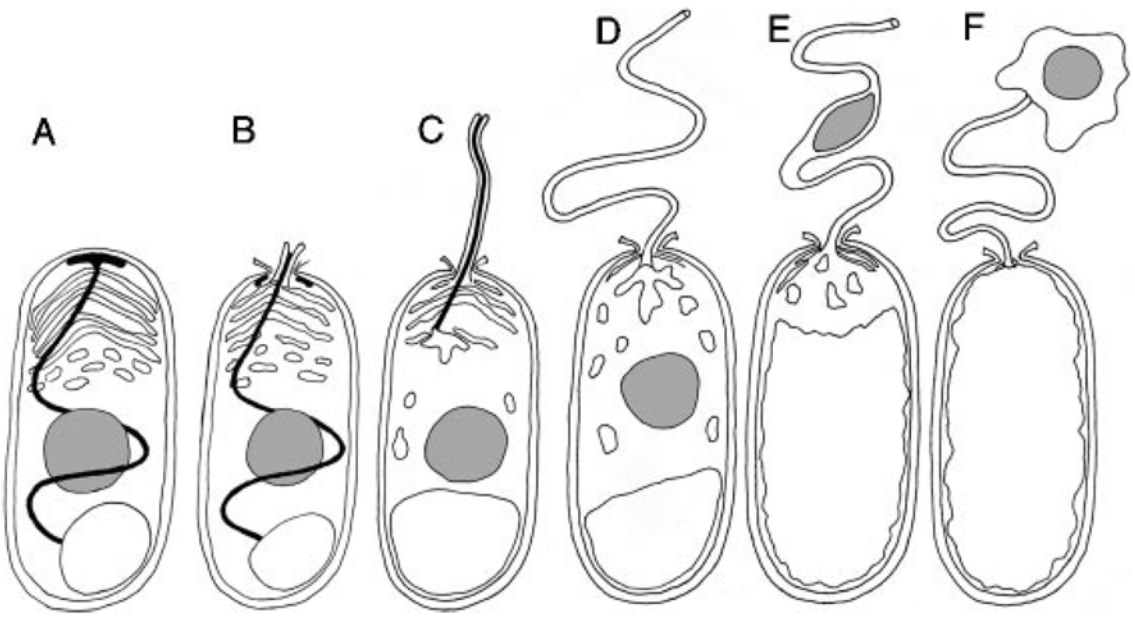

Figure 5. Model of the spore germination (Keeling and Fast, 2002). (A) Dormant spore, showing polar filament (black), nucleus (grey), polaroplast and posterior vacuole. (B) Polaroplast and posterior vacuole swells, anchoring disk ruptures, and polar filament begins to emerge and evert. (C) Polar filament continues to evert. (D) Once the polar tube is fully everted, the sporoplasm is forced into and (E) through the polar tube. (F) Sporoplasm emerges from the polar tube bound by a new membrane.

not apparent until the beginning of sporogony (Cali and Takvorian, 1999). Their plasmalemma is in direct contact with the host cell cytoplasm (Cali, 1971). The transition to sporogony include a general increase in cytoplasmic density due to increased ER and ribosomes and a change in the appearance of plasmalemma. A meront becomes a sporont with the onset of the plasmalemma thickening. Once the sporont thickened membrane (the early cell wall) is formed, the sporonts (0.5~1.5 μm in diameter) divide by binary fissions. Every sporont cell produces two sporoblasts which will undergo a series of metamorphosis during maturation: the extrusion apparatus including the polar filament, its anchoring disk complex, the polaroplast membranes and/or tubules, and the posterior vacuole begin to form; large quantities of ER and ribosomes are produced; the Golgi complex enlarges; they crenate and decrease in size and their cytoplasm becomes more electron-dense. Finally every sporoblast matures into a spore with their shape, polar filament and spore wall with exospore and endospore well established (Cali, 1971; Cali and Takvorian, 1999) .

N. bombycis completes its relatively simple life cycle with two sporulation sequences both with diplokaryotic sporont and disporoblastic sporogony (Cali, 1971, Kawarabata and Ishihara, 1984; Iwano and Ishihara, 1989, 1991a, b). The primary (early) sporulation sequence produces a thin-walled binucleate spore [called “primary spore, internal spore or FC (few coils of polar tube) spore”] with 4 coils of short polar filament and a large posterior vacuole. The primary spore can germinate quickly after formation in the infected cells and serve to disseminate infection within *B. mori* (autoinfection) and they are responsible for the transovarial transmission because of the infection of the gonads. In cultured insect cells or *in vivo*, the primary spores are present at 48 h after infestation (Kawarabata and Ishihara, 1984; Iwano and Ishihara, 1991b). The second sporulation sequence produce a binucleate spore with a thicker spore wall and 10~13 coils of long polar filament in one row arrangement that was previously described in section 1.3.1 (Ishihara, 1969; Iwano and Ishihara, 1991a, b). They are detected 72 h after infestation of the insect cell cultures (Ishihara and Sohi, 1966). These external or environmental spores are involved in the infestation of new hosts and function to infect the new host in horizontal transmission.

1.3.3. *N. bombycis* germination and cell invasion

As the unique biological phenomena of microsporidia, germination plays a very important

Table 5. The stimuli inducing *Nosema bombycis* germination *in vitro*

Stimulus	Description of stimulus	Reference
digestive fluid of *Bombyx mori*	boiled digestive fluid of *Bombyx mori*	Oshima, 1927
	digestive fluid of *Bombyx mori*	Trager, 1937
H_2O_2	30% H_2O_2 or 30% H_2O_2 +1% $NaHCO_3$	Kudo, 1918
	1.5~3% H_2O_2	Oshima, 1966
	3% H_2O_2	Oshima, 1927
buffered monovalent ions	0.1N KOH followed by preheated *Bombyx mori* hemolymph	Ishihara, 1968
	0.375 M KCl + 0.05 M glycine + 0.05 M KOH, pH 9.4~10	Oshima, 1964
monovalent ions and pH change	NaOH (N/10 to N/160) pH 11~13 neutralized with HCl to pH 6.0~9.0	Oshima, 1937
	KOH (N/7 to N/640) neutralized with HCl to pH 6.5~8	Oshima, 1964
other	liver extract medium, pH > 8	Trager, 1937

Table 6. Comparision of genome size and chromosomal DNA bands from 13 microsporidian species (Méténier and Vivarès, 2001; Cornillot E., personal communication for *Nosema bombycis*)

Species of microsporidia	Genome size estimate (Mbp)	Number of bands	Chromosomal size range (Kbp)	Host
Glugea atherinae	19.5	16	420~2700	fish
*Nosema bombycis**	12~15	39	440~1815	insect
Nosema pyrausta	10.5	13	130~440	insect
Nosema furnacalis	10.2	13	130~440	insect
Vairimorpha sp.	10.2	8	720~1790	insect
Vavraia oncoperae 1	10.2	16	140~1830	insect
Vavraia oncoperae 2	8.0	14	130~1930	insect
Nosema costelytrae	7.4	8	290~1810	insect
Spraguea lophii	6.2	12	230~980	fish
Nosema locustae	5.4	18	139~651	insect
*Paranosema grylli**	4.4~4.7	17	135~485	insect
Encephalitozoon cuniculi	2.9	11	217~315	mammal
Encephalitozoon hellem	2.5	12	175~315	mammal
Encephalitozoon intestinalis	2.3	11	190~280	mammal

*, based on KARD 2-D PFGE data; for other microsporidian, based on PFGE data. PFGE, pulsed-field gel electrophoresis; KARD 2-D PFGE, karyotype and restriction display two -dimensional PFGE

role in perpetuating microsporidian life cycle though its exact mechanism is not well understood. The germination is a very quick process often occurring in less than 2s and including a chain of events leading to discharge of the polar filament and sporoplasm (**Figure 5**): (1) spore activation with a set of appropriate stimuli; (2) rapid increase in intrasporal osmotic pressure; (3) explosive eversion of the polar filament and formation of a hollow "polar tube" and (4) quick passage of sporoplasm through the polar tube, and exit of the sporoplasm in the form of a minute cell at the tip of the everted polar tube (Keohane and Weiss, 1999).

Although the initiation steps of germination appear to be more variable and largely unknown, the propulsive force is probably osmotic (Oshima, 1927; Undeen and Frixione, 1990). The polar tube function studies of *N. bombycis* led to the first experimental demonstration of the relationship between the osmotic pression and spore germination. When hatched in H_2O_2 and various concentration of NaCl, the rate of *N. bombycis* germination decreased with increasing saline concentration (Oshima, 1927, 1937). Undeen believed that the increase in intrasporal osmotic pressure was due to the hydrolysis of trehalose into glucose (Undeen, 1990; Undeen and Vander Meer, 1994). Recently, the oxidation of fatty acids in the posterior vacuole has been considered to also provide the force needed for germination (Findley *et al*., 2005).

The identified stimuli for microsporidian germination *in vitro* are ions, pH change, rehydration, direct pressure, and hydrogen peroxide. Temperature is also an important variable (Keohane and Weiss, 1999). The stimuli used for *N. bombycis* gemination *in vitro* include the digestive fluid of silkworm (Trager, 1937; Oshima, 1927), hydrogen peroxide (H_2O_2) (Kudo, 1918; Oshima, 1966), buffered monovalent ions (Oshima, 1964) and pH change (Ohshima, 1937, 1964) or their combination (**Table 5**). *In vivo*, the conditions promoting the germination of microsporidia appear to be very different: *N. bombycis* primary spores can germinate immediately in the same host cell cytoplasm (Ishihara, 1969; Iwano and Ishihara, 1991b) and its environmental spores germinate in the midgut of silkworm (Oshima, 1937), while other species of microsporidia were found germinating from the phagosome (Franzen, 2004). Perhaps the microsporidian germination *in vivo* mainly depends on the interactions between microsporidian spores and host cell cytoplasm and involves a series of signal pathways not yet identified.

When triggered by appropriate stimuli, *N. bombycis* polar filament rapidly discharges from

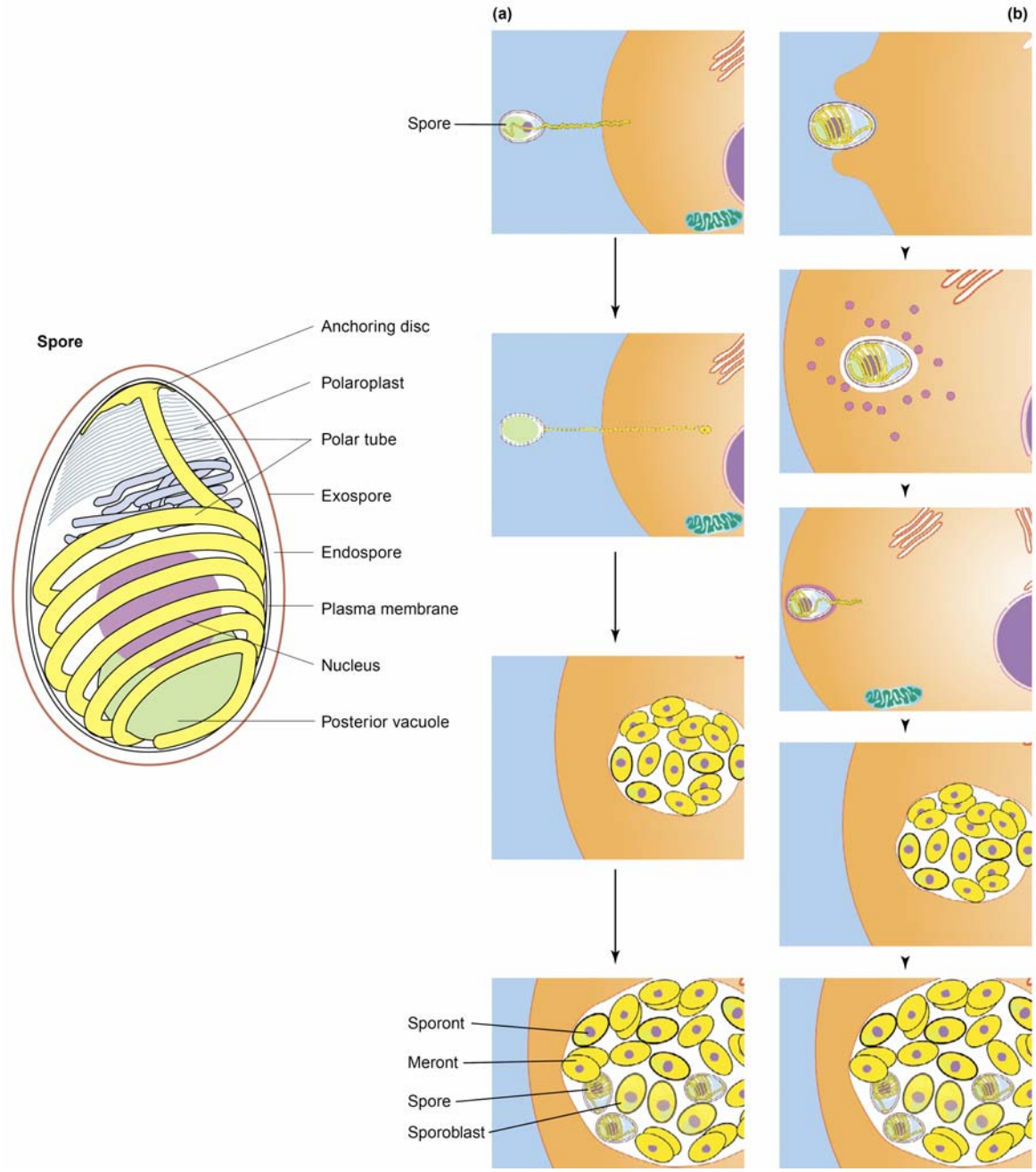

Figure 6. Models of host-invasion routes of microsporidia proposed from *in vitro* experiments: active invasion and phagocytosis (Franzen, 2004). (a) In active invasion, the spore extrudes its polar tube, the infective sporoplasm is released into the cytoplasm of the host cell, and the remaining empty spore and polar tube are degraded. The sporoplasm matures into a meront, which is in direct contact with the host cell cytoplasm like *Nosema bombycis* or surrounded by a parasitophorous vacuole. The meront undergoes several rounds of asexual reproduction (merogony), leading to the production of 50 to several hundred meronts in a single cell. The meronts develop further to become sporonts, then into sporoblasts. Eventually, the host cell bursts releasing the spores. (b) In the alternative model, the extracellular spore is taken up by the host cell by phagocytosis. The spore is enclosed in a phagosome, which is attacked by the host cell lysosomes (violet dots). The spore uses its polar tube to escape from the phagolysosome, thus releasing the infective sporoplasm into the host cell cytoplasm. The sporoplasm matures into a meront and undergoes asexual reproduction as described in (a).

the anterior pole of the spore forming a hollow polar tube that remains attached to the anterior end of the spore and the sporoplasm flows through the tube appearing as a droplet at its distal end. This evagination of the polar filament has been likened to 'reversing a finger of a glove' (**Figure 5**) (Oshshima 1937; Ishihara, 1968).

The microsporidian germination from the digestive fluid, host cell cytoplasm or phagosome seems the unique means for their host cell invasion. The "active invasion" (spore germination from digestive fluid, host cell cytoplasm) and "phagocytosis" (after phagocytosis, the spore can escape the killing of phagosome by germination and injecting the infective sporoplasm into host cell cytoplasm to multiply) have been proposed as the two main host-invasion routes of microsporidia (**Figure 6**) (Franzen, 2004)

1.4. Molecular studies on microsporidia

1.4.1. Genomes and genomics

The unicellular microsporidia have small genomes in remarkably diversified size from 2.3 to ~20 megabases (MB) (**Table 6**) (Biderre *et al*., 1994). The genomic resources for microsporidia have steadily increased in the last few years. Presently the first complete microsporidian genome 2.9 Mbp sequence for *Encephalitozoon cuniculi* Levaditi, Nicolau et Schoen, 1923, a monokaryotic microsporidian infecting mammals including human (genoscope.cns.fr/externe/English/Projets/Projet_AD/AD.html), has revealed about ~2,000 coding sequence genes densely distributed over 11 small chromosomes which range from 217 to 315 kb and are made up of gene-rich cores flanked on both ends by rRNA operons, non-coding subtelomeric regions and telomers (Katinka *et al*., 2001). Statistical analyses for *E. cuniculi* completed genome and predicted proteome, are available in the EBI Integr8 web site (http://www.ebi.ac.uk/integr8/EBIIntegr8-HomePage.do). The genome *Antonospora locustae*, also known as *Nosema locustae* infecting grasshoppers, is estimated at 5.4 Mb (Streett, 1994). The *Antonospora locustae* Genome Project (Marine Biological Laboratory at Woods Hole (funded by NSF award number 0135272), using whole genome shotgun (WGS) sequencing, has released 648 contigs of over 3000bp at the site http://jbpc.mbl.edu/*Nosema*/Nannotation.html. So far other genomic resources include genome sequence surveys (GSS) from the fish parasite

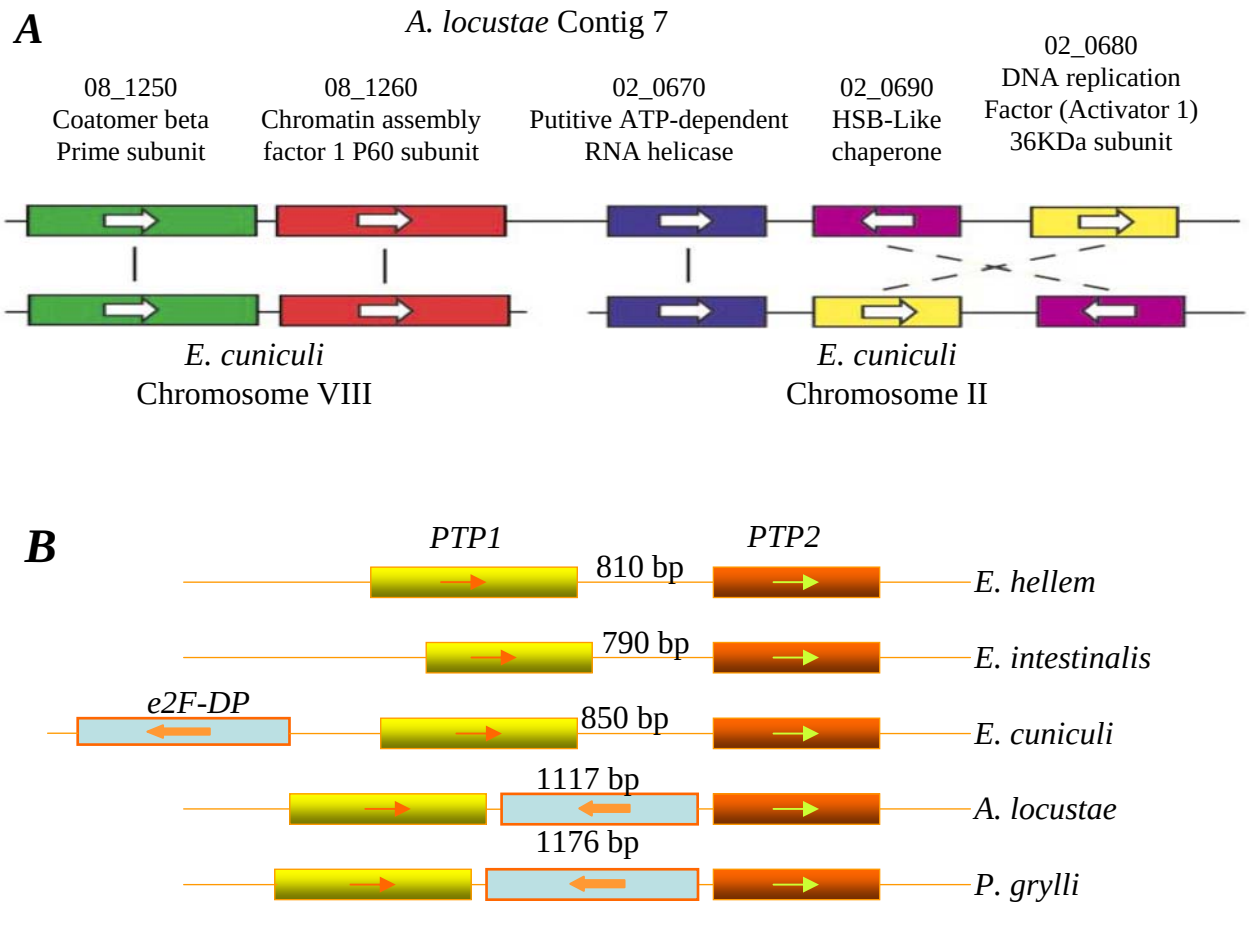

Figure 7. A) Examples of gene order conservation between *Antonospora locustae* and *Encephalitozoon cuniculi* (Slamovits *et al.*, 2004); **B) Syntenic region in five microsporidian species, centered on two ptp genes (*PTP1* and *PTP2*)** (Polonais *et al.*, 2005). The five species are three mamalian parasites *Encephalitozoon intestinalis, Encephalitozoon hellem, Encephalitozoon cuniculi* and two insect parasites *Antonospora locustae and Paranosema grylli* (ptp, polar tube protein; e2F-DP, E2F dimerization partner)

Spraguea lophii (jbpc.mbl.edu/Spraguea-HTML/) (Hinkle *et al*., 1997), the opportunistic human pathogen *Vittaforma corneae* (Mittleider *et al*., 2002), and *Antonospora locustae* (botany.ubc.ca/keeling/Antonospora GSS.html) (Slamovits *et al*., 2004), and an expressed sequence tag (EST) survey for *A. locustae* (amobidia.bcm.umontreal.ca/pepdb/pep.php). *Brachiola algerae* (mammalian parasite, Génoscope, France) and *Nosema bombycis* (insect parasite, Chongqing, China) complete genome sequencing projects are currently running.

Nosema bombycis has 18 chromosomes and the genome is approximatly 15,330 kb (Kawakami *et al*., 1994). Recently the analyses of eight complete long-terminal repeat retrotransposon (Nbr) elements (3~4 kb) which have been identified in the *N. bombycis* genome indicated that they are associated with genome size variation and syntenic discontinuities and play a major role in reorganization of the microsporidian genome (Xu *et al*., 2006).

The comparison of *E. cuniculi* and *A. locustae* genome shows an extreme reduction of gene numbers by non-random loss of genes, a genome compaction with very small intergenic space, and a genome structure conservation in microsporidian genomes (Slamovits *et al*., 2004; Keeling and Slamovits, 2004). The *E. cuniculi* genome contains relatively few protein-coding genes (1,997 identified), suggestive of massive gene loss due to host dependence (Katinka *et al*., 2001). In terms of compaction, the gene-rich cores in *E. cuniculi* chromosomes are composed of protein-coding genes in very high density (about 0.97 genes/Kbp). Genes are separated by short intergenic regions (average of 129 bp), have few introns (Katinka *et al*., 2001), and the genes themselves are on average 17% shorter than homologues in yeast. The gene density of *A. locustae* sequenced regions is about 0.94 genes/Kbp and the average intergenic region is about 200 bp, with gene lengths similar to *E. cuniculi* homologues (Slamovits *et al*., 2004). The gene density of these two microsporidian genomes is considerably higher than any other well-sampled eukaryote, twice as high as in *Saccharomyces cerevisiae* but about the same as in typical bacteria. Another characteristic found to be similar between the *E. cuniculi* and *A. locustae* genomes is the relative order of genes or synteny (13% of genes are in the same context) as demonstrated by the analysis of polar tube proteins genes (**Figure 7**) (Delbac *et al*., 2001; Slamovits *et al*., 2004; Polonais *et al*., 2005; Texier *et al*., 2005).

Table 7. Major characteristics of microsporidian polar tube proteins

(data from Delbac *et al*. 1998, 2001; Peuvel *et al*., 2002; Polonais *et al*., 2005; Polonais, personnal communication)

Protein	Number of AA		pI*	M.W.* (kDa)	Major AA (%)		No. of cycteine	No. of potential glycosylation sites	
	Precurser	Mature protein			Pro	Gly		O-Glyc	N-Glyc
Ec-PTP1	395	373	4.7	37	13.4	11.8	17	37	3
Ei-PTP1	371	349	4.5	35	13.7	8.3	17	56	3
Eh-PTP1	453	431	4.4	43	14.6	12.9	21	32	0
Al-PTP1	355	337	5.2	34.4	19.8	10.6	12	19	1
Pg-PTP1	351	333	5.2	33.3	21.6	14.7	12	19	1
					Lys	Glu			
Ec-PTP2	277	264	8.6	35	12.1	9.5	8	3	1
Ei-PTP2	275	262	8.6	30	11.8	6.2	8	4	1
Eh-PTP2	272	259	8.6	30	10.8	9.5	8	5	2
Al-PTP2	287	268	9.1	29.1	12.3	9.3	8	1	0
Pg-PTP2	287	268	8.9	29.2	12.3	8.6	8	2	1
					Pro	Glu			
Ec-PTP3	1256	1241	6.5	136	16	17	1	0	6
					Glu	Ser			
Ec-PTP4	276	260	7.5	29.7	10.4	7.3	6	2	2
Al-PTP4	381	364	8.5	42.4	7.4	7.7	5	2	3
Pg-PTP4	381	366	9.2	42.4	7.6	9.6	5	0	3
					Lys	Leu			
Ec-PTP5	252	239	9.6	27.6	12.5	9.6	6	1	0
Al-PTP5	242	230	8.9	26.9	9.1	8.7	6	0	0

AA, amino acid; *, the calculated pI and molecular weights (M.W.), for Ec-PTP1, the oberserved molecular weight in SDS-PAGE is 55 kDa; PTP, polar tube protein; *Ec, Encephalitozoon cuniculi*; *Ei, Encephalitozoon intestinalis*; *Eh, Encephalitozoon hellem*; *Al, Antonospora locustae*; *Pg, Paranosema grylli*;

1. 4. 2. Proteins and proteomics studies of microsporidia

Microsporidian protein studies mainly concentrate on: 1) the parasite invasion related proteins such as polar tube or spore wall proteins, most of them being microsporidian-specific proteins (Peuvel *et al*., 2006); 2) the mitochondrial-related proteins (see 1.1. of this chapter) and 3) the potential drug target for therapeutics such as polyamine oxidase (PAO) (Bacchi *et al*., 2002) and methionine aminopeptidase type 2 (MetAP2) (Didier *et al*., 2003).

An important set of microsporidian-specific proteins are the polar tube proteins. Two polar tube proteins (PTP1 and PTP2) have been identified in five microsporidian species *Encephalitozoon intestinalis*, *Encephalitozoon hellem*, *Encephalitozoon cuniculi*, *Antonospora locustae* and *Paranosema grylli* (**Table 7**). PTP1, an acid protein rich in proline, is the major polar tube O-mannosylated protein (~70% of the mass of the polar tube). Its glycosylation has a functional role in polar tube adherence to the host cell surface during host cell invasion (Xu *et al*., 2004; Polonais *et al*., 2005). Carbohydrate moieties of PTP1 and anchoring region are targeted by immunoglobulin G in immunocompetent individuals (Peek *et al*., 2005). PTP2 is a basic protein rich in lysine. The cysteine-rich PTP1 and PTP2 can only be extracted with reducing agents such as DTT. They are encoded by two tandemly arranged genes (**Figure 7**) (Delbac *et al*. 1998, 2001; Keohane *et al*. 1998; Polonais *et al*., 2005). A large-sized PTP3 (1,256 aa) which is solubilised in the presence of SDS alone has also been localized to the polar tube of *E. cuniculi* (Peuvel *et al*., 2002). Chemical cross-linking experiments support the involvement of the three proteins in the formation of a large multimeric complex (Peuvel *et al*., 2002). More recently, two basic proteins PTP4 and PTP5, have also been characterized in *Encephalitozoon cuniculi*, *Antonospora locustae* and *Paranosema grylli* (**Table 7**) (Polonais, personal communication). Of three polar-tube proteins in *P. grylli*, p56 is considered to be a member of PTP1 family while p34 and p46 belonging to PTP2 family due to their biochemical characteristics (Dolgikh *et al*., 2005).

Another set of microsporidian-specific proteins is the microsporidian spore wall proteins, including those of exospore and endospore. So far the identified exospore proteins are restricted to two *Encephalitozoon* species: two spore wall proteins (SWP1 and SWP2) which are glycoproteins and have several conserved cysteines in *E. intestinalis* (Hayman *et al*., 2001) and one SWP1 in *E. cuniculi* (Bohne *et al*., 2000). They are cysteine-rich polypeptides with similar

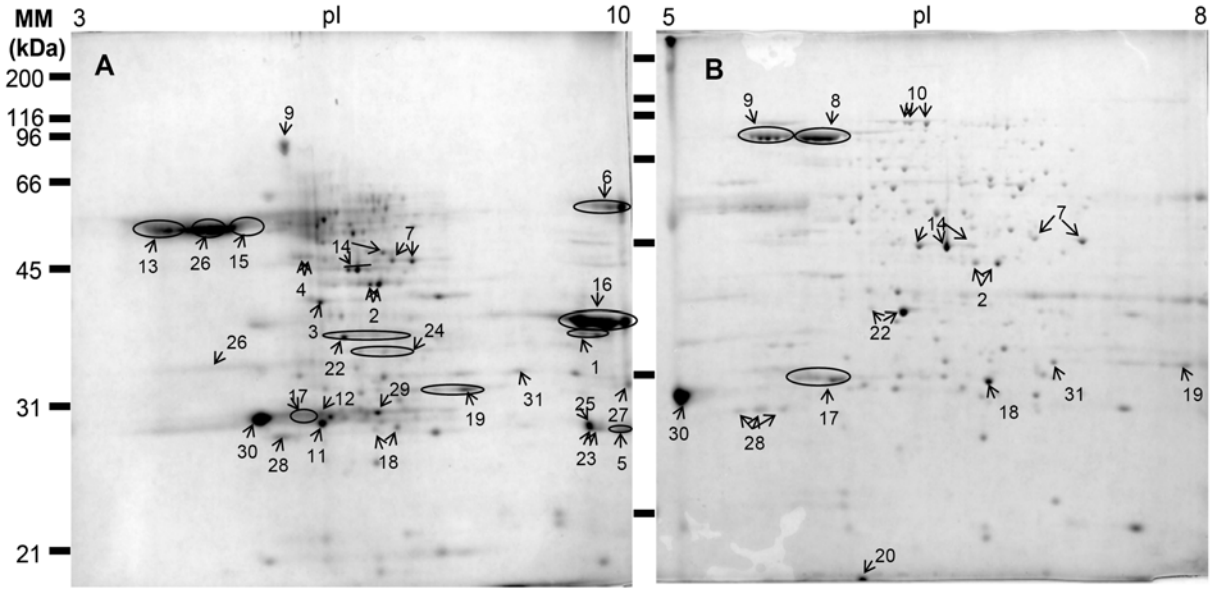

Figure 8. Two-dimensional electrophoresis maps of proteins from a spore-rich *E. cuniculi* fraction (Brosson *et al*., 2006). Isoelectric focusing was carried out using either a pH 3-10 (A) or a pH 5-8 (B) gradient. Numbers refer to abundant proteins in Table 8.

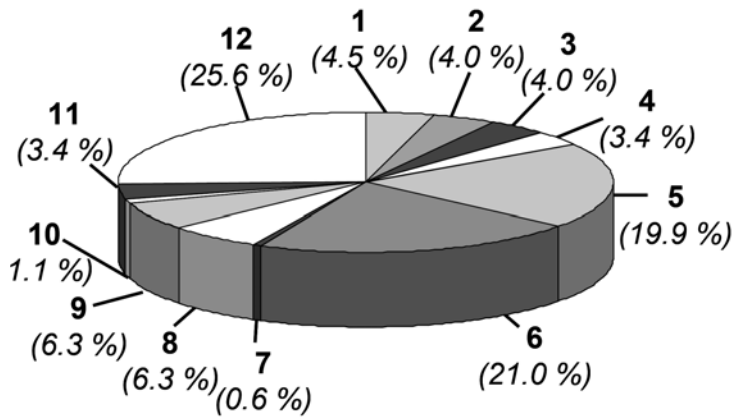

Figure 9. Functional distribution of 177 *E. cuniculi* proteins among 12 classes (Brosson *et al*., 2006)**.** Classes: 1, Metabolism; 2, Energy; 3, Cell growth, cell division and DNA synthesis; 4, Transcription; 5, Protein synthesis; 6, Protein destination; 7, Transport facilitation; 8, Intracellular transport; 9, Cellular organization and biogenesis; 10, Cellular communication, signal transduction; 11, Cell rescue, defence, cell death and ageing; 12, Unassigned function.

N-terminal domains and repeating amino acid units at their C-terminus. The onset of deposition of *E. cuniculi* exospore SWP1 correlated with the formation of lamellar protuberances during meront-to-sporont conversion and *swp1* mRNA was preferentially synthesized in early sporogony (Taupin *et al*., 2006). An alkaline-saline solubilized protein p40 in *P. grylli* has been localized to its exospore (Dolgikh *et al*., 2005). Recently four endospore proteins in *E. cuniculi* have been identified: a putative chitin deacetylase which has been localized at the endospore-plasmalemma interface (Brosson *et al*., 2005); EnP1 (40 kDa, cysteine-rich) which was detected early on the plasma membrane of meronts prior to extensive accumulation within the chitin-rich layer of sporoblasts, while *enp1* mRNA was transcribed during merogony and a large part of sporogony (Taupin *et al*., 2006); EnP2 (22 kDa; serine-rich) and SWP3 (< 20 kDa). EnP2 and SWP3 are predicted to be O-glycosylated and GPI-anchored (Peuvel *et al*., 2006; Xu *et al*., 2006). The high proportion of cysteine residues in these identified spore wall proteins suggests that the disulfide bridges may have a significant role in spore wall assembly.

Concommitant to more and more microsporidian genomics studies and genome projects, post-genomic studies of microsporidia such as proteomics begin to emerge. The large-scale analysis of proteins expressed at a particular time, offers an excellent way to characterize the microsporidian biology, the host-microsporidia interactions or the mechanism of host manipulation by parasite. But until recently, there are only a few reports of large scale protein analyses of microsporidia. The first two proteomic analysis of microsporidia based on the 2-DE (two-dimensional electrophoresis) gels have been used for the species discrimination of microsporidia and the study of host-microsporidia interaction without protein identification. To distinguish three insect-infecting microsporidia *Antonospora locustae*, *Nosema bombycis* and *Vairimorpha necatrix*, the 2-DE spore protein patterns after isoelectric focusing (IEF) and nonequilibrium isoelectric focusing (NIEF) were compared (Langley *et al*., 1987). Mourra and Visvesvara compared the 2-D protein profiles of purified *Encephalitozoon intestinalis* spores, infected host cell with *E. intestinalis* spores and unifected host cell. Of more than 200 protein spots, 95 were found to be immunogenic on the basis of their reactivity with a rabbit anti-*E. intestinalis* serum, some of these spots providing potential markers for either merogonial or sporogonial stages (Mourra and Visvesvara, 2001). In another study, whole spores and soluble

Table 8. Classification of highly abundant proteins identified in *Encephalitozoon cuniculi* (Brosson *et al*., 2006)**.**

Class function	Spot* Number	ORF Number	Protein function
1. Metabolism	1	ECU01_0970	aldose reductase
	2	ECU11_0870	ethanolamine phosphate cytidyltransferase
3. Cell growth, cell division and DNA synthesis	3	ECU09_1330	DNA replication factor C subunit
	4	ECU01_1370	septin-like protein
5. Protein synthesis	5	ECU09_1250	40S ribosomal protein S3
	6	ECU04_1100	translation elongation factor eEF1α
	7	ECU11_0530	tryptophanyl-tRNA synthetase
6. Protein destination	8	ECU03_0520	heat-shock protein, HSP70 family
	9	ECU02_0100	HS70 protein cognate 4 (HSC70)
	10	ECU01_1230	protein of the CDC48/PAS1/SEC28 family of ATPases (AAA)
	11	ECU01_1010	ubiquitin-conjugating E2 subunit
8. Intracellular transport	12	ECU05_0090	GTP binding protein, SAR-type, ARF family
9. Cellular organisation and biogenesis	13	ECU10_1660	spore wall protein 1 (SWP1)
	14	ECU01_0460	actin
	15	ECU06_0250	polar tube protein 1 (PTP1)
	16	ECU06_0240	polar tube protein 2 (PTP2)
10. Cellular communication / signal transduction	17	ECU04_1480	ZRP1
11. Cell rescue, defence, cell death and ageing	18	ECU05_1590 = ECU11_0140	3-methyl-adenine DNA glycosylase
	19	ECU02_0580	hydroxyacyl gluthatione hydrolase
	20	ECU01_0930	thioredoxin H-type
12. Unassigned role	21	ECU01_0820	cysteine-rich protein (endospore protein EnP1
	22	ECU07_0920	exonuclease-phosphatase family domain
	23	ECU08_1610	UPF0023 family (hypothetical proteins)
	24	ECU08_2020	member of a multigenic subtelomeric family / domain: ricin B lectin (QxW lectin repeat)
	25	ECU09_1470	possible RNA binding protein
	26	ECU11_0510	Possible chitin deacetylase
	27	ECU01_0420	
	28	ECU05_0510	
	29	ECU05_0590	
	30	ECU07_0400	
	31	ECU09_1820	

*, Spot numbers refer to Figure 8.

fractions of three *Encephalitozoon* species and *Brachiola algerae* were directly analyzed by MALDI-TOF-MS, providing species-specific markers within the molecular size range of 2~8 kDa (Moura *et al*., 2003).

More recently, the first sequenced *E. cuniculi* genome (2.9 Mbp) has been used for a descriptive proteomic study which combined a classical 2-DE approach followed by MALDI-TOF/MS and nanoLC-MS/MS and a high-throughput 2-DE free strategy (nanoLC-MS/MS) (Brosson *et al*., 2006). A reference 2-DE map of about 350 major spots with multiple isoforms was obtained for the first time in Microsporidia (**Figure 8** and **Table 8**), in which the identification of a large set of unique proteins (177) including proteins with unknown function gave the first global view of proteins expressed in late sporogony of the microsporidian parasite life cycle. Besides mainly eukaryotic housekeeping proteins, *E. cuniculi* proteins have been distributed into 12 functional classes in which two-third of these proteins account for only three classes: protein synthesis (19.9%), protein destination (21%) and unassigned function (25.6%) (**Figure 9**). Four classes (energy, protein synthesis, protein destination and cell defence) are over-represented in the proteome when compared to the genome. *E. cuniculi* protein subgroups are currently being characterized, including the phosphoproteins which might be invovled in several signal transduction pathways besides initiating polar tube extrusion, and the glycoproteins in which no N-linked glycans were detected and O-linked glycans have been demonstrated to be linear manno-oligosaccharides containing up to eight α1,2-linked mannose residues (Taupin *et al*., 2006).

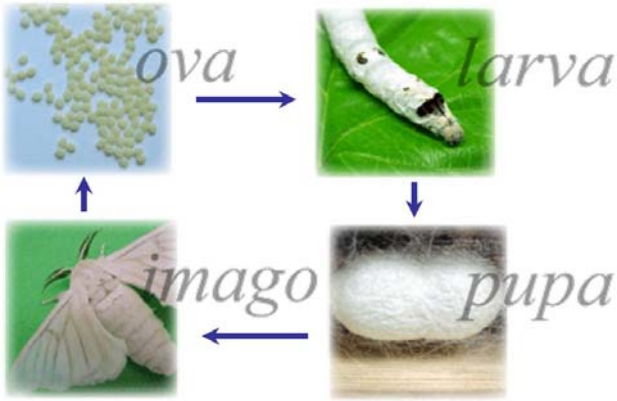

Figure 10. The four different developmental stages of *Bombyx mori*

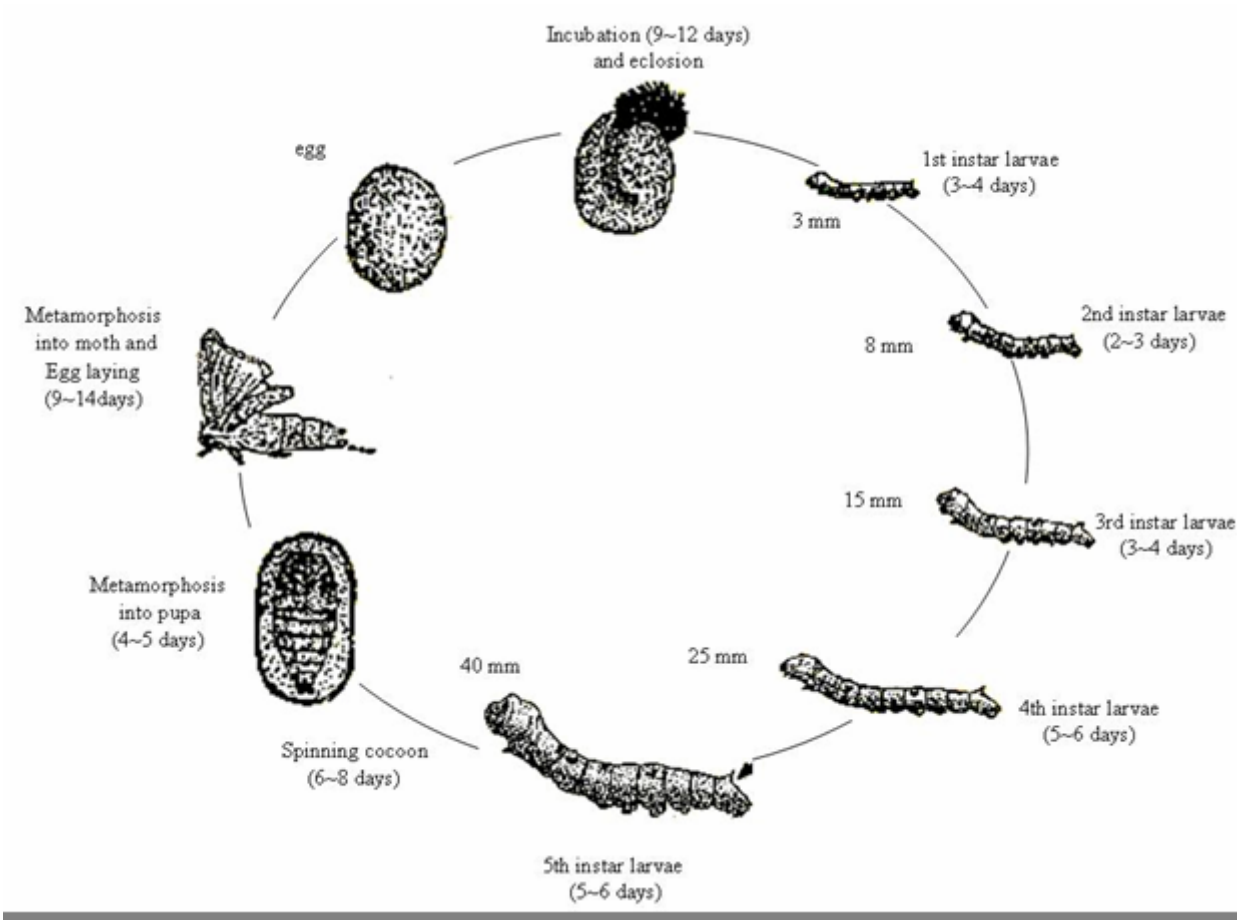

Figure 11. The life cycle of *Bombyx mori*

2. *Bombyx mori* (Arthropoda: *Lepidoptera*), an important economic insect

Archaeological evidence has suggested that sericulture began in the Middle to Lower Yangtze delta about 6,000 years ago, whereas *Bombyx mori* was domesticated from *Bombyx mandarina* inhabiting Central to Northern China (Kawarabata, 2003). The discovery of silk production from *B. mori* led that sericulture spread through China and silk became a precious commodity highly sought by other countries during the following centuries. In 139 B.C., the world longest highway "Silk Road" named after its most important commodity was opened, and stretched from Eastern China to the Mediterranean sea. The sericulture was introduced into western Asia and Europe in the 6th century A.D. and into North America in the 18th century and *B. mori* became an important economic insect for the silk industries in these conutries. But in 1845, the outbreak of pebrine or "pepper disease" that started in Italy and France, two leading countries in the sericulture in the early 19th century, nearly destroyed the silkworm industry of Europe. In 1857, the etiological agent of the pebrine, the first recognized microsporidium, was named *Nosema bombycis* by Nägeli (Nägeli, 1857). So far, pebrine caused by *N. bombycis* is still the most devastating mulberry silkworm disease and inflicts severe economic losses in the silkworm rearing industries for lack of efficient and thorough therapy.

2.1. Biology of the Lepidopteran *Bombyx mori*

The completely domesticated *Bombyx mori* (*Phalaena mori* Linnaeus, 1758, China) is classified in the Arthropoda phylum, Insecta class, *Lepidoptera* order, *Bombycidae* family and belongs to the complete metamorphosis insects. *B. mori* is essentially monophagous and the food needed for its larval stage is almost restricted to mulberry leaves (*Morus alba*). So far, the silkworm rearing techniques have been greatly improved. The duration of the developmental stages can be completely controlled throughout the life cycle and even the hatching day can be scheduled by applying artificial hatching treatment such as changing the incubation temperature in combination with cold storage. The hatching timings and synchronization can also be controlled by photoperiodic cycles and illumination (Yu *et al*., 1994).

With this easiness of handling, the introduction of artifical diets and the development of

Table 9. The structure of *Bombyx mori* larva

	Head	Thorax	Abdomen
segments	two sets of 6 ocelli; antenna; mouth and spinneret	3	11
spiracles (pair)		1	8
legs (pair)		3 (thoracic legs)	4 (abdominal legs) 1 (caudal legs)
other			one caudal horn

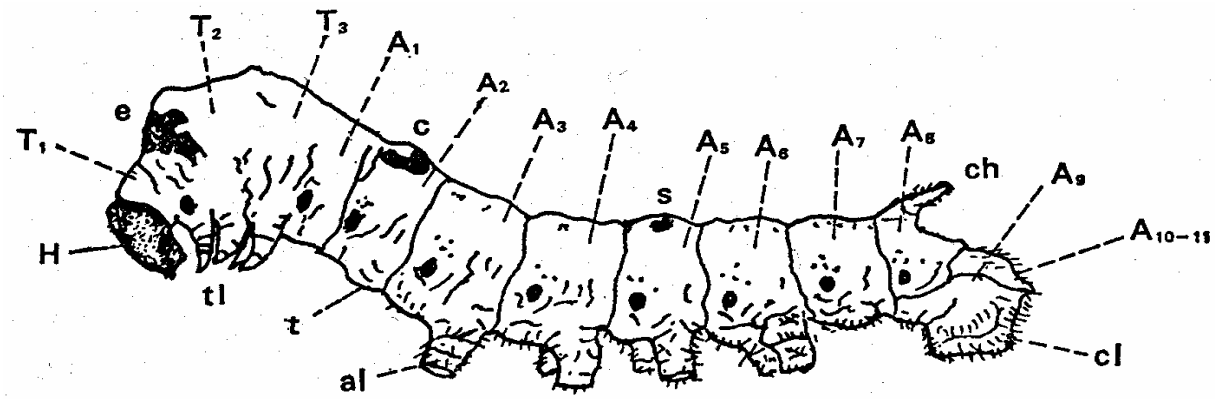

Figure 12. The fifth instar larva of *Bombyx mori*. H, head; T1~3, thoracic segments; A1~11, abdominal segments; e, eye spots; c, crescents; s, star spots; ch, caudal horn; cl, caudal legs; al, abdominal legs; t, spiracles; tl, thoracic legs.

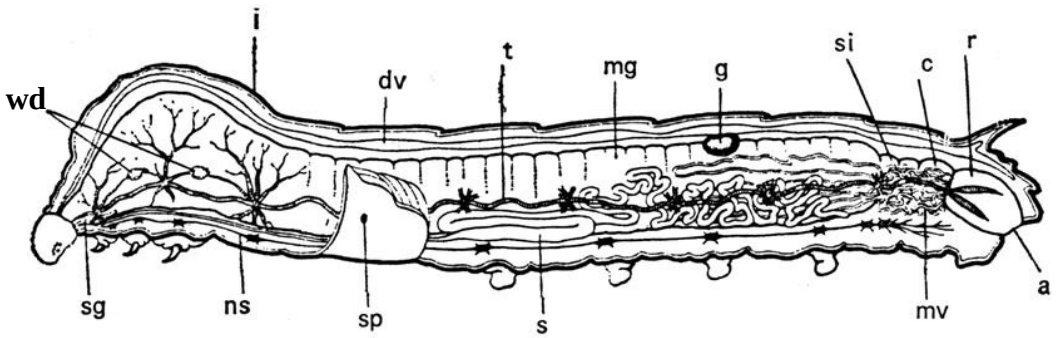

Figure 13. Internal structure of the 5th instar *Bombyx mori* larva. a, anus; c, colon; dv, dorsal vessel; g, gonad; i, integument; mg, mid-gut; mv, Malpighian vessel; ns, nervous system; r, rectum; si, small intestine; sg, salivary gland; s, silk gland; sp, spiracle; t, trachea; wd, wing disc.

the molecular linkage maps, EST databases, a draft genome sequence, transgenic transformation and RNAi technologies, *B. mori* has been increasingly used as an experimental model for basic insect science, a “bioreactor” for proteinaceous drugs and a source of biomaterials (Goldsmith *et al*., 2005; Tomita *et al*., 2003). And importantly, *B. mori* reasonable size, easy injection of microbial pathogen, conveniency for studies of drug pharmacodynamics, increasing knowledge about its innate immunity, commercial availability and the possibility of genetic modification by germiline transformation made it a promising insect model for the host-pathogen interactions as *Drosophilia melanogaster* and *Caenorhabditis elegans* (Kaito *et al*., 2002; Garcia-Lara *et al*., 2005; Mylonakis and Aballay, 2005; Taniai *et al*., 2006)

The life cycle of *B. mori* demonstrates the most advanced form of metamorphosis. Termed holometabolous, the serial progressions of four different metamorphosing stages of development in about 50 days complete one generation of *B. mori*: egg, larva, pupa and adult (moth). Of this life cycle, about half is the larval stage (**Figure 10** and **11**)

The eggs of *B. mori* are very small and hard structures with the size of a pin head and resembling a poppy seed. The egg shell provides a protective covering for embryonic development. When first laid, an egg is light yellow. Fertile eggs darken to a blue-gray within a few days. The larva is the vegetative stage where growth takes place. The larva constitutes the only feeding stage in silkworms. During growth, the larva will molt 4 times. The period between successive molts is called an instar. The *B. mori* larvae are divided into three parts: head, thorax and abdomen (**Figure 12** and **13**; **Table 9**). After a final molt inside the cocoon formed by a single, continuous thread (300~1,500 m in length) of the protein complex secreted from salivary glands, the larva develops into the brown, chitin covered structure called the pupa. Metamorphic changes of the pupa result in an emerging moth which is flightless and lack functional mouth part. It is the reproductive stage where adults mate and females lay 200~500 lemon-yellow eggs. Then the adults die within five days.

2.2. Genetic, genomics studies and genetic engineering of *Bombyx mori*

Extensive genetic studies have been carried out with *B. mori*. Rapid progress has been made in the past 10 years in applying molecular and genomic technologies to *B. mori*.

Table 10. The number of *Bombyx mori* strains in different stock centers

Country	*Bombyx mori* strains	Stock center
China	~600	Southwest Agricultural University, Chongqing
	~1000	Institute of Sericultural Research, Chinese Academy of Agricultural Sciences, Zhenjiang,
Japan	>400	Kyushu University
	>450	National Institute of Agrobiological Sciences
Korea	>300	Rural Development Administration, Suwon

2.2.1. Genetic studies

The wealth of silkworm strains (spontaneous ones, genetically improved strains, irradiation and chemical mutagenesis-induced) and inbred lines (such as geographic "races", e.g., Chinese, Japanese, Korean, European, Tropical) makes *B. mori* a unique experimental model for genetic study of insect. More than 400 Mendelian strains have been described (**Table 10**).

Classical and molecular linkage maps: The classical linkage maps for *B. mori* consist of ~240 visible and biochemical markers on 28 linkage groups, with a recombination length of ~900 cM (Fujii, 1998; Lu *et al*., 2001). Marker density per linkage group varies from 1~3 (for 5 linkage groups) to ~20, with an average of 8 markers. Initial molecular linkage maps were of low-to-medium density and composed of anonymous markers genotyped by PCR [RAPDs, 169 markers; (Promboon *et al*., 1995)] or cDNAs and known genes characterized as RFLPs [61 markers; (Shi *et al*., 1995)]. More complete maps followed, composed of RAPDs [1018 markers; (Yasukochi, 1998)], AFLPs, [356 markers; (Tan *et al*., 2001)], integrated RAPDs and SADFs [544 markers; (He *et al*., 2001)], and RFLPs based on ESTs [~200 markers; (Kadono-Okuda *et al*., 2002)]. Maps with microsatellites, several hundred of which are polymorphic in many strains, have been developed (Reddy *et al*., 1999; Nagaraju and Goldsmith, 2002). Molecular markers that are tightly linked to economically important traits have been mapped, including refractoriness to densonucleosis virus (DNV), a serious pathogen in sericulture (Li *et al*., 2001 and 2006), NPV, a potentially devastating pathogen (Yao *et al*., 2003) and resistance to high fluoride levels encountered on mulberry leaves (Chen *et al*., 2003).

B. mori EST databases**:** ESTs are powerful tools used to find genes, annotate large-scale genome sequencing projects, and perform comparative genomics. Currently more than 110,000 silkworm ESTs from independent projects are available in SilkBase which covers >55% of all genes of *Bombyx* and contains 11,000 nonredundant ESTs with the average length of 1.25 kb (http://papilio.ab.a.u-tokyo.ac.jp/silkbase/index.html) (National Institute for Agrobiological Sciences in Tsukuba, Japan; Mita *et al*., 2003) and Silkworm Knowledgebase (SilkDB) (http://silkworm.genomics.org.cn). SilkDB provides an integrated representation of the large-scale, genome-wide sequence assembly, cDNAs, clusters of expressed sequence tags (ESTs), transposable elements (TEs), mutants, single nucleotide polymorphisms (SNPs) and

functional annotations of genes with assignments to InterPro domains and Gene Ontology (GO) terms (Southwest Agricultural University in Chongqing, China; Wang *et al*., 2005). A precise analysis of the SilkBase EST database revealed Lepidoptera-specific genes (Hara and Yamakawa, 1995a, b). The horizontal gene transfers between lepidopterans and bacteria or between lepidopterans and baculovirus have been confirmed by the analysis of *B. mori* EST and WGS (Whole-Genome Shotgun sequences) (Huang *et al*., 2001; Luque *et al*., 2002; Mita *et al*., 2003)

2.2.2. Genomic studies

The haploid genome size of *B. mori* is 428.7 Mb , which is respectively 2.4 and 1.53 times larger than that of fruitfly *Drosophilia melanogaster* (175 Mbp) and mosquito *Anopheles gambiae* (280 Mbp) and the estimated gene count is 18,510, which exceeds the 13,379 genes reported for *Drosophila melanogaster* (Xia *et al*., 2004). The most prominent feature of the *B. mori* genome is the abundance of transposable elements that are frequently truncated to fragments (Mita *et al*., 2004). There are a greater number of introns in genes than in *D. melanogaste*r and the introns of *B. mori* genes are also longer than their orthologs in *Drosophila* (Komoto *et al*., 1999; Goldsmith *et al*., 2005).

2.2.3. Genetic engineering

Germline transformation and transient expression technologies have been used in *B. mori* for its functional studies, to produce specialized silks (Mori and Tsukada, 2000) or value-added products such as human therapeutic proteins (Tomita *et al*., 2003), or to improve the silkworm by enhancing features such as productivity and pathogen resistance needed for its traditional role in sericulture.

Vectors derived from the transposable element *piggyBac*, originally discovered in the lepidopteran *Trichoplusia ni*, allowed the first, and surprisingly efficient germline transformation of *B. mori* by a transposon-based method (Tamura *et al*., 2000). The drawback of the earliest promoter *BmA3 (B. mori* cytoplasmic actin promoter) was eliminated by using the artificial eye- and nervous system-specific 3×P3 promoter (Horn *et al*., 2002; Horn and Wimmer, 2000;

Table 11. The development of *Bombyx mori* germline transformation

Vector	Introduction method	Promoter	Reporter	Description and transformation efficiency
piggyBac	egg injection (preblastoderm embryos; with a helper plasmid)	*BmA3*	EGFP	*piggyBac* transposase gene was carried on a separate helper plasmid; 0.7~3.9% (Tamura *et al*., 2000)
		artificial 3×P3 promoter	EGFP	easily screen the transgenic individuals at embryonic stages and evaluate the frequency of transgenesis; 0.08% (Thomas *et al*., 2002)
			DsRed	rapidly distinguish transgenic from wild–type worms through all development stages except the early embryonic stages; 18.3~27.6% (Tomita *et al*., 2003)
		hsp70 promoter	EGFP	the first system for conditional control of transgene expression; 1.7% (Uhlirova *et al*., 2002)
		Fib-L promoter	EGFP	the recombinant protein expressed at high level; 18.3~27.6% (Tomita *et al*., 2003)
AcNPV	larvae injection or *per os*	*Fib-L* promoter	GFP	AcNPV was converted into a gene-targeting (homologous recombination) vector by replacing the viral polyhedrin gene with a full-length chimeric Fib-L gene carrying GFP in place of exon 7; 0.16% (Yamao *et al*., 1999)

BmA3, *Bombyx mori* cytoplasmic actin gene; EGFP, enhanced green fluorescent protein; 3×P3, three tandem copies of the binding sites for the well conserved eye- and nervous system-specific transcription factor, PAX-6; *DsRed*, the gene for red fluorescent protein; *hsp70*, the gene for heat shock protein 70; AcNPV, *Autographa californica* nuclear polyhedrosis virus; GFP, green fluorescent protein; *Fib-L*, the gene for fibrion light chain.

Thomas *et al*., 2002). An inducible *Drosophila* heat shock 70 (*hsp70*) promoter was used to establish the first conditional control system of transgene expression in *B. mori* (Uhlirova *et al*., 2002). This system opens up possibilities for many functional studies, such as controlled ectopic or misexpression of regulatory proteins involved in development and introduction of dominant-negative mutations, conditional knockouts, or knock-downs via antisense or double-stranded siRNA constructs (Goldsmith *et al*., 2005). Owing to an improved egg injection method and the improvement of vectors, transformation efficiencies have been ranged up to 27.6% from the earliest 0.7% (**Table 11**). *B. mori* germline transformation was first used successfully to synthesize a value-added product, collagen, which is used in many medical applications, including tissue engineering and drug delivery materials, by modifying a *piggy-Bac*3×P3 vector to carry a chimeric gene with a procollagen III minichain sequence inserted between the coding sequences for *Fib-L* and EGFP, under control of posterior silk gland-specific *Fib-L* promoter elements (Tomita *et al*., 2003).

Sindbis virus is a single-stranded enveloped RNA virus (family Togaviridae, genus Alphavirus). The Sindbis replication cycle results in dsRNA and offers the possibility to knock down expression of specific genes through RNAi. RNAi and Sindbis-mediated RNAi have been also used as an important new tool for uncovering gene function in the silkworm (Pierro *et al*., 2003; Quan *et al*., 2002; Uhlirova *et al*., 2003).

2.3. Proteomic studies of *Bombyx mori*

Compared to the extensive genomic studies of *B. mori*, its proteomic analyses emerged only a few years ago. The earliest large scale proteomic study by 2-DE and MALDI-TOF has been used to analysis the innate immunity of the 5^{th} instar larvae injected with lipopolysaccharide (LPS) from *Escherichia coli* (Wang *et al*., 2004). The changes of inducible polypeptides (antibacterial peptides) in the hemolymph, fat body and midgut were examined within a pI range of 3~10 and a size range of 14~97 kDa. Besides the novel polypeptides, LPS was confirmed to induce attacin, an immune polypeptide active against Gram-negative bacteria, in *B. mori* hemolymph. The amounts of all induced polypeptides decreased at 48h after the injection. More recently, the large scale analysis of up-regulated proteins in the hemolymph of *B.*

Table 12. The infectious diseases of *Bombyx mori*

Disease	Name of disease	Pathogens
viral disease	nuclear polyhedrosis	BmNPV: *B. mori* nuclear polyhedrosis virus
	cytoplasmic polyhedrosis	BmCPV: *B. mori* cytoplasmic polyhedrosis virus
	flacherie virus	FV: Flacherie Virus
	densovirus disease	DNV: Densovirus
bacterial disease	septicemia	*Serratia; Enterocbactec; Bacillus; Aeromonas*
	sotto disease	*Bacillus thuringiensis*
	bacterial gastroenteric disease	*Streptococcus; Staphylococcus ;Pseudomonas*
fungal disease	white muscardine	*Beauveria bassiana Vuillemin*
	yellow muscardine	*Beauveria bassiana* (Balsama) *Vuillemin*
	green muscardine	*Nomuraea prasina*
	aspergillosis	*Aspergillus flavus* Liuk; *A. parasiticus Speare*
	grey muscardine	*Spicaria* sp.
	black muscardine	*Oospora destructer Delacroix*
	(purplish) red muscardine	*Isaria fumoso - rosea* (Casimir) *Wize*
	fusarum disease	*Fusarum semifeotum*
	yeast disease	*Rhodotoruca* sp.
protozoonoses	pebrine disease	*Nosema bombycis* and other microsporidia
	trypanosemiasis	*Trypanosoma*
	coccidiosis; amoebiasis	Coccidia; Amoebae

mori larvae immunized with heat-inactivated bacteria (*Bacillus megaterium*) were realized by 2-DE and Q-TOF MS/MS (Song *et al*., 2006). After the bacterial injection, more than 30 spots were up-regulated and 11 spots were down-regulated. The heat shock 70 kDa protein cognate was one of the up-regulated hemocytic proteins, while peptidoglycan recognition protein, antichymotrypsin (ACT) precursor [a member of the serine protease inhibitor (serpin) family], and four gloverin-like protein were newly synthesized in the plasma. Antennal binding protein 7 [ABP7, insect odorant binding protein (OBP) family] was up-regulated in the plasma.

Zhang *et al* (2005) analysed the isoforms of P25 component of *B. mori* fibroin which is composed of the heavy chain, light chain and P25 glycoprotein (fibrohexamerin) in the form of [(H-L)6-P25] complex. Four of the eight isoforms were identified as *Bombyx mandarina* (the ancestor of *B. mori*) P25s. Further analysis indicated that this diversity of P25 isoforms depends on phosphorylation modification in addition to glycosylation. Recently, more than 700 protein spots were resolved in different developmental stages (pupa and moth) from the secretory region of *B. mori* colleterial glands and most of the proteins were distributed in the mass range from 30 to 70 kDa with pH 4~8 (Jin *et al*., 2006). Three proteins (two proteins are cytosolic actins and one is not identified) were found only expressed in the later pupa stage/moth stage and not expressed in the Ng (No glue) mutant in which female moth secreted only very little glue-like substance and laid loose eggs naturally. Results indicated that actins participated or regulated the exocytosis of colleterial gland and might be related to colleterial gland development or the secretion of a glue-like substance. Proteome analysis of silk gland proteins from *B. mori* indicated that they can be categorized into groups involved in silk protein secretion, transport, lipid metabolism and defense (Zhang *et al*., 2006).

2.4. The contagious, inherited and fatal pebrine disease of *Bombyx mori*

B. mori suffers from a number of diseases involving viral, bacterial, fungal and protozoan agents (**Table 12**). The pebrine disease of *B. mori* is caused by the first recognized microsporidium *Nosema bombycis*. The infection of *B. mori* by *Nosema bombycis* is systemic. Most tissues such as the inner cuticle, fat body, trachea, midgut, silk gland, Malphighian tubules, nervous system, gonad and dorsal vessel can be infected except the external cuticle, spiral

Table 13. Typical symptoms of *Bombyx mori* pebrine disease

Stage	Typical symptoms
egg	irregular form, size and arrangement; piled eggs; unfertilized and dead eggs increase
larva	early instars: stunted, small and thin, dark in color; die in the 1st~3rd instars
	late instars: 1. the typical larvae: “the shrinked newly-hatched larva with the color of rust” “the demi-molted or non-molted larva” “non-spining larvae or spinning irregular form cocoon, thin cocoon” 2. the typical external symptoms: covered by brownish or dark irregular dots, spots or blotches (“pepper”) loss of appetite, sluggish, weak, dull in color inactiveness and lethargic condition, show unequal and irregular growth; extended development period silk gland weight and silk production declined significantly dead larvae: soft, shrinked and non-decayed 3. the typical internal symptoms: silkgland: small milkwhite spots ↓ irregular white blotches ↓ irregular zebra crossings in appearance (milk white/ transparent wall) ↓ milkwhite and fragile silkgland Malphigian tubules: dark spots or section midgut: dark spots or blotches wrapped in irregular snowflake-like white focus
pupa	“naked pupa”; lacklustre skin; loose abdomen; irregular dark spots or blotches on the cuticle; dead in cocoon or late-eclosion pupa; cocoons are not uniform
moth	“ large-abdomen moth”, “bare moth”; elongated corp, crouched wing, dark blotches or blain on the wing; reduction in ovary weight, fecundity and fertility; egg chorionation was affected; emergence of moths is very irregular; infected female moths lay few eggs

filament of trachea, inner wall of the fore- and hind-gut, the cutinized parts like mouthparts (Yu *et al*., 1994).

2.4.1. Typical symptoms and diagnosis

The typical symptoms of pebrine disease in the different developmental stages of *B. mori* are summarized in **Table 13**. For the early diagnosis of pebrine disease, the larvae with the external symptoms (stunted, sluggish, demi-molted or non-molted, shrinked and rusty newly-hatched, *etc*) listed in **Table 13**. can be immediately inspected by microscope. The dark spots or blotches covered on the cuticle or around the spiracles and the milkwhite blotches in the silkgland wall are evidences for pebrine disease.

2.4.2. How to obtain healthy larvae?

In 1870, Louis Pasteur recorded that *Nosema bombycis* can be transmitted transovarially and demonstrated that the pebrine disease can be prevented and controlled through simple microscopic examination of adult moths, which led to the establishment of “whole mother-moth microscopic inspection”. This method is still the most reliable way practised in world-wide grainages (egg producing centres) to eliminate pebrinised layings (transovarial transmission). Often the whole homogenate of egg-laying female moths are examined. The whole batch of eggs laid by female moths infected by *N. bombycis* should be burned. Only the eggs from uninfected female moths are used. Patil *et al* (2002) studied the role of male moths of *B. mori* in the spread of *N. bombycis* and showed that this “whole mother-moth examination” does not discriminate between transovarial transmission and venereal transfer leading to the development “wing and wing base examination” to eliminate losses due to false positives. For the horizontal transmission, spores adhering to the surface of the eggs can be destroyed by treating the eggs with some disinfectant such as sodium hypochlorite. Different sterilization methods and drugs treatment such as albendazole (Costa and Weiss, 2000) are also necessary for the prevention and control of pebrine disease.

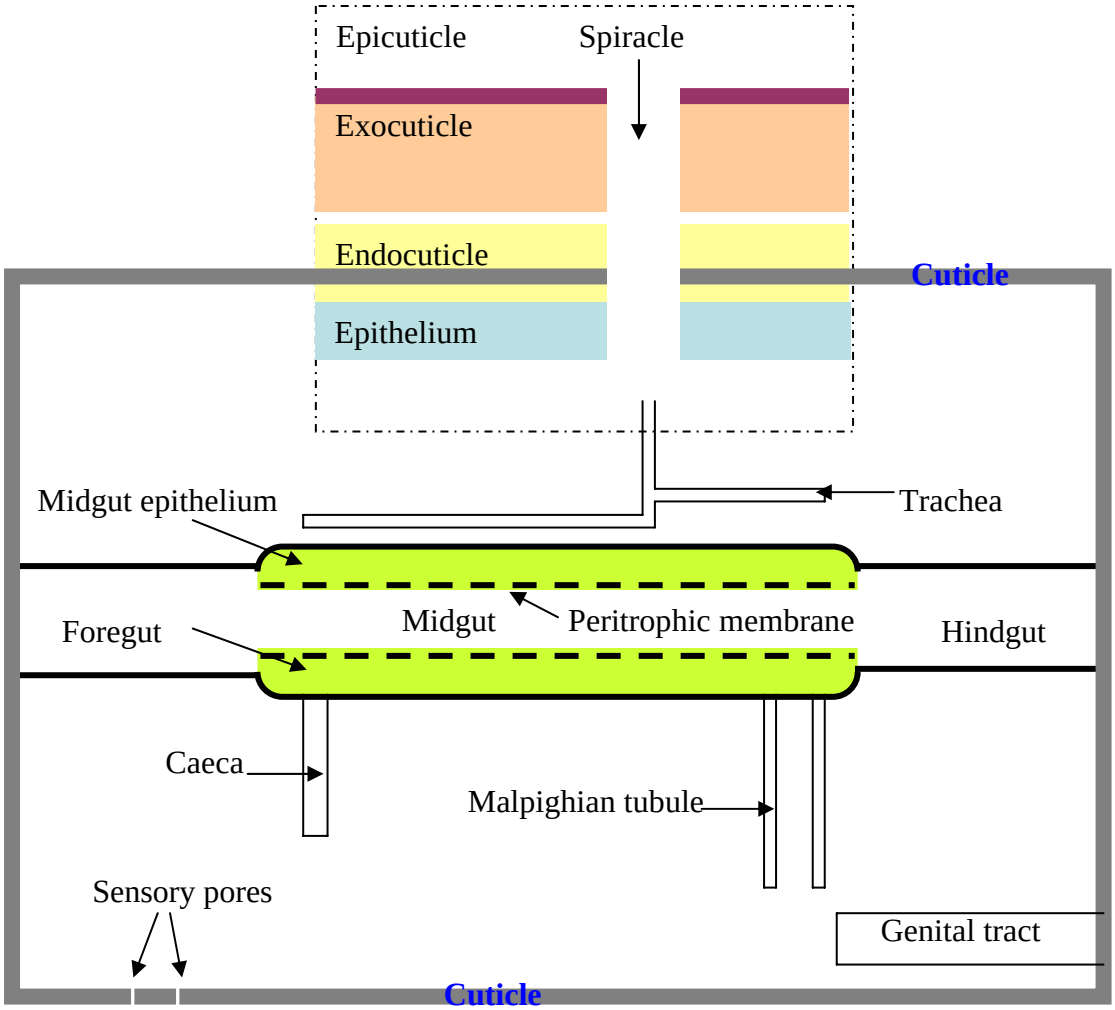

Figure 14. A schematic figure of the first-line barrier defenses of insect, showing the regions where the invasion is likely (Siva-Jothy *et al*., 2005). These regions mainly include insect cuticle, intestin, trachea, Malpighian tubules and genital tract. The dotted box reveals detail within the integument.

3. Insect-parasite interactions

The insect-parasite relationship can be a coexistence that is harmless to the microbe and insect (commensalism, for example, bacteria *Wolbachia* and their host wasp *Trichogramma dendrolimi*: bacteria manipulate the reproduction of their host and wasp provide the nutritions for bacteria), a mutual benefit to both the insect and the microbe (mutualism, for example, the caterpillars such as *Lycaenidae* butterflies need ants to transport their newly emerged larvae to the host plants and attend the older larvae sheltered under nearby rocks and stones, and ants feed on copious secretions of liquid from the caterpillar honeyglands), or a benefit to the microbe at the expense of the insect (parasitism). Parasitism is carried out by viruses, bacteria, protozoa (these usually being endoparasitic), and various metazoan groups (multicellular eukaryotic animals). In "insect parasitism", the benefiting parasite is referred to as a pathogen and the host (insect) is harmed or damaged in some manner. The damage to insect may result from pathogen-encoded structures or products and/or the insect's response to the infection (Sadd and Siva-Jothy, 2006). The insect innate immune system and immune response to the pathogen infection, *Anopheles-Plasmodium* and insect-microsporidia interactions are the main subjects discussed here.

3.1. Insect innate defense system against pathogens

Insects possess a complex and efficient system of biological defense against pathogens. Unlike vertebrates, insects do not have an acquired immune system. They solely depend on "innate immunity", which refers to a variety of physical, cellular, and molecular features that provide the first lines of defense against infections (Govind and Nehm, 2004). Insect innate defense system is comprised of three lines of defense to avoid infection: (1) the physical barriers such as exoskeleton and epithelial barriers to infection, (2) the cellular immune responses: which are coordinated responses of several subpopulations of hemocytes that occur when their physical barriers are breached, and (3) the humoral immune responses such as the induced synthesis of antimicrobial peptides and proteins. The insect innate immune system plays an important role in

Table 14. The epithelial and tissue distribution of antimicrobial peptides (AMPs) in fruit fly (data from Bulet *et al*., 2003)

Tissue	AMP
epidermis	cecropin
digestive tract	metchnikowin, diptericin, drosocin, attacin
respiratory tract	drosomycin, drosocin
Malpighian tubules	cecropin, metchnikowin
salivary glands	drosomycin
genital tracts	metchnikowin, attacin
labellar glands	defensin, metchnikowin
seminal receptacle and spermatheca	drosomycin, defensin

self-integrity, discrimination of self from not-self and clearance of foreign pathogens.

3.1.1. Insect first-line defense barriers: cuticle, chitin-included barriers and epithelial cells

The first line of insect innate defense against the majority of pathogens is the physical barriers between the internal and external environment (**Figure 14**).

The insect cuticle, analogous to the skin in mammals, is an important line of defence to provide an effective physical and chemical complex barrier designed to prevent or retard the entry of pathogens into the hemocoele (the body cavity) (Clarkson *et al*., 1998). The outer layer of the cuticle (the epicuticle) is covered in a waxy layer containing lipids, fatty acids and sterols, which may display anti-microbial properties by its mechanical resistance to penetration, its resistance to degradation by many pathogen enzymes, and its impermeability to pathogen secretions. The inner cuticle is thought to consist of polymerized lipoprotein stabilized by quinines which implies toughness (Hajek and Leger *et al*., 1994).

Besides insect chitin exoskeletons (cuticle), the chitinous lining of the trachea system, the chitinous peritrophic membrane (PM) lining the midgut composed the important chitin-included barriers in which chitin and its polymers are common components providing a structured shield against the intruders (Levashina, 2004). The binding of a multidomain serine protease to the chitin of the trachea or cuticle has been showed to induce effective insect immue reponses (Gorman *et al*., 2000).

Another class of physical barriers is the epithelial barriers such as epithelial cells of the midgut, trachea, genital tract and Malpighian tubules which can constitutively or inducibly produce antimicrobial peptides in a tissue-specific manner (local response, **Table 14**) (Ferrandon *et al*., 1998; Tzou *et al*., 2000; Hoffmann, 2003; Govind and Nehm, 2004). In *Bombyx mori* silkworm larva, cecropin mRNA is induced in the epithelial cells underlying the cuticle when it is lightly abraded in the presence of live bacteria (Brey *et al*., 1993).

Additionally, the midgut of most insects is maintained at a hostile acid pH which inhibits the growth of most bacteria and incorporates a peritrophic membrane to keep microbes that enter

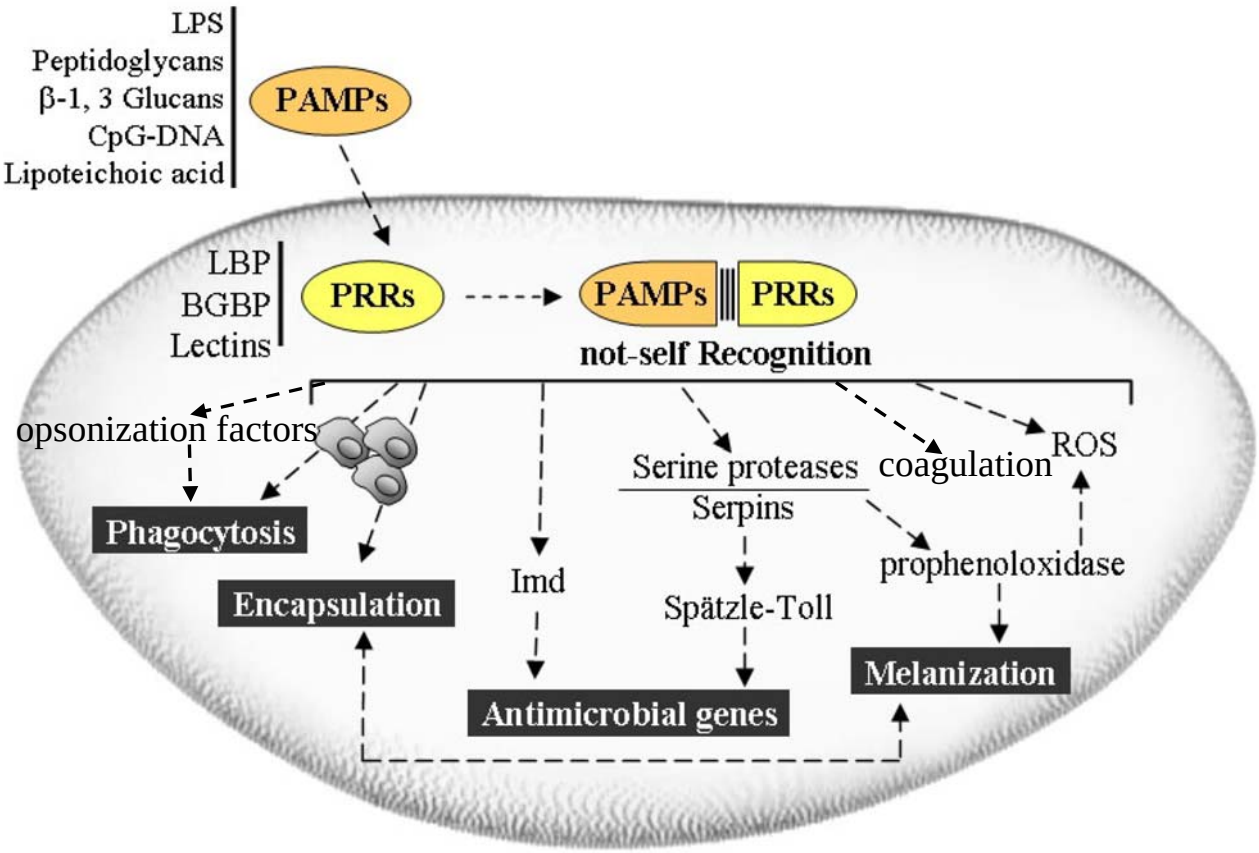

Figure 15. PAMPs-PRRs interactions during in insect "non-self" recognition and insect typical immune defense responses (Brivio *et al.*, 2005). 1. PAMPs-PRRs interactions: Perceiving of not-self in insect seems to be modulated by the presence of PAMPs (pathogen-associated molecular patterns) which interact with free or membrane-bound receptors called PRRs (pattern-recognizing receptors). These interactions lead to the activation of different cell-mediated and humoral effector immune processes. 2. Insect cellular immune responses: phagocytosis, nodule formation and encapsulation. 3. Insect humoral immune responses: the synthesis of antimicrobial peptides, activation of the prophenoloxidase system and melanization, opsonization, the generation of reactive intermediates of oxygen (ROIs) or nitrogen (RNIs) and other inducible immune-related proteins. These two immune systems cooperatively function in clearance of invading pathogens from insect hemolymph. LPS, lipopolysaccharide; BGBP or βGBP, β-1,3-glucan-binding protein; ROS, reactive oxygen species.

the digestive tract with food from entering the hemocoele through the gut wall.

3.1.2. Insect humoral and cellular immune responses in hemocoele

Once the first-line physical barriers are breached and pathogens enter the insect hemocoele, insect can recognize these "non-self" infectious pathogens by PAMPs-PRRs interactions (see the following "3.1.2.1. section") which can activate complex and effective humoral and cellular immune responses to the invaders (Lavine and Strand, 2002; Kanost *et al.*, 2004). In insect, the synthesis of antimicrobial peptides (Bulet *et al*., 1999; Hetru *et al*., 2003) and activation of the prophenoloxidase system (Ashida and Brey, 1998; Cerenius and Söderhäll, 2004) are important humoral immune responses, whereas hemocytes participate in insect cellular immune responses such as phagocytosis, nodule formation, and encapsulation (Lavine and Strand, 2002). These two immune systems cooperatively or overlappingly (in hemolymph clotting, see 3.1.2.4.) function in clearance of invading pathogens from insect hemolymph (**Figure 15**).

3.1.2.1. Recognition of "non-self" and PAMPs-PRRs interactions

Insects lack finely tuned immunorecognition receptors but they recognize non-self infectious pathogens through a series of humoral and cellular pattern recognition receptors (PRRs) (Janeway and Medzhitov, 2002). PRRs are conserved receptors encoded by germ line cells (Janeway, 1992; Hoffmann *et al*., 1999). Insect PRRs such as lipopolysaccharides and β-1,3-glucan-binding protein (LGBP), β-1,3-glucan-binding protein (βGBP), and peptidoglycan (PGN) binding protein (PGBP) specifically recognize microbial structurally conserved pathogen-associated molecular patterns (PAMPs) such as lipopolysaccharides, peptidoglycan and β-1,3-glucan, which are cell wall components of Gram-negative, Gram-positive bacteria and fungi respectively (Medzhitov and Janeway, 2002; Dimopoulos, 2003). The earliest described insect PRRs are *B. mori* PGBP and βGBP which provide the first evidence for specific PRRs mediating an immune reponse in any organism (Williams, 2001).

PAMPs-PRRs interactions in insect is a key process among the discriminatory steps of insect innate immunity that usually precede the defensive humoral and cellular responses

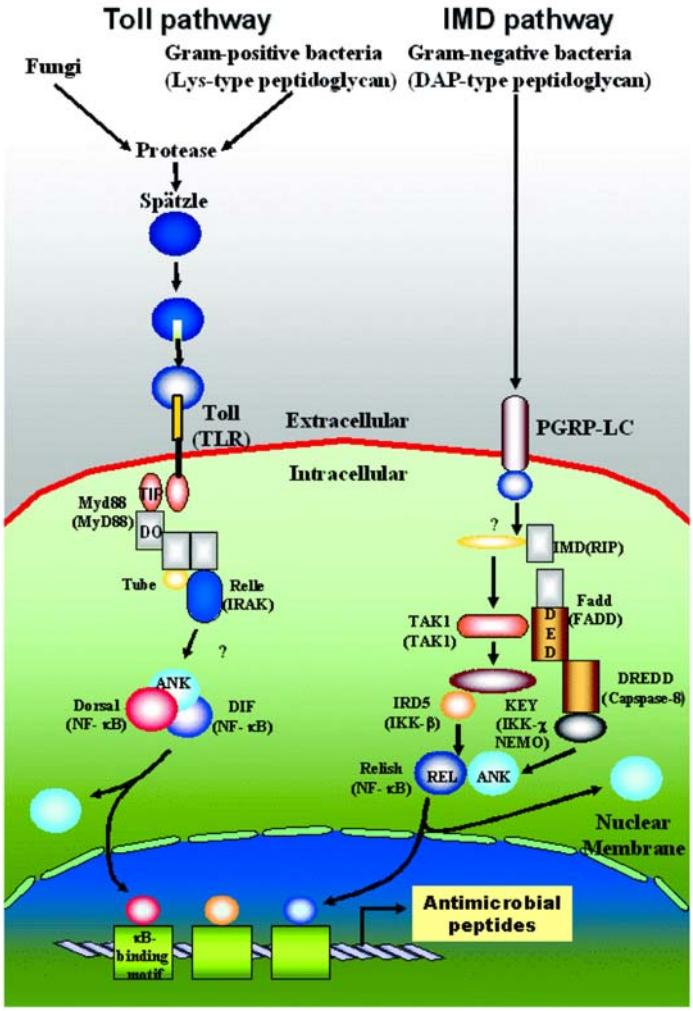

Figure 16. The Toll and IMD pathways involved in Drosophila immunity (Iwanaga and Lee, 2005). 1.Toll pathway: Toll pathway is activated mainly by fungi and Gram-positive bacteria. Toll activation leads to intracellular signaling via cytoplasmic proteins Tube and Pelle, leading to the degradation of Cactus and nuclear localization of NF-κB proteins Dorsal and Dif. These transcription factors bind to promoters of target genes, such as drosomycin, activating their transcription. 2. IMD pathways: The immune deficiency (IMD) pathway is activated mainly by Gram-negative bacteria. The NF-κB protein for the Imd pathway, Relish, activates diptericin transcription.

responsible for the elimination of not self (Medzhitov, 2001; Kanost *et al*., 2004; Brivio *et al*., 2005) (**Figure 15**). It can immediately trigger the activation of the important prophenoloxidase (proPO) cascade (for details, see the following "3.1.2.2.3. section") and the synthesis of antimicrobial peptides (Gillespie *et al*., 1997). On insects hemocytes, cell receptors involved in Toll and IMD pathways (**Figure 16**) activation can be considered as the main PRRs involved in cellular PAMPs sensing leading to antimicrobial peptides (AMPs) synthesis (De Gregorio *et al*, 2002). Surface molecules present on Gram-positive bacteria and fungi are PAMPs recognized by the receptors "Toll", which results in the NF-κB-like transcription factors Dorsal and Dif being translocated to induce the expression of the antimicrobial peptide drosomycin. The binding of Gram-negative bacteria PGN to PGN recognition protein-LC (PGRP-LC) activates the IMD pathway which results in the nuclear translocation of Relish (an NF-κB-like transcription factor), and the induction of antimicrobial peptides (AMPs) such as cecropin, drosocin, defensin and diptericin (Hoffmann and Reichhart, 2002; Meister *et al*., 2005).

3.1.2.2. Insect humoral defenses

Insect humoral defenses include the production of antimicrobial peptides (Meister *et al*., 1997; Bulet *et al*., 2005), the generation of reactive intermediates of oxygen (ROIs) or nitrogen (RNIs) (Nappi and Vass, 2001), the activation of proteolytic cascades such as insect proPO-activating systems that lead to localized melanization reactions (Nappi and Christensen, 2005), the induction of lectin synthesis, the release of stress responsive proteins such as insect thioester-containing protein (TEP) protein and molecules believed to function in opsonization and iron sequestration (Gillespie *et al*., 1997; Ursic-Bedoya *et al*., 2006)

3.1.2.2.1. Insect antimicrobial peptides (AMPs)

The isolation of antibacterial peptides from the giant silkmoth *Hyalophora cecropia* (Lepitoptera) has opened the area of animal antibiotics (Steiner *et al*., 1981). The production of antimicrobial peptides (AMPs) is an important aspect of insect humoral defence. These small and endogenous peptides share common features such as a low molecular weight (often below 5

Table 15. The immune-related proteins in *Bombyx mori*

Immune-related proteins			Description	Activity	References
antimicrobial peptides	cecropin		~40 aa, two α-helices, three subtypes (A/B/D)	bacteria	Morishima *et al*., 1990; Hara *et al*., 1994
	attacin		20 kDa, glycine-rich	bacteria	Sugiyama *et al*., 1995
	lebocin		32 aa and proline-rich, four analogues	bacteria	Hara and Yamakawa, 1995 a; Furukawa *et al*., 1997
	moricin		42 aa, basic, in hemolymph	bacteria	Hara and Yamakawa, 1995 b
	gloverin		glycine-rich, in the fat body	bacteria	Axen *et al*., 1997; Song *et al*., 2006
	lysozyme*		in fat body, hemocytes and epidermal cells	bacteria	Lee and Brey, 1995; Dunn *et al*., 1985
lectin	hemocytin (lectin)		3133 aa, in hemocytes specific for glucuronic acid	hemostasis or encapsulation of foreign substances	Kotani *et al*., 1995
	PRR	BmLBP	C-type lectin, two different CRDs	hemocyte nodule formation	Koizumi *et al*., 1997, 1999
		BmMBP	C-type lectin, binding to teichoic acid, mannan and PGN and hemocyte directely	hemocyte nodule formation	Ohta *et al*., 2006
proPO system		PGRP*	19 kDa, in fat body, hemocytes and epidermal cells	bacteria	Yoshida *et al*., 1986; Ochiai and Ashida, 1999
		βGRP*	62 kDa, in fat body, hemocytes and epidermal cells	fungi	Ochiai and Ashida, 2000
	serine protease zymogen		39 kDa, in hemolymph plasma	mediate the melanization pathway	Katsumi *et al*., 1995
	pro-PO		a heterodimeric protein, synthesized by hemocytes (oenocytoids)		Kawabata *et al*., 1995
	ppA		glycosylated; two isozymes (ppA I/ II) in the integument, hemocytes, and salivary glands but not in the fat body or midgut		Satoh *et al*., 1999

aa, amino acid; *, constitutively expressed (for lysozyme, at a low level); PRRs, pattern recognition receptors; BmLBP, *B. mori* lipopolysaccharide (LPS)-binding protein; BmMBP, *B. mori* mannan-binding protein; CRD, carbohydrate-recognition domain; pro-PO, prophenoloxidase; ppA, prophenoloxidase-activating enzyme (serine proteinase); PGRP, peptidoglycan recognition protein; βGRP, β-1,3-glucan recognition protein.

kDa, containing <100 residues), a positive net charge (cationic) at physiological pH and for most of them, amphiphilic α-helices or hairpin-like β-sheets or mixed structures. So far, more than 250 different AMPs have been described from different insect orders (Ursic-Bedoya *et al*., 2006) (see database AMSDb, http: //www.bbcm.univ.trieste.it/).

In insects undergoing metamorphosis (holometabolous) such as *Bombyx mori*, systemic expression of AMPs are rapidly and transiently synthesized by the fat body and various epithelia (Bulet *et al*., 2003). AMPs produced by the fat body are secreted into the hemolymph, from where they can easily diffuse to act throughout the whole animal (For *B. mori* AMPs, see **Table 15**). Epithelial expression of AMPs in epithelial cells of the midgut, trachea, genital tract and Malpighian tubules appears to be a general feature of host defense (Bulet *et al*., 2003) (**Table 14**). In contrast, in insect with incomplete metamorphosis (heterometabolous), AMPs are produced by hemocytes in the healthy individuals and secreted into the hemolymph upon infection (Lamberty *et al*., 2001).

Insect antimicrobial peptides (AMPs) can be grouped into three families based on their main biological targets (**Table 16**): (i) anti-bacteria peptides: including anti-Gram-positive bacteria peptides, anti-Gram-negative bacteria peptides; (ii) anti-fungi peptides; (iii) peptides which have a broad spectrum of activity against both Gram-positive and Gram-negative bacterial strains as well as against filamentous fungi, protozoan and metazoan parasite or virus. On the basis of sequence and structural features, the insect AMPs can be roughly categorized into five groups (**Table 17**): (i) Linear and amphipathic α-helical AMPs: linear peptides forming amphiphilic α-helices and deprived of cysteine residues; (ii) S-S bridged AMPs (cysteine-stabilized peptides); (iii) Peptides with an overrepresentation in a certain amino acid, most often proline and/or glycine residues; (iv) aromatic dipeptides; (v) peptides derived from oxygen-binding proteins.

Despite the marked molecular diversity of AMPs described above, their biological activity can be generally ascribed to two principal mechanisms of action (Brogden, 2005): (i) Through non-specific peptide-lipid interaction: their amino acid composition, amphipathicity, cationic charge and size allow them to attach to and insert into microbial membrane bilayers to form pores. The intensive study of AMP-membrane interactions has given rise to molecular models of

Table 16. The insect representive antimicrobial peptides (AMPs) with different antimicrobial activity

AMP groups	AMPs	Antimicrobial activity and Description	Reference
anti-bacteria AMPs	attacin	G^--bacteria; >190 residues	Imler and Bulet, 2005 Bulet *et al*., 1999
	drosocin	G^--bacteria; 19 residues, cysteine-free, O-glycopeptide, proline-rich (>30%),	Imler and Bulet, 2005 Bulet *et al*., 1999
	diptericin	G^--bacteria; 83 residues, O-glycopeptide, proline-rich (>35%)	Imler and Bulet, 2005
	MPAC	G^--bacteria; 23 residues, O-glycopeptide	Imler and Bulet, 2005
	gloverin	G^--bacteria; 14 kDa, glycine-rich	Bulet *et al*., 1999
anti-fungi AMPs	drosomycin	44 residues	Imler and Bulet, 2005
	metchnikowin	26 residues, proline-rich, cysteine-free,	Imler and Bulet, 2005 Bulet *et al*., 1999
	AFP	7 kDa	Iwanaga and Lee, 2005
	tenecin 3	75 kDa	Iwanaga and Lee, 2005 Bulet *et al*., 1999
	holotricin 2/3	75 kDa	Iwanaga and Lee, 2005 Bulet *et al*., 1999
AMPs with broad spectrum of activitiy	thanatin	G^+ and G^--bacteria and filamentous fungi; 21 residues	Bulet *et al*., 1999
	defensin	G^+-bacteria, fungi, protozoa; 40 residues, three internal S-S bridges	Imler and Bulet, 2005 Bulet *et al*., 1999 Vizioli and Salzet, 2002
	cecropin	bacteria, fungi, virus, protozoa, metazoan; 29~42 residues; linear, cysteine-free	Imler and Bulet, 2005 Bulet *et al*., 1999
	gambicin	bacteria, fungi, protozoa	Vizioli *et al*., 2001
	heliomicin	bacteria, fungi	Lamberty *et al*., 2001
	stomoxyn	bacteria, fungi, trypanolytic activity; 42 residues	Bulet *et al*., 2004

AFP, antifungal protein; 5-S-GAD, *N*-β-alanyl-5-*S*-glutathionyl-dopa; MPAC, maturated prodomain of attacin C.

membrane disruption that include both the formation of discrete channels by 'barrel-stave' or 'toroidal-pore' mechanisms (**Figure 17**) and more non-specific detergent-like 'carpet' processes (**Figure 18**); (ii) Through receptor-mediated recognition processes (intracellular killing): specific interactions with membrane associated or intracellular molecular targets, resulting in disruption of vital metabolic processes and cell death (Tossi *et al*., 2002). Several observations suggest that translocated AMPs such as pyrrhocoricin, drosocin and apidaecin can alter cytoplasmic membrane septum formation, inhibit cell-wall synthesis, inhibit nucleic-acid synthesis, protein synthesis or enzymatic activity (Otvos *et al*., 2000). These two mechanisms may in many cases be complementary rather than alternative. While most AMPs are considered to exert their microbicidal activity principally by inducing membrane permeabilisation (mechanism i), the mechanism ii allows AMPs penetration into the cytoplasm and subsequent interaction with intracellular targets (Park *et al*., 1998) and it has been proposed that the mechanism ii may be as, if not more, important than membrane permeabilization (Hancock *et al*., 2000).

3.1.2.2.2. Reactive intermediates of oxygen (ROIs) and nitrogen (RNIs)

Various reactive intermediates of oxygen (ROIs) and nitrogen (RNIs**)** generated in response to immune challenge can modify the structural integrity and function of various target molecules, and ultimately destroy invading pathogen. They provide an effective immune arsenal for insects (**Figure 19**) (Nappi and Christensen, 2005).

ROIs have been shown to be involved in encapsulation responses in *Anopheles gambiae* (Kumar *et al*., 2003). Nappi *et al* (1993, 2005) have found melanization-associated superoxide generation and these enzyme-mediated melanogenic responses contribute to hemocyte-mediated, target specific cytotoxicity in immune challenged insects. Superoxide $^{\bullet}O_2^-$ has been detected in the plasma of several species of *Lepidopteran* larvae (Arakawa, 1995a, b; Arakawa *et al*., 1996; Whitten *et al*., 2001).

Nitric oxide (NO), produced during the oxidation of L-arginine to L-citrulline by NO synthase (NOS), is both an unstable free radical biological messenger and a highly reactive and killing molecule. In insects, two main types of NO synthases have been found: constitutive (cNOS) and inducible (iNOS) (Luckhart *et al*., 1998; Imamura *et al*., 2002). The first molecular

Table 17. The different groups of insect AMPs based on their structures
(Bulet *et al*., 1999; Vizioli and Salzet, 2002; Imler and Bulet, 2005)

AMP Groups	Description	Example
linear and amphipathic α-helical AMPs*	linear, amphiphilic α-helices, cysteine-free	cecropin
S-S bridge stabilized peptides*	cyclic, containing cysteine residues, mixed α-helical /β-sheet, triple-stranded β-sheet, β-hairpin-like structures	defensins, drosomycin, thanatin, andropin, moricin
peptides with an overrepresentation in a certain amino acid*	1. Pro-rich, 2. Pro/Gly-rich, 3. Pro/Arg rich, 4. His-rich, 5. His/Gly-rich, 6. Trp-rich	Pro-rich: drosocin Pro/Arg rich: apidaecin Glee-rich: diptericin, attacin
aromatic dipeptides	low molecular weight (5-S-GAD: 573 Da)	p-Hydroxycinnamaldehyde($C_9H_8O_2$); 5-S-GAD
peptides derived from oxygen-binding proteins	low molecular weight (3.2 kDa)	hemoglobin derived

*, cationic peptides; 5-S-GAD, N-β-alanyl-5-S-glutathionyl-3,4-dihydroxy phenylalanine

evidence of an immune-inducible NOS was reported from insects: NOS expression and NO production in the mosquito *Anopheles stephensi* (Diptera) limit malaria parasite development in the insect host (Luckhart *et al*., 1998). Since then, in several insect species NO has been shown to be inducibly synthesized in response to parasite infection (Dimopoulos *et al*., 1998; Whitten *et al*., 2001; Hahn *et al*., 2001; Colasanti *et al*., 2002). Inducible NO has a ubiquitous pathogen-killing mechanism and no other invertebrate immune mechanism has such a broad spectrum of action (Rivero, 2006). *In vitro* and *in vivo* studies have demonstrated the direct toxicity of inducible NO towards virtually every tested pathogen, from viruses to metazoan parasites, such as the filarial nematode *Brugia* and the trematode *Schistosoma* (Colasanti *et al*., 2002).

The interactions between these reactive intermediates of oxygen (ROIs) and nitrogen (RNIs) with DNA, metal centres and thiols are the main molecular mechanisms for pathogen-killing of ROIs and RNIs (Fang, 2004). Direct DNA damage is of central importance to the antimicrobial actions of ROI, whereas RNI inhibit respiration and interfere with DNA replication through the inactivation of zinc metalloproteins. Both ROIs and RNIs can mobilize iron from iron-sulphur-containing dehydratases, which further potentiates ROIs toxicity. The diversity of targets for ROIs and RNIs acting individually or synergistically with other systems results in a broad spectrum of antimicrobial activity that encompasses bacteria, fungi, protozoan and metazoan parasites and viruses.

3.1.2.2.3. Prophenoloxidase (proPO)-activating system (proPO system) and melanization

A major innate defense system in insects is the melanization of pathogens and damaged tissues. This important process is controlled by the enzyme phenoloxidase (PO) which is a key and terminal enzyme activated from proPO through proteolysis in the insect proPO-activating system (reviewed in Cerenius and Söderhäll, 2004).

Insect proPO-activating systems appear to be similar to the complement system of mammals. Insect proPO-activating system can be activated through PAMPs-PRRs interactions upon infection (see 3.1.2.1.section) and is considered to be a critical and efficient humoral

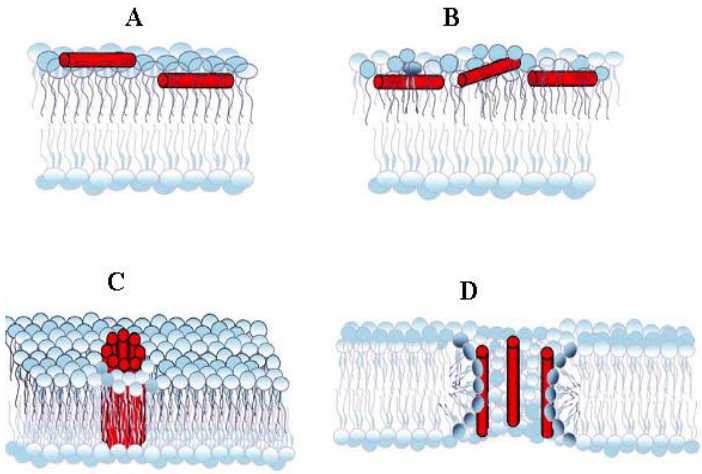

Figure 17. The "barrel-stave and toroidal pore model" of insect AMP microbicidial mechanism (Matsuzaki *et al*., 1996; Huang *et al*., 2006). Models of transmembrane channel formation mechanism: (A) Peptide α-helices (red cylinders) initially associate parallel to the membrane surface, either superficially (left) or embedded just below the aqueous interface (right). (B) Peptides continue to accumulate at or near the bilayer surface, disrupting lipid packing and causing membrane thinning. This step may or may not involve peptide-peptide aggregation. Once a critical peptide/lipid ratio is reached, peptides either insert into the membrane as a barrel-stave type pore (C), or induce the localized formation of toroidal pores (D).In the barrel-stave model, the peptides need to be long enough to traverse the hydrophobic core of the bilayer and directly contact between peptides upon channel formation (Ludtke *et al*., 1996). In the toroidal model, channels are composed of a mixture of peptides and lipids and thus are not required to span the complete bilayer. Toroidal pores are proposed to form subsequent to peptide-induced membrane thinning, which may also allow the penetration of short peptides to form a peptide/lipid pore.

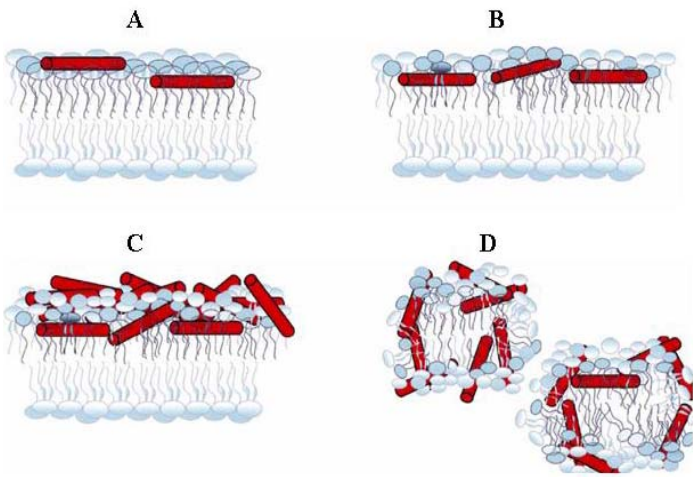

Figure 18. The "carpet model " of insect AMP microbicidial mechanism (Sato *et al*., 2006)**.** Model of membrane disruption by the carpet mechanism: as in channel formation, peptide α-helices (red cylinders) initially bind (A) and accumulate in an orientation parallel to the membrane surface (B). Membrane-bound peptides which associate with the phospholipid head-groups continue to accumulate and eventually cover (i.e., carpeting) the bilayer (C) which lead to detergent-like membrane disintegration (D). 2. In detergent-like "carpet" mechanism, peptides accumulate at the bilayer surface like a carpet and, above a threshold concentration of monomers, the membrane is permeated and disintegrated in a detergent-like manner without the formation of discrete channels.

defense reaction against microbial infection and parasitization in insect hemolymph (Ashida, 1990). As a complex enzyme cascade, insect proPO-activating system is composed of pattern-recognition receptors (PRRs), serine proteases and their zymogens, pro-ppA (proenzyme of ppA), ppA (proPO-activating enzyme), proPO (proenzyme of PO), PO (phenoloxidase) as well as proteinase inhibitors (serpins: serine protease inhibitors), which are important regulatory factors to avoid activation of the system where it is not appropriate (Cerenius and Söderhäll, 2004) (**Figure 20**). For insect proPO system, ppA and PO are synthesized as an inactive zymogen (pro-ppA and proPO), which can be activated by proteolytic cleavage. While PRRs are considered as the activators of this system, the terminal enzyme PO can oxidize phenols into quinones, that in turn will convert into melanin autocatalytically resulting in wound healing, melanization of foreign organisms trapped in capsules or hemocyte nodules and sclerotization (Nappi *et al*., 2004; Yu *et al*., 2006).

Concomitant with proPO system activation, besides the melanization many other immune reactions will be produced, such as the induced synthesis of antimicrobial peptides, the cytotoxic reactions, the opsonization and the stimulation of cellular immune responses such as phagocytosis, nodule formation and encapsulation by hemocytes (Hoffmann *et al*., 1996; Gillespie *et al*., 1997; Cerenius and Söderhäll, 2004).

Bombyx mori proPO-activating systems (**Table 15**): *B. mori* PGRP (peptidoglycan binding protein) and βGBP (β-1,3 glucan binding protein, 62 kDa) are the earliest described insect PRRs that mediates the activation of proPO cascade (Yoshida *et al*., 1986; Ochiai and Ashida, 1988, 1999, 2000). *B. mori* PGRP is constitutively expressed in the fat body, epithelial cell and hemocytes of naïve silkworms (Ochiai and Ashida, 1999). In *B. mori* hemolymph plasma, a serine protease zymogen (39 kDa) is activated by the presence of PGN or yeast cell wall (Katsumi *et al*., 1995). *B. mori* proPO is synthesized by the hemocytes (oenocytoids) (Kawabata *et al*., 1995). After being released from the hemocyte, hemocyte-derived proPO can be post-translationally modified and transported through the *B. mori* cuticle by an unknown mechanism (Asano and Ashida, 2001). These findings could mean that hemocytes may be responsible for proPO synthesis in many tissues. In *B. mori*, proPO-activating enzyme (ppA) is a glycosylated serine protease synthesized as pro-ppA with 441 amino acid residues and activated

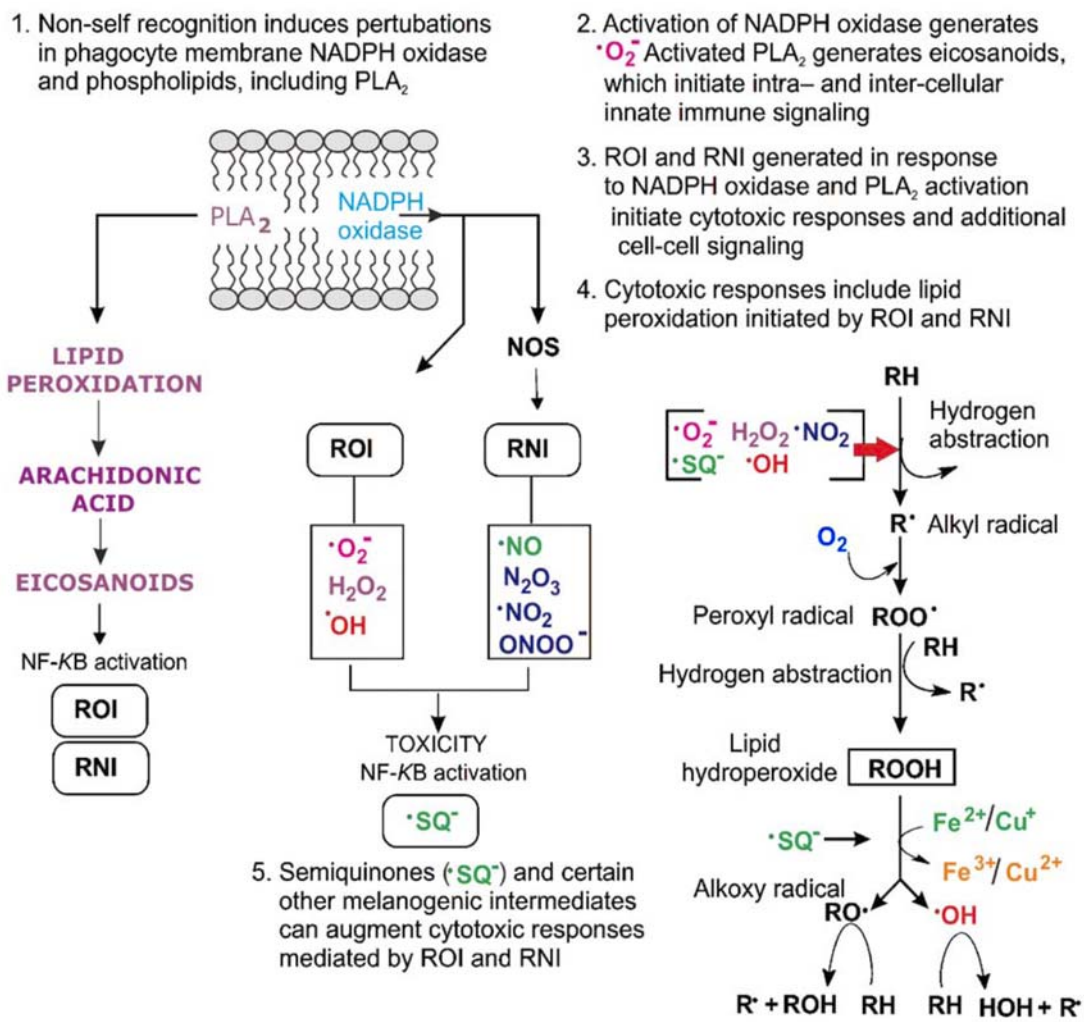

Figure 19. Some cytotoxic reactions reported in immune challenged insects (Nappi and Christensen, 2005). In insects the cytotoxic responses of ROI and RNI to the invading pathogen can be augmented by certain melanogenic intermediates of phenoloxidase(PO)-mediated melanogenesis, including semiquinone ($^{\cdot}SQ^{-}$), which has the same reactivity as superoxide anion ($^{\cdot}O_2^{-}$). NADPH, nicotinamide adenine dinucleotide phosphate; ROI, reactive intermediates of oxygen, including the superoxide anion ($^{\cdot}O_2^{-}$), hydrogen peroxide (H_2O_2), hydroxyl radical (·OH) and hypochlorous acid (HOCl); RNI, reactive intermediates of nitrogen, including the nitric oxide (NO), nitrous anhydride (N_2O_3), peroxinitrite anion ($ONOO^{-}$), nitrite (NO_2) and nitrate (NO_3); PLA, phospholipase A; RH, lipid.

from pro-ppA by proteolytic cleavage of a peptide bond between Lys152 and Ile153 (Satoh *et al*., 1999).

3.1.2.2.4. Induction of lectin synthesis

Insect lectins are carbohydrate-binding proteins with a highly specific multivalent capacity to bind to certain sugar residues on cell surface molecules. The carbohydrate-recognition domains (CRD) of lectins recognize specific carbohydrate patterns on the surfaces of bacteria, viruses and fungi, that are not present as surface carbohydrates of higher eukaryotes and so help to distinguish self from non-self (Jack and Turner, 2003; Gadjeva *et al.*, 2004). They are multimeric proteins (70~1,500 kDa) composed of 30- to 40-kDa subunits (Gillespie *et al*., 1997).

Insect lectins participate in a variety of innate immune responses, including stimulation of prophenoloxidase (proPO) activation (Yu *et al*., 2002), phagocytosis, hemocyte nodule formation encapsulation, melanization and protecting larvae from microbial infection (Yu and Kanost, 2000 a, b; Ling and Yu, 2006 a, b). Insect C-type lectins (CTLs) which are extracellular or membrane-bound proteins can bind to the invading pathogen surface and function as pattern recognition receptors (PRRs) in innate immunity which results in lectin-linked aggregates of target cells (Gillespie *et al*., 1997; Williams, 2001; Yu *et al*., 2006). The agglutinated foreign cells vary from bacteria, fungi to parasites such as trypanosomes (Pereira *et al*, 1981; Yu *et al*., 2006).

Lectin is made constitutively in insect larvae and pupae (Komano *et al*., 1980). A C-type lectin with two different CRDs that binds to LPS constitutively expresses in *B. mori* hemolymph and participates in hemocyte nodule formation (Koizumi *et al*., 1997, 1999) (For *Bombyx mori* lectins, **Table 15**). A lectin named scolexin of *Manduca sexta* is synthesized and released mainly by epidermal cells and to a minor extent by midgut cells, but not by hemocytes (Kyriakides, 1993, 1995) while four C-type lectins in *M. sexta* is inducibly synthesized in fat body and then released to hemolymph (Yu *et al*., 2006). *B. mori* hemocytin is a very different type of lectin homologous to mammalian von Willebrand platelet aggregation factor and coagulation factor V and VIII with its mRNA elicited in hemocytes (Kotani *et al*., 1995)

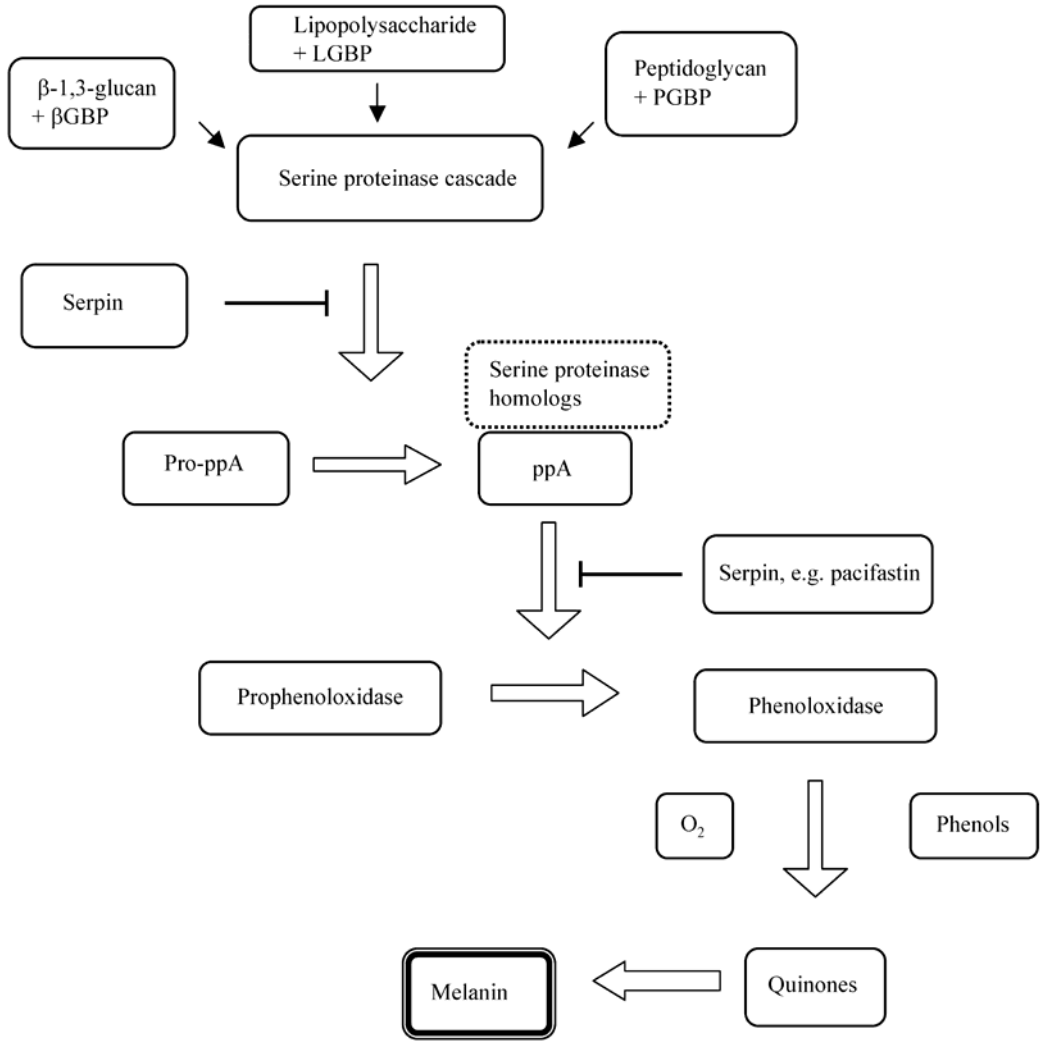

Figure 20. The insect prophenoloxidase (proPO)-activating system (Cerenius and Söderhäll, 2004; Michel and Kafatos, 2005). The insect prophenoloxidase (proPO) system is activated by pattern-recognition proteins (PRRs) that have bound to microbial conserved pathogen-associated molecular patterns (PAMPs) such as LPS (lipopoly-saccharide), PGN (peptidoglycan), β-1,3-glucans. The activities of these PRRs, i.e. LGBP (LPS and β-1,3-glucans-binding protein), PGBP (PGN-binding protein) and βGBP (β-1,3-glucans-binding protein), may be carried out by separate proteins or individual proteins with several binding activities, depending on species and protein). The proPO system can also be activated by other compounds such as endogenous factors produced upon tissue damage. A cascade of serine proteinases, which are not yet characterized, will result in the cleavage of the pro-form of the prophenoloxidase-activating enzyme (pro-ppA) into active ppA. The box containing serine proteinase homologs is dotted, as some ppAs require them and some ppAs are capable of cleaving proPO directly into active phenoloxidase with the synthesis of quinones then melanin. Melanin synthesis plays important roles in the development and physiology of all insects; it is required for the hardening of the exoskeleton and pigmentation during the life cycle, and for wound healing after injury. In addition, pathogens and parasites can be immobilized by formation of a surrounding melanotic capsule and are killed apparently by the production of free radicals and toxic quinone intermediates produced during capsule formation.

Lectin can also be induced by injury or by injecting larvae with bateria, LPS or PGN (Hurlbert, 1985; Kyriakides, 1993, 1995; Kotani *et al*., 1995; Ourth *et al*., 2005). An inducible LPS-binding lectin was found in a cockroach (Jomori and Natori, 1992). Two different inducible LPS-binding C-type lectins which involved in phenoloxidase activation have been recovered from *Manduca sexta* (Yu *et al*., 1999; Yu and Kansot, 2000).

Several insect lectins are specific for galactose (Takahashi *et al*., 1985; Stebbins and Hapner, 1985; Castro *et al*., 1987, Haq *et al*., 1996). The function of M13, a lectin-like protein in larvae of the tobacco hornworm was inhibited by glucose (Minnick *et al*., 1986). A mannan-binding lectin exists in adult mosquito *Anopheles stephensi* (Liston) hemolymph and its agglutination is inhibited by mannan and nitrophenol-modified sugar derivatives, but not by simple sugars (Chen and Billingsley, 1999). Recently, a mannose-binding C-type lectin (36 kDa) is firstly isolated from tobacco budworrn *Heliothis virescens* (*Lepidoptera*) immune pupal hemolymph (Ourth *et al*., 2005). The aboved-mentioned *B. mori* hemocytin shows specificity for glucuronic acid and its function is inhibited by D-mannose, N-acetyl-D-galactosamine, and D-maltose (Kotani *et al*., 1995).

3.1.2.2.5. Insect thioester-containing protein (TEP) protein

Members of the α 2-macroglobulin/thioester-containing protein (TEP) protein superfamily are widespread among metazoans (Blandin and Levashina, 2004), and have recently been found in bacteria, probably acquired by horizontal transfer (Budd *et al*., 2004). Members include vertebrate complement factors, α 2-macroglobulins and insect TEPs, which play an important role in innate immunity. These proteins are characterized by a thioester motif that forms an intra-chain, unstable highly reactive bond which is normally buried within the protein structure to prevent precocious inactivation. Proteolytic cleavage of the protein causes a change in conformation and exposure of the thioester bond, which mediates binding of the molecules to nearby target surfaces (in the case of complement factors) or a wide spectrum of proteases (in the case of α 2-macroglobulins).

In *Anopheles gambiae*, TEP1 was shown to bind to the surface of $Gram^+$ and $Gram^-$

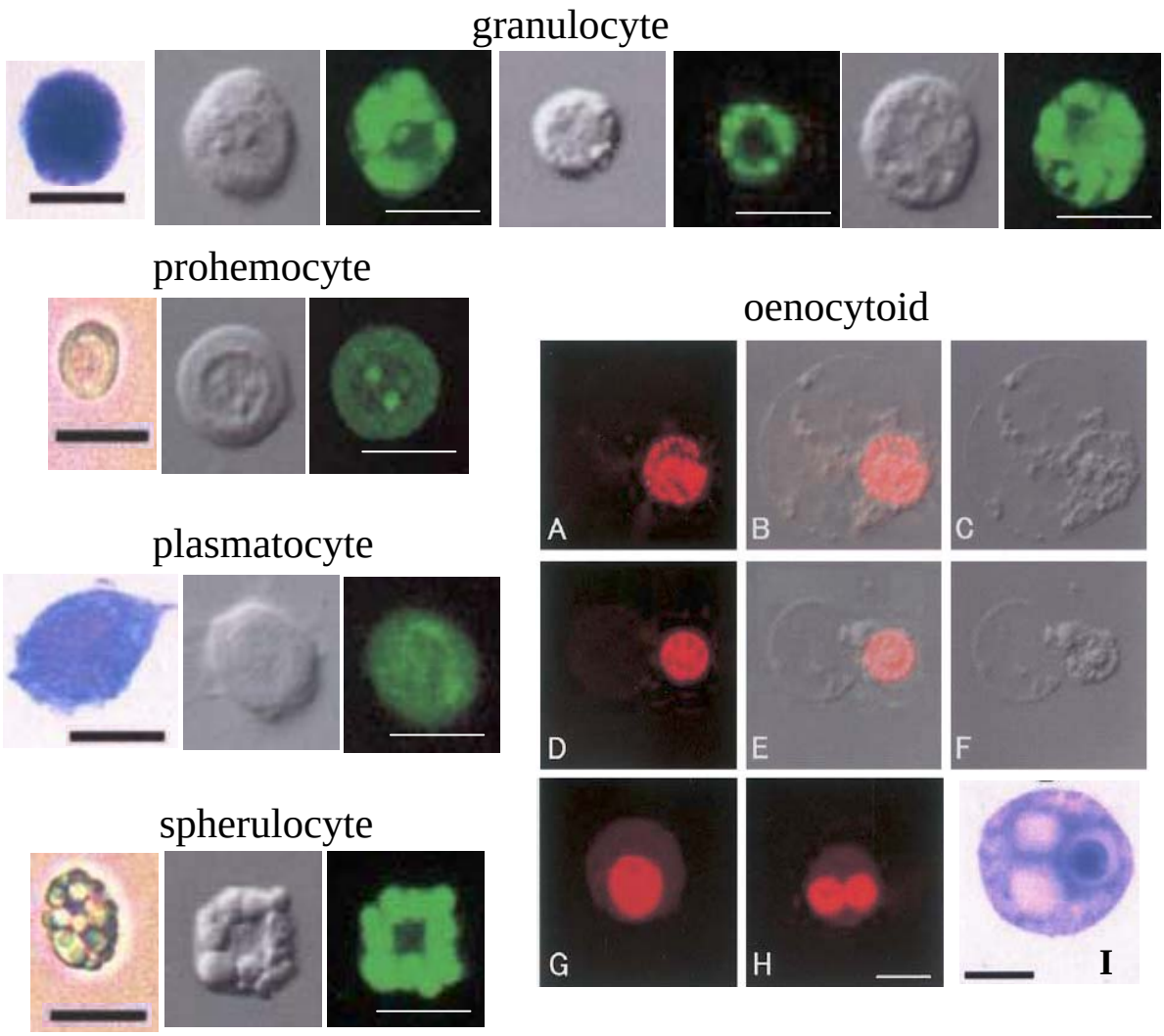

Figure 21. Morphology of five types of *Bombyx mori* hemocytes using Gimesa staining, phase contrast, differential interference contrast and fluorescence microscopy (Ling *et al*., 2003)**.** Blue hemocytes are Gimesa-stained; hemocytes with green fluorescence are stained by acridine orange and oenocytoids with red fluorescence are stained by propidium iodide, Bar for all hemocytes: 10 μm. *Bombyx mori* hemocytes are classified as the granulocyte, prohemocyte, spherulocyte, plasmatocyte and oenocytoid. Circulating granulocytes, which appear either a little irregularly shaped, small or round, contain many green granules of different sizes. Prohemocytes (the left cell is unstained) and plasmatocytes are stained a faint green by acridine orange. In prohemocytes, the nuclei appear dark within the background of faint green fluorescence and one or two weak green fluorescent bodies are observed within the nuclei. Nuclei are invisible in plasmatocytes that are irregularly shaped with extended pseudopodia. In spherulocytes (the left cell is unstained), these green granules are generally larger and similar in size. In oenocytoids (A-I), B is combined from A and C, and E from D and F. Most oenocytoids have intact membranes (A, G, H). Because of their fragile characteristics, the membranes of some oenocytoids rupture and their nuclei are expelled (E, F). Some oenocytoids were shown to have two nuclei (H). I is a Gimesa-stained oenocytoid.

bacteria and binding was stronger when the thioester bond was intact. Importantly, TEP1 opsonizes $Gram^+$ and $Gram^-$ bacteria for phagocytosis and therefore resembles vertebrate complement function (Levashina *et al*., 2001). Recently, TEP1 was shown to bind to the surface of *Plasmodium berghei* sporozoites and promote parasite killing by lysis in the basal labyrinth of the midgut epithelium (Blandin *et al*., 2004a). This was the first report of a putative PRR that can indeed reduce *A. gambiae* susceptibility towards *Plasmodium* infection.

In insects, TEP genes have been described in *Drosophila* (*Diptera*)(Lagueux *et al*., 2000) and *Anopheles* (Levashina *et al*., 2001; Oduol *et al*., 2000). Six TEP genes were found in the genome of *D. melanogaster*, dTep1, 2 and 4 are up-regulated after bacterial challenge in larval and adult stages, and dTep1 is induced under the control of the JAK/STAT signal transduction pathway (Lagueux *et al*., 2000). 15 TEP genes were identified in the mosquito *A. gambiae* in which several of them have been shown to be up-regulated after bacterial and/ or *P. berghei* infection (Oduol *et al*., 2000; Levashina *et al*., 2001; Christophides *et al*., 2002; Blandin *et al*., 2004b). *TEP4* were up-regulated after bacterial challenge (Oduol *et al*., 2000).

3.1.2.3. The insect cellular defenses: hemocyte-mediated immune responses

The cells in insect hemolymph are collectively called hemocytes (Theopold *et al*., 2004). The insect hemocytes are highly immunoreactive cells playing a central role in maintaining host integrity and involves in various defense mechanisms such as phagocytosis (largely aimed at small pathogens, such as virus, bacteria and fungi), nodule formation and encapsulation (aimed mostly at larger pathogens, such as protozoan and metazoan parasites) (Bulet *et al*., 1999; Kanost *et al*., 2004; Ribeiro and Brehélin, 2006).

3.1.2.3.1. Typical insect hemocytes and hemocyte adhesion receptors

In *Lepidoptera*n larvae such as *Bombyx mori*, there are mainly five hemocyte types: two adhesive hemocytes: granular cells and plasmatocytes, and three non-adhesive hemocytes: spherule cells, oenocytoids and prohemocytes (Lavine and Strand, 2002; Ling *et al*., 2003; Jiravanichpaisala *et al*., 2006). In *Drosophila* (Diptera), the hemocytes are classified into three

Table 18. The characterization of typical insect hemocytes (Lavine and strand, 2002; Jiravanichpaisala *et al*., 2006)

Hemocyte types of *Lepidoptera*	Characterization	Function	Corresponding three hemocyte types in *Diptera*: *Drosophila*
granular cells (granulocytes)	small spherical and adhesive cells (5~8 μm), including heterogeneous granules (phagocytised material), numerous pseudopods and pinocytotic vesicles	phagocytosis; opsonisation (the first cells contact the foreign body and their following exocytosis of opsonin attracts plasmatocytes and help them to build the capsule or nodule)	**plasmatocytes** adhesive cells, the only hemocyte in embryogenesis, the most abundant hemocyte type in circulation
plasmatocytes	irregular shape (spherical , oval or spindle-shaped), adhesive cells, narrow cisternae of the RER, no granular inclusion, rare pinocytotic vesicles and pseudopods	capsule or nodule formation (synthesize desmosomes forming the bulk of capsules around foreign bodies too large to be phagocytosed, or nodules around masses of bacteria and necrotic melanised material)	**lamellocytes** adhesive cells that only occur after infection with foreign bodies
spherule cells (spherulocytes)	spherule, non-adhesive cells, including granules more homogenous and larger	transport cuticular components	No
oenocytoids	regular shape, non-adhesive cells, eccentric nucleus and paucity in cytoplasmic organelles with exception of free ribosomes	synthesis of phenoloxidase (PO); melanization of hemolymph	**crystal cells** non-adhesive cells
prohemocytes	round, non-adhesive cells	stem cells that differentiate into other hemocyte types	No

types: adhesive plasmatocytes, adhesive lamellocytes and non-adhesive crystal cells which correspond functionally to the granular cells, plasmatocytes and oenocytoids in *Lepidoptera* (Ribeiro and Brehélin, 2006). The morphology of *Bombyx mori* hemocytes is shown in **Figure 21**. The characterization and functions of insect hemocytes are listed in **Table 18**.

The granular cells and plasmatocytes are two main classes of hemocytes involved in insect cell-mediated immune responses. In response to a foreign surface, they can suddenly transform from circulating, non-adherent cells to adherent cells that adhere to each other and interact with the foreign surface (Nardia, *et al*, 2005). Two known adhesion receptors of insect hemocytes are integrin and neuroglian, a member of the immunoglobulin superfamily which are integral membrane proteins (Hortsch, 1996; Wiegand *et al*., 2000; Nardi *et al*., 2003; Levin *et al*., 2005). It has been indicated that activation of ligand binding by the hemocyte specific integrin plays a key role in stimulating plasmatocyte adhesion leading to encapsulation (Levin *et al*., 2005).

3.1.2.3.2. Insect cellular defense mechanisms: phagocytosis, nodulation and encapsulation

Insect hemocyte-mediated immune defenses mainly include phagocytosis, nodule formation, and encapsulation (Bulet *et al*., 1999; Kanost *et al*., 2004) (**Table 19)**.

Phagocytosis refers to the engulfment of entities by an individual cell. In phagocytosis, the granular cells and plasmocytes are the main functional hemocytes in *Lepidoptera* and in *Drosophila* respectively. This evolutionarily conserved process is essential for a variety of biological events including the elimination of microorganisms, activation of innate and adaptive immune responses, removal of apoptotic cells, and tissue remodeling during development. Receptor-mediated recognition of infectious microbes is a key early step in phagocytosis. Previous studies in insects have identified a number of conserved proteins, including pathogen receptors, complement-like factors, and cytoskeletal proteins that are involved in phagocytosis (Rämet *et al*., 2001; Pearson *et al*., 2003; Moita *et al*., 2005). Recently it has been demonstrated that ecdysone modulates phagocytosis of foreign particles by *Rhodnius prolixus* hemocytes *in vivo* and this is also the first report that the neuroendocrine system in insects is involved in

Table 19. The insect cellular immune reponses and involved hemocytes
(Kanost *et al*., 2004)

Cellular defense	Mechanism definition	Hemocytes involved	Targets
phagocytosis*	engulfment of entities by an individual hemocyte	granular cells (in *Lepidoptera*) plasmatocytes (in *Drosophila*)	small pathogens, such as virus, bacteria and fungi
nodule formation	multiple hemocytes binding to aggregations of bacteria	granular cells and plasmatocytes (in *Lepidoptera*) lamellocytes and crystal cells (in *Drosophila*)	larger pathogens, such as protozoan and metazoan parasites
encapsulation	multiple hemocytes binding to larger targets like parasitoids, nematodes		

*, in *Bombyx mori*, prohemocytes have the function of phagocytosis *in vitro* (Ling *et al*., 2005a).

modulating hemocyte phagocytosis (Figueiredo *et al.*,2006)

Nodulation refers to multiple hemocytes binding to aggregations of bacteria while encapsulation refers to the binding of hemocytes to larger targets like parasitoids and nematodes. Nodule and capsule are essentially the same process though against different targets (Lavine and Strand, 2002). Unlike phagocytosis, nodulation and encapsulation result in the formation of an overlapping sheath of hemocytes around a target. The granular cells and plasmatocytes involved in encapsulation in *Lepidoptera* while lamellocytes in *Drosophila* (Schmidt *et al*., 2001; Vass and Nappi, 2001). Both humoral and cellular receptors are involved in recognition of encapsulation targets (Lavine and Strand, 2001). After granular cells or humoral opsonins such as extracellular matrix (ECM) proteins lacunin and a ligand for peanut agglutinin (PNA) lectin released by granular cells bind to the target, they induce plasmatocytes to change from non-adhesive to strongly adhesive cells that form the majority of the capsule (Nardia, 2005). Encapsulation is terminated by the attachment of granular cells to the capsule periphery. Nodule and capsule formation in some insect species often become melanized, through the action of phenoloxidase (Lavine and Strand, 2002; Cerenius and Söderhäll, 2004; Iwanaga and Lee, 2005).

3.1.2.4. Hemolymph clotting: overlapping of insect humoral and cellular immune defenses

Insects have an open circulatory system. Therefore, after injury, insect hemolymph clotting (hemolymph coagulation, hemostasis) is critical in preventing hemolymph loss. Hemolymph clotting is also an important part of innate immune system quickly forming a secondary barrier against infection, which can help in the trapping and immobilizing of microbes from entering, spreading throughout the hemocoele, thereby promoting their killing and initiating wound healing. It overlaps the insect humoral and cellular immune defenses and involves a combination of soluble and cell-derived factors. However, hemolymph clotting is one of the least understood immune responses in insects (Theopold *et al*., 2002, 2004; Scherfer *et al*., 2006).

Insect hemolymph clotting strictly depends on Ca^{2+} ions and the activity of

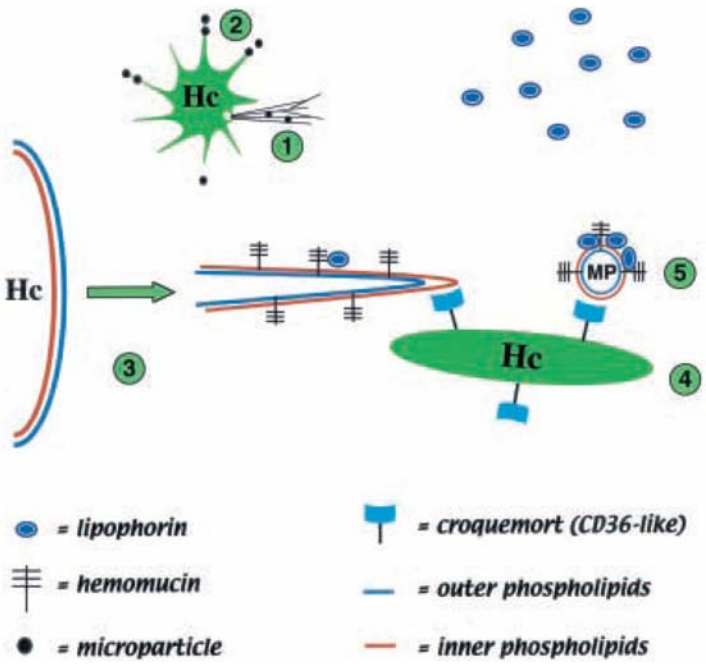

Figure 22. Scheme of hemolymph clotting (coagulation) in insects (Theopold *et al*., 2002). Insect hemolymph clotting comprises the activation of both hemocyte and hemolymph coagulogen activity. Hemocytes (Hc) show two reactions, namely degranulation (the release of granular components such as hemomucin) (1), and the formation of membranous vesicles called microparticles (MP) (2). Microparticle formation is accompanied by a reversal in membrane polarity, leading to the exposure of (mostly negatively charged) lipids from the inner leaflet of the membrane lipid bilayer on the cell surface (3). These lipids can be recognized by scavenger receptors like the *Drosophila* croquemort protein or other CD36-like proteins on hemocytes (4). The hemocyte coagulogen such as hemomucin attracts hemolymph coagulogen comprising lipophorin (5) and possibly other factors and finally resulting hemolymph clotting.

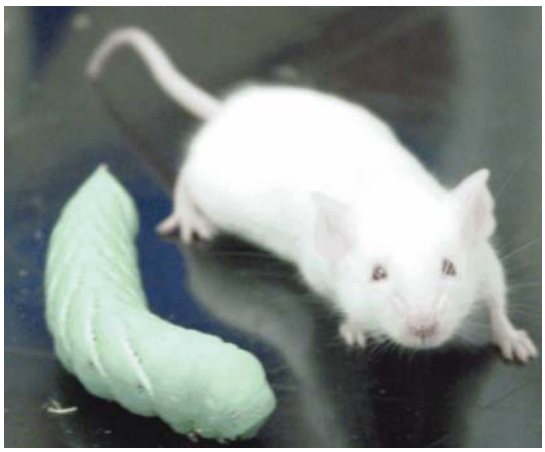

Figure 23. Comparison of the sizes of a fifth instar *Manduca sexta* larva and an adult mouse (Kanost *et al*., 2004). A fifth-instar *Bombyx mori* can be nearly the same size of (4~7cm) as a fifth instar *Manduca sexta* larva**.** Hemolymph samples that can be collected from such insects (1~2 mL) are of the same magnitude that can be obtained from small mammals.

transglutaminase (TG, Ca^{2+}-dependent enzyme) (Li *et al*., 2002). It is often considered consisting of four steps (Theopold *et al*., 2004). First, the degranulation or disintegration of hemocytes (a subpopulation of granular cells or so-called coagulocytes) leads to establishment of extracellular aggregates, which include hemocytes, cell debris and extracellular matrix. These aggregates seal the wound (termed the primary or soft clot). Second, the activation of the transglutaminase and/or proPO cascade, leads to crosslinking of the clot (hard clot). Third, the plasmatocytes are attracted and they spread across the clot and seal it off from the hemocoele (scab formation). The spreading of plasmatocytes is triggered by a factor released from plasmatocytes (plasmatocyte spreading factor) (Lavine and Strand, 2002). Last, regeneration of the epidermis occurs, growing across the wound site and replacing the scab.

In many insects, full activation of hemolymph clotting cascade is only achieved when cellular and soluble procoagulant components (also called coagulogen) are brought together (**Figure 22**) (Li *et al*., 2002). Hemomucin (a hemocyte surface mucin) and lipophorin (lipid-carrying protein, a major serum component of the hemolymph) have been identified as major coagulogens (Barwig, 1985; Duvic and Brehélin, 1988). During cell attachment, hemomucin released from hemocytes binds to lipophorin, which initiates establishing of extracellular aggregates (Theopold and Schimidt, 1997). An ecdysone-regulated mucin, gp150, found in *D. melanogaster* hemocytes, midgut and salivary glands and released from larval hemocytes, is a component of the clot and participates in the entrapment of bacteria (Korayem *et al*., 2004). Hexamerin, a storage protein in the hemolymph plasma acts as a pro-coagulant (Scherfer *et al*., 2004; Ma *et al*., 2005). Hemofibrin, a 22-kDa protein found in *Manduca sexta*, forms a fibrous clot that can be visualized using electron microscopy (Geng and Dunn, 1988). A hemolymph galactoside-binding lectin markedly enhanced the activation of clump formation of hemocyte monolayers with an increase in clump size and hemocyte aggregation. This lectin is also one of the few described lectins in insects with agglutination activity independent of Ca^{2+} ions (Mello *et al*., 1999). The above-mentioned lectins such as M13 (Minnick *et al*., 1986) and scolexin (Finnerty *et al*., 1999) from *M. sexta* as well as hemocytin (Kotani *et al*., 1995) from *B. mori* have also been implied in induction of coagulation reactions. By RNAi knockdown and pull-out assay, hemolectin and fondue found in the hemolymph of *Drosophila* have been

Table 20. Some insects being increasingly used as reference models

Order	Insect		References
	Name	Larva	
Lepidoptera	*Bombyx mori* (silkworm)		Garcia-Lara *et al*., 2005; Kaito *et al*., 2002, 2005
	Manduca sexta (tobacco hornworm)		Garcia-Lara *et al*., 2005; Kanost *et al*., 2004
	Galleria mellonella (greater wax moth)		Kavanagh and Reeves, 2004; Altincicek and Vilcinskas, 2006; Cytrynska *et al*., 2006
	Spodoptera littoralis (Egyptian armyworm)		Krishnan and Sehnal, 2006
Diptera	*Drosophila melanogaster* (fruit fly)		Martinelli and Reichhart, 2005; Imler and Bulet, 2005; Mylonakis and Aballay, 2005
	Anopheles gambiae (mosquito-malaria vector)		Barillas-Mury and Kumar, 2005; Aguilar *et al*., 2005; Boete *et al*., 2005; Michel and Kafatos, 2005
	Sarcophaga peregrina (flesh fly)		Natori *et al*., 1999; Itoh *et al*., 1985
Coleoptera	*Tenebrio molitor* (mealworm beetle)		Moret, 2006; Moret and Siva-Jothy, 2003; Barnes and Siva-Jothy, 2000

demonstrated that they are required for efficient hemolymph clotting in which the clot entraps bacteria and can form in the absence of PO activity (Scherfer *et al*., 2004, 2006).

3.2. Insects as reference models for innate immune and host-pathogen interactions studies

The study of silkworm *Bombyx mori* response to microsporidian *Nosema bombycis* pioneered by Pasteur in the 19th century demonstrated the possibility of using insects to study of innate immunity against different pathogens. Given the role of the innate immune response in protecting mammals from microbial infection (Romani, 1999; Levy, 2001) and the high degree of similarity that exists between the mammalian and insect innate immune responses (Vilmos and Kurucz, 1998; Salzet, 2001; Kavanagh and Reeves, 2004; Hoffmann, 2003), studying the insect response to infection may provide comparable data to those which may be obtained using mammals.

3.2.1. Current insect models

The discovery of human Toll-like receptor (TLR) in *Drosophila* represented a turning point in the study of the mammalian immune system and opened many new research possibilities, which supports the notion that *Drosophila* presents a good model for the analysis of immune-response pathways (Tzou *et al*., 2002; Iwanaga and Lee, 2005). *Bombyx mori* and *Manduca sexta* have proven to be good model systems for studying pro-PO activation system (Iwanaga and Lee, 2005). Their reasonable sizes (**Figure 23**), the easiness of pathogen injection, the low cost of maintaining, the commercial availbility, the increasing knowledge about insect molecular and genetic biology and genomics have made some insects being increasingly used as reference models for the study of innate immune reponses against pathogen, evaluating microbial pathogenicity or analysis of host-pathogen interaction (**Table 20**).

3.2.2. *Plasmodium-Anopheles,* an example of an integrative insect-parasite interaction

3.2.2.1. *Plasmodium* life cycle in vertebrate host and mosquito (**Figure 24** and **25**)

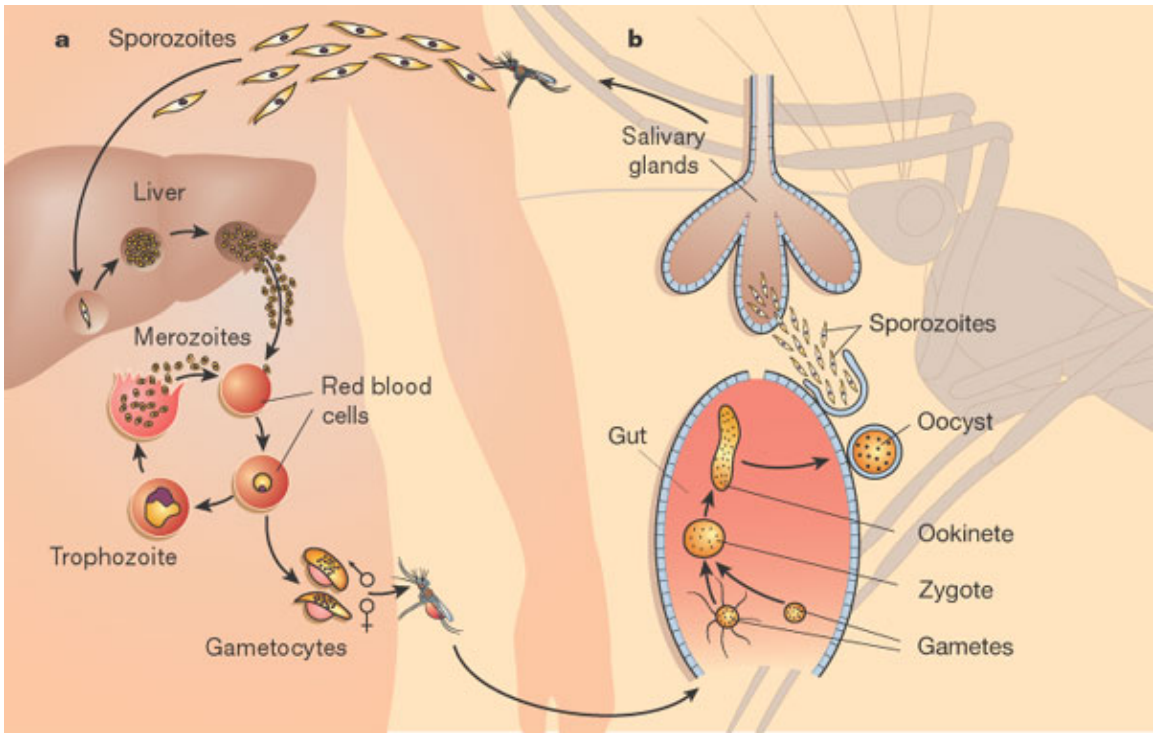

Figure 24. ***Plasmodium falciparum*** **life cycle: in human and mosquito** (from http://www.sanger.ac.uk/PostGenomics/plasmodium/images/lifecycle.jpg). **a. In human**: During a blood meal, a malaria-infected female *Anopheles* mosquito inoculates sporozoites into the human host and two main phases of multiplication follow. Exo-erythrocytic schizogony stage (in the liver): Sporozoites infect liver cells and mature into schizonts. The host cell ruptures and releases as many as 200,000 merozoites. Asexual or sexual erythrocytic schizogony stage (in the red blood cell): merozoites infect red blood cells and mature asexually to produce another 10~20 merozoites via the trophozoite stage, which are in turn released into the blood to re-infect more red cells (asexual stage). The merozoites in a subset of infected red blood cells then develop into haploid gametocytes (sexual stage). **b. In an *Anopheles* mosquito** (sporogonic cycle): when another mosquito bites the infected human, it takes up blood containing gametocytes. In the mosquito stomach they develop into male and female reproductive cells (gametes: ♂-microgametocytes; ♀-macrogametocytes). The microgametes penetrate the macrogametes generating zygotes which in turn become motile and elongated ookinetes. The ookinetes invade and traverse the midgut wall of the mosquito and arrive at the basal membrane of midgut where they develop/transform into sporozoite-filled oocysts. The oocysts grow, rupture, and release sporozoites, which make their way to the mosquito's salivary glands. Inoculation of the sporozoites into a new human host perpetuates the malaria life.

In vertebrate host: During a blood meal, a malaria-infected female mosquito inoculates sporozoites into the host. Then they attend the liver cells and mature into meronts, which rupture and release merozoites. Merozoites then infect red blood cells where they undergo asexual and sexual multiplication. In asexual erythrocytic stages, the ring stage trophozoites mature into meronts, which rupture releasing merozoites then re-infect the red blood cells. In sexual erythrocytic stages some merozoites differentiate into haploid gametocytes.

In mosquito: the gametocytes, including male (microgametocytes) and female (macrogametocytes), are ingested by a mosquito during a blood meal. While in the mosquito stomach, a microgamete penetrate a macrogamete generating a diploid zygote. A zygote mature into the ookinete stage, a 'banana-shaped' motile and elongated form. The ookinete invades and traverses the midgut wall of the mosquito and arrive at the basal membrane of midgut where it develops/transforms into an oocyst. The oocyst grows, ruptures, and releases thousands of sporozoites over a 2-week period. These sporozoites make their way from the hemolymph to the mosquito salivary glands. Inoculation of the sporozoites into a new vertebrate host perpetuates the malaria cycle.

3.2.2.2. Interactions between mosquito and *Plasmodium* ookinete

3.2.2.2.1. Barriers presented by the mosquito midgut

Physical barrier I-peritrophic matrix (PM) (**Figure 25** and **26A, B**)**:** Soon after ingesting a blood meal, mosquito midgut epithelial cells synthesize the peritrophic matrix (PM) that surrounds the blood bolus and separates it from the midgut epithelium. The PM is a thick (1~20 μm) noncellular layer and composed of chitin (ranging from ~1% to 15% by weight) cross-linked by chitin-binding proteins known as peritrophins. The structure of the peritrophic matrix varies between mosquito species but has been demonstrated to present a physical barrier to ookinete invasion and to prevent physical trauma to the delicate microvillar surface of the midgut epithelial cell (Villalon *et al*., 2003).

Physical barrier II-mosquito midgut epithelium: After breaching the PM barrier, the ookinete encounters the mosquito second physical barrier: the midgut epithelium. Mosquito midgut epithelium is composed of a single layer of polarized epithelial cells with their apical

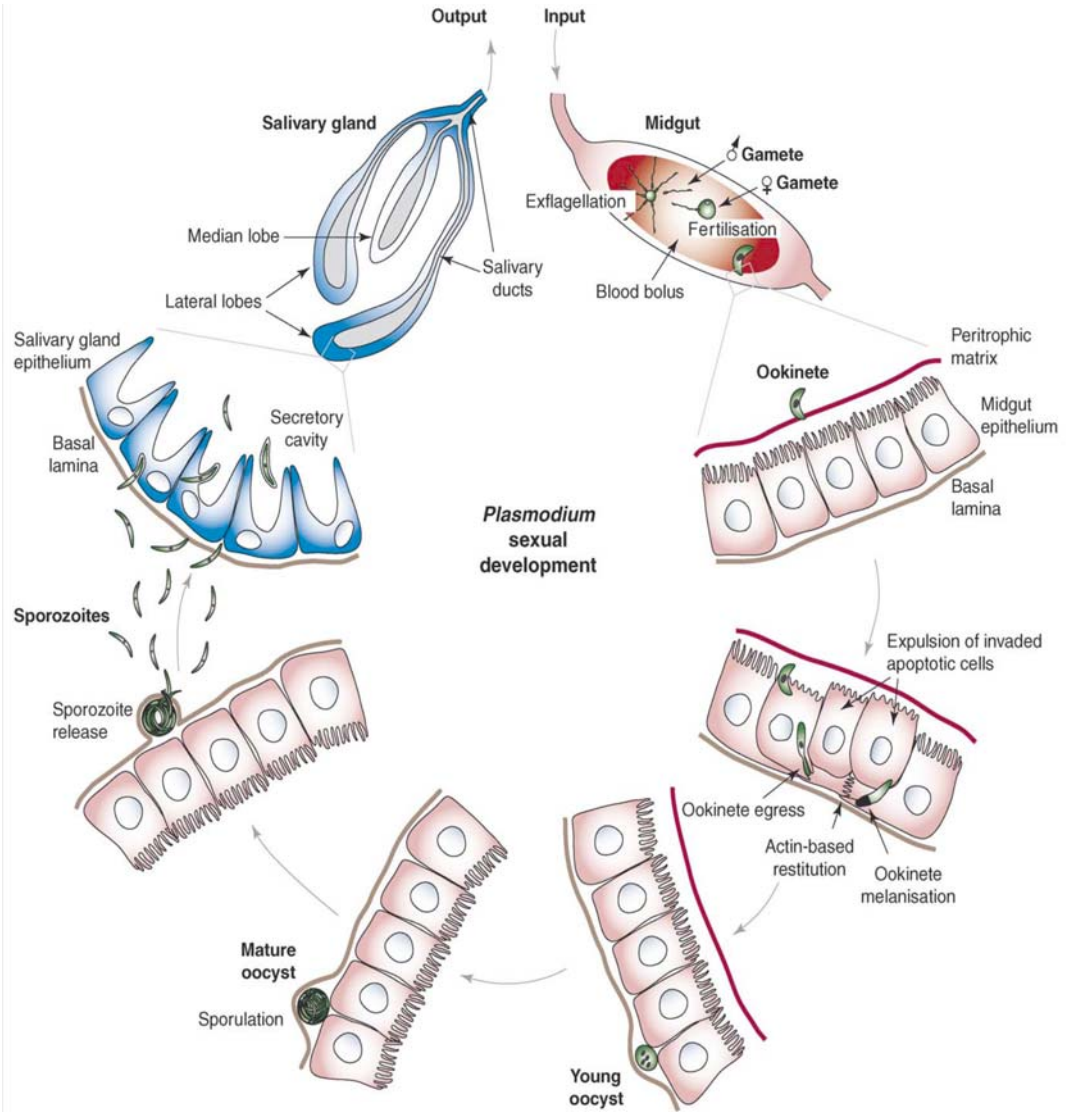

Figure 25. *Plasmodium* development in the mosquito host (Vlachou *et al.*, 2006). *Plasmodium* life cycle in the mosquito starts with a female mosquito bite and blood meal on a malaria-infected vertebrate host. It ends with a new bite approximately three weeks later. Soon after blood feeding, ingested parasite gametocytes produce male and female gametes that fertilise and form the zygotes. Still in the gut lumen, the zygotes transform into motile ookinetes. Approximately one day after blood feeding, the ookinetes traverse the midgut epithelium; the invaded epithelial cells become apoptotic and are extruded from the midgut epithelium. Mosquito immune reactions result in processes, such as lysis and melanisation, mainly mediated by proteins that are present in the mosquito hemolymph. These processes drastically reduce the number of ookinetes that successfully develop to the next parasite stage, the oocyst, on the basal side of the epithelium. Approximately two weeks later-this length of time depends on the parasite-mosquito species combination-multiple nuclear divisions within each oocyst are followed by membrane partitioning and budding off of several thousand haploid sporozoites. Upon oocyst burst, this army of sporozoites is released into the haemocoel; many reach and infect the median and the distal lateral salivary gland lobes. Invasion of the salivary gland epithelial cells is thought to occur through the formation of a parasitophorous vacuole, following the interaction of sporozoites with the basal lamina and invagination of the host cell plasmalemma. A similar parasitophorous vacuole is formed around the sporozoites during their escape from the salivary glad cells into the secretory cavity of the glands. The final act of the parasites in the mosquito is the breakdown of this second vacuole and migration of sporozoites into the salivary ducts, from where they are ejected into a new vertebrate host upon the next mosquito bite.

surfaces folded into a dense array of microvilli. The midgut epithelial cells are connected to each other at their lateral borders by junctional complexes that act as mechanical linkages (i.e. tight and adherent junctions). These junctions are only observed between the apical portions of the cells, and the basal regions appear to be mainly connected only by membrane interdigitation. This arrangement may have profound consequences for the penetration behaviour of *Plasmodium* ookinetes. Because the junctional complexes at the apical surface are rigid, and their integrity is vital to the survival of the cell, the parasite may attempt the mechanically less demanding and damaging process of intracellular penetration of the epithelial cells than intercellular penetration (Abraham and Jacobs-Lorena, 2003; Whitten *et al*., 2006).

Biochemical barriers: The hostile mosquito midgut milieu is a very important biochemical barrier for the *Plasmodium* ookinetes. The mosquitoes secrete high levels of proteases into the midgut and impose the proteolytic damage/pressure to the zygotes and immature/mature ookinetes. Melanization of ookinetes and intra-epithelial lysis of invading ookinetes within the epithelial wall constitute two well-known mechanisms used by the mosquitoes to limit midgut invasion and to reduce the number and quality of invading parasite (Collins *et al*., 1986; Vernick *et al*., 1999). Their underlying molecular mechanisms involve proPO cascade, peroxidase and other biochemical pathways (Kumar *et al*. 2003), as well as innate detection of invading parasites likely mediated by pattern recognition receptors (PPRs) in the mosquito midgut (Dimopoulos, 2003).

3.2.2.2.2. "Tips" of *Plasmodium* ookinete and invasion of the mosquito midgut

Ookinete different morphologies and different motility types: The ookinete must be versatile insofar as it must be able to recognize and cross both cellular and acellular structures during its invasion process. It has been demonstrated that the ookinete is able to adopt a number of different, viable morphologies *in vivo* (**Figure 27**). First, the ookinete must squeeze through an enzymatically digested hole in the peritrophic matrix (**Figure 26**) (Sieber *et al*., 1991; Torii, *et al*., 1992; Vinetz, 2005). Interacting with a structure termed the 'microvilli associated network', and within the midgut lumen and within epithelial cells, the ookinete takes on a variety of elongated, stalked and dumbell-shaped forms (Zieler *et al*., 1998; Vernick *et al*., 1999;

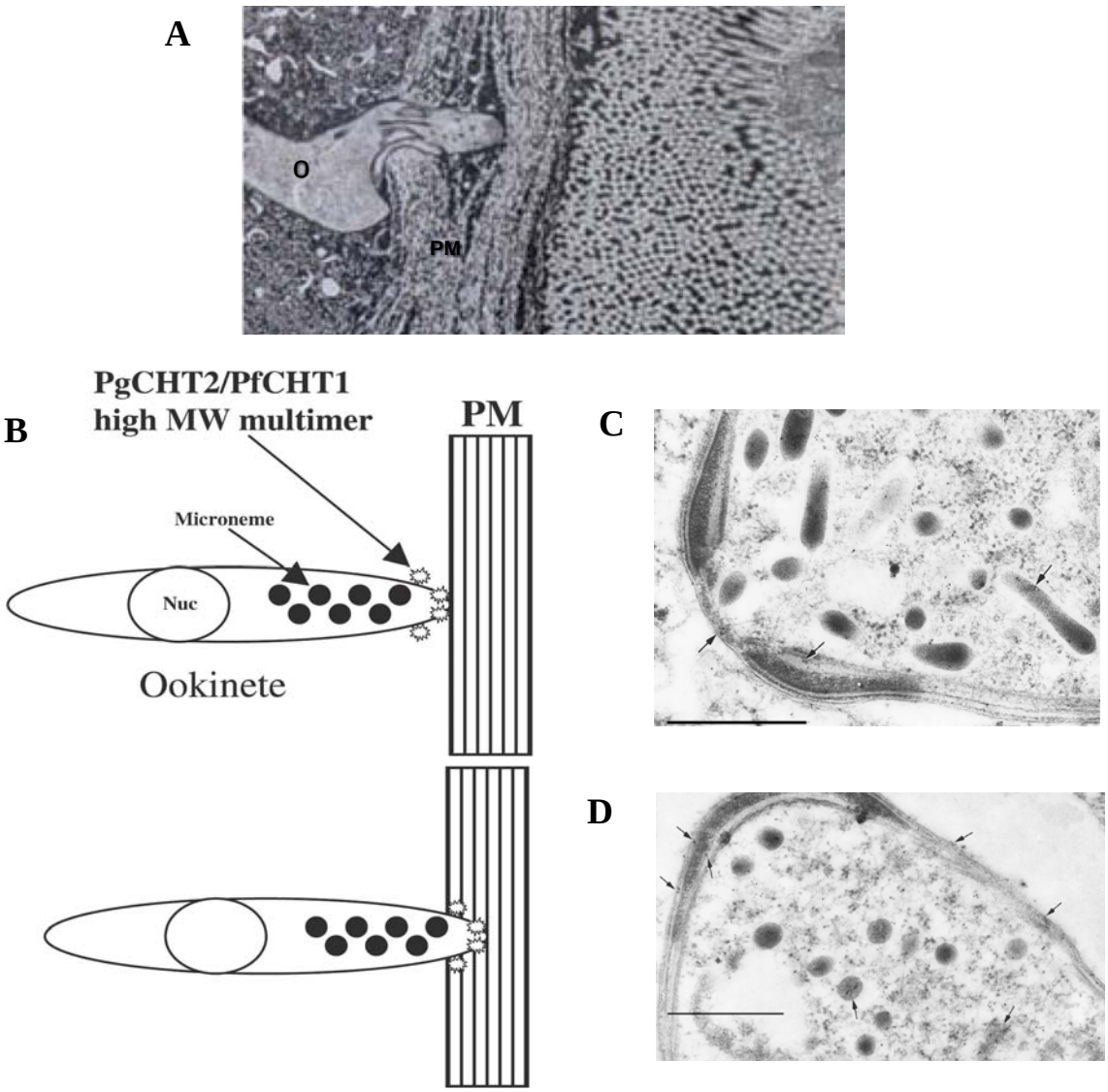

Figure 26. *Plasmodium* ookinete invasion (A), model of interaction with peritrophic matrix (B) and chitinase present on the *Plasmodium gallinaceum* ookinete cell surface (C and D) (Sieber *et al.*, 1991; Vinetz, 2005). **A.** Ookinete penetration of the peritrophic matrix. The parasite is exiting the blood meal and produing chitinase to focally disrupt the peritrophic matrix en route to the microvilli of the midgut epithelial surface. **B.** Proposed model of interaction with peritrophic matrix: a high molecular mass complex containing chitinase (PgCHT2/PfCHT1) might interact with the peritrophic matrix (PM), coupling gliding motility to penetration and crossing of the PM. **C.** Immunoelectron microscopy of *P. gallinaceum* ookinete with mAb1C3, raised against PfCHT1 that recognizes the ortholog chitinase in *P. gallinaceum*, PgCHT2. PgCHT2 is present within micronemes, the apical end of the parasite within the electron-dense region previously identified as part of a protein secretion apparatus, and on the ookinete cell surface (D). PfCHT, *Plasmodium falciparum* chitinase; PgCHT, *Plasmodium gallinaceum* chitinase. Bar, 0.5 μm for C and D.

Vlachou *et al*., 2004). Associated with its differing morphologies, the ookinete displays several types of motility including stationary rotation, translocational spiraling and straight-segment motility (Vlachou *et al.,* 2004). These morphological and functional features are present as the ookinete travels both extracellularly and intracellularly within one or more adjacent midgut epithelial cells.

Ookinete surface and secreted survival/invasion-related molecules (**Table 21**): As a sole identifiable secretory organelle, the microneme of *Plasmodium* ookinete is presumed to constitutively secretes proteins to function within the hostile milieu of the midgut: to resist proteolytic attack, to cross the acellular peritrophic matrix, and to interact with midgut epithelial cells (Han *et al*., 2000). It has shown that the *Plasmodium* ookinete secretes chitinase(s) that punch an "enzymatic hole" and facilitate the movement of the ookinete across the peritrophic matrix (**Figure 26**) (Huber *et al*., 1991; Shahabuddin *et al*., 1993; Vinetz *et al*., 1999 and 2000; Langer and Vinetz, 2001). Interference with the function of *Plasmodium*-secreted chitinase impairs the ability of the ookinete to continue on to the sporogonic forms of the parasite, as demonstrated by chemical interference (Shahabuddin *et al*., 1993), antibody inhibition of chitinase activity (Langer *et al*., 2002), and *Plasmodium* chitinase gene truncation/deletion studies (Dessens *et al*., 2001; Tsai *et al*., 2001). Ookinete-secreted protease(s), acting synergistically with ookinete-produced chitinase, are shown to be important in parasite penetration of the peritrophic matrix (Abraham and Jacobs-Lorena, 2004; Langer and Vinetz, 2001). *P. gallinaceum* plasmepsin (an aspartic protease) can 'drill' a hole in the peritrophic matrix and allow egress of the ookinete from the blood meal towards invasion of the epithelial surface (Vinetiz *et al*., 2005).

***Plasmodium* ookinetes invasion of mosquito midgut**: The mechanisms by which the ookinete recognizes and traverses mosquito midgut epithelial cells are complex and incompletely understood. Ookinetes were observed entering cells through the lateral apical membrane at sites were three cells converged (**Figure 28**). *In vivo*, the ookinete appears to interact with an acellular, network-like matrix on the midgut epithelium microvillar surface termed the microvilli-associated network (Zieler *et al*., 1998). No specific epithelial cell subtype appears to be a target cell for the ookinete (Han *et al*., 2000; Zieler and Dvorak, 2000; Sinden and Billingsley, 2001;

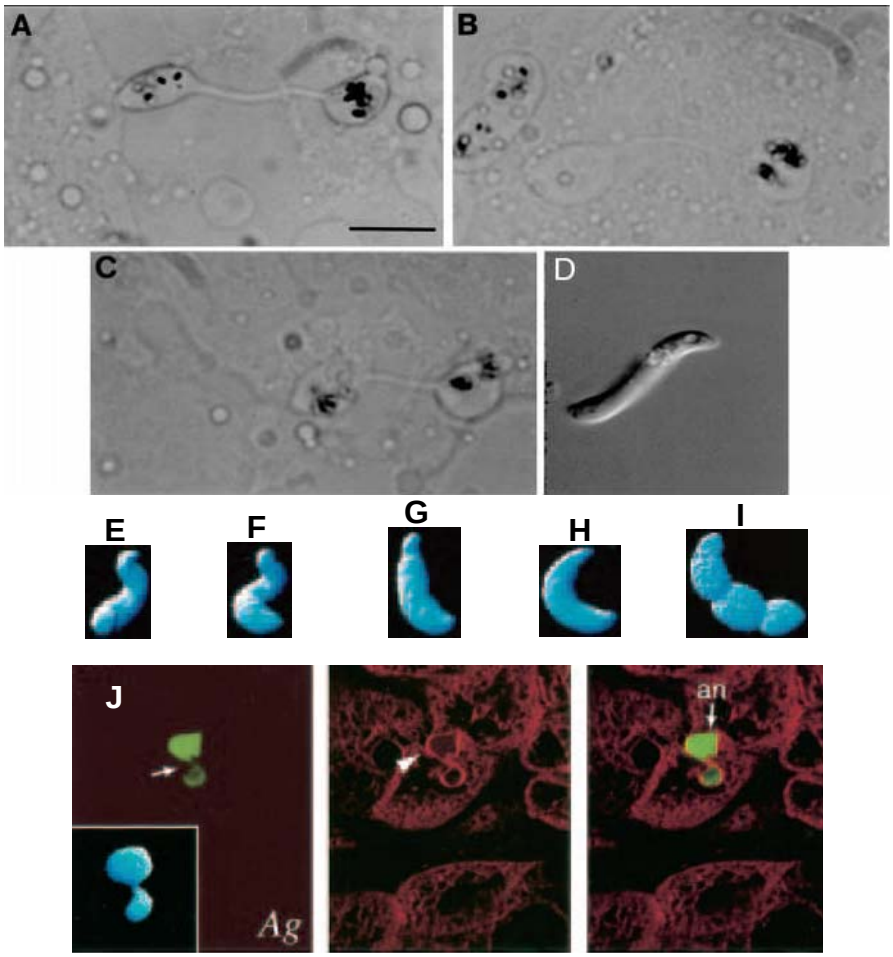

Figure 27. *Plasmodium* ookinete different morphologies (Vernick *et al*., 1999; Vlachou *et al*., 2004). A~D: light micrographs of *Plasmodium gallinaceum* ookinetes in dissected midguts of susceptible *Anopheles gambiae* mosquitoes 30 h post-bloodmeal. Note long stalk separating anterior and posterior portions of ookinetes. In A and C, hemozoin pigment granules are present in anterior and posterior portions of ookinetes. In B, granules are found only in one portion. No granules are seen within the stalks. D, DIC image of a typical non-stalked ookinete, with elongated banana shape and dispersed pigment granules. Size bar, 5 μm , applies to panels A~D; E~I, an ookinete undergoes dramatic shape changes while exiting a midgut cell. E, the ookinete achieves a double corkscrew shape as it starts to exit the cell. F, During this process, strong contortions can be observed. G~H, the parasite is outside of the cell and assumes a crescent shape; I, high-resolution 3D imaging of an ookinete in a living mosquito midgut cells reveals multiple constrictions. J, selected 3D confocal image dataset of living midguts infected with the PbCTRPp-GFP green parasite. Basolateral cell membranes are stained by FM4-64 (red). A constricted ookinete (arrow in the left panel) emerges from the basolateral side of the cell with its anterior end (an) in the extracellular space and the posterior end inside the cell. Inset in the left panel shows a 3D reconstruction of the ookinete. The ookinete is covered by a thick membranous hood (arrowhead), best seen in the singlechannel image of the middle panel.

Vlachou *et al*., 2004). Elegant real-time *in vivo* microscopy studies have demonstrated that the ookinete glides smoothly over the surface of the epithelial cell, before an abrupt engagement occurs between the apical end of the ookinete and an epithelial cell surface with the ookinete plunging into the cell (Vlachou *et al*., 2004). Once in midgut epithelial cells, ookinetes do not form a vacuole and glide freely in direct contact with the cytoplasm of the invaded cell (Meis *et al*., 1989). Just before exiting, ookinetes have been observed gliding on the membrane folds of the basolateral domain of the invaded epithelial cell and egressing the cell through the basolateral intercellular spaces or at three-cell junctions (Zieler and Dvorak 2000). Ookinete invasion resulted in the loss of midgut microvilli, apoptosis of the invaded cell and the degenerated cells budding off into the midgut lumen (Baton and Ranford-Cartwright, 2004).

3.2.2.2.3. Mosquito immune responses to *Plasmodium* ookinetes, oocysts and sporozoites

Mosquito immune responses to *Plasmodium* ookinetes, oocysts and sporozoites include all the above-described insect innate immune defenses. *Plasmodium* cells are challenged by the mosquito complex immune humoral defense mechanisms system like AMP synthesis and the triggering of proPO system and melanization (Collins *et al*., 1986; Christensen *et al*., 2005) and a variety of cellular immune responses mediated by hemocytes such as melanotic encapsulation of oocysts or phagocytosis of sporozoites (Vernick *et al*., 1995; Hillyer *et al*., 2003; Kappe *et al*., 2004; Michel and Kafatos, 2005). The mosquito immune defenses greatly limit the parasite survival so that only a fraction of the 100~1,000 gametocytes transform into tens of ookinetes which then mature into a few oocysts (but one oocyst can produce thousand of sporozoites) (Vinetz, 2005). Finally, only about 20% of sporozoites released from the oocyst can reach the mosquito salivary glands (**Figure 29**) (Kappe *et al*., 2004) and it indicates that a number of sporozoites have been killed by immune defense in the mosquito hemocoele since sporozoites are rarely found attached to other mosquito organs and that they preferentially invade the median and distal lateral lobes of the salivary glands through specific receptor-mediated interaction (Kappe *et al*., 2004; Myung *et al*., 2004).

Invasion of *Anopheles* by *Plasmodium berghei* induced expression of NOS, peroxidase

Table 21. *Plasmodium* ookinete surface and secreted survival/invasion-related molecules

Ookinete molecules	Protein	Function	References
surface molecules	P25 and P28 families	ookinete survival: resistance to proteolytic activity	Tomas *et al*., 2001
	CTRP	ookinete gliding motility	Templeton *et al*., 2000; Yuda *et al*., 1999
secreted molecules	SOAP	ookinete invasion	Dessens *et al*., 2003
	MAOP (perforin family)	ookinete invasion	Kadota *et al*., 2004
	CDPK3	regulating ookinete motility	Ishino, *et al*., 2006
	chitinase	ookinete invasion: 'drilling' an "enzymatic hole" in PM	Dessens *et al*., 2001; Tsai *et al*., 2001
	protease (plasmepsin in *P. gallinaceum*)		Vinetiz, 2005

CTRP, circumsporozoite- and TRAP-related protein; TRAP, thrombospondin-related anonymous protein; MAOP, membrane-attack ookinete protein; SOAP, secreted ookinete adhesive protein; CDPK, calcium-dependent protein kinase; PM, peritrophic matrix.

activity and tyrosine nitration, but these reactions were not observed when *Anopheles aegypti* or *Anopheles stephensi* were invaded by *P. gallinaceum* (Gupta *et al*., 2005), indicating that the immune responses of different mosquito-parasite combinations are not the same. Induction of nitric oxide synthase (NOS) plays an important role in limiting parasite survival (Luckhart *et al*., 1998). 2-Cys peroxiredoxin (AsPrx-4783), an enzyme known to detoxify reactive nitrogen oxide species (RNIs), is induced in the *A. stephensi* midgut by parasite infection to protect midgut cells against the toxicity of NO (nitric oxide)-mediated defense response (Peterson and Luckhart., 2006).

The first reported putative PRR of *Anopheles gambiae*, aboved-mentioned thioester-containing protein TEP1 secreted by mosquito haemocytes, binds to the surface of *P. berghei* ookinetes, triggers melanization and promotes ookinete killing and lysis in the basal labyrinth of the midgut epithelium (Blandin *et al*., 2004). A Leucine-Rich Repeat Immune Protein 1 (LRIM1), was recently identified as a participant in the *A. gambiae-P. berghei* antiparasitic responses. Melanization of dead ookinetes appears to be LRIM1-dependent (Whitten *et al*., 2006) (**Figure 30**). The expression of *SRPN6*, a member of the serine protease inhibitor (serpin) family, is strongly induced in both *A. stephensi* and *A. gambiae* midguts during ookinete invasion. SRPN6 acts in synergy with CTL4 (C-type lectin) (see 3.1.2.2.4. section) as a component of the midgut epithelial immune-response system (proPO system) (Abraham *et al*., 2005).

3.3. Insect-microsporidia interactions

Microsporidia have been described from all insect orders. Almost half of the 143 described genera and over 1200 species of microsporidia have insects as hosts. The genera of microsporidia with an insect as the type host are present by insect order in **Table 22** (Wittner and Weiss, 1999; Becnel and Andreadis, 1999). Compared to the Apicomplexa parasites or the human-pathogenic microsporidia, the microsporidia in insect hosts and microsporidia-insect interactions *in vivo* are very poorly understood.

Microsporidia infection of insect can be tissue-/cell type-specific or systemic (Becnel and Andreadis, 1999; Solter and Becnel, 2000; Johny *et al*., 2006). The infected larvae and pupa are typically stunted. Overt signs of infect in larvae include the formatiom of dark spots, or areas on

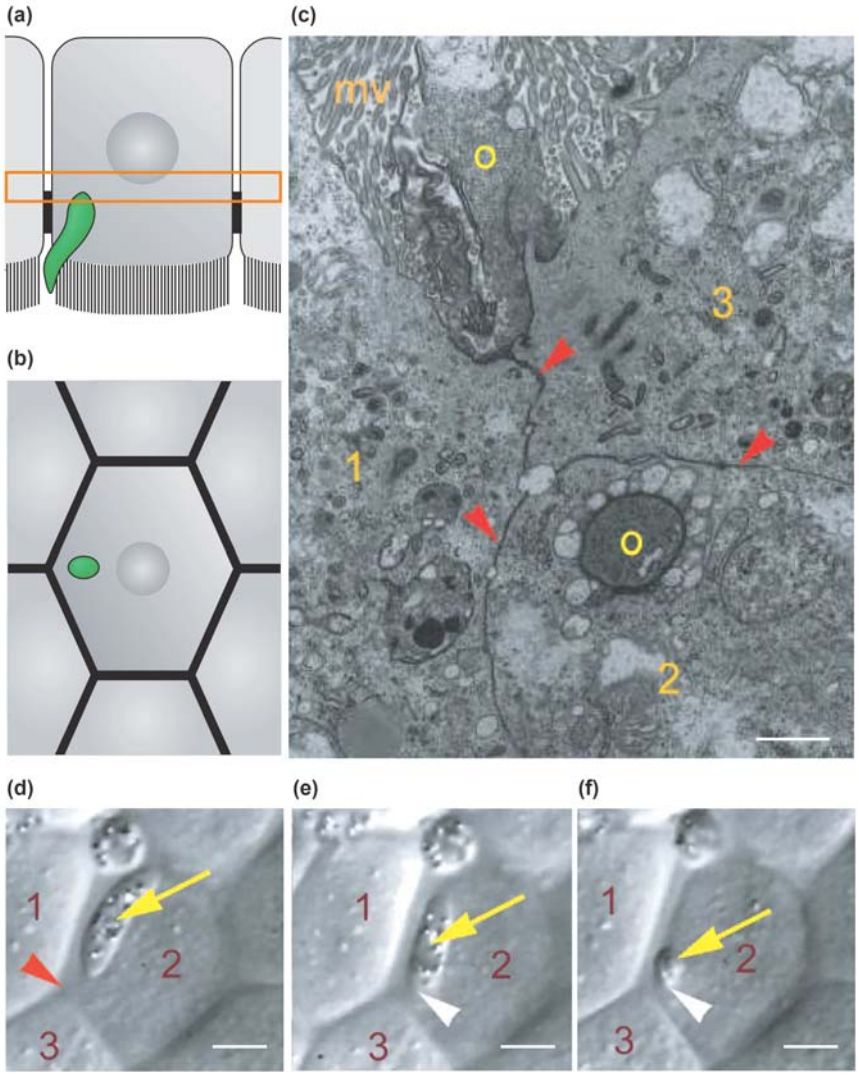

Figure 28. Ookinete entry into midgut epithelial cells (Baton and Ranford-Cartwright, 2005). (a): Ookinetes enter midgut epithelial cells through the lateral apical membrane at sites where three adjacent epithelial cells converge. (b): A cross-section through the plane boxed in orange in (a) (the ookinete is coloured green). Re-interpretation of previously published observations also suggests ookinete entry occurs at such sites. (c): Electron micrograph of an ookinete of the rodent malaria parasite *Plasmodium yoelii nigeriensis* entering the midgut wall of *Anopheles omorii*. This ookinete (o) is invading intracellularly where three epithelial cells (numbered 1, 2 and 3) appear to converge. The lateral membranes (red arrowheads) of the epithelial cells are visible. Part of the ookinete resides within the middle epithelial cell (2), surrounded by vacuoles, whereas part of the ookinete is extracellular within the microvilli (mv). (d–f): Light micrographs using differential interference contrast, looking down onto the apical surface of the midgut wall, showing sequential temporal stages of an ookinete of the avian malaria parasite *Plasmodium gallinaceum* entering the midgut wall of *Aedes aegypti*. Yellow arrow indicates the ookinete. Red arrowhead indicates site where the lateral membranes of three adjacent epithelial cells (1, 2 and 3) converge. White arrowhead indicates the entry site of the ookinete, which is moving downwards, into one of the epithelial cells (2). Scale bars=1μm (c); 5 μm (d–f).

the cuticle that often appear puff in comparison to the healthy individual. The two most commonly infected insect tissues are the fat body and midgut epithelium. The infected midgut cells is porcelain-white. The infected fat body tissue is often lobate and also porcelain-white (Becnel and Andreadis, 1999).

3.3.1. Microsporidia-induced insect immune reponses

3.3.1.1. Non-cellular or humoral immune reponses

The microsporidia-induced most typical insect defense reaction is the melanization of spores released into the hemolymph (Becnel and Andreadis, 1999). The infection of *Lymantria dispar* (*Lepidoptera*) larvae with different microsporidia, induced a significant activation of the prophenoloxidase (proPO) system leading to melanization. The activation was highest when the pathogen caused heavy infections of the fat body, which was the case with two microsporidia originally isolated from *L. dispar*. Infection of only the silk glands or light infection of the fat body by two *Vairimorpha* spp. from other *Lepidoptera*n hosts elicited a lower response (Hoch *et al*., 2004).

Proteome analysis of *Aedes aegypti* larvae exposed to the microsporidian *Vavraia culicis* have showed that proteins induced or suppressed during the infection by *V. culicis* are linked directly or indirectly to the immune defense against invading microorganisms and indicates that *A. aegypti* larvae try to control or clear *V. culicis* infection (Biron *et al*., 2005a). The induction of a peritrophic matrix protein suggested that *A. aegypti* larvae had detected the presence of a pathogen and were actively investing in protection against infection by reinforcing this physical barrier and reduce the chances of further infection. The induced expression of odorant binding proteins (OBP) was also notable. Some OBPs are thought to play a role in recognizing or neutralizing viral and bacterial infections, and Levy *et al* (2004) found one OBP to be particularly over-expressed in response to a fungal infection. This latter result is of special interest given the phylogenic proximity of microsporidia and fungi. Other known immune constitutive proteins with a modified expression in infected *A. aegypti* larvae include protease inhibitor, serine protease, serine/threonine phosphatase, actin, thioester-containing protein (TEP),

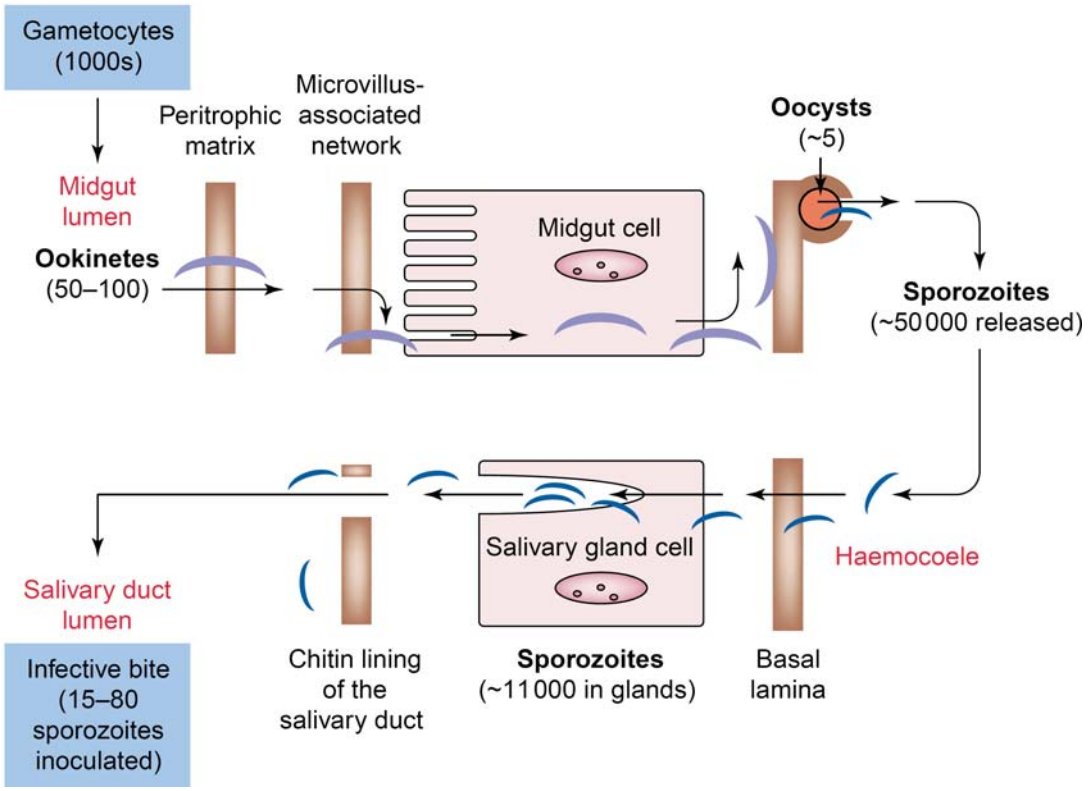

Figure 29. The passage of *Plasmodium* through the mosquito vector, indicating the barriers to be crossed (both cellular epithelia and extracellular matrices) and the parasite numbers commonly found at each stage of development (Sinden and Billingsley, 2001).

NF-kB, Gasp (precursor), phosphatidyl-ethalolamine binding protein (PEPB), alcohol dehydrogenase, glutathione-Stransferase (GST). The analysis of differential expression for six proteins involved in the L-arginine and L-ornithine metabolic pathways indicate that *V. culicis* probably impairs the immune defense of its host via arginases-NOS competition. However, not all changes in protein expression were necessarily due to the host as some of the proteins involved in cell maintenance may have actively been manipulated by the parasite (Biron *et al*., 2005b). Scanlon *et al* (2000) have suggested that microsporidia actively arrest mitosis and division of host cells to maintain the integrity of their cellular environment.

3.3.1.2. Cellular mediated immune reponses

3.3.1.2.1. Nodule formation and encapsulation

The earliest report of immune responses of insects to microsporidian infection is the hemocytes reaction of the tobacco hornworm *Manduca sexta*, to the microsporidian *Nosema sphingidis*. Nodule formation on the posterior portion of the midgut epithelium was detected within 24 hr post-exposure to spores. By 120 h, the inflammatory response was striking, with extensive nodule formation at the site of infected midgut cells labial glands, Malpighian tubules, and adipose tissue. In the late stages of infection, the posterior portion of the midgut was extensively deranged, with intense hemocytic infiltration and melanization (Brooks, 1971). One *Vairimorpha* species induced a significant increase in total numbers of *Lymantria dispar* (L.) larvae hemocytes while the other microsporidian infections led to temporarily decreased numbers. Microscopic examinations showed that parts of infected tissue were encapsulated by hemocytes (Hoch *et al*., 2004).

3.3.1.2.2. Phagocytosis and how can phagocytosed spores invade other insect cells?

It has been shown that insect hemocytes can phagocytose microsporidian spores. *Paranosema grylli* spores are reported to be quickly phagocytized by *Gryllus bimaculatus* (Orthoptera) hemolymph-derived hemocytes incubated *in vitro* (Nassonova *et al*., 2001). After 12h of co-incubation, the index of phagocytosis (average amount of spores per phagocyte) was

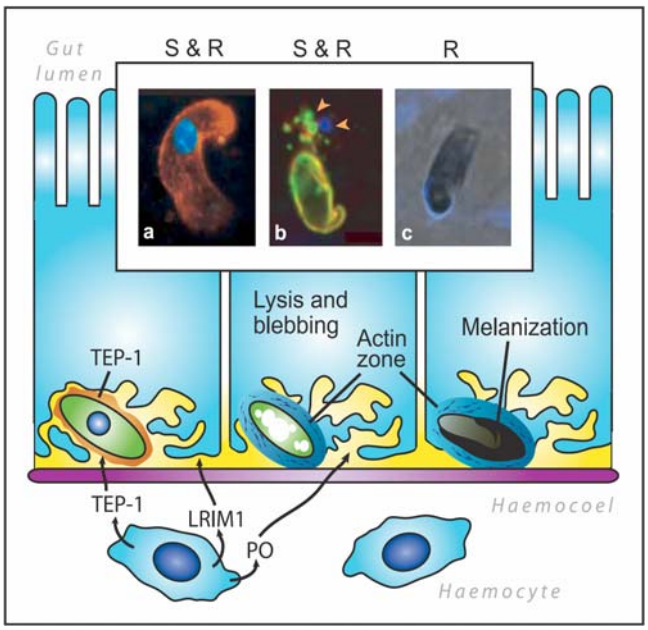

Figure 30. Killing and clearance events in the *A. gambiae* midgut in response to *P. berghei* infection (Whitten *et al.*, 2006). The soluble factors TEP1, LRIM1 and components of the phenoloxidase (PO) cascade all originate from the haemocoel, and are secreted by haemocytes into the midgut to play key roles in these events. Left panel: ookinetes are bound by TEP1 in the midgut extracellular space in both susceptible (S) and refractory (R) mosquitoes, resulting in lysis of the parasite (middle panel) by an as yet uncharacterized mechanism. LRIM1 also enhances killing. Later *TEP1* expression probably replenishes the spent protein. In R mosquitoes, the phenoloxidase (PO) cascade initiates in the haemocoel and results in melanotic encapsulation of the dead ookinete (right panel). Actin polymerization in the basal labyrinth serves to envelope dead or dying lysed parasites in both R and S mosquitoes, and melanized parasites in R mosquitoes (middle and right panels). Melanization and actin polymerization are probably clearance events. Box a: 3-D reconstruction of confocal sections demonstrating TEP1 binding (orange channel) to an ookinete (nucleus, blue channel). Box b: an ookinete undergoning lysis and labelled with TEP1 (green channel) in an S strain mosquito. Membrane blebs are of parasite origin as evidenced by the presence of P28 (closed arrowhead, red channel). Note also the eccentric nucleus (blue channel, arrowhead). Box c: merged phase contrast and confocal image of a melanized ookinete surrounded by a zone of polymerized actin (blue channel, phalloidin staining).

2.38. The hemocyte phagocytosis is suspected to play the most essential role in *P. grylli* spore internalization. When exposed to *P. grylli*, *G. bimaculatus* hemocytes produce long cytoplasm protrusions and form clamps. Some spores adhere to the hemocyte surface and are phagocytized. Giant round cells loaded with spores can be observed in the host hemolymph. They are surrounded by a sheath composed of flattened cells and resemble xenomas. The infection significantly reduced the phenoloxidase (PO)-positively stained cells. Based on their analysis, Sokolova *et al* (2000) summarized that microsporidia do not suppress such cellular immune reactions as a clamp formation and phagocytosis of spores liberated from the infected tissue while at the same time they suppress activities of enzymes involved in immune response.

Besides the infection by microsporidian "syringe-like" polar tube extruding from the spores and penetrating the membranes of insect host cells, the above studies have shown that microsporidia also gain access to insect host cells by phagocytosis. After phagocytosed, microsporidian spores are able to prevent acidification of the phagosomes they reside in (Nassonova *et al*., 2001; Tokarev *et al*., 2005). The prevention of acidification is important for microsporidian survival in phagosome. Kurtz *et al* (2000) demonstrated that *Vairimorpha sp.* spores fluorescently labeled with fluorescein isothiocyanate (FITC) were efficiently phagocytosed by hemocytes (mainly plasmatocytes and granular cells) of *Plutella xylostella* (*Lepidoptera*). An additional DNA staining with 4,6-diamidino-2-phenylindole (DAPI) showed that the ingested spores contained DNA and were not only empty spore walls. These studies suggest that hemocytes, which are mobile within the insect body cavity, probably mediate the spread of infection to all susceptible tissues and also confirmed that in insects after phagocytosis, the spore uses it polar tube to escape from the phagosomes, thus releasing the infective sporoplasm into the host cell cytoplasm (Franzen, 2004) (**Figure 6**).

3.3.2. *Bombyx mori-Nosema bombycis* interactions

With the *Bombyx mori* as type host, *Nosema bombycis* can infect more 30 species of *Lepidoptera* (Kashkarova and Khakhanov, 1980; Canning, 1993).

Generally, *B. mori-N. bombycis* interactions are still less understood. What happens in *B.*

Table 22. The genera of microsporidia with an insect as the type host present by insect order
(Wittner and Weiss, 1999)

Insect order	No. of microsporidian genera	Microsporidian genus or genera
Diptera	42	*Amblyospora, Bohuslavia, Campanulospora, Caudospora, Chapmanium, Coccospora, Cristulospora, Culicospora, Culicosporella, Cylindrospora, Edhazardia, Evlachovaia, Flabelliforma, Golbergia, Hazardia, Helmichia, Hessea, Hirsutusporos, Hyalinocysta, Janacekia, Merocinta, Napamichum, Neoperezia, Octosporea, Parathelohania, Pegmatheca, Pernicivesicula, Pilosporella, Polydispyrenia, Ringueletium, Scipionospra, Semenovaia, Spherospora, Spiroglugea, Striatospora, Systenostrema, Toxoglugea, Toxospora, Trichoctosporea, Tricornia, Vavraia,Weiseria*
Coleoptera	5	*Anncaliia, Canningia, Chytridiopsis, Endoreticulatus, Ovavesicula*
Ephemeroptera	5	*Geusia, Mitoplistophora, Stempellia, Telomyxa, Trichoduboscqia*
Lepidoptera	4	*Cystosporogenes, Nosema, Orthosomella, Vairimorpha*
Trichoptera	3	*Epriseptum, Issia, Tarrdivesicula*
Orthoptera	2	*Heterovesicula, Johenrea*
Odonata	2	*Nudispora, Resiomeria*
Siphonaptera	2	*Nolleria, Pulcispora*
Collembola	1	*Auraspora*
Thysanura	1	*Buxtehudea*
Hymenoptera	1	*Burenella*
Isoptera	1	*Duboscqia*
Total	69	

mori upon *N. bombycis* infection, how *N. bombycis* spores traverse the peritrophic matrix, how they access to and interact with the midgut epithelium microvillar surface (microvilli-associated network), whether they invade midgut epithelial cells mainly by spore germination, by host cell phagocytosis or both , if there is one or more specific epithelial cell subtypes to be their target cells, how they can disseminate to hemocoele and other tissues, still remain to be characterized.

Results

Results I

4. Microsporidian-insect interactions *in vivo*: *Nosema bombycis* ISC-ZJ complete TEM life cycle and its dissemination route in *Bombyx mori*-Role of *B. mori* hemocytes

(To submit to "*Journal of Invertebrate Pathology*")

4. Microsporidian-insect interactions *in vivo*: *Nosema bombycis* ISC-ZJ complete TEM life cycle and its dissemination route in *Bombyx mori*-Role of *B. mori* hemocytes

4.1. Introduction

The unicellular and eukaryotic Microsporidia, defined by their formation of a small resistant spore, are a large group of obligate intracellular (Sprague and Vávra, 1977; Sprague *et al*, 1992; Sprague and Becnel, 1998, 1999) and fungi-related parasites (Weiss *et al*., 1999; Keeling, 2003; Thomarat *et al*., 2004). They can infect all major animal groups ranging from protists to mammals (Wittner, 1999) by their distinctive spore germination in addition to phagocytosis (Franzen, 2004) and inflict great economic losses to the breedings of economic animals (Wittner and Weiss, 1999; Wasson and Peper, 2000). *Nosema bombycis*, the first identified microsporidian (Naegëli, 1857), is the causative agent of the silkworm *Bombyx mori* epidemic "pepper disease" or pebrine, which nearly destroyed the silkworm industry of Europe in the middle of the 19th century (Sprague and Vávra, 1977; Wittner, 1999; Legay and Chavancy, 2004). Pasteur's landmark studies firstly proved that *N. bombycis* can be transmitted both horizontally and transovarially in *B. mori* and developed an effective practical method of control (Pasteur, 1870).

Since then, the further studies of *N. bombycis* are limited to biology, histopathology, immunological studies (Ishihara and Sohi, 1966; Ishihara, 1968; Kawarabata and Ishihara, 1984; Kawarabata and Hayasaka, 1987; Ke *et al*., 1990; Kawarabata, 2003), and recent molecular phylogeny (Wang *et al*., 2001; Rao *et al*., 2004, 2005) which are essential for a correct species identification of *N. bombycis*; or ultrastructural descriptions of its mature spore (Sato *et al*., 1982) and *N. bombycis* life cycle model (Kawarabata and Ishihara, 1984; Iwano and Ishihara, 1989, 1991a, b).

Of different geographical major reference strains of *N. bombycis* in the world (Wang *et al*., 2001; Kawarabata, 2003; Rao *et al*., 2005), Japanese strain *N. bombycis* NIS-001 life cycle model has been proposed mainly based on *in vitro* studies by light microscopy (Kawarabata and Ishihara, 1984) and the *in vitro* and *in vivo* ultrastructual observations of sporogonial dimorphism

(Iwano and Ishihara, 1989, 1991a, b): *N. bombycis* is diplokaryotic, disporoblastic and apansporoblastic, developed in direct contact with the host cytoplasm throughout all its life cycle. *N. bombycis* complete life cycle present three different phases: the environmental phase-*N. bombycis* dormant and resistant environmental spore, which can be activated to evert its polar tube, inject the infectious sporoplasm to host cell and initiate its parasitism; and two proliferative intracellular phases which multiply by binary fission, namely merogony and sporogony. Sporogony is characterized by their production of both the primary spores which are characterized by their thin wall, short polar filament and spontaneous germination *in vivo* and environmental spores equipped with a thick wall and long polar tube (called "sporogonial dimorphism"). However except the primary spore and environmental spore of *N. bombycis* NIS-001 (Iwano and Ishihara, 1989, 1991a, b), an electron microscopy investigation *N. bombycis* complete life cycle *in vivo*, including that of Chinese reference strain *N. bombycis* ISC-ZJ in this study, has not been conducted.

The peroral infection of silkworm larvae with *N. bombycis* NIS-001 has been demonstrated to start in the midgut epithelium and surrounding muscles (Sato and Watanable, 1986). The primary spores formed in the silkworm midgut epithelium, which can spontaneously germinate *in vivo*, are considered to be the source of spreading parasite infection within the host and result in the severe and complete infection of silkworm larvae in the end (Iwano and Ishihara, 1991a, b). However, since their polar tube is so short that arranged into only 3~4 coils in the spore (Iwano and Ishihara, 1991b), how *B. mori* other tissues and organs beyond their reach can be infected by *N. bombycis* primary spores formed in the midgut epithelial cells still needs elucidation.

On the other hand, the foreign microorganism invasion of insects including *B. mori* can elicit their robust innate immune responses, which involve humoral and cellular components (Lavine and Strand, 2002). Of these, the phenoloxidase-based melanization of spores released into the hemolymph is the most typical insect humoral defense reaction induced by microsporidian (Becnel and Andreadis, 1999). The hemocyte-mediated cellular immune responses to microsporidian invasion, including phagocytosis, encapsulation and nodule formation have also been reported (Brooks, 1971; Nassonova *et al*., 2001; Hoch *et al*., 2004 ; Tokarev *et al*., 2005). So far, *B. mori* immune responses studies mainly focused on those elicited

by injected bateria and yeast or their wall components: the induced synthesis of antimicrobial peptides (Yamakawa and Tanaka, 1999; Tanaka *et al*., 2005), the phenoloxidase-melanization pathway (Ashida *et al*., 1988; Ashida, 1990; Asano and Ashida, 2001); hemocyte-mediated immune responses (Akai and Sato 1973; Beaulaton 1979; Wago 1991; Ling *et al*., 2005 a). *B. mori* hemocytes are highly immunoreactive cells and mediate important cellular immune responses such as phagocytosis, nodule formation and encapsulation (Kotani *et al*., 1995; Koizumi *et al*., 1997, 1999; Ochiai and Ashida, 2000; Ohta *et al*., 2006). Unfortunately, very little is known about *B. mori* immune reactions to *N. bombycis* infection and the roles of *B. mori* immune reactions especially hemocyte-mediated immune responses in *N. bombycis* dissemination *in vivo*.

The objective of the present research is thus to characterize *N. bombycis* ISC-ZJ life cycle *in vivo* at the ultrastructural level and to better understand its *in vivo* dissemination and interactions with *B. mori.*

4.2. Materials and methods

4.2.1. **Nosema bombycis** *spore and its polyclonal antibody production*

Nosema bombycis (Zhenjiang isolate, named *Nosema bombycis* ISC-ZJ) spores [(3.59 ± 0.16) µm × (2.07 ± 0.12) µm] were produced and purified as previously described (Wang *et al*., 2001). Briefly, they were harvested from infected larvae of its natural host, the silkworm *Bombyx mori* (75xin×7532 strain). Third instar larvae were exposed for 8h to mulberry leaves previously immersed in a *N. bombycis* spore suspension (5000 spores/mL). Heavily infected larvae were crushed in distilled water and large silkworm and mulberry debris were removed by filtration on 4 cheesecloth layers. After centrifugation (300×g, 15 min), spores were washed in distilled water until the pellet was white. Spores were further purified on an incontinuous sucrose gradient with equal volume of 30%, 40% and 60% sucrose where they concentrated as a thin band between the 40% and 60% sucrose fractions. After washes in distilled water, the parasite fraction purity was checked by phase-contrast microscopy and fluorescent microscopy after DAPI staining.

For polyclonal antibody (PAb) production, the purified *N. bombycis* spores were fixed with 4% formaldehyde. Every two weeks, SWISS mice (Charles River, France) were injected intraperitoneally with these fixed spores homogenized in Freund's adjuvant (complete for the

first injection and incomplete for the four next ones). Serum was collected 2 weeks after the last injection and stored at -20°C. The animal house (agreement B63014.5) and the experimental staff (agreement 63-146) have been approved by the French veterinary services, and experiences were conducted according to ethical rules.'

4.2.2. Bombyx mori *rearing and infestation by* Nosema bombycis

The eggs of *Bombyx mori* (Indian polyvoltin strain Nistari) and silkworm artificial diet powder (Italian) were kindly provided by Dr. Gérard Chavancy of Unité Nationale Séricicole, INRA (La Mulatière, France). The artificial diet were prepared by adding distilled water to artificial diet powder (26ml ddH_2O:10g powder) and sterilized at 105°C for 30 min. After hatching, *Bombyx mori* larvae were fed with the sterilized artificial diet and reared at a temperature of 25±1 °C, 60%~70% humidity, and a 16 h/8 h light / dark photoperiod.

Different concentrations of purified *Nosema bombycis* spores (10^4~10^6 spores/gram diet) were either mixed with sterilized artificial diet or smeared on the surface of artificial diet. The second, third and fourth instars of *Bombyx mori* larvae were perorally inoculated by feeding with the *N. bombycis* spore-treated diet for 8h. Then they were fed with the sterilized artificial diet and reared as previous described.

4.2.3. Detection of Nosema bombycis *in* Bombyx mori *intestine and other tissues*

4.2.3.1. Intestine cryosections preparation for transmission electron microscopy.

The intestine focus of infected *Bombyx mori* larvae were dissected into small pieces (2~3 mm× 2~3mm) and fixed with 4% paraformaldehyde and 0.1% glutaraldehyde in 0.1M phosphate buffer pH 7.2 for 1~2h. After three PBS washes, the samples were impregnated with a cryoprotective agent (25% glycerol, 5% DMSO in phosphate buffer) and frozen in pasty nitrogen before storage in liquid nitrogen. 90 nm ultrathin sections were performed using a Leica Ultracut ultramicrotome equipped with FCS system. The FCS sections were picked up on collodion -coated nickel grids and stored on 2.3M sucrose. These sections were embedded directly with 0.5% aqueous uranylacetate and 1.6% methylcellulose for 10 min, left to dry and then observed with a JEOL 1200EX transmission electron microscope.

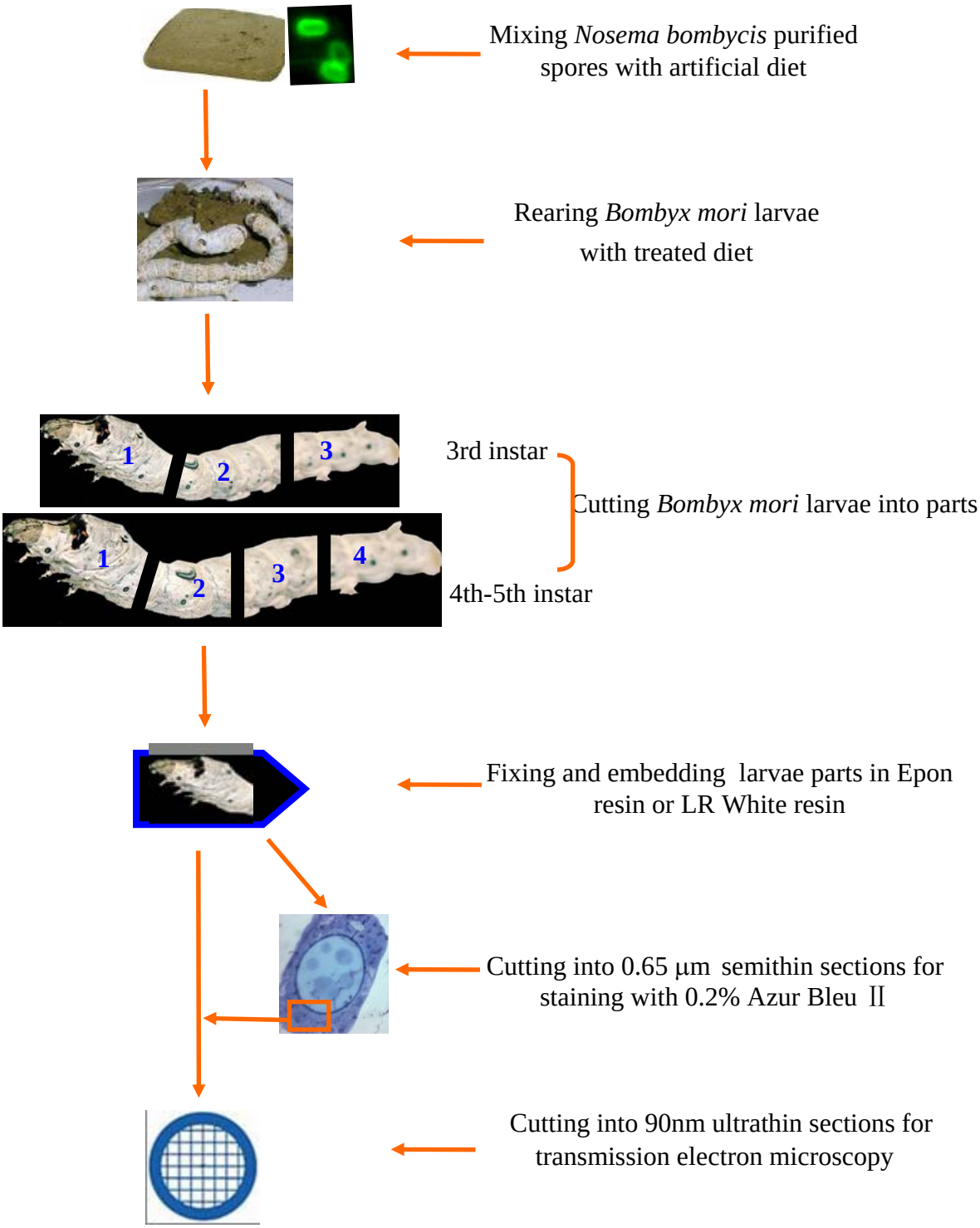

Figure 31. Protocol followed for the study of *Bombyx mori-Nosema bombycis* interaction *in vivo*

4.2.3.2. Embedding of infected Bombyx mori *larvae in Epon resin*

The infected larvae (from the 3rd to 5th instar) were cut into three or four parts (**Figure 31**) and each part was fixed independently. After 1~2 h of fixation in 0.07 M cacodylate buffer (CB, pH7.4) containing 2% glutaraldehyde, 0.05% ruthenium red, the samples were washed in 0.07 M cacodylate buffer (pH7.4) 2 times for 1h and postfixed with 4% OsO_4 in 0.07 M cacodylate buffer (pH7.4) for 1h. They were then dehydrated in increasing ethanol concentrations: 50% ethanol 3×5min; 70% ethanol 3×10min; 90% ethanol 3×20 min; 100% ethanol 3×20 min. The dehydrated samples were then infiltrated with 100% propylene oxide 3×20 min and increasing concentrations of Epon embedding medium (prepared as following) in propylene oxide at room temperature (RT) as follows: 50% Epon for 24 h; 100% Epon for 24 h. Polymerization was performed at 50℃ for 3 days in fresh 100% Epon. The Epon embedding medium was prepared by mixing solution A [Embed 812:DDSA (dodecenyl succinic anhydride) (v/v) = 81:100] and solution B [Embed 812: NMA (nadic methyl anhydride) (v/v) = 81: 89] in a v/v =1/1) and adding 1.7% DMP-30 [2,4,6-Tris (dimethyl-aminomethyl)-phenol].

4.2.3.3. Embedding of infected Bombyx mori *larvae in LR White resin*

The infected larvae (from the 2rd to 3th instar) were cut into two or three parts (**Figure 31**). After fixation overnight at 4℃ in 4% paraformaldehyde, 0.1 M phosphate buffer (pH 7.2), the larval samples were rinsed in 0.1 M phosphate buffer (pH 7.2) 6 times for 10 min and then dehydrated in increasing ethanol concentrations at 4℃: 50% ethanol 3×5min; 70% ethanol 3 × 15 min; 100% ethanol 3×20 min. After dehydration, tissues were infiltrated with increasing concentrations of LR White resin (Agar scientific, R1281) at -20℃ as follows: 100% ethanol /resin (v/v = 2/1) 2×15 min; then 100% ethanol : resin (v/v = 1/2) for 15 min; 100% LR White for 1h; fresh 100% LR White for 24 h. Embedding was then performed in fresh 100% LR White and polymerized over UV light at -20℃ for 3 days.

4.2.3.4. Azur Blue staining and transmission electron microscopy (TEM) of resin blocks

For Azur Blue staining, 0.65 μm semithin sections from the infected *Bombyx mori* larvae embedded in Epon resin and LR White resin were performed using a Leica Ultracut ultramicrotome. Sections were picked up individually, transferred to a droplet of 5% ethanol on a

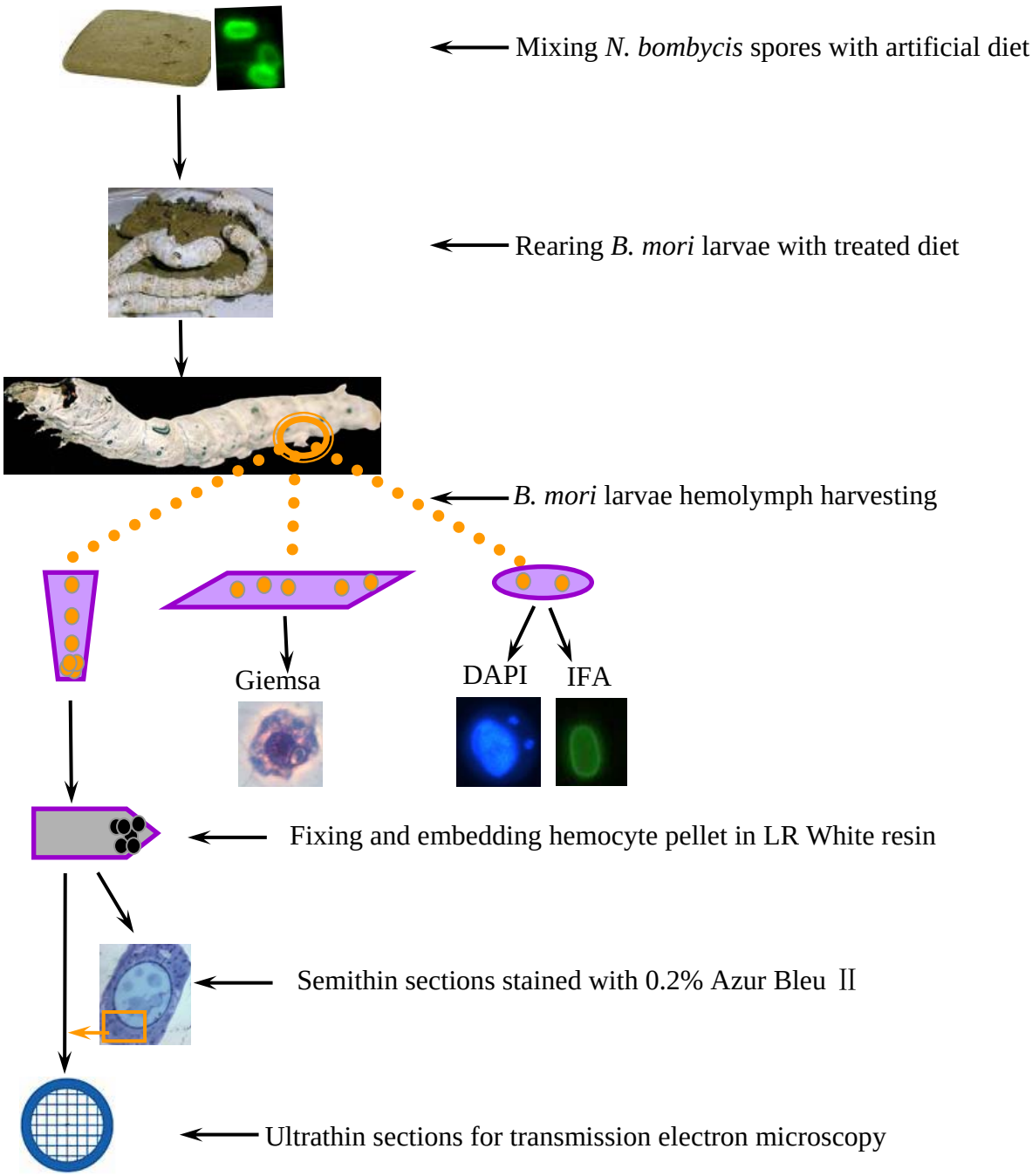

Figure 32. Protocol followed for the study of interactions between *Nosema bombycis* and silkworm hemolymph and hemocytes *in vivo*

glass slide, and dried on a hotplate for 20 min. The slides were stained with 0.2% Azur Blue II (pH 8.5) for 2~5 min. The slides were directly observed with a Leica DMIRB microscope.

For transmission electron microscopy (TEM), 90 nm ultrathin sections from the infected *Bombyx mori* larvae embedded in Epon resin and LR White resin were obtained using a Leica Ultracut ultramicrotome and picked up on collodion-coated nickel grids. For ultrastructure observation, the sections were directly stained with 2% uranyl acetate for 5 min.

4.2.4. Detection of Nosema bombycis *in* Bombyx mori *hemolymph and hemocytes*

4.2.4.1. Bombyx mori *hemolymph harvesting* (Figure 32)

For the optic and fluorescent microscopy, hemolymph of naïve and infected *Bombyx mori* 3^{rd}~5^{th} larvae was harvested by cutting the abdominal legs or the tail horn of caterpillar. Samples were either directly coated on the glass slides or stored in insect phosphate saline (IPS) (150 mM NaCl, 5 mM KCl, 4 mM $CaCl_2$).

For transmission electron microscopy, hemolymph was perfused directly into microfuge tubes containing 6% paraformaldehyde and 0.75% glutaraldehyde in 0.1M phosphate buffer pH 7.2. During the course of hemolymph collection the fixative was diluted 2:3, such that by the end of the procedure it was 4% paraformaldehyde and 0.25% glutaraldehyde. The hemolymph were allowed to fix for 5~6h.

4. 2. 4. 2. Giemsa staining and DAPI staining

The hemolymph coated on glass slides was fixed in 100% methanol for 10 min at room temperature. These slides were either stained with Giemsa staining solution (Sigma) for 10~20 min (Giemsa staining), or then permeabilized with 70% ethanol-0.5% TritonX-100 for 30 min and stained with 150µl of DAPI in 1 µg/mL for 5~10 min (DAPI staining). The slides were observed with a Leica DMIRB phase or fluorescence microscope.

4.2.4.3. Indirect immunofluorescence assays (IFA)

The hemolymph coated on the glass slides was fixed with 100% methanol for 10 min at -80°C. Some slides were permeabilized with 70% ethanol-0.5% TritonX-100 for 30 min. Slides with or with out the permeabilization treatment were then incubated for 1h with appropriate

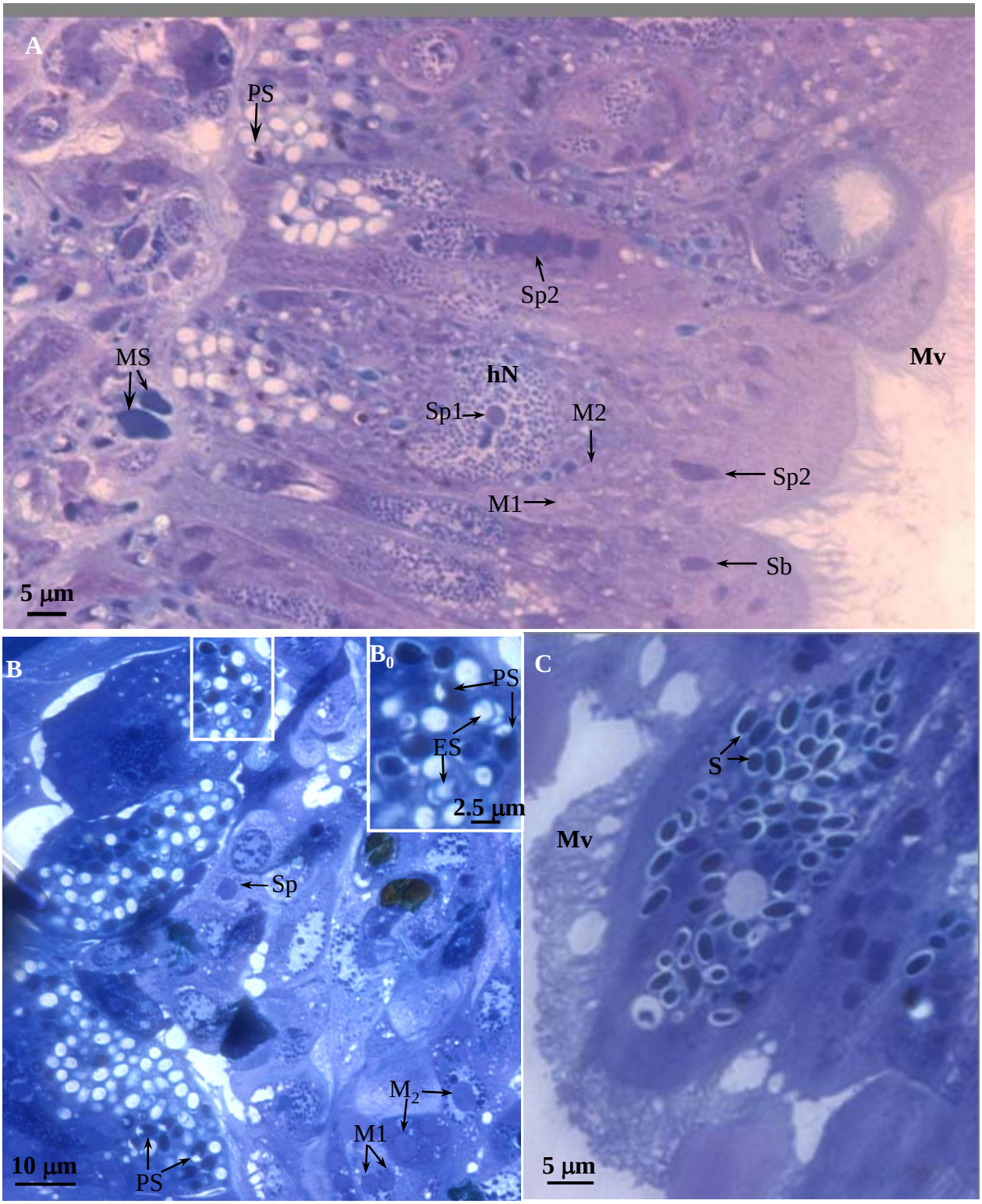

Figure 33. All developmental stages of *Nosema bombycis* life cycle revealed in the semithin sections of silkworm *Bombyx mori* intestine infected focus embedded in Epon resin. The sections were stained by 0.2% Azur blue II, pH 8.5 for 2~5 min and directed observed with a phase contrast microscope. M1, meront; M2, meront; Sp1, sporont; Sp2, sporont in binary fission; Sb, sporoblast; PS, intact primary spore; ES, germinated primary spore; S, mature/external spore; MS, malformed spore; hN, host cell nucleus; Mv, microvilli. The inset B_0 is the enlargement of the left rectangle.

dilutions of PAb anti-fixed *N. bombycis* spores (prepared as 4.2.1.) diluted in PBS-0.1% TritonX-100. Bound antibodies were detected with a 1:1,000 dilution of Alexa Fluor® 468 goat-anti-mouse IgG (Molecular Probes). DNA was stained by a 5-min incubation in 150µl 1 µg/mL DAPI solution. Slides were observed with a Leica DMIRB immunofluorescence microscope.

4.2.4.4. Transmission electron microscopy (TEM)

Fixed hemolymph was centrifuged at 2,300×g for 20 min. The cell pellet was rinsed in 0.1 M phosphate buffer (pH 7.2) 6×10 min and then embedded in LR White resin as described in section 4.2.3.2. For TEM ultrastructure observation or immunocytochemistry see 4.2.3.3.

4.3. Results

4.3.1. Complete life cycle of Nosema bombycis *ISC-ZJ in* Bombyx mori *larvae intestine*

Since *N. bombycis* primary spores are characterized by their spontaneous germination *in vitro* and considered to spread infection within the host, *N. bombycis* complete life cycle *in vivo* is an important prerequisite for the investigation of its dissemination route in *B. mori*, we firstly characterized the complete life cycle of *Nosema bombycis* ISC-ZJ in *Bombyx mori* larvae intestine. The intestine focus of infected silkworm larvae were dissected, fixed and embedded in Epon resin or frozen in pasty nitrogen. The complete life cycle of *N. bombycis* ISC-ZJ in *B. mori* larvae intestine was characterized by light microscopy of Azur blue stained 0.65µm semithin Epon sections and transmission electron microscopy of 90nm ultrathin cryosections.

4.3.1.1. Detection of N. bombycis *different developmental stages in* B. mori *intestine*

The different developmental stages of *N. bombycis* ISC-ZJ in *B. mori* intestine can be clearly identified by Azur Blue staining (**Figure 33**). In host cell, *N. bombycis* ISC-ZJ is in direct contact with the host cell cytoplasm, so all stages of *N. bombycis* ISC-ZJ are randomly distributed in the host cell cytoplasm. The meronts are slightly stained as pearl-blue or grayish purples round cells with their nuclei stained as a dark-blue dot in the center. The meronts in fission are dumbbell-like in the same color of meronts and their nuclei are stained as two separated dark-blue dots. Sometimes the meronts or meronts in fission are stained so weakly that

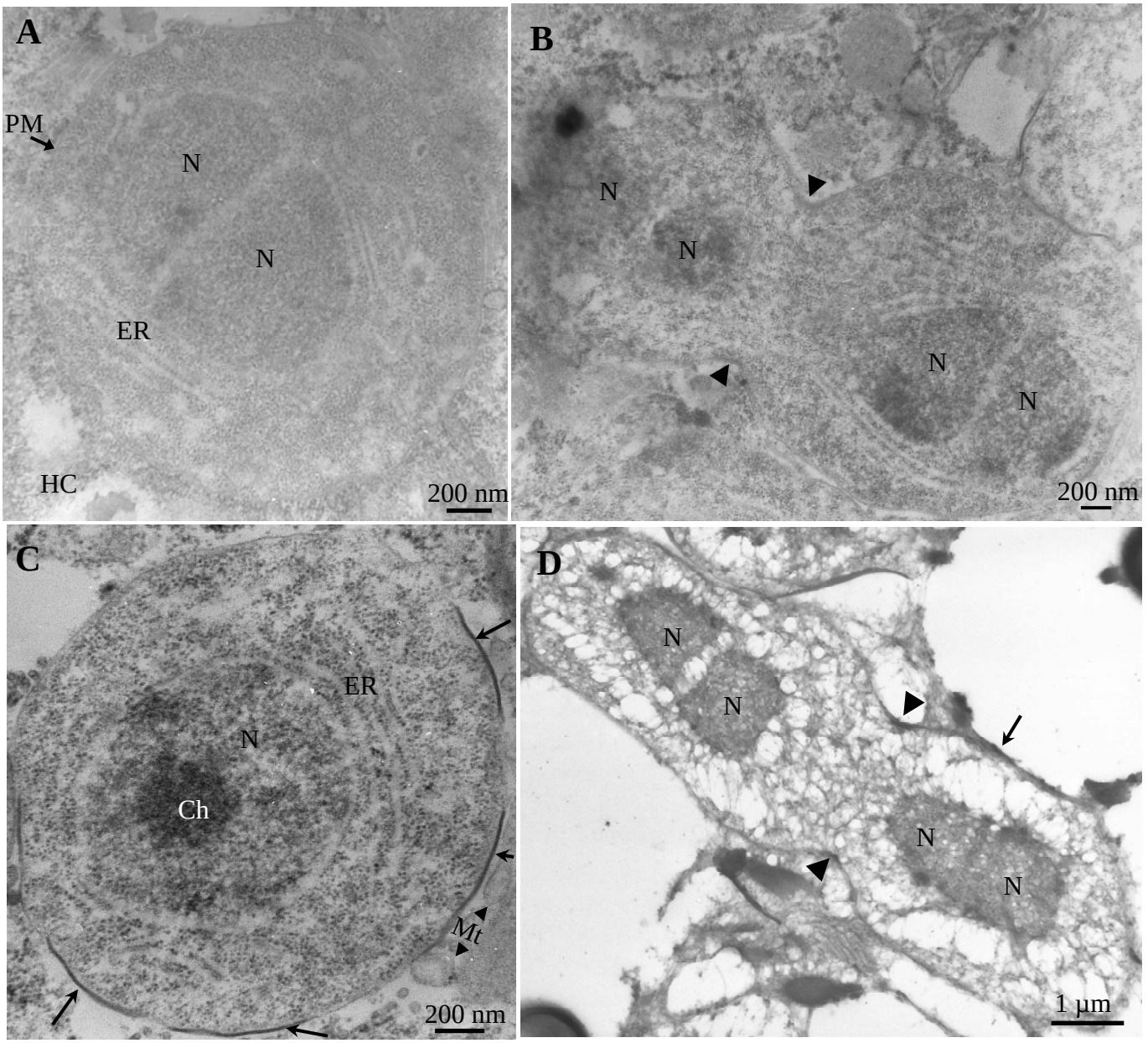

Figure 34. ***Nosema bombycis*** **in cycle: meront and sporont stages observed by transmission electron microscopy.** N, nucleus of *Nosema bombycis*; ER, endoplasmic reticulum; PM, plasma membrane; Mt, mitochondria; HC, host cell cytoplasm; Ch, chromatin. The merogony phase: Panel A, meront, Panel B, meront in binary fission. The sporogony phase: Panel (C~K), Panel C shows a young sporont with electron-dense materials (arrows) being deposited on the plasmalemmal surface of the parasite. Note the centrally located chromatin (Ch). In the cytoplasm, strands of endoplasmic reticulum surrounded the nucleus and free ribosomes were evenly dispersed. The arrowheads show the host mitochondriae (Mt) are in close contact with the proliferative parasite. Panel D, the sporont mutiplies by binary fission.

Figure 35 (next verso). ***Nosema bombycis*** **in cycle: sporoblasts in progressively maturing observed by transmission electron microscopy**. N, nucleus of *Nosema bombycis*; ER, endoplasmic reticulum; PM, plasma membrane; Mt, mitochondria; PF, polar filament; PV, posterior vacuole. Panel A, one sporont produced two sporoblasts. Panel B is a maturing sporoblast with the voluminous and actively developing polar filament. The anchoring disk is forming (asterik). The polar filament (PF) in this stage is under extensively rearrangement. The arrowheads indicates the uniformly electron dense cell wall. In Panel C, the posterior vacuole begins to appear. The polar filament has nearly finished its arrangement. The upper eight coils of polar filament have arranged in one row while the lower four coils of polar filament are in two rows. The polar filament lumen is largely electron-lucent with only a dark eccentric spot. In panel D, more electron-dense material (asterik) appears in the polar filament lumen Some layers of electron-lucent and electron-dense material with the different thickness are now discernible.

it is difficult to distinguish from the intestine cytoplasm. Compared to the meronts, the sporonts, sporonts in binary fission and sporoblasts are evidently deeply stained as large dark grayish blue round cells (sporonts), (irregular) dumbbell-like cells (sporonts in binary fission cells) and small irregular or regular ovoid cells (sporoblasts). The primary spores and environmental spores are stained in indigotin and can be easily distinguished by their white spore walls which looks like a layer of frost covered on the surface of spores. The primary spores are characterized by their obvious depressions at the spore apex and shown as the dentiform cells. After the primary spores discharged most of their sporoplasms and polar filaments, the remaining parts of spores were sparsely stained as tubular structures and these spores were shown as empty cells, namely germinated primary spores. The environmental spores are often regular and of ovoidal form. Different developmental stages of *N. bombycis* ISC-ZJ cells can often be found in the same intestine epithelial cell.

4.3.1.2. N. bombycis *ISC-ZJ complete life cycle at the ultrastructural level*

Since the different developmental stage of *N. bombycis* ISC-ZJ cells can be found in *B. mori* intestine, further characterization of every developmental stages of *N. bombycis* ISC-ZJ have been performed by transmission electron microscopy of intestine focus cryosections.

N. bombycis ISC-ZJ merogony begins with the maturation of sporoplasm into meront (**Figure 34A**). Meronts are round cells surrounded by a unit membrane and has a large nuclear region including double D-shaped diplokarya and a weakly developed cytoplasm with relatively sparse dispersed ribosomes and endoplasmic reticula (ER). Meronts multiply by binary fission (karyokinesis linked to cytokinesis). **Figure 34B** shows that a meront is undergoning cytokinesis after the diplokaryon has completed its division. The cytokinesis has begun with the occurrence of two "isthmus" between the two diplokaryotic parts of the cell. The first sign of sporogongy is the deposition of secretory material on the plasmalemmal surface of the parasite which thus turns into sporont. The deposited material forms electron-dense patches at the sporont periphery (**Figure 34C**). Once this thickening finished, the sporont undergoes a single binary fission (**Figure 34D**) to produce two sporoblasts (**Figure 35A**). As sporoblasts continue their maturation, they undergo great morphogenesis: they crenate and decrease in size and their cytoplasm becomes more electron-dense with the result of the rapid production of ER and ribosome,

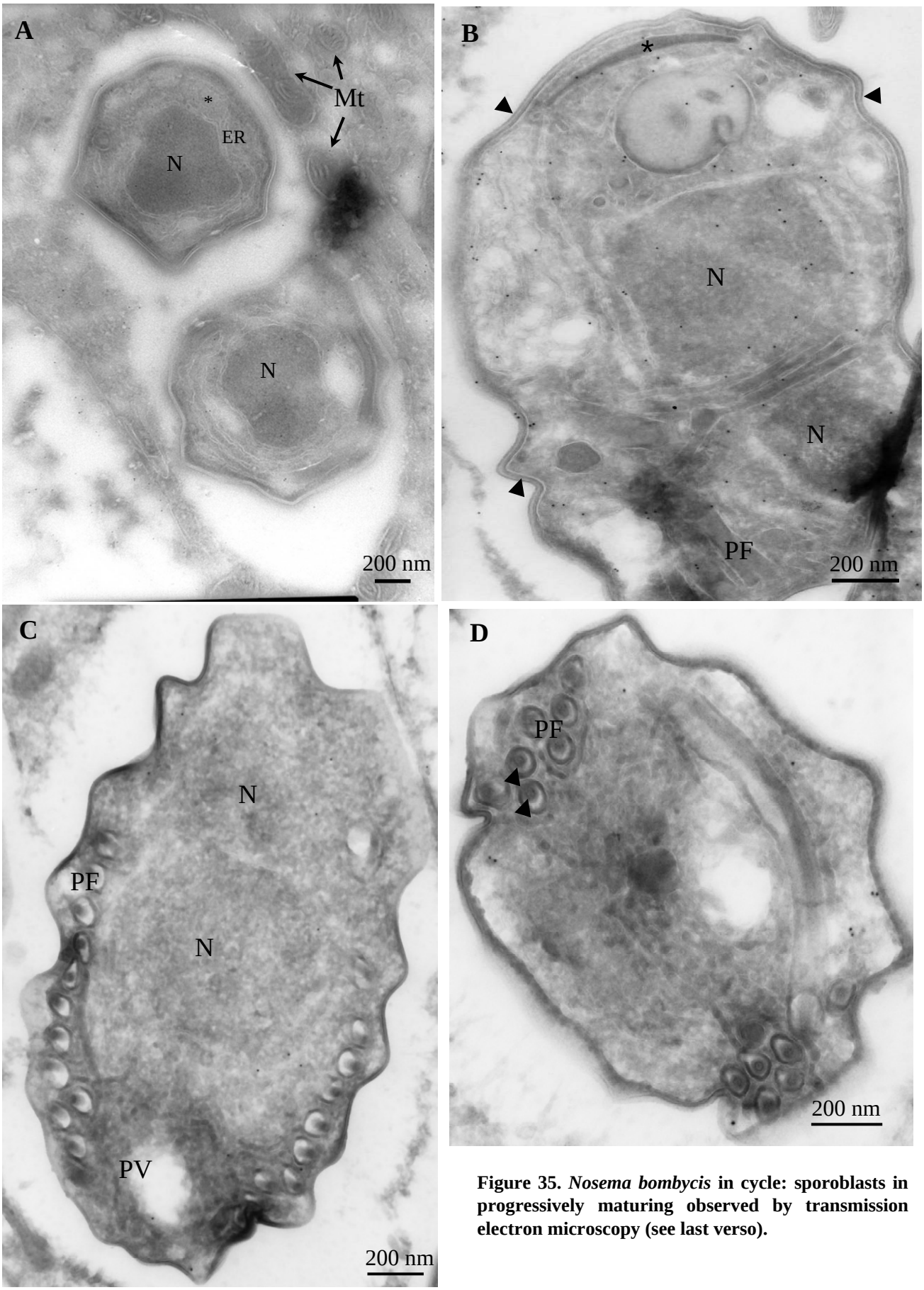

Figure 35. ***Nosema bombycis*** **in cycle: sporoblasts in progressively maturing observed by transmission electron microscopy (see last verso).**

enlargement of the Golgi complex. They form the extrusion apparatus which consist of the polar filament, the anchoring disk, the polaroplast lamellae or vesicles and the posterior vacuole (**Figure 35B~Figure 36A**). As the sporoblast nears maturation into a spore (**Figure 36B**), the spore shape and the polar filament appear as well established; the posterior vacuole and the endospore coat structures are produced. Finally, they transform into spores (**Figure 36C**). *N. bombycis* ISC-ZJ environmental spores is oval in shape. Its spore wall is composed of an outer thinner three-layered exospore wall (two electron-dense layers and one middle electron-lucent layer) (30~40 nm) and an inner thicker endospore wall (40~50 nm) (**Figure 36C-SW,** see also **Figure 2**). The mushroom-shaped anchoring disk complex is situated close to the spore apex and appears as an electron-dense area. It connects to the manubrium of the polar filament. The polaroplast is composed of two parts: its anterior lamellae are tightly packed and regularly arranged organized while posterior regions are less compressed and organized. The isofilar polar filament is well arranged in a single row and its 12~14 coils are closely abutted. At least five electron-dense and electron-lucent concentric rings are discernible in the cross section of polar filament (**Figure 36B-PF**). The posterior vacuole at the basal region contains a glomerular-like structure and flocculent material.

During *N. bombycis* ISC-ZJ development in *B. mori* larvae, occasionally, *N. bombycis* ISC-ZJ cells can be found in the nucleus of intestine epithelial cell (**Figure 37**). By Azur blue staining, the intestine epithelial cell nuclei are characteristically stained with many small deep-colored granule-like heterochromatins and can be easily distinguished from the cytoplasm. When *N. bombycis* ISC-ZJ cell occurred in the host cell nuclus, its development seems need a large space and push the heterochromatins to the periphery of inner membrane of nucleus. In this case, *Nosema bombycis* ISC-ZJ cell is often situated in the center of host cell nucleus and separated from the heterochromatins by the surrounding slightly-colored substance. Compared with the hetero- chromatins, *N. bombycis* ISC-ZJ cells looks like a “giant” round or ovoid cell. TEM observations further confirmed that *Nosema bombycis* ISC-ZJ cell can present in the host cell nucleus. **Figure 37C** shows two *Nosema bombycis* ISC-ZJ meronts (characterized by their weakly developed cytoplasm with relatively sparse dispersed ribosomes and ER) coexist in one intestine cell nucleus. The meront in the left is a longtitudinal section with its two nuclei discernible while only one nucleus is visible in the cross section of right meront. These meronts

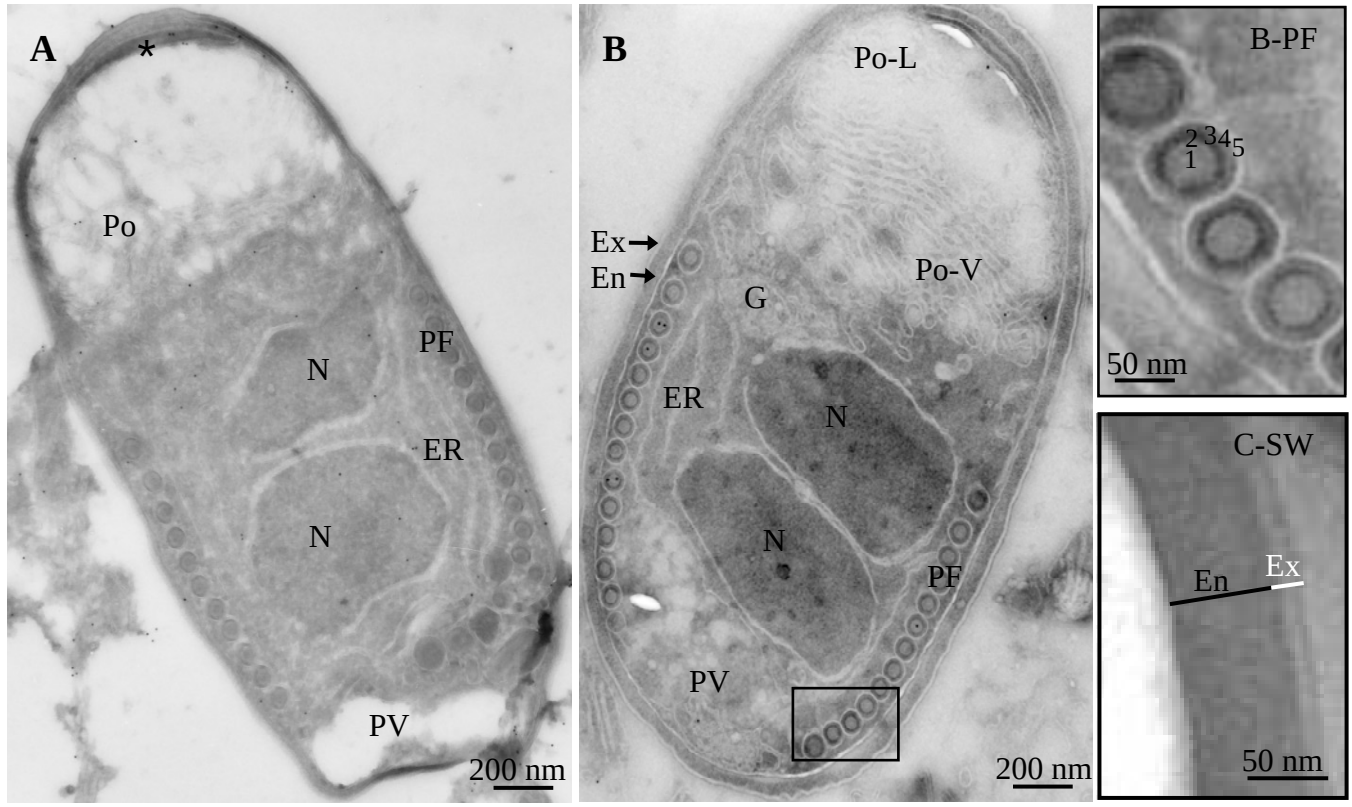

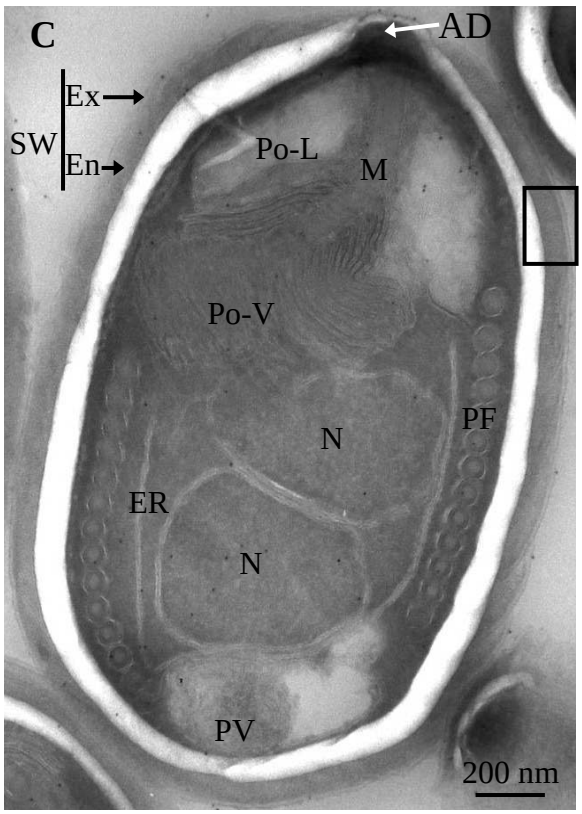

Figure 36. *Nosema bombycis* in cycle: sporoblasts in advanced stages and spore by transmission electron microscopy. N, nucleus of *Nosema bombycis*; ER, endoplasmic reticulum; PM, plasma membrane; Mt, mitochondria; HC, host cell cytoplasm; PF, polar filament; PV, posterior vacuole; Po, polaroplast; Po-L, polaroplast laminar region; Po-V, polaroplast vesicular region; G, Golgi complex; AD, anchoring disk; M, manubrium of polar filament; SW, spore wall; Ex, exospore; En, endospore.

Panel A, this late sporoblast or immature spore has reached the ovoid shape of mature spore. The anchoring disk is still in formation (asterik). The voluminous polaroplast (Po) is actively forming and appears as the irregular electron-lucent chambers in the anterior region and vesicles in the posterior region. The polar filament is well developed and arranged. Large quantities of ER and ribosomes are produced. Panel B, an advanced sporoblast or immature spore. The endospore coat has evidently thickened. The polar filament appears distinctly multilayered (5 layers), composed of a number of concentric rings of varying thickness and electron density (showed in B-PF: the enlargement of cross sections of 4 coils polar filament in the rectangle region in Panel B). It is well arranged into one row. The posterior vacuole is well eastablished. The well-developed polaroplast has reached its final arrangement. In this stage two different polaroplast regions can be seen: the anterior region (Po-L) is composed of the regular arrays of lamellae followed by the less compressed and more irregular posterior region (Po-V) in a vesicular appearance. The Golgi complex (G) appears to enlarge. Panel C shows a mature spore in the longitudinal axial section. *Nosema bombycis* mature spore has two nuclei (N). Its invasion apparatus have been well established: anchoring disk complex; polaroplast with tightly packed lamellae or regular arranged vesicles; polar filament arranged in 12~14 closely abutted coils; posterior vacuole. Panel C-SW is the enlargement of the spore wall in the rectangle region shown in Panel K. Panel K-SW shows that *N. bombycis* spore wall is composed of three-layered exspore (two electron dense layers and one middle electron-lucent layer) and one electron-dense thick endospore.

are also surrounded by the electron-dense heterochromatins mainly distributed around the nuclear envelope, similar to the findings in the Azur blue-stained sections.

4.3.2. Nosema bombycis *dissemination kinetics in* Bombyx mori *larvae*

4.3.2.1. Nosema bombycis ISC-ZJ dissemination in Bombyx mori tissues

For following *N. bombycis* ISC-ZJ dissemination in *B. mori* tissues, four increasing concentrations of *N. bombycis* ISC-ZJ spores were inoculated *per os* to the 2nd newly moulted silkworms (2×10^4, 10^5, 5×10^5 spores/ml) (**Figure 38**) and the 3rd newly moulted silkworms (10^6 spores/ml) (**Figure 39**). The infected larvae were analysed at different time intervals postinfestation (PI).

N. bombycis ISC-ZJ infection can not be detected at any tissue at 64h PI (**Figure 38**). At 112h PI, they can be detected both at the anterior midgut and its basal membrane, although no parasite was observed at 160h PI. At 208h PI, *N. bombycis* ISC-ZJ infection began to spread to the muscles surrounding the intestine and then to the posterior tissues such as muscle, tracheae, fat body and silk glands, while the middle and posterior midguts seem to be kept intact. From 256h, *N. bombycis* ISC-ZJ infection has evidently disseminated to nearly all tissues and organs in all directions. These tissues and organs include the epithelial cells of cuticle and trachea, the muscle, the dorsal vessel, the fat body, the silk gland, the neural cells of nervous system, the salivary gland (**Figure 40**), the gonad and the Malpighian tubules.

In other serial analysis (**Figure 39**), *N. bombycis* ISC-ZJ infection seems to spread more quickly than in **Figure 38**. At 48h PI, *N. bombycis* ISC-ZJ cells can not be detected. They are firstly observed also in the anterior midgut and its basal membrane at 96h PI, and then at 143h PI, in intestine surrounding muscles and tracheae, silkgland. At 192h, *N. bombycis* ISC-ZJ infection has disseminated to many interior tissues and cuticle.

From **Figures 38** and **39**, no matter which concentration of spores was used, *N. bombycis* ISC-ZJ spores firstly establish their infection in the anterior midgut epithelial cells. Then the parasite infection began to spread to those muscles and tracheae closely surrounding the anterior intestine. Gradually, other distant tissues or organs such as fat body, middle and posterior midguts, silk glands, the nervous system and the dorsal vessel were infected. Finally, the systemic infection follows. i.e., *N. bombycis* ISC-ZJ disseminates from the anterior midgut to

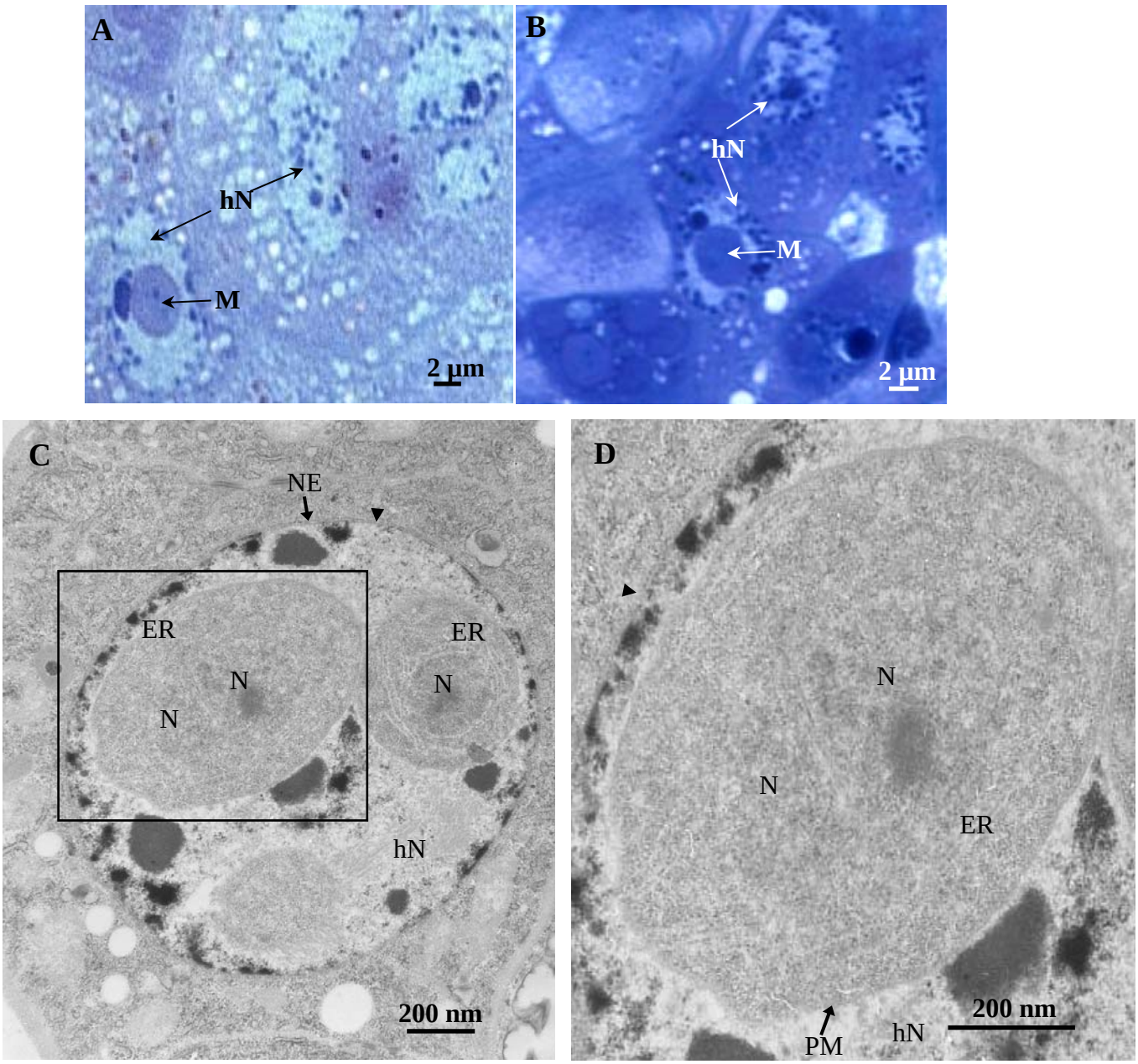

Figure 37. *Nosema bombycis* can be found in the host cell nucleus. Semithin sections of infected silkworm larvae embedded in Epon resin were stained by 0.2% Azur blue II, pH 8.5 (A~B). The intestine epithelial cell nuclei are characteristically stained with many small deep-colored granule-like heterochromatins and and can be distinguished from cytoplasm. N. bombycis large meronts (M) (4~5 µm ×5~6 µm) have been found in the host cell nuclei. Ultrathin sections from these resin blocks were also analysed by transmission electron microscopy (C~D). In panel C, two meronts of *N. bombycis* are present in the nucleus of host cell. Panel D is the enlargement of the rectangle region in panel C, one *N. bombycis* meront with two nuclei (N). Arrowheads show the nuclear pores in the host cell nuclear envelope (NE). hN: host cell nucleus. N: *N. bombycis* nucleus; ER; endoplasmic reticulum; NE, host cell nuclear envelope; PM, plasma membrane of *N. bombycis* meront.

their surrounding muscles or tracheae and then other tissues or organs, from the anterior part of larvae to the posterior part.

Because the surrounding muscles and tracheae are in direct contact with the intestine epithelial wall, it is reasonable to suggest that they are directly infected by the *in vivo* spontaneous germination of *N. bombycis* ISC-ZJ primary spores developped in the anterior midgut. However, since the other different tissues are spacially separated from the intestine and evidently beyond the reach of primary spores short polar filament, we wonder how they can be gradually and finally systemically infected. Because all insects including *B. mori* have an open circulating system with all interior tissues or organs immersed in the hemolymph, we hypothesize that *B. mori* hemolymph and hemocytes may function as vectors or disseminators which can carry *N. bombycis* ISC-ZJ cells to get close to those distant tissues or organs and then infect them. So we also analyzed the interactions between *N. bombycis* ISC-ZJ and *B. mori* hemocytes and hemolymph.

4.3.2.2. Nosema bombycis *presence in* Bombyx mori *hemolymph and infection of* Bombyx mori *hemocytes*

For analyzing *N. bombycis* ISC-ZJ interactions with *B. mori* hemolymph and hemocytes, high concentration of *N. bombycis* ISC-ZJ environmental spores (10^{10} spores/ml) were perorally inoculated to the 4^{th} newly moulted larvae. With the hemolymph of naïve silkworms as negative control, the hemolymph samples of infected silkworms were analyzed by Giemsa/DAPI staining or by transmission electron microscopy.

Both Giemsa/DAPI staining and TEM can clearly detect *N. bombycis* ISC-ZJ spores in the hemolymph or hemocytes. By Giemsa staining, the cytoplasm of *N. bombycis* ISC-ZJ spores is pink with the nuclei in blue (data not shown). By DAPI staining, the nuclei of *Nosema bombycis* developing in the hemocytes can be stained in blue as that of host cell nucleus. In transmission electron microscopy analysis, the ultrastructures of *Nosema bombycis* in hemocyte such as the spore wall and polar filament can be identified (**Figure 41**).

Our results show that *N. bombycis* ISC-ZJ can infect and develop in all five known types of hemocytes of *Bombyx mori*: oenocytoid, prohemocyte, spherulocyte, plasmatocyte and granulocyte (**Figure 41**). In all these hemocytes, *Nosema bombycis* cells are in direct contact

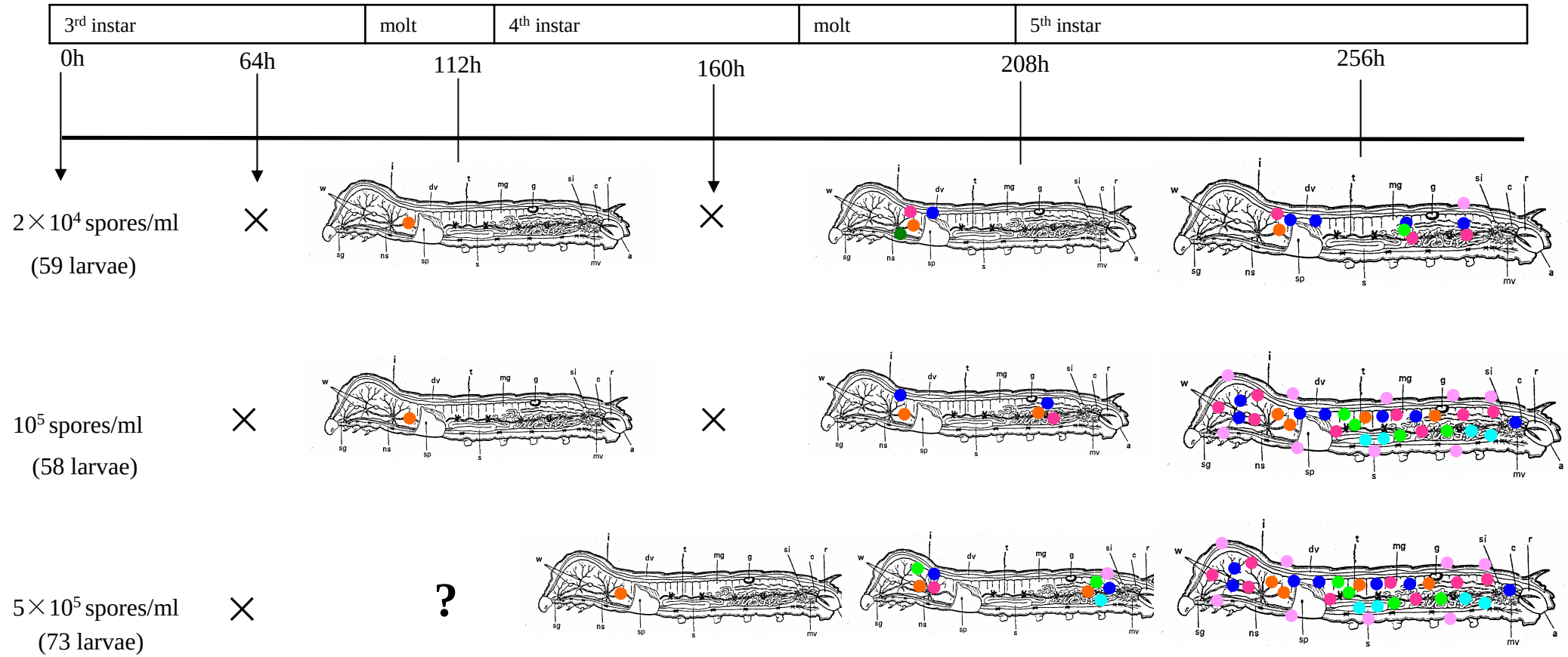

Figure 38. *Nosema bombycis* dissemination kinetics in *Bombyx mori* larvae (I). The 2rd newly moulted silkworms were perorally innoculated with *N. bombycis* spores in different concentrations (2×10^4, 10^5, 5×10^5 spores/gram artificial diet). The infected larvae were cut into three (64h, 112h, 160h, 208h) or four parts (256h) and each part was seperately fixed and embedded in Epon resin at 64h, 112h, 160h, 208h and 256h postinoculation. 0.65 μ m semithin sections were obtained from these resin blocks and stained by 0.2% Azur Blue II (pH 8.5) for 2~5 min. The slides were directly observed with a Leica DMIRB microscope. At every time point, one larva was analysed. The dots in different colors showed the different infected tissues and organs respectively: ● intestine; ● muscle; ● fat body; ● trachea; ● cuticle; ● silk gland; ● nervous system.

with the host cell cytoplasm. Because of optical transparence of oenocytoid, eight *Nosema bombycis* meronts in their cytoplasm are clearly observed (**Figure 41A~C**). In the prohemocyte, only a few *N. bombycis* ISC-ZJ cells were found at the two poles with the host cell nucleus induced to change their shape and adopt the development of parasites (**Figure 41 D~F**). **Figure 41G~I** showed that a spherulocyte is full of *N. bombycis* ISC-ZJ cells in its cytoplasm. The irregular or spindly plasmatocyte can also be infected by *N. bombycis* ISC-ZJ (**Figure 41J~L**). *N. bombycis* ISC-ZJ cells are also present in the granulocytes with pseudopods shown (**Figure 41M**) or not shown (**Figure 41P~R**). In **Figure 41P**, at least seven *N. bombycis* ISC-ZJ cells develop in one hemocyte. The polar filament of *N. bombycis* ISC-ZJ spore in **Figure 41Q~R** can be clearly identified.

Besides the five known types of hemocytes, it is possible to observe that some hypertrophic hemocytes (diameter: 12~18 μm) also support the development of *N. bombycis* (**Figure 42C~H**). Though these hypertrophic hemocytes can be in the same size as some oenocytoids, but they have more high nucleus/cytoplasm ratio and far less optical than oenocytoids (**Figure 41A~C**, **Figure 42A**). When stained by Giemsa solution, they are full of a large number of small violet granulae (**Figure 42B**), very different from Giemsa-stained oenocytoids (**Figure 42A**). In these hypertrophic hemocytes, *Nosema bombycis* cells are also in directly contact with cytoplasm (**Figure 42C~H**).

4.3.2.3. Time of N. bombycis *presence in* B. mori *hemolymph and invasion of hemocytes*

Since *B. mori* hemocytes have been proved to support the multiplication of *N. bombycis* ISC-ZJ, for further characterizing the role of *B. mori* hemocytes in *N. bombycis* ISC-ZJ dissemination *in vivo*, we then analyzed the time of *N. bombycis* ISC-ZJ presence in *B. mori* hemolymph and invasion of *B. mori* hemocyte. After the 4th newly moulted larvae were infected by *N. bombycis* ISC-ZJ, hemolymph samples were collected from infected *B. mori* larvae with the hemolymph of naïve silkworms as the negative control (**Figure 32**). *N. bombycis* ISC-ZJ in the hemolymph and hemocyte were detected by DAPI staining and IFA.

4.3.2.3.1. Presence in B. mori *hemolymph* (**Table 23**)

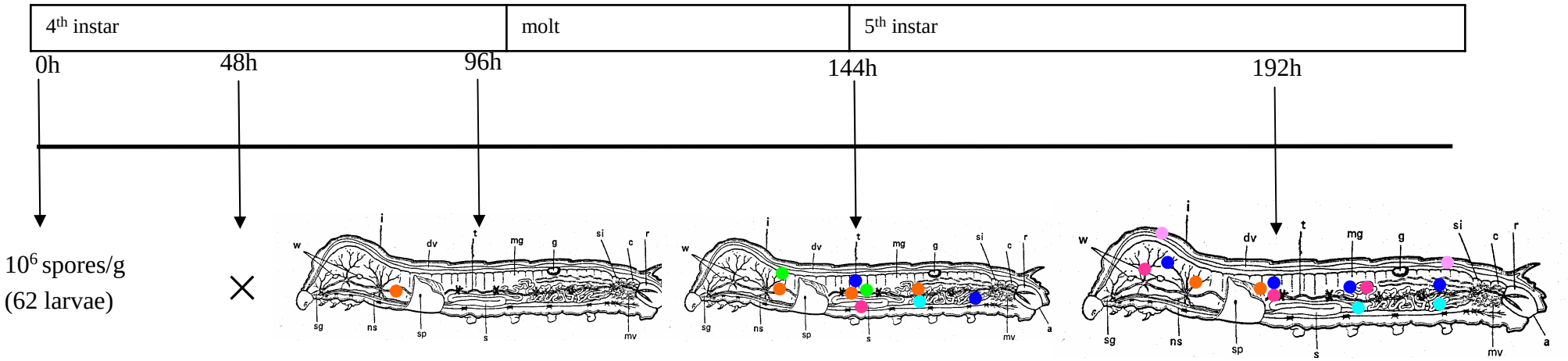

Figure 39. *Nosema bombycis* dissemination kinetics in *Bombyx mori* larvae (II). The 3rd newly moulted silkworms were perorally innoculated with *N. bombycis* spores (10^6 spores/gram artificial diet). The infected larvae were cut into three (48h, 96h) or four parts (144h, 192h) and each part was seperately fixed and embedded in Epon resin at 48h, 96h, 144h and 192h postinoculation. 0.65 μ m semithin sections were obtained from these resin blocks and stained by 0.2% Azur Blue II (pH 8.5) for 2~5 min. The slides were directly observed with a Leica DMIRB microscope. Six larvae were analysed at 48h and 96h with four larvae 144h and two larvae at 192h. The dots in different colors showed the different infected tissues and organs respectively: ● intestine; ● muscle; ● fat body; ● trachea; ● cuticle; ● silk gland.

From 2.5h PI to 82h PI, the presence of *N. bombycis* ISC-ZJ in hemolymph is at a relatively low rate, either without detection or with the detection proportion of every time point one larva of three. The total detection proportion is 10 larvae of 66 (15.2%). Between 71h PI and 91h PI, the detection proportion of every time point began to increase to two larvae of three. The total detection proportion also increases to 9 larvae of 21 (42.9%). From 94h PI to 192h PI, *N. bombycis* ISC-ZJ can be detected in all *B. mori* larvae hemolymph.

At 2.5h, 5h and 19h, some environmental spores were observed in the hemolymph [1~4 cell(s) /field] by DAPI staining, which has been then proved by IFA experiment (**Figure 43**). The spore walls of *N. bombycis* ISC-ZJ cells in these hemolymph samples have been intensely labeled by the polyclonal antibody against formaldehyde-fixed *N. bombycis* spores in IFA analysis. Between 34h PI and 149h PI, only a few *N. bombycis* ISC-ZJ early stage cells [1~2 cell(s) /field] (sporoplasm, meront, sporont) and germinated empty spores can be observed in the hemolymph. At 192h PI, *N. bombycis* ISC-ZJ cells in hemolymph greatly increased in number and can be at every developmental stages, but mainly the late stage cells such the intact or germinated empty primary spores and environmental spores.

4.3.2.3.2. Invasion of B. mori *hemocytes* (Table 23)

Between 2.5h and 69h, though *N. bombycis* ISC-ZJ cells have been present in *B. mori* hemolymph, the hemocytes are still intact. At 71h, the hemocytes became oocasionally infected for the first time and one or two *N. bombycis* ISC-ZJ meronts can be observed in hemocytes by DAPI staining. At 139.5h, the infected hemocytes increased and some hemocytes were occupied with *N. bombycis* ISC-ZJ spores but still keep their integrities. Up to 192h, many *B. mori* hemocytes were so severely infected that they began to lyse and release a large number of *N. bombycis* ISC-ZJ cells in different developmental stages into the hemolymph (**Figure 44**), including the primary spores (**Figure 45**)

4.3.2.4. B. mori *hemocytes and hemolymph immune reponses to* N. bombycis *infection*

Upon *N. bombycis* ISC-ZJ infection, insect typical immune responses such as phagocytosis (the engulfment of entities by an individual cell) and melanization (melanin synthesis pathway; pathogens were immobilized by the surrounding melanotic layers or capsules and killed by the

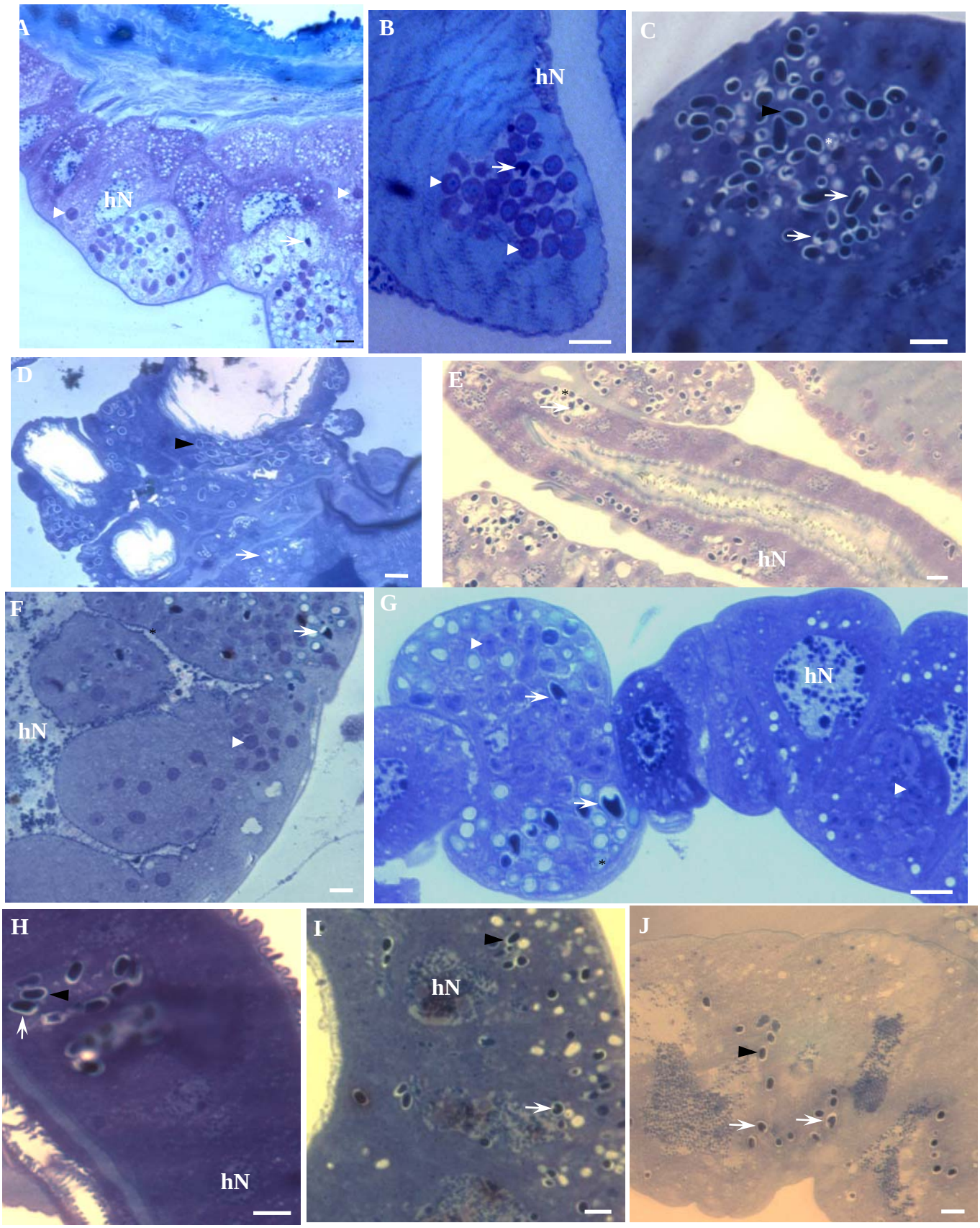

Figure 40. ***Nosema bombycis*** **can develop in different organs or tissues of** ***Bombyx mori*** **larvae**. They are revealed on semithin sections of infected silkworm larvae embedded in Epon resin. The sections were stained by 0.2% Azur blue II, pH 8.5 for 2~5 min and directed observed with a phase contrast microscope. A, cuticle; B-C, muscles; D-E, tracheae; F, nervous system; G, fat boby; H, dorsal vessel; I, silk galnd; J, salivary gland. White arrowheads, meront or sporont; Black arrowheads, mature spores; White arrows, primary spores; Asteriks, germinated primary spores; hN, host cell nucleus. Bars = 5 μm.

cytotoxic derivatives or intermediates produced in this pathway) were observed in *B. mori* hemocyte and hemolymph (**Figure 46** and **47**). In **Figure 46A~C**, a prohemocyte with high nucleus cytoplasm ratio is phagocytosing an intact *N. bombycis* ISC-ZJ spore. This prohemocyte has been induced to form a "mouth"-like cupped depression to phagocytose the parasite. **Figure 47A~N** show the melanization of both hemocyte and *Nosema bombycis* cells in hemocyte or hemolymph. The melanization has just begun in the hemocyte in **Figure 47A~C**. When the forming melanotic layer is enclosing the whole hemocyte, the penetration of DAPI is so limited that its nucleus is sparsely stained in dark blue and the whole hemocyte nearly appears as a dark cell (**Figure 47B**). **Figure 47C** shows that its nucleus is in appearance of an apoptosis cell and distributed around the cell membrane. In **Figure 47D~I**, the hemocytes in different sizes are highly melanized. When stained by DAPI, they are observed as dark cells and their nuclei can not be stained. In **Figure 47J~N**, nine *N. bombycis* ISC-ZJ cells and one melanized meront or sporont of *N. bombycis* ISC-ZJ are observed in the cytoplasm of a plasmatocyte. By DAPI staining, this meront or sporont is shown as a dark cell while the nuclei of *N. bombycis* ISC-ZJ cells and host cell are stained in blue. This dark *Nosema bombycis* cell probably developped in the cytoplasm and was then melanized or was firstly melanized in the hemolymph and then phagocytosed. Compared to **Figure 41P~R**, *N. bombycis* ISC-ZJ in hemolymph (**Figure 47M**) or hemocytes (**Figure 47N**) is highly melanized and is shown as a black cell (note one melanized hemocyte in **Figure 47M** is also shown as a black cell) by acetate uranyl staining. The melanized parasites in resin blocks are so hard to cut that they are separated from the embedding resin.

4.4. Discussion

4.4.1. **Nosema bombycis** *ISC-ZJ complete life cycle in* **Bombyx mori**

Nosema bombycis ISC-ZJ is Chinese reference strain with a long history. Nowadays it still inflicts the great losses in the sericulture. Its life cycle in *B. mori* intestine has been studied by Giemsa staining (Yu *et al*., 1994) and the ultrastructure of its environmental spores has been reported and compared with other microsporidian pathogenic to silkworms (Gao *et al*., 1999). We documented the hitherto unreported complete life cycle of *N. bombycis* ISC-ZJ in *Bombyx mori* at the ultrastrucutral level. *N. bombycis* ISC-ZJ is diplokaryotic, disporoblastic and apansporoblastic and develops in direct contact with the host cytoplasm throughout all its life

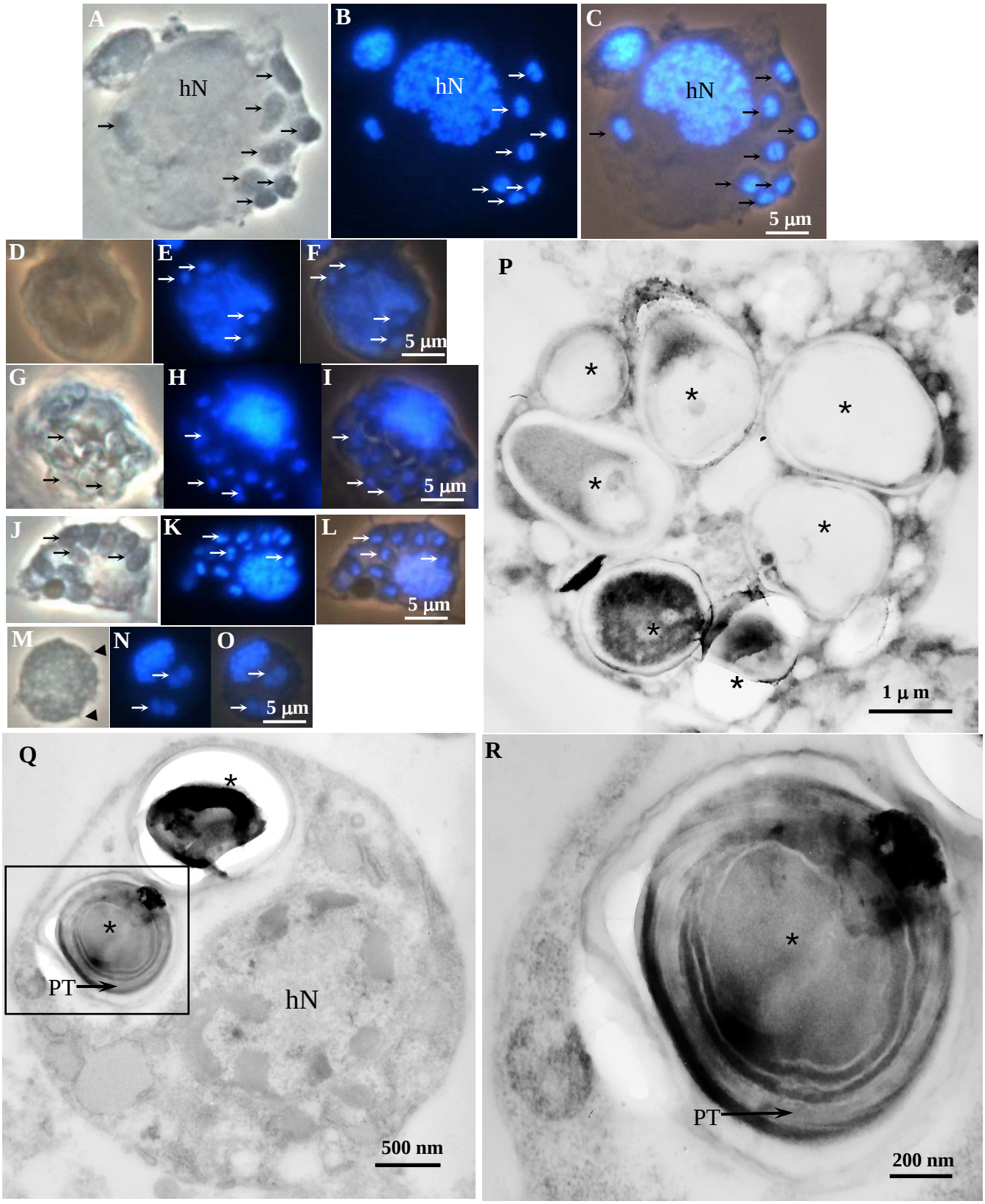

Figure 41. *Nosema bombycis* present in the cytoplasm of different *Bombyx mori* hemocytes. A~C, oenocytoid; D~F, prohemocyte; G~I, spherulocyte; J~L, plasmatocyte; M~R, granulocyte. A, D, G, J, M: phase contrast microscopy; B, E, H, K, N: DAPI staining; C, F, I, L, O: superposition of phase contrast and DAPI staining; P, Q, R: transmission electron micrographs. Panel R is the enlargement of the rectangle region in panel Q. Arrows in A~O and asterisks in P~R: *Nosema bombycis* cells in hemocyte cytoplasm. Arrowheads: pseudopods of *B. mori* granulocytes. hN: hemocyte nucleus.

cycle. *N. bombycis* ISC-ZJ sporogonial stage forms both the primary and environmental spores by binary fission, which is called "sporogonial dimorphism" (Kawarabata, 2003). These charateristics were consistent with the observations on *N. bombycis* NIS-001 development in cultured cells *in vitro* (Kawarabata, 1984) and also considered by Sprague *et al* (1992) to be generic characters for the genus *Nosema*.

In this study, *N. bombycis* ISC-ZJ primary spores with a depression at the posterior end are shown as the dentiform cells by IFA experiment (**Figure 45**) or when stained by 0.2% Azur Blue. *N. bombycis* ISC-ZJ environmental spores are regular ovoidal cells with their polar filament arranged in 12~14 coils. When stained by 0.2% Azur Blue, the spore walls of *N. bombycis* ISC-ZJ primary spores and environmental spores are both colored in white (**Figure 40C**), it seems there are some common compenents in their spore walls. Iwano and Ishihara (1991b) firstly studied the ultrastructure differences of *N. bombycis* NIS-001 primary spores and environmental spores formed in silkworm larvae gut epithelium: *N. bombycis* NIS-001 primary spores, which are variable in size with 3~5 coils of polar tube and a depression at the posterior end, appear in silkworm midgut as early as 46h after inoculation; *N. bombycis* NIS-001 relatively uniformly environmental spores show 10~13 coils of polar filament and there is no depression at the posterior end and can be detected in silkworm midgut 72h after inoculation.

N. bombycis sporogonial dimorphism has been considered as a highly adaptive nature to survive and perpetuate its life according to different conditions (Iwano and Ishihara, 1991b). The dormant environmental spores with a thick spore wall can suffer the drastic external environment and when they enter into the silkworm digestive tube, with appropriate stimuli, their long polar filaments can function as a syringe to transfer their infective sporoplasms into the host cell or haemocoel. The primary spore was considered as an intermediate which can only survive in host cell with their thin spore wall facilitating their spontaneous germination and their short polar filaments allowing the sporoplasm to be deposited to the same host cell cytoplasm or adjacent host cells (Ishihara, 1985; Iwano and Ishihara, 1991b).

Notwithstanding that a uninucleate parasite has been supposed to exist during the early merogonial development of *N. bombycis* (Ohshima, 1973) and in *Nosema* genus (Sprague *et al*., 1992), the uninucleate *N. bombycis* NIS-001 cells has not been observed in cultured cells by Gimeas staining (Kawarabata and Ishihara, 1984). Our investigation by Giemsa staining and

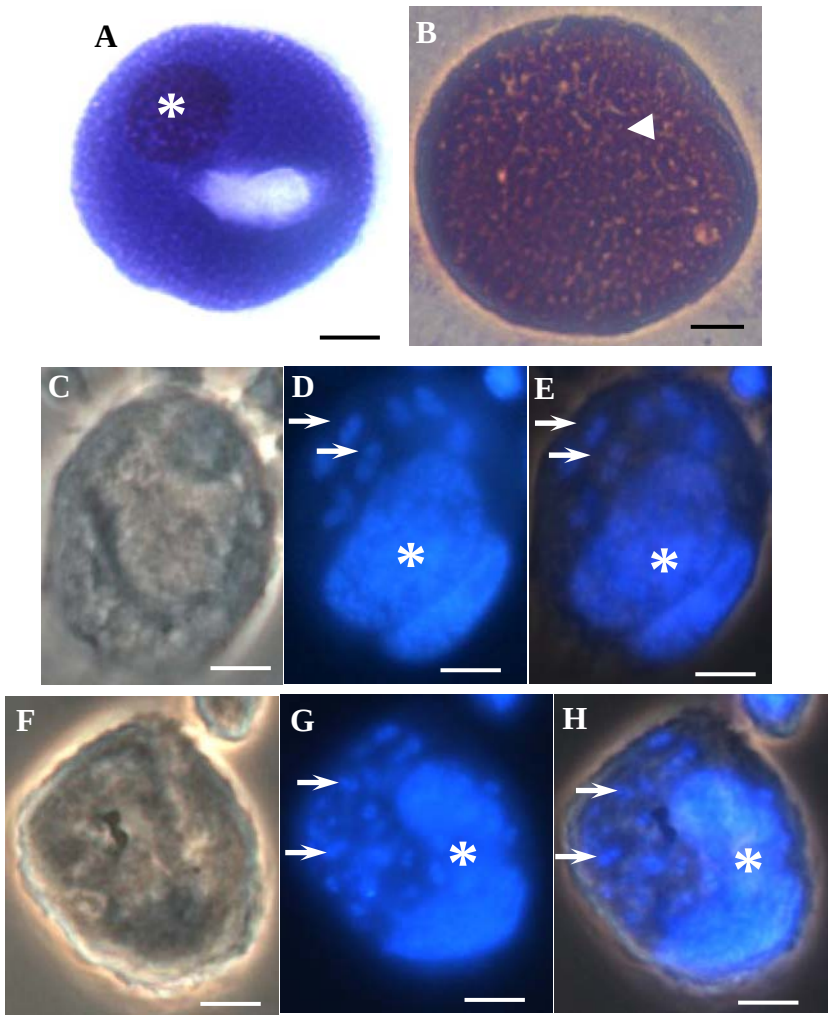

Figure 42. *Bombyx mori* hypertrophic hemocytes: comparison with oenocytoid and its interactions with *Nosema bombycis*. Bar=5 μm. A~B, Giemsa staining; C, F, phase contrast microscopy; D, G, DAPI staining; E, H, Superposition of phase contrast microscopy and DAPI staining. A, oenocytoid, B~H, hypertrophic hemocytes. White arrows show *Nosema bombycis* in hemocyte cytoplasm; Asterik, hemocyte nucleus. When compared with oenocytoids (A and Figure 41 A~C), they have more high nucleus/cytoplasm ratio and are far less optical than oenocytoids. When stained by Giemsa solution, a large number of small violet granulae (arrowhead in B) nearly occupy the whole hemocyte, very different from Gimesa-stained oenocytoids (A).

TEM has showed that *N. bombycis* ISC-ZJ is dikaryotic during all developmental stages *in vivo.* The earlier supposition of a uninucleate stage in *N. bombycis* life cycle seems to be very unlikely.

N. bombycis ISC-ZJ develops in the host cell cytoplasm, but our light and electron microscopy analyses show incidences also in the host nucleus. But often the earlier developmental stages of *N. bombycis* ISC-ZJ such as meront, sporont and sporoblast were found in host nucleus. This fact inferred that host cell nuclei can not meet the great needs such as protein synthesis during *N. bombycis* ISC-ZJ cell maturation and these parasite of early developmental stages can not mature into spore in the host nucleus. It differs from the complete *Enterocytozoon salmonis* cycle which develops inside the nucleus of leucocytes and epithelioid cells of salmon (Desportes-Livage *et al*., 1996). Therefore, the earlier same observation of *N. bombycis* in host nucleus (Takizawa *et al*., 1973) was further strengthened by our ultrastructural analyses.

The internal ultrastucture of *N. bombycis* NIS-001 including the invasion apparatus have been reported (Sato *et al*., 1982) while with no description of its spore wall. In this report, we observed the exospore wall of *N. bombycis* ISC-ZJ is as electron-dense as its endospore wall, contrary to the acknowledged spore wall electron-density order (the electron-dense exospore and electron-lucent endospore) (Vávra and Larsson, 1999), and composed of three layers, different from one layer of *N. bombycis* NIS-001 exospore (Sato *et al*., 1986; Iwano and Ishihara, 1991a, b). Since the layer number of exospore shown in the micrograph of microsporidian mature spore has been proved to relate to the different fixative in addition to the fixation time and temperature (Larsson, 2005), it seems that the combination of fixation by paraformaldehyde/glutaraldehyde and cryosection-cutting used in this study are suitable for the better ultrastructure conservation of *N. bombycis* mature spore.

4.4.2. Dissemination of Nosema bombycis *ISC-ZJ in* Bombyx mori *larvae*

4.4.2.1. Primary spore in the dissemination of N. bombycis *ISC-ZJ in* B. mori *larvae*

Microsporidian sporogonial dimorphism was firstly characterized in *N. bombycis* NIS-001 and *N. bombycis* Sd-NU-IW8381 by light and electron microscopy (Iwano and Ishihara, 1991a, b). As a milestone which changed the life cycle models of many microsporidians, the definition

Table 23. *Nosema bombycis* presence in the hemolymph-hemocytes of *Bombyx mori* 5th instar larvae

Time after infestion		Presence of *N. bombycis* in hemolymph		Invasion of hemocyte	Positive larva Percent
		Number of positive larvae	*N. bombycis* stage		
1st day	2.5h	1/3	environmental spores		
	5h	1/3	environmental spores		
	7.5h	0/3			
	10h	0/3			
	17h	0/3			
	19h	1/3	environmental spores		
	21h	0/3			
	23h	0/3			
2nd day	25h	0/3			
	27.5h	0/3			
	34h	1/3	sporoplasm, primary spores		
	36.5h	2/3	sporoplasm, primary spores		
	39h	1/3	germinated empty spores		
	41.5h	0/3			
	44.5h	1/3	germinated empty spores		
3rd day	47.5h	1/3	meront		
	50.5h	0/3			
	53h	0/3			
	55.5h	0/3			
	65h	1/3	sporont		
	67h	0/3			
	69h	0/3			
		Total : 10/66 larvae			**15.2%**
3rd day	71h	2/3	sporoplasm, sporont	*	
4th day	73h	0/3			
	75h	1/3	sporoplasm		
	82h	1/3	sporoplasm		
	86h	2/3	sporoplasm, meront	*	
	89h	1/3	germinated empty spores		
	91h	2/3	sporoplasm		
		Total : 9/21 larvae			**42.9%**
4th day	94h	3/3	sporoplasm, meront		
	96h	1/1	sporoplasm, meront		
5th day	98.5h	1/1	sporoplasm, meront	*	
	100.5h	1/1	sporoplasm		
	106h	1/1	meront	*	
	112.5h	1/1	sporoplasm, meront	*	
	115h	1/1	sporont, sporoblast	*	
	118h	1/1	meront, sporont	*	
	121h	1/1	meront, sporont	*	
6th day	139.5h	1/1	sporoplasm, meront, sporont	*	
7th day	149h	1/1	sporoplasm,meront, sporont	*	
8th day	192h	1/1	all stages	*	
		Total : 14/14 larvae			**100%**

At different time points the hempolymph and hemocytes of three larvae (2.5~94h postinfection) or one larva (96~192h postinfection) were analysed respectively by DAPI staining. So “Number of positive larvae” is shown as x/3 or x/1.

of the sporogonial sequence and the terminology of microsporidians (Kawarabata, 2003), it is also very useful for us to uncover parasite dissemination mechanism *in vivo*.

The primary spores with short polar filaments are in a non-resting state. They can germintate within the cytoplasm of host cell immediately after maturation (spontaneous germination), protrude sporoplasm like the germs which are called "secondary infective forms" and spread infection within a host (autoinfection) (Iwano and Ishihara, 1991a, b; Kawarabata, 2003).

Our histochemical analyses of infected silkworm larvae showed that *Nosema bombycis* ISC-ZJ intact primary spores and germinated primary spores can be found in nearly all tissues and organs, Furthermore, as shown in **Figure 33A~B** and **Figure 40A,C,G**, *Nosema bombycis* ISC-ZJ primary spores can be formed in such a large number (high spore productivity) in *B. mori* that the intact and germinated parimary spores can be up to two-third of all parasites, especially at the earlier stage after inoculation, while it has been estimated that *Nosema bombycis* NIS-001 primary spores are only approximately one-fourth to one-sixth of environmental spores produced in the life cycle (Kawarabata and Ishihara, 1984; Kawarabata, 2003). Finally, our investigation of *N. bombycis* ISC-ZJ dissemination from intestine epithelium to other tissues has shown that no matter which concentration of perorally inoculated spores, the secondly infected tissues/organs are those muscles and tracheae closely surrounding the anterior midgut. All these finding suggested that the primary spores play a very important role in the adjacent dissemination of *N. bombycis* ISC-ZJ in *B. mori* larvae by their spontaneous germination.

4.4.2.2. Phagocytosis and melanization in the dissemination of N. bombycis *ISC-ZJ in* B. mori *larvae*

4.4.2.2.1. Phagocytosis-killer and potential promoter

The phagocytosis is the uptake or engulfment of particulate ligand/entities, usually measuring >0.5μm, into cytoplasmic vacuoles by mechanisms that require actin polymerization. The phagosome containing the ingested material matures into phagolysosomes by a series of fusion events with endosomal vesicles (Couzinet *et al*., 2000). While phagocytosis has been long considered as a conventional cellular immune response to the pathogen invasion and it may lead to the killing and digestion of microbes (Lavine and Strand, 2002), there is accumulating

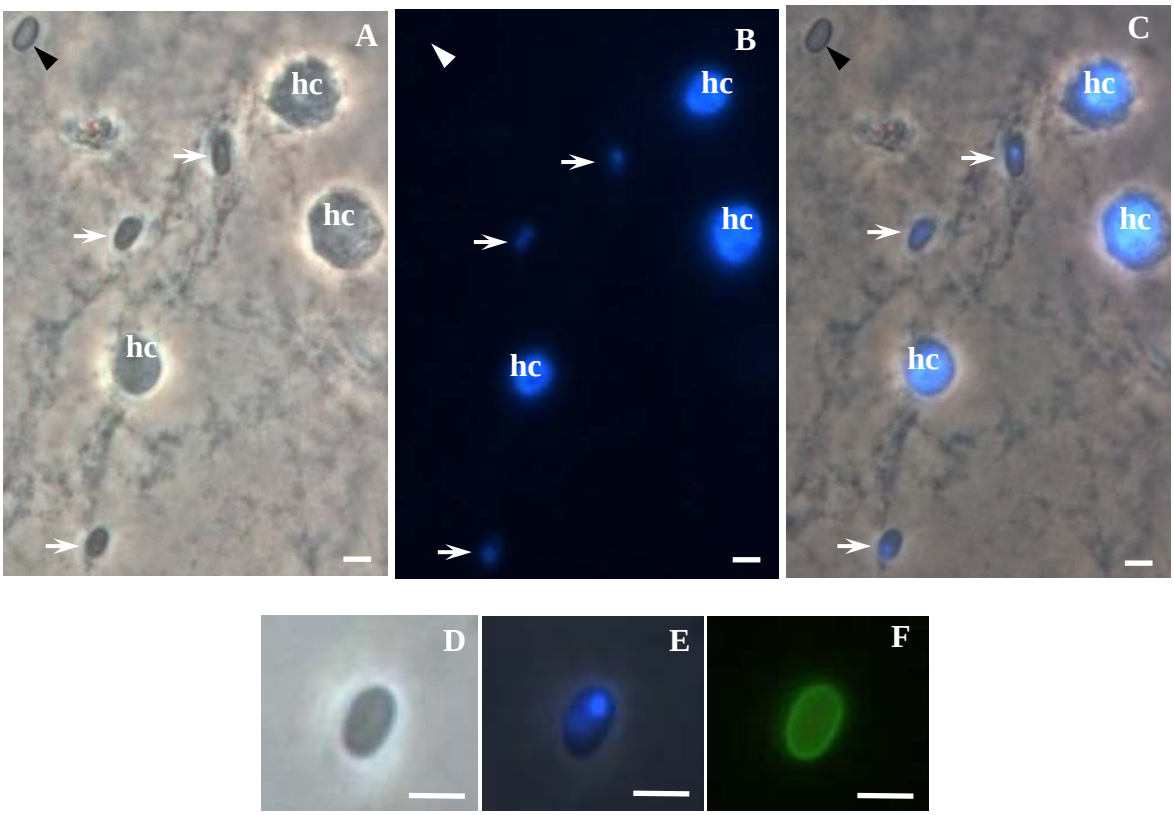

Figure 43. ***Nosema bombycis*** **external spores present in** ***Bombyx mori*** **hemolymph at 19h after infestation.** A, D: phase contrast; B, DAPI staining; C, E: superposition of phase contrast and DAPI staining; F, immunofluorescence microscopy (Ac, Anti-fixed spores of *Nosema bombycis*). Bars=2.5µm. hc, hemocyte; arrows, *N. bombycis* external spores; arrowheads, germinated empty spore.

evidence for their role of internalizing intact microsporidia (Couzinet *et al*., 2000; Bigliardi and Sacchi, 2001; Franzen *et al*., 2005) and disseminating the microsporidian infection. Phagocytosis has been found as the other efficient mechanism for microsporidian to give access to and actively invade host cells (Couzinet, 2000; Franzen, 2004). The internalized spores by phagocytosis are able to prevent acidification of the phagolysosomes they reside in (Weidner and Sibley, 1985; Nassonova *et al*., 2001; Tokarev *et al*., 2005), as the case for other intracellular protozoans including *Toxoplasma gondii* and *Trypanosoma cruzi* (Garcia-del portillo and Finlay, 1995). The prevention of acidification is important for microsporidian survival in phagolysosome. The viable spores can escape from the phagolysosome by germination and infect the host cells (Franzen, 2004). In this case, the phagocytoic uptake represent one route used by microsporidian unique germination mechanism to infect the host cells and disseminate the infection within the host in concert with the vehicle role of blood cells.

As a microsporidian with high pathogenity to *B. mori*, it is possible that *N. bombycis* can invade its host and disseminate their infection *in vivo* by means of germination not only from the known digestive fluid, but also from phagolysome formed in different epithelial cells, hemocytes or tissues, though this has to be confirmed. In fact, three of five *B. mori* hemocyte types (prohemocyte, granulocyte, plasmatocyte) have the function of phagocytosis (Akai and Sato 1973; Beaulaton 1979; Han *et al*. 1998; Yamashita and Iwabuchi 2001; Ling *et al*., 2003, 2005a). Besides the conventional "insect macrophages" or professional phagocytes-granulocytes and plasmatocytes, *B. mori* prohemocytes, which have been demonstrated as stem cells as in other insects (Yamashita and Iwabuchi 2001), can adopt the morphology of plasmatocytes and have the capacity to phagocytose (Ling *et al*., 2005a). In the current study, we also observed a prohemocyte, a nonprofessional phagocyte, phagocytosing an intact *N. bombycis* ISC-ZJ cell. To our knowledge, this is the first report showing phagocytosis of *N. bombycis* by *B. mori* hemocytes. Though the intracellular fate of the phagocytosed spores is unknown, it is strongly suggested that phagocytosis may have been used for *N. bombycis* ISC-ZJ dissemination in *B. mori* larvae.

4.4.2.2.2. Melanization-inhibitor or cleaner

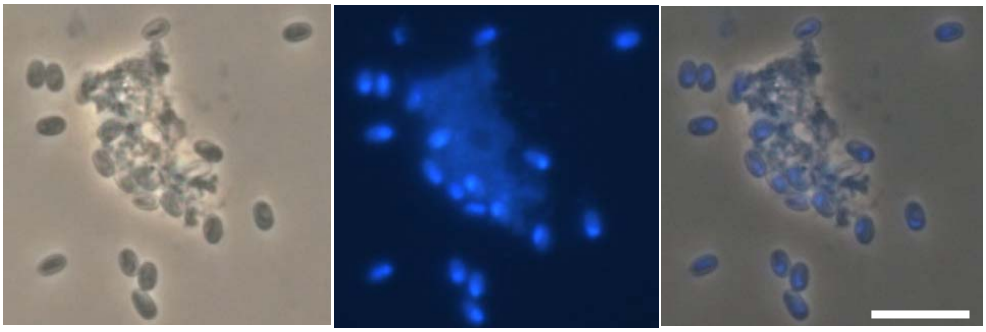

Figure 44. The hemocyte of the severely infected *Bombyx mori* 5th instar larva was triggered to lyse at 192h postinoculation and released a large number of *Nosema bobmycis* cells in the hemolymph of *B. mori* 5th instar larvae. The larvae are perorally inoculated with 10^{10} *Nosema bobmycis* spores/gram artificial diet. A, phase contrast; B, DAPI staining; C, superposition of phase contrast and DAPI staining. Bar=10 μm.

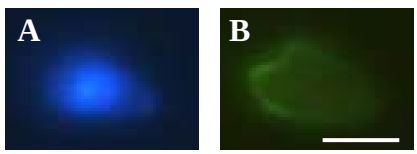

Figure 45. Primary spore present in the hemolymph of *Bombyx mori* 5th instar larva. The larvae are perorally inoculated with 10^{10} *Nosema bobmycis* spores/gram artificial diet. A, DAPI staining; B, IFA analysis. By immunolabeling with PAb against of formaldehyde-fixed *N. bombycis* spores, a depression at the posterior end of spore wall can be clearly shown. Bar=2 μm.

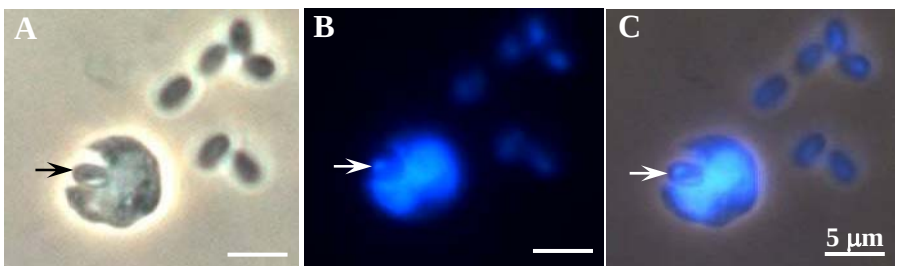

Figure 46. *Bombyx mori* hemocyte immune reponse to *Nosema bombycis* invasion: phagocytosis. A prohemocyte is phagocytosing an intact *N. bombycis* spore. A, phase contrast microscopy; B, DAPI staining; C, superposition of phase contrast and DAPI staining. Arrow shows the intact *N. bombycis* spore.

The phenoloxidase-based melanization involves a complex series of reactions that include the phenoloxidase-catalyzed oxidation and sequential conversion of phenolic substances such as tyrosine and DOPA, to melanin (Söderhäll and Cerenius, 1998; Asano and Ashida, 2001). Melanin was deposited over the surface of various pathogens and parasites or damaged host cells/tissues to form a surrounding melanotic layers or capsule and immoblize them. Pathogens or parasites are killed apparently by free radicals and toxic quinone intermediates produced during oxidation and melanin biosynthetic pathway (Cerenius and Söderhäll, 2004; Michel and Kafatos, 2005). Melanization has been shown to be able to kill not only bacteria but also the unicellular protozoan parasite *Plasmodium* sporozoite (Hillyer *et al*., 2003a, b).

As most typical insect defense reaction to microsporidian (Becnel and Andreadis, 1999), melanization can be observed in insect different tissue or hemocoele (Hoch *et al*., 2004; Johnson *et al*., 1997; Tokarev *et al*., 2007).Though the molecular mechanism of melanization-mediated microsporidian killing is unclear, it has been shown that the cytotoxic derivatives in melanin synthesis pathway can lead to the abnormal sporogony and have the deteriorating effect on spore morphogenesis (Tokarev *et al*., 2007). In the present study, *N. bombycis*-induced melanization have been optically observed in *B. mori* intestine, Malpighian tubules, and at the late stage of parasite infection, *B. mori* skin was covered with many dark dots and blotches, which is also the origin of *B. mori* "pepper disease". The melanization of infected hemocyte and *N. bombycis* cells in hemocyte or hemolymph have been observed by fluorescence and transmission electron microscopy. It indicates that the melanization elicited by *N. bombycis* is robust and has been used to immobilize and/or kill *N. bombycis* cells. However, compared with *N. bombycis* mighty survival and multiplication capabilities, the intense melanization in *B. mori* induced by *N. bombycis* seems still not enough to stop the dissemination of parasite infection in the whole body

4.4.2.3. Hemocyte and hemolymph in the dissemination of N. bombycis *ISC-ZJ in* B. mori *larvae*

To date, very little is known about the vector/vehicle role of insect hemocytes and hemolyph in microsporidian dissemination *in vivo*. In vertebrate, mechanisms of transportation of microsporidian by host cell such as leucocytes (macrophages), undifferentiated mesenchyme

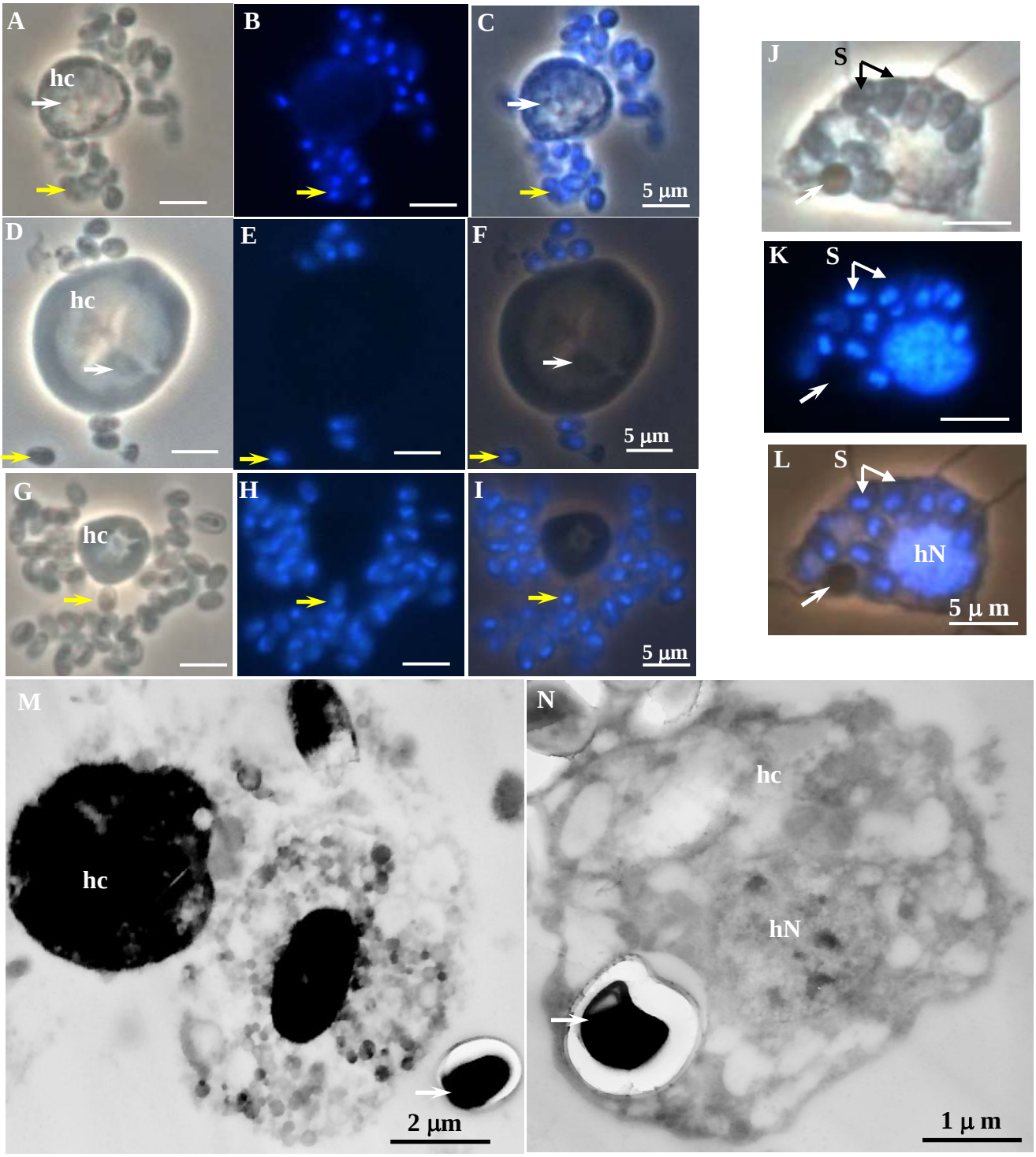

Figure 47. *Bombyx mori* hemocytes and hemolymph immune reponse to *Nosema bombycis* invasion: Melanization. Melanization or melanin synthesis pathway can form melanotic layers or capsules on the surfaces of invading organisms and infected host tissues, which are immobilized by these hard melanotic layers or capsules and killed by the cytotoxic derivatives or intermediates produced in this pathway. A, D, G, J: phase contrast microscopy; B, E, H, K: DAPI staining; C, F, I, L: superposition of phase contrast and DAPI staining; M, N: transmission electron micrographs. The hemocytes in A~I, M are melanized. White arrows in A, C, D, F, J~N are the melanized *N. bombycis* cell; The melanized *N. bombycis* spores in M and N are so hard to cut that they seperated from the resin medium. The yellow arrows in D-L and S in J~L show the intact *N. bombycis* spores. hc, hemocyte; hN, hemocyte nucleus.

cells and body fluids (blood) have been suggested (Canning *et al*., 1986). By using the infected hemolymph of silkworm previously inoculated per os with spores, Trager succeeded in infecting primary ovarian tissue cultures of *B. mori* with *N. bombycis* (Trager, 1937). Ohshima also realized the infection of silkworm larvae with *N. bombycis* by hemocoelic inoculation of spores primered under alkaline conditions (Ohshima, 1937). These findings strongly indicated that *B. mori* hemolymph and hemocytes, which are mobile within *B. mori* body cavity, play an undeniable role in mediating the spread of infection to all susceptible tissues .

In our study, *N. bombycis* ISC-ZJ sporoplasm can present in hemolymph as early as 34h PI. Whether they are directly deposited by *N. bombycis* ISC-ZJ environmental spores still in the digestive tube is not unclear. In fact, the environmental spores has been suggested that they can also deposit their sporoplasms directly at the body cavity by their long polar tubes penetrating through the intestine epithelial wall (Ishihara, 1985; Canning *et al*., 1986; Dyková, 1995). But this needs further confirmation.

From 34h PI to 149h PI, *N. bombycis* ISC-ZJ sporoplasm, meront and sporont can be infrequently observed. Similarly, where do these young parasite come from? It seems that they are not released by hemocyte, since the hemocytes were only infected at 71h for the first time and till 121h the infection of hemocyte is very slight with only one or two parasite in it. Moreover, whether these early stage parasites in hemolymph will degenerate or they can further disseminate infection by invading other hemocytes or tissues is unknown. In *N. bombycis*-inoculated *B. mori* ovarian tissue culture medium, while many sporoplasms emerged from spores usually decreased in volume, degenerated and failed to invade host cells, some sporoplasm changed karyotype and the cytoplasm increased (Ishihara and Sohi, 1966). Whether it means young stage *N. bombycis* ISC-ZJ cells in hemolymph observed in this study can disseminate parasite infection *in vivo* or not needs future investigation.

At 192h PI, a large number of free *N. bombycis* ISC-ZJ cells, hemocytes which are lysing and releasing many parasites, sloughed tissue pieces crowded with parasite can be observed in hemolymph. Since *B. mori* hemocytes and some tissues have been severely infected at this time, *N. bombycis* ISC-ZJ cells present in the hemolymph can be considered to be released both by hemocytes and by other tissue cells such as sloughed fat body cells.

The primary spores present in the hemolymph can move with the hemolymph, get close to

other hemocytes and silkworm interior tissues and organs "immersed" in hemolymph and finally invade them by their spontaneous germination. At the same time, though whether *N. bombycis* environmental spores can germinate in hemolymph or not is not unclear, we can not exclude the possibility of environmental spores in hemolymph can further disseminate the parasite infection to other hemocytes and host cells by phagocytosis mechanism.

The occasional incidence of environmental spores in hemolymph at 2.5h, 5h and 19h is worth of further investigation for better understanding parasite invasion and dissemination mechanism. Where did they come from? How can they reach the hemolymph? Can these environmental spores in circulating hemolymph spread infection by host cell phagocytosis?

On the other hand, *B. mori* hemocytes are also highly immunoreactive cells and can function cooperately with hemolymph as an inhibitor or cleaner in the elimination of invading microorganisms (Koizumi *et al*., 1997, 1999; Ochiai and Ashida, 2000; Ohta *et al*., 2006). While hemocyte-mediated phagocytosis is a potential promoter of *N. bombycis* infection dissemination *in vivo* as above described, it may also lead to the deteriorate effects on parasite development or the killing of parasite, as the case of *Plasmodium* sporozoites killed by mosquito hemocytes (Hillyer *et al*., 2003b). Hemocyte-mediated encapsulation and nodule formation around parsites or infected tissues can also help to immobilize and/or killing *N. bombycis* cells. Moreover, *B. mori* hemocytes are responsible for the synthesis of prophenoloxidase and phenoloxidase, two absolutely necessary enzymes in the phenoloxidase-melanization pathway, which can then be secreted into the hemolymph or other tissues (Ashida *et al.*, 1988; Asano and Ashida, 2001; Ling *et al*., 2005 b). At the same time, *B. mori* humoral and cellular pattern recognition receptors (PRRs), which can specifically recognize microbial structurally conserved pathogen-associated molecular patterns (PAMPs) in non-self recognition have been found in hemolymph or localized to the surface of hemocytes (Koizumi *et al*., 1997, 1999; Ohta *et al*., 2006). In addition, numerous antimicrobial peptides (AMPs), which are inducibly synthesized in the fat body and epithelia and have different microbicidal activity, are secreted in *B. mori* hemolymph (Yamakawa and Tanaka, 1999; Bulet *et al*., 2003; Tanaka *et al*., 2005). It is plausible that these AMPs should have the capacity to lyse or kill *N. bombycis* cells released in hemolymph, as the case of insect AMPs to Trypanosome (Bulet *et al*., 2004). However, in this study, the parasite dissemination is always systemic, it indicates that *B. mori* humoral and hemocyte-mediated

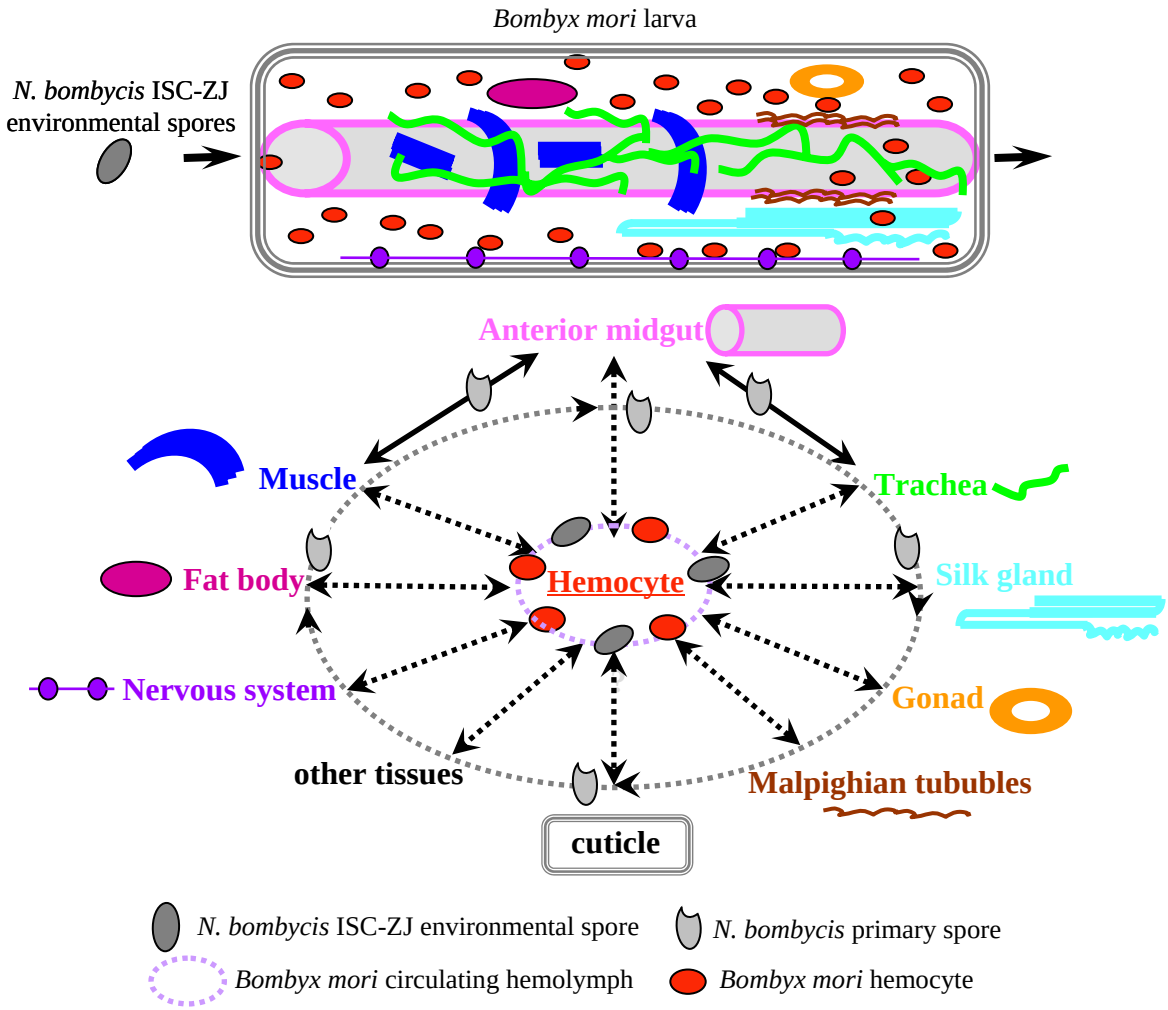

Figure 48. Hypothesis of *Nosema bombycis* ISC-ZJ dissemination route in *Bombyx mori* larvae from *in vivo* experiments: *N. bombycis* ISC-ZJ environmental spores first establish the infection in the anterior midgut epithelial cells and midgut basal membrane by spore germination or host cell phagocytosis. Then, the primary spores formed in the midgut can disseminate the infection to the midgut surrounding muscles/tracheae by their spontaneous germination *in vivo*. At the same time, the primary spores formed in midgut and its surrounding muscles/tracheae can spread the infection to the circulating hemocytes. Once the hemocytes in the hemolymph are invaded, the comprehensive dissemination networks will soon be established: 1) the primary spores formed in the midgut, muscles and trachea continue to spread infection to adjacent hemocytes and tissues or organs; 2) at the early stage of hemocyte infection, the primary spores in hemocytes can move with the hemocyte-hemolymph and invade both other hemocytes and distant tissues and organs, in this case, the hemocyte and hemolymph function as the vehicle or disseminator to help the primary spores to reach distant host cells, 3) at the late stage, as the hemocytes and other tissues like fat bodies were severely infected, a large number of primary spores and environmental spores are released into the hemolymph by the lysis of hemocytes or sloughed host cells. The primary spores in hemolymph continue to disseminate their infection as described in 1) and 2), and environmental spores can gain access to host cells by phagocytosis and infect them by germination from phagolysosome. At this stage, all *B. mori* interior tissues and organs immerse in parasite-rich hemolymph and can be infected. The complete infection of *B. mori* larvae will follow.

immune reponses are very limited and weak.

Notwithstanding the complexity of *N. bombycis* interactions with *B. mori* hemocytes and hemolymph, the current study has shown that on the one hand, *B. mori* hemocytes can function as a producer of parasites with hemolymph as an efficient transporter and they work together to actively disseminate *N. bombycis* ISC-ZJ infection *in vivo* on a large scale, on the other hand, *B. mori* immunoreactive hemocytes and hemolymph may play an certain role in parasite deteriorating and killing, but they can not stop the parasite systemic dissemination *in vivo*.

4.4.2.4. Hypothesis of N. bombycis *dissemination route of in* B. mori *larvae*

It has been believed that the peroral infection of silkworm by microsporidians starts from the germination of environmental spores in the larval midgut (Kawarabata, 2003). Our investigation demonstrated that the peroral infection of silkworm larvae with *N. bombycis* ISC-ZJ starts in the midgut epithelium and then surrounding muscles/tracheae, gradually spreads to distant other tissues or organs and finally the whole body. *N. bombycis* ISC-ZJ revealed the high infectivity and pathogenicity to silkworm larvae without parasite tropism or invasion speicificity for some subtypes of host cells, which is very similar to the case of *N. bombycis* NIS-001 (Sato and Watanable, 1986; Fugiwara, 1985).

On the basis of our finding in the present study, one hypothesis is proposed to outline the invasion and dissemination route of *N. bombycis* ISC-ZJ in *B. mori* larvae (**Figure 48**): After *N. bombycis* ISC-ZJ dormant environmental spores entered *B. mori* intestine along with the food, they can get access to the midgut epithelial cells or other host cells by two mechanisms, 1) spore germination: with the appropriate stimuli in the digestive fluid, the spores are activated to discharge of polar tubes to deposit their sporoplasms into the nearest midgut epithelial cells to begin their developmental cycle, 2) phagocytosis: first, those outside sporoplasms in intestine deposited by random spore germination can be phagoctosed by the midgut epithelial cells and result in the infection; second, the ungerminated intact environmental spores can be phagocytosed by midgut epithelial cells and the spore can still infect host cells by germinating from the phagosome; rarely, the environmental spores in the intestine can also directly deposit their sporoplasms into the haemocoel and these sporoplasms can be phagocytosed by hemocytes

or other tissues and lead to the infection of these host cells. *N. bombycis* ISC-ZJ sporoplasms in the midgut epithelial wall differentiate into meront, sporont, primary sporoblast, then primary spores. These primary spores germinate spontaneously within the host cell and spread parasite infection to the same or adjacent epithelial cells, closely surrounding muscles, tracheae and fat body. At this period, it is mainly the primary spores spread parasite infection within host in a small scale. Once the hemocytes in the hemolymph are invaded, the comprehensive invasion networks will soon be established: 1) the primary spores formed in the midgut epithelial cells, muscles, trachea and fat body continue to spread infection to adjacent hemocytes and tissues or organs; 2) at the early stage of hemocyte infection, the primary spores in hemocytes can move with the hemocyte-hemolymph and invade both the other hemocytes and other distant tissues and organs, in this case, the hemocyte and hemolymph function as the vehicle or disseminator to help the primary spores to reach distant host cells, 3) at the late stage, as the hemocytes and other tissues like fat bodies were severely infected, a large number of primary spores and environmental spores are released into the hemolymph by the lysis of hemocytes or sloughed host cells. The primary spores in hemolymph continue to disseminate their infection as described in 1) and 2), and environmental spores can gain access to host cells by phagocytosis and infect them by germination from phagolysosome. At this stage, all *B. mori* interior tissues and organs immerse in parasite-rich hemolymph and can be infected. The complete infection of *B. mori* larvae will follow.

As a whole, our understanding of *N. bombycis* dissemination mechanism *in vivo* is far from complete. Additional studies are needed to determine *B. mori* midgut epithelial cell invasion and penetration mechanism, the complex interactions between *N. bombycis* and *B. mori* hemocyte and hemolymph, the fate of environmental spores released into the hemolymph and *B. mori* immune response to *N. bombycis* infection.

Results II

5. A proteomic-based approach for the characterization of some major structural proteins involved in host-parasite relationships from the silkworm parasite *Nosema bombycis* (Microsporidia).

Submitted to "*Proteomics*" and accepted

A proteomic-based approach for the characterization of some major structural proteins involved in host-parasite relationships from the silkworm parasite *Nosema bombycis* (Microsporidia).

Jian-Yang Wang[a,b,c], Christophe Chambon[d], Chang-De Lu[b], Ke-Wei Huang[c], Christian P. Vivarès[a], Catherine Texier[a*]

[a] Equipe Parasitologie Moléculaire et Cellulaire, LBP, UMR CNRS 6023, Université Blaise Pascal, 63177 Aubière, France

[b] Institute of Biochemistry and Cell Biology, Shanghai Institutes for Biological Sciences, Chinese Academy of Sciences, Shanghai 200031; Graduate School of the Chinese Academy of Sciences, China 200031

[c] Institute of Sericultural Research, Chinese Academy of Agricultural Sciences, Zhenjiang, China 212018

[d] Institut National de la Recherche Agronomique, Qualité des produits animaux – Plateforme Protéomique, Saint Genès Champanelle, France

*** Corresponding author:** Dr Catherine TEXIER

Equipe Parasitologie Moléculaire et Cellulaire, LBP, UMR CNRS 6023, Université Blaise Pascal, 63177 Aubière, FRANCE

catherine.texier@univ-bpclermont.fr

tel: +33 4 73 40 74 34

fax: +33 4 73 40 76 70

Abbreviations:

DAPI: 4',6-Diamidino-2-phenylindole dihydrochloride; IFA: immunofluorescent assay; PAb: polyclonal antibodies; PT: polar tube; PTP: polar tube protein; SW: spore wall; SWP: spore wall protein; TEM: transmission electron microscopy

Keywords:

2-DE maps, Microsporidia, MS/MS *de novo* sequencing, *Nosema bombycis*, polar tube proteins

Abstract:

Nosema bombycis is the causative agent of the silkworm *Bombyx mori* pebrine disease which inflicts severe worldwide economical losses in sericulture. Little is known about host-parasite interactions at the molecular level for this spore-forming obligate intracellular parasite which belongs to the fungi-related Microsporidia phylum. Major microsporidian structural proteins from the spore wall and the polar tube are known to be involved in host invasion. We developed a proteomic-based approach to identify few *N. bombycis* proteins belonging to these cell structures. Protein extraction protocols were optimized and four *N. bombycis* spore protein extracts were compared by SDS-PAGE and 2-DE to establish complementary proteomic profiles. Three proteins were shown to be located at the parasite spore wall. Moreover seventeen polyclonal antibodies were raised against major *N. bombycis* proteins from all extracts, and three spots were shown to correspond to polar tube proteins (PTPs) by IFA and transmission electron microscopy immunocytochemistry on cryosections. Specific patterns for each PTP were obtained by MALDI-TOF-MS and MS/MS mass spectrometry. Peptide sequence tags were deduced by d*e novo* sequencing using Peaks Online and DeNovoX, then evaluated by Mascot and Sequest searches. Identification parameters were higher than false-positive hits, strengthening our strategy that could be enlarged to a non-genomic context.

1. Introduction

The spore-forming obligate intracellular parasites called Microsporidia are unicellular eukaryotes that can infect a wide variety of animals ranging from protists to mammals, and constitute emerging pathogens and important pests for sericulture, fishery or shrimp farms. The internalized parasite cycle comprises a proliferative phase or merogony, followed by a multi-step differentiation phase or sporogony leading to mature spores that are released in the environment by host cell disruption [1]. Phylogenetic analyses based on conserved proteins [2, 3], rDNA sequences [4, 5] and the complete microsporidian *Encephalitozoon cuniculi* genome sequence [6, 7] have shown that Microsporidia are related to fungi. First considered as amitochondriate, these organisms are now supposed to have retained a mitochondrion-derived organelle called mitosome [6, 8].

Microsporidia display an original invasion mechanism, involving the polar tube, a cylindrical and very long structure coiled within the spore. Suitable stimuli promote an increasing intrasporal osmotic pressure that leads to the discharge of the polar tube and propels the spore content or sporoplasm through the polar tube into a host cell (review: [9]). Polar tube proteins (PTPs) are the most extensively studied microsporidian structural proteins. The cysteine-rich PTP1 and PTP2 which were only solubilized in reducing conditions, were characterized at the sequence level for the mammal-infecting species *Encephalitozoon cuniculi*, *E. hellem* and *E. intestinalis* [10-12] and for the insect-infecting species *Antonospora locustae* and *Paranosema grylli* [13, 14] and presented highly divergent sequences among species. Nevertheless the PTP1 family encompassed acidic mature proteins (333 to 431 aminoacids, proline- and glycine- rich) with apparent molecular masses of 50-55 kDa, while the PTP2 group comprised basic mature proteins (259-268 aminoacids, lysine- and glutamate- rich) of ~35 kDa. Their coding genes clustered in a syntenic region with identical gene order and orientation. Moreover PTP1 was shown to be O-mannosylated [13, 15], this modification being involved in some interactions with an unknown host cell mannose-binding molecule. Chemical cross-linking and co-expression experiments suggested interactions between PTP1 and PTP2 ([16] and data not published). A slightly acidic PTP3 (1256 aminoacids) was also described for *E. cuniculi* [16], as well as two additional PTPs for *E. cuniculi*, *A. locustae* and *P. grylli* (data not published).

While the classical concept of the parasite penetration mode into a host cell involves the polar tube acting as a needle-syringe system, microsporidian spores are also internalized after interactions between the parasite spore wall and the host plasma membrane, then phagocytosis [17-19]. This attachment depends on interactions between spore wall components and sulfated host cell glycosaminoglycans [20, 21]. To date, the knowledge of the primary structure of microsporidian spore wall proteins (SWPs) is limited to the *Encephalitozoon* genus with (i) three exospore (the outer electron-dense layer) components: SWP1 (50 kDa) in both *E. cuniculi* [22] and *E. intestinalis* [23], SWP2 (150 kDa) in *E. intestinalis* only [23], and ExP1 (27 kDa) in *E. cuniculi* [24], and (ii) three endospore (the innermost electron-lucent layer) components of *E. cuniculi*: EnP1/SWP3 (40 kDa) [25, 26], EnP2 (22 kDa) [25], *Ec*CDA (33 and 55 kDa) [27].

Nosema bombycis, a silkworm (*Bombyx mori*) parasite, was the very first microsporidian identified by Naegëli in 1857. This disporous and diplokaryotic organism develops at the direct contact of the host cytoplasm [28-30]. It was recognized as the orally- and transovarially-transmitted causative agent of the pebrine disease which almost destroyed the European silkworm industry in the mid 19th century [31, 32] and which still inflicts severe silk cocoon crop loss. Nevertheless very little is known about the molecular interactions between this historic microsporidian and its host of economic importance, and in particular about the two microsporidian structures involved in host-cell invasion (only a putative spore wall protein available in the NCBI database). We thus intended to unravel polar tube (PT) and spore wall (SW) proteins for *N. bombycis*. Since high evolution rates of microsporidian genes [7] render difficult the design of primers for PCR approaches, since the structural PT and SW proteins represent major landmarks in the *E. cuniculi* proteomic maps [24], and since *N. bombycis* genome is under sequencing [33], we developed a proteomic-based strategy to identify *N. bombycis* structural proteins. We thus established mono- and bi-dimensional protein patterns for the *N. bombycis* mature spore after optimization of extraction methods. Several polyclonal antibodies were raised against fixed spores and some major proteins allowing the description of three SW and three PT proteins, the latter being characterized by mass spectrometry *de novo* sequencing.

2. Materials and methods

2.1. Nosema bombycis *spore production and purification*

Nosema bombycis (Zhenjiang isolate ISC-ZJ) spores were produced and purified as previously described [34]. Briefly, they were harvested from infected larvae of its natural host, the silkworm *Bombyx mori* (75xinx7532 strain). Third instar larvae were exposed for 8h to mulberry leaves previously immersed in a *N. bombycis* spore suspension (5000 spores/mL). Heavily infected larvae were crushed in distilled water and large silkworm and mulberry debris were removed by filtration on 4 cheesecloth layers. After centrifugation (300xg, 15 min), spores were washed in distilled water until the pellet was white. Spores were further purified on an incontinous sucrose gradient with equal volume of 30%, 40% and 60% sucrose where they concentrated as a thin band between the 40% and 60% sucrose fractions. After washes in distilled water, the parasite fraction purity was checked by phase-contrast and fluorescent microscopy after DAPI staining.

2.2. Protein extraction

N. bombycis spore germination was induced at 25°C by 0.1 M KOH (30 min), then by 0.05 M KOH-0.25 M KH_2PO_4 (30 min). Cells were collected by centrifugation (20000xg, 10 min) and submitted to protein extraction. **Method 1**: Parasites (10^9 cells/mL) were disrupted in a lysis buffer containing 100 mM DTT, 4% CHAPS and 0.5% Triton X-100, by a 1-to-2-min-treatment with 0.4-0.5 mM acid-washed glass beads (diameter: 0.45 µm) followed by repeated cycles of freezing-thawing and sonication (Deltasonic 1320, 300 W, 28 kHz). Proteins from broken cells were first extracted with a solution containing 7 M urea, 2 M thiourea, 100 mM DTT, 4% CHAPS and 0.5% Triton X-100 for 6h at room temperature. After centrifugation (20800xg, 5 min), the supernatant was collected ("urea extract"). The sedimented material was treated with 30 mM NaOH for 16h at 4°C and centrifuged (15000xg, 5 min) to collect the supernatant ("NaOH extract"). The NaOH-insoluble material was finally boiled for 5 min in Laemmli solution containing 2.5% SDS, 0.125 M Tris HCl pH 6.8, 20% glycerol, 2 mM EDTA and 100 mM DTT ("Laemmli extract"). **Method 2**: Parasites (10^9 cells/mL) were disrupted in a buffer containing 10 mM Tris HCl pH 7.6 and 1 µM E64 (protease inhibitor, Sigma), with glass beads as in Method 1. After centrifugation (1000xg, 5 min), the insoluble material was treated with 2% Nonidet P40, 9.5 M urea and 5% 2-mercaptoethanol for 2h at room temperature. Soluble proteins (PEL extract) were collected after centrifugation (1000xg, 15 min). After quantification using the Plus-One 2D Quant Kit (Amersham), all protein samples were stored at -20°C.

2.3. Gel electrophoresis and Western blotting

Protein samples were characterized by standard SDS-PAGE on 12% polyacrylamide gels. Two-dimensional electrophoresis (2-DE) was performed as previously described [27] with 7-cm linear immobilized pH gradient strips. For image analysis, gels were stained using the PlusOne Silver Staining kit (Amersham). For mass spectrometry analysis and polyclonal antibody production, proteins were detected with Coomassie blue (Biosafe, Biorad). For immunoblotting studies, they were transferred onto polyvinylidene difluoride (PVDF) membranes (Millipore). After blocking for 1h in PBS-5% skim milk, membranes were incubated for 3h with appropriate dilutions of polyclonal mouse antibodies in PBS 0.1% Triton X-100. Bound antibodies were detected with a 1:10000 dilution of alkaline phosphatase – conjugated goat anti-mouse IgG (H+L)

(Promega) for 1h at room temperature and revealed with NBT/BCIP (Promega).

2.4. 2-DE gel analysis

Silver stained 2-DE gels were scanned with a GS-700 Densitometer (BioRad) and image analysis was performed with the PDQuest 7.0.0 software (BioRad). The relative abundance of each spot (RA) in a given gel was determined as a percentage of the total spot intensity in the gel. To compare intensity of a given spot common to two gels, the ratio (RA in gel A divided by RA in gel B) was calculated and three cases were delineated: the spot was more abundant either in A than in B (ratio ≥ 2) or in B than in A (ratio ≤ 0.5), or of equal abundance ($0.5 <$ ratio < 2).

2.5. Polyclonal antibody (PAb) production and purification

Polyclonal antibodies (PAbs) were raised against either *N. bombycis* 4% formaldehyde-fixed spores or major *N. bombycis* SDS-PAGE bands and 2-DE spots that were crushed in sterile PBS. Every two weeks, SWISS mice (Charles River, France) were injected intraperitoneally with samples homogenized in Freund's adjuvant (complete for the first injection and incomplete for the four next ones). Serum was collected 2 weeks after the last injection and stored at -20°C. The animal house (agreement C63014.19) and the experimental staff (agreement 63-146) have been approved by the French veterinary services, and experiences were conducted according to ethical rules. The anti-PEL1, anti-PEL2 and anti-PEL3 PAbs were further purified according to [14]. Briefly, PVDF membrane strips with SDS-PAGE-separated *N. bombycis* proteins were saturated 1h in PBS-5% skim milk and incubated with the corresponding PAbs (1:1000 in saturation buffer). After washing with TTBS (50 mM TrisHCl pH 7.4, 150 mM NaCl, 0.05% Tween 20), PAbs were eluted with 0.2 M glycine-HCl (pH 2.5), neutralized with 1.0 M Tris-HCl (pH 8.0) and conserved in TBS (50 mM Tris HCl pH 7.4, 150 mM NaCl).

2.6. Indirect Immunofluorescence Assays (IFA)

Germinated spores (see section 2.2.) were coated on poly-lysine treated glass slides, fixed with 100% methanol for 10 min at -80°C and permeabilized with 70% ethanol - 0.5% TritonX-100 for 30 min. Slides were then incubated for 1h with appropriate dilutions of PAbs in PBS-0.1% TritonX-100. Bound antibodies were detected with a 1:200 dilution of Alexa Fluor® 488

goat-anti-mouse IgG (Molecular Probes). DNA was stained by a 5-min incubation in a 1 µg/mL DAPI solution. Slides were observed with a Leica DMIRB immunofluorescence microscope.

2.7. Transmission electron microscopy (TEM) immunocytochemistry

Ultrathin *N. bombycis* spore cryosections were obtained as previously described [27]. After a 1h-blocking with 1% ovalbumin in PBS, they were incubated 2h with various dilutions of PAbs and then 1h with a 1:100-dilution of goat-anti-mouse IgG conjugated with 10-nm colloidal gold particles (Sigma). Grids were stained and embedded with 0.5% aqueous uranylacetate and 1.6% methylcellulose, prior to examination with a JEOL 1200EX transmission electron microscope.

2.8. Trypsic digestion for mass spectrometry analysis

Protein spots were manually excised from Coomassie blue-stained 2-D gels. Excised gels were washed with destaining solutions (25 mM NH_4HCO_3 – 5% acetonitrile for 30 min and 25 mM NH_4HCO_3 - 50% acetonitrile for 30 min). After dehydration in 100% acetonitrile and drying, the volume spot was evaluated and three volumes of a 10 ng/µL trypsin (V511, Promega, Madison, WI, USA) solution in 25 mM NH_4HCO_3 were added. Digestion was performed at 37°C for 5h. After centrifugation, trypsic peptides were extracted by acetonitrile. The mixture was then sonicated for 5 min and centrifuged.

2.9. MALDI-TOF analysis

For MALDI-TOF analysis, 1 µL of trypsin peptide mixture was loaded onto the MALDI target and the matrix solution (5 mg/mL α-cyano-4-hydroxycinnamic acid in 50% acetonitrile/0.1% trifluoroacetic acid (v/v)) was added immediately and allowed to dry at room temperature. The MALDI-TOF mass spectrometer (Voyager DE-Pro, Perspective BioSystems, Farmingham, MA, USA) was used in positive-ion reflector mode for peptide mass fingerprinting. External calibration was performed with a standard peptide solution (Proteomix, LaserBio Labs, Sophia-Antipolis, France), while internal calibration was performed using peptides from porcine trypsin auto-lysis. Protein databases from *Encephalitozoon cuniculi* (local one) and *Antonospora locustae* ("*Nosema locustae* Genome Project, Marine Biological Laboratory at Woods Hole, funded by NSF award number 0135272", http://jbcp.mbl.edu/Nosema/index.html) were explored

using the Mascot software version 2.1 (http://www.matrixscience.com; mass tolerance: 25 ppm, miss cleavages: 1, variable modifications: carbamidomethylation, oxidised methionine). Peptide masses were assumed to be monoisotopic.

2.10. NanoLC-MS/MS analysis

HPLC was performed with an Ultimate LC system combined with Famos autosample and Switchos II microcolumn switching for preconcentration (LC Packings, Amsterdam, Netherlands). The samples were loaded on the column (PEPMAP C18, 5 µm, 75 µm ID, 15 cm; LC Packings) using a preconcentration step in a microprecolumn cartridge (300 µm ID, 1 mm). Six µL of each sample were loaded on the precolumn at 40 µL/min. After 3 min, the precolumn was connected with the separating column and the gradient was started at 200 nL/min. The solvents with 0.5% formic acid were 95% water / 5% acetonitrile (A) and 95% acetonitrile / 5% water (B) and a 45-minutes linear gradient from 10% to 90% of B was applied. For ion trap-MS, a LCQ deca with a nano electrospray interface (ThermoElectron, Les Ulis, France) was used. Ionization (1.8 kV ionization potential) was performed with a liquid junction and a noncoated capillary probe (New Objective, Cambridge, USA). Peptide ions were analyzed by the data-dependant "triple-play" method as follows: (i) full MS scan (m/z 400-2000), (ii) ZoomScan (scan of the major ion with higher resolution), (iii) MS/MS of this ion. The databases (ncbi.nr, *E. cuniculi* and *A. locustae* ones) were searched by Mascot version 2.1 (miss cleavages set to 1; m/z tolerance set to 1.5 and 0.8 for the parent ions and the fragment ions, respectively) and Sequest in Bioworks 3.1 (ThermoElectron; miss cleavages set to 1; m/z tolerance set to 2.0 and 0.5 for the parent ions and the fragment ions, respectively).

2.11. De novo sequencing

MS/MS *de novo* sequencing was performed on ion trap data using DeNovoX version 1.0 (ThermoElectron, San Jose, CA) and Peaks Online (http://www.bioinformaticssolutions.com/peaksonline/) softwares. DeNovoX was run with default parameters (standard amino acid table, mass tolerance set to 0.8). Different analysis parameters were tested with Peaks: mass tolerance (0.4 and 0.8), amino acid table (standard and some variable modifications as acetylation, carbamidomethylation, and oxidation). In order to test if the Mascot and Sequest softwares were

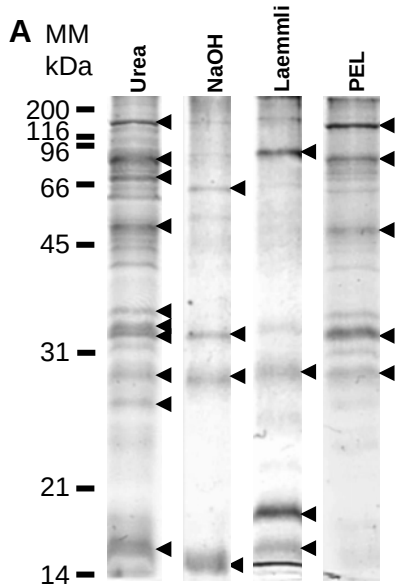

Figure 49. Mono- and two-dimensional electrophoresis patterns of proteins from *N. bombycis* spore extracts. A) SDS-PAGE profiles of *N. bombycis* protein extracts. Seven µg of each extract were separated on a 12%-polyacrylamide gel and revealed by silver staining. The urea extract (lane 1) is characterized by 10 major bands at 148, 77, 62, 52, 38, 36, 35, 30, 27 and 16 kDa. The NaOH extract (lane 2), the Laemmli extract (lane 3) and the PEL extract (lane 4) present four or five intense bands (60, 35, 30 and 15 kDa; 83, 30, 18 and 16 kDa; 138, 72, 52, 35 and 30 kDa, respectively). Arrowheads label these major bands. The urea (B, D) and the PEL (C, E) extracts were submitted to 2-DE. For IEF, 20 µg of proteins were loaded on a pH 3-10 linear gradient. After SDS-PAGE on a 12%-acrylamide gel, proteins were revealed by silver staining. Gels were representative of three independant ones. D and E correspond to enlargements of the 25-40 kDa / pI 4.85-6.10 windows in B and C respectively, and were compared by image analysis. Specific spots of the urea and PEL extracts are labelled "Ux" and "Px", respectively, and a star shows their theoretical position on the gel where they are absent. Common spots of both extracts fall into three categories: more abundant in the urea extract ("UPx") or in the PEL extract ("PUx"), and equal abundance ("=x").

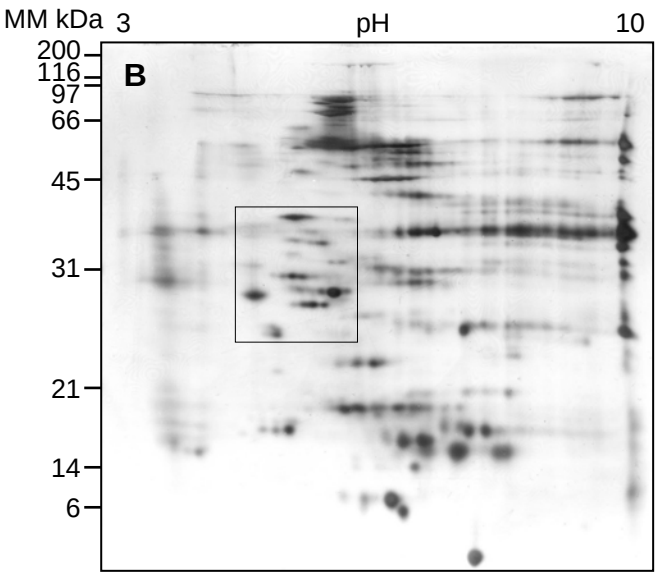

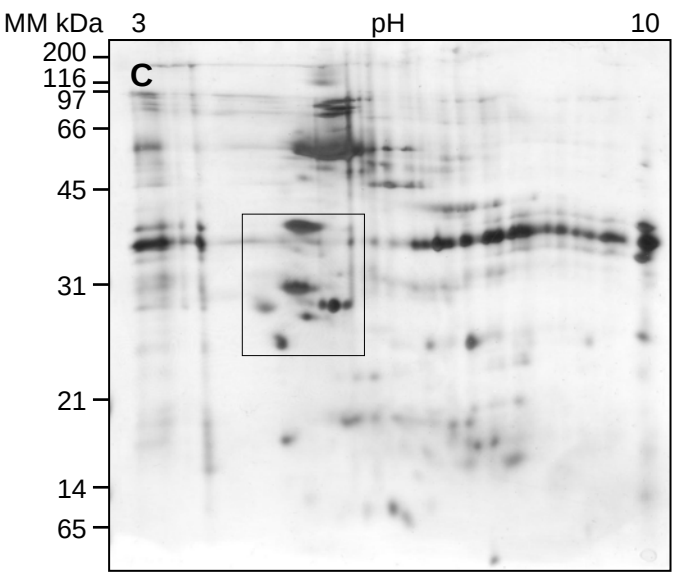

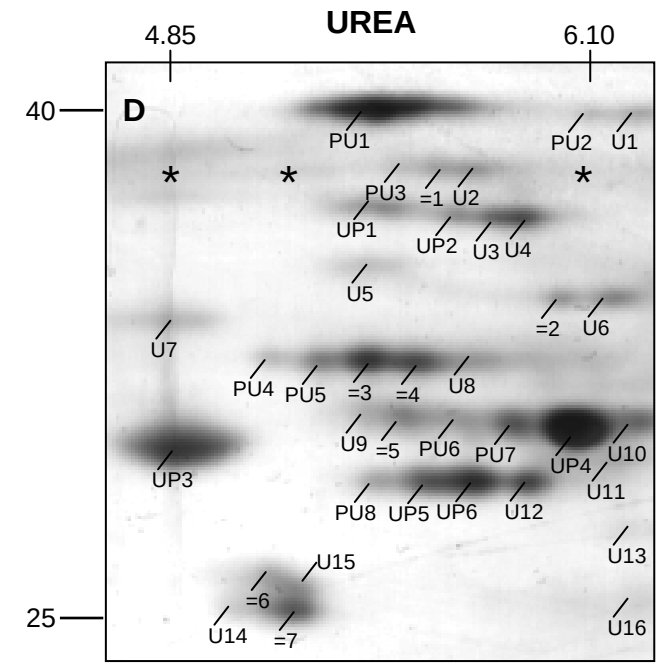

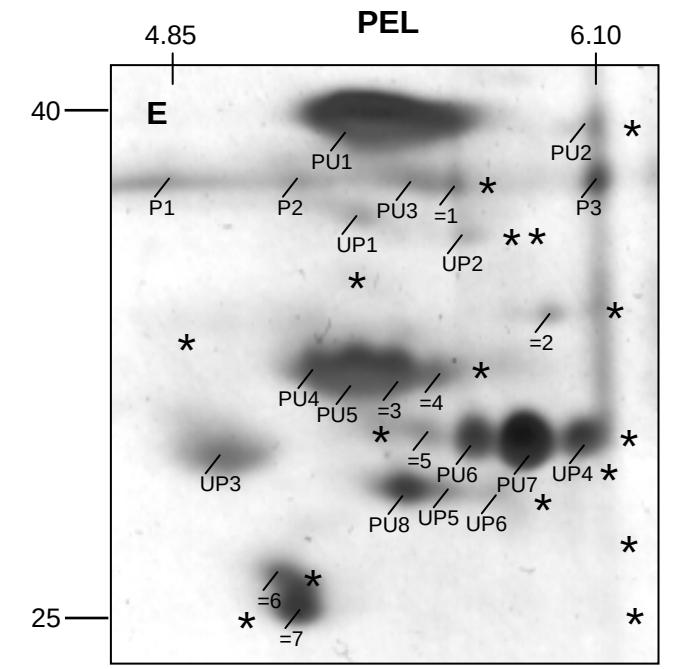

able to associate with significant scores the MS/MS data and the *de novo* peptide sequences, a "protein environment" was provided to the *de novo* peptide sequences obtained for a given *Nb*PTP protein (see table 1) by incorporating them between trypsin proteolysis sites in the corresponding *E. cuniculi* PTP sequence. Two "chimera" proteins were constructed for each *Nb*PTP: one with Peaks peptides and one with DeNovoX peptides. These hybrid proteins were then integrated in an unrelated local protein database (about 45565 entries from poplar) which was then searched, as well as the total Swissprot database (2006 July, 228630 entries), by Mascot and Sequest as described in section 2.10. and using the MS/MS raw data of each 2-DE spot.

3. Results

3.1. Extraction and 2-DE patterns of the microsporidian Nosema bombycis *proteome*

Since the microsporidian polar tube and cell wall are involved in host-microsporidia relationships, their components may play an important part in cell invasion and in the silkworm infestation. In order to describe major structural *Nosema bombycis* proteins, we first developed protein extraction and separation procedures. *N. bombycis* can only be propagated in its natural host larvae [34, 35]. Spores are the main developmental stages recovered after purification and their thick proteino-chitinous cell wall requires harsh breakage conditions combined with sequential protein extraction treatments. The extraction strategy previously described for the *Encephalitozoon cuniculi* spore proteome was thus applied [24]. Briefly, a soluble fraction in a highly denaturing mixture ("urea extract") was collected after spore disruption. The alkaline treatment of the insoluble material ("NaOH extract") was known to solubilize fungal O-glycosylated-linked spore wall proteins [36]. Finally, alkali-resistant proteins were solubilized by boiling in standard Laemmli solution ("Laemmli extract"). A second strategy, adapted from Langley et al. [37], solubilized proteins associated with insoluble material after spore breakage (spore wall and polar tube fragments, membranes) and the "PEL extract" we obtained should be thus richer in structural proteins. The four extracts exhibited rather different SDS-PAGE patterns (**Figure 49A**). As the "urea" and "PEL" 2-DE-compatible treatments were designed to target proteins with different physico-chemical properties, the extracts were analysed by 2-DE (**Figure 49B-E**). Wide pH gradient gels (pH 3-10) reproducibly revealed about 450 and 335 different silver-stained spots for the urea extract (**Figure 49B**) and the PEL extract (**Figure 49C**),

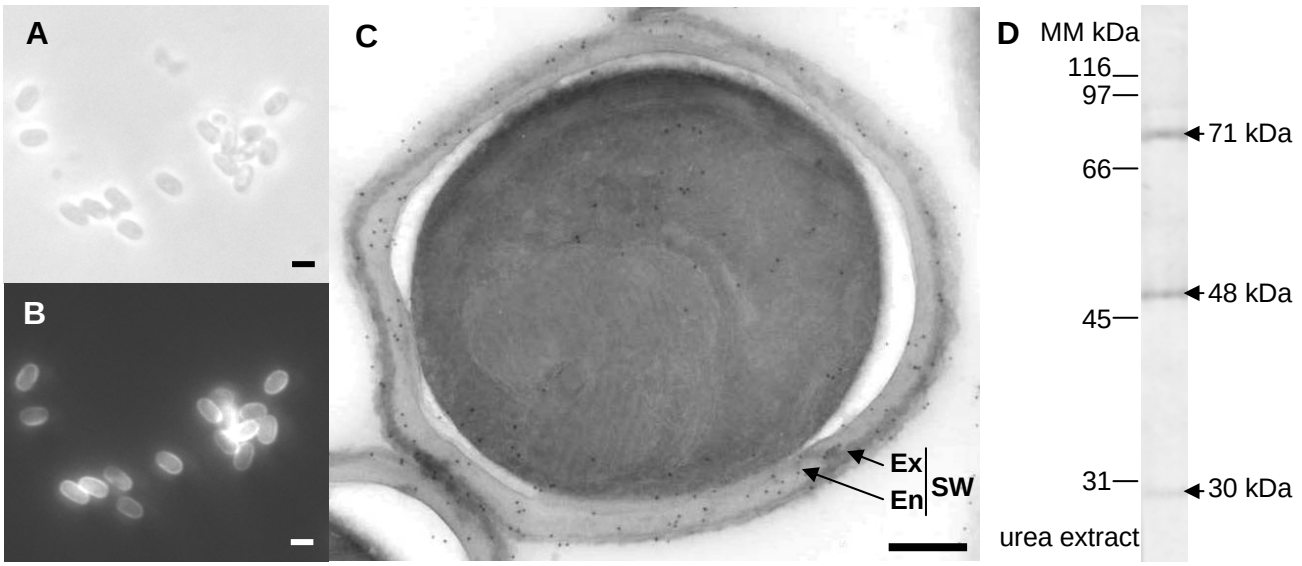

Figure 50. Identification of *N. bombycis* spore wall proteins. A mouse polyclonal antibody (anti-Nb PAb) was produced against formaldehyde-fixed spores and presented a typical spore wall labelling either by IFA (spores coated on slides observed in phase contrast (A) and immunolabelled with the anti-Nb PAb (B) at the 1:300 dilution, bar = 3 µm) or by TEM immunocytochemistry (C, dilution 1:100 , bar = 200 nm). D) Reactivity of the anti-Nb PAb on a western blot of the urea extract. Three bands at 71, 48 and 30 kDa were recognized. *SW: spore wall; Ex: exospore; En: endospore*.

respectively. While major proteins at 53-81 kDa/pI 6 or at 37 kDa/pI>6.8 appeared as common features, several spot patterns differences were mainly observed. For example, proteins of low molecular mass (<27kDa) were more diverse and abundant in the urea extract (119 versus 69 spots). Moreover, in the window (25-40 kDa/pI 4.85-6.10), the urea extract harboured 37 spots, 16 of them being urea extract-specific (**Figure 49D**), while only 3 spots among 24 were characteristic of the PEL extract (**Figure 49E**), and among the 21 common spots, 6 were more abundant in the urea extract and 8 in the PEL extract while 7 presented an equal abundance.

3.2. Production of N. bombycis*-specific antibodies*

Then we intended to produce specific probes for *N. bombycis* polar tube (PTPs) and spore wall proteins (SWPs). Polyclonal antibodies (PAbs) raised against formaldehyde-fixed spores strongly reacted with *N. bombycis* spore wall components located either in the exospore or the endospore (**Figure 50A-C**). Three bands at 71, 48 and 30 kDa of the urea extract were labelled by this serum (**Figure 50D**) and thus must contain SWPs. As PTPs and SWPs represented major landmarks of the *E. cuniculi* proteomic map [24], specific PAbs were raised against some *N. bombycis* major proteins excised from SDS-PAGE and 2-DE gels. Two bands from the "urea" (148 and 52 kDa), "NaOH" (35 and 15 kDa) and "Laemmli" (83 and 18 kDa) extracts and 11 spots from the PEL extract were thus injected to mice. PAbs were tested in western blot assays after SDS-PAGE and 2-DE. When tested on the corresponding protein extract, 6 among the 17 sera gave no or not interpretable signals in western blot assays after SDS-PAGE (data not shown). Ten reacted specifically with a single band at the corresponding size while one which was produced against a 25-kDa spot reacted with a 52-kDa band (not shown). The anti-PEL1 (**Figure 51A**, 54 kDa, pI 5.4) and anti-PEL2 (**Figure 51A**, 36 kDa, pI 10) sera highlighted a single band (54 and 36 kDa, respectively) on SDS-PAGE western blots of the PEL extract (not shown). On 2-DE blots, PEL1 exhibited ~8 acidic isoforms (**Figure 51B**) while PEL2 was characteristically distributed on the whole pH 3-10 range (**Figure 51C**). Similar SDS-PAGE- and 2-DE- patterns were obtained when the anti-PEL1 and anti-PEL2 sera were tested on the urea extract (data not shown), suggesting that the PEL1 and PEL2 proteins were also solubilized by this treatment. When tested on the PEL proteins, the anti-PEL3 (**Figure 51A**, 150 kDa, pI 7.1) PAbs labelled a 150-kDa band/spot and several lower ones which probably resulted from protein degradation

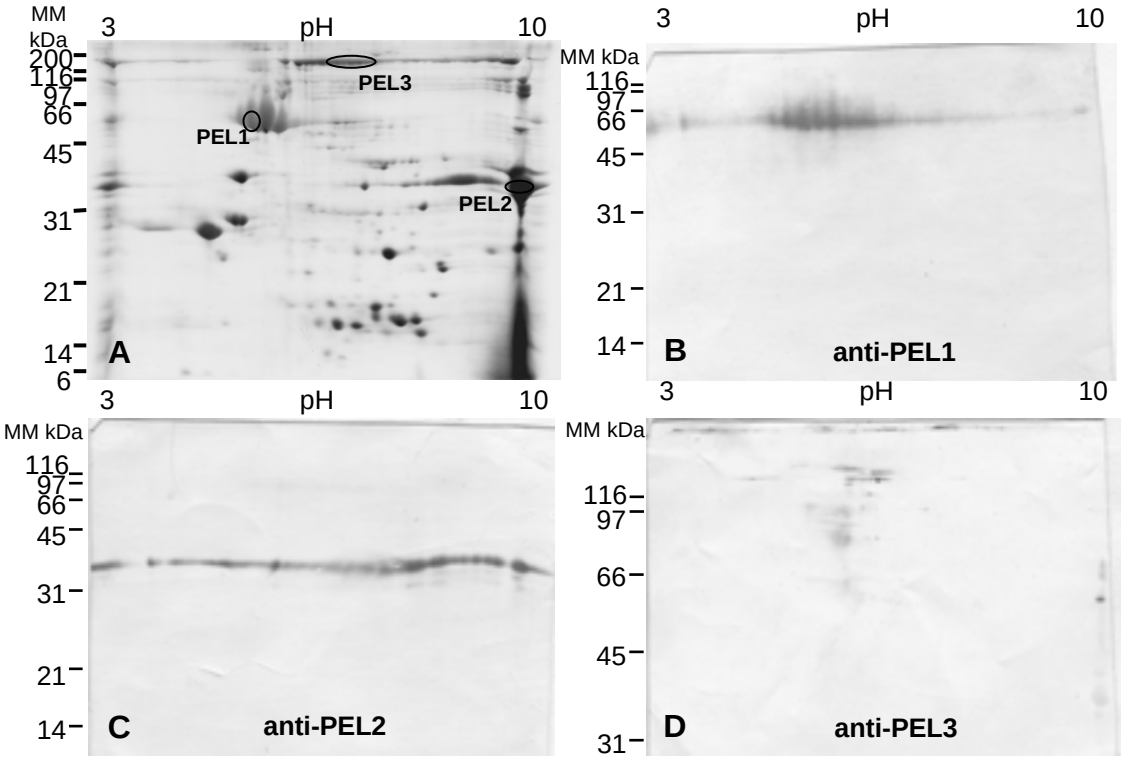

Figure 51. Anti-PEL1, anti-PEL2 and anti-PEL3 *N. bombycis*-specific polyclonal antibody production and their characterization by western blot. A) 2-DE profile of the PEL extract. Fifty µg of proteins were loaded on a pH 3-10 IEF gel before SDS-PAGE and revealed by Coomassie blue staining. Labelled spots were injected into mice to produce specific PAbs. The reactivity of each PAb was determined by western blot against the PEL extract separated by 2-DE (B, C, D).

(**Figure 51D**).

3.3. Identification of three N. bombycis *polar tube proteins*

The target location of our *N. bombycis*-specific antibodies were then screened for polar tube and spore wall location by IFA experiments on germinated spores. Only three PAbs, anti-PEL1, anti-PEL2 and anti-PEL3, labelled extruded polar tubes (**Figure 52**). The target location of anti-PEL1, anti-PEL2 and anti-PEL3 sera was thus further assayed by immunocytochemistry with purified PAbs on *N. bombycis* spore cryosections by transmission electron microscopy (TEM). In mature spores, the polar tube (PT) is fully organized. The PT anterior part called manubrium is a straight portion embedded in the polaroplast lamellar membranes and anchored in the polar cap, a thinner cell wall region the disruption of which allows the PT extrusion during germination. The PT posterior part which is coiled around the nuclei and the posterior vacuole with about 12 turns [38] is pushed at the cell periphery. Immunocytochemical experiments at the ultrastructural level with the three PAbs, revealed a gold labelling of the polar tube (**Figure 53**). The anti-PEL1 (**Figures 53A-C**), anti-PEL2 (**Figures 53E-F**) and anti-PEL3 (**Figure 53G**) PAbs seem to preferentially label the PT coiled section periphery. The coiled region-manubrium connection also reacted strongly with the anti-PEL1 PAb (**Figure 53D**). Thus we described *N. bombycis* polar tube proteins (*Nb*PTPs) for the first time.

PTPs from mammalian- [10-12, 16, 39] and insect- [13, 14] infecting microsporidia have been previously described and classified into three families. PTP1 group members exhibit apparent molecular masses of 50-55 kDa and acidic pIs (4.4 to 5.2). PTP2 are 35-kDa basic proteins that migrate as a whole-pH smear on 2-D gels, while PTP3 is a slightly acidic protein of high molecular weight (150 kDa). The physico-chemicals properties of the *Nb*PTPs described in this work (PEL1: 54 kDa/pI 5.4; PEL2: 36 kDa/pI 10; PEL3: 150 kDa/pI 7.1) thus match the ones of the three microsporidian PTP families, allowing us to renamed the PEL1, PEL2 and PEL3 proteins into *Nb*PTP1, *Nb*PTP2 and *Nb*PTP3, respectively.

3.4. Characterization of N. bombycis *polar tube proteins*

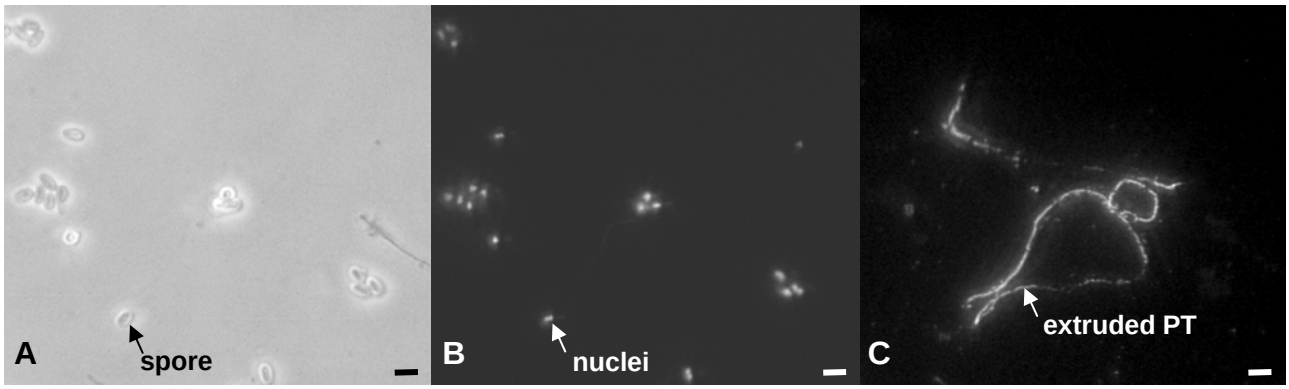

Figure 52. Reactivity of the anti-PEL3 PAb against germinated *N. bombycis* spores. Each PAb reactivity was evaluated by IFA on germinated *N. bombycis* spores coated on slides. Here is presented the same microscopic field observed in phase contrast (A), stained with DAPI (B) and immunolabelled with the anti-PEL3 PAb (C, dilution 1:100) which reacted with extruded polar tubes. Bar = 3 µm

As mass spectrometry is an efficient and convenient method to identify proteins in a post-genomic context, MALDI-TOF-MS and ESI-IT MS/MS analyses were performed on the PEL1, PEL2 and PEL3 spots after trypsin digestion. Despite of precise and distinguishable signals, MALDI-TOF (**Figure 54**) and ESI-IT (not shown) spectra could not lead to protein identification even when the microsporidian *E. cuniculi* and *A. locustae* databases were used as templates. MS/MS data were thus used to *de novo* sequence some trypsic peptides of the *Nb*PTPs, using softwares with different algorithms that allow automated interpretation of peptide tandem mass spectra (DeNovoX [40] and Peaks Online [41]). We retained peptides for which both methods gave a similar sequence (**Table 24** and supplementary **Figure 55** for an example). In order to have a more precise idea of the pertinence of the *de novo* sequence tags we obtained, we incorporated the *N. bombycis* sequence tags obtained for a given PTP protein in its *E. cuniculi* homologue sequence (not shown). The database in which we added these "chimera" proteins was then searched using our MS/MS raw data by two well-known cross-correlation algorithms (Mascot and Sequest) which have score results easy to read by the proteomic community (**Table 24**). No significant hits were observed among unrelated proteins and *E. cuniculi* sequences. While only five out of nine *N. bombycis* DeNovoX-sequences significantly matched the corresponding MS/MS data, all nine Peaks-sequences were significantly attributed by at least one algorithm with usually higher individual peptide scores than for DeNovoX-peptides (**Table 24**). In order to estimate false-positive hits, the Swissprot database was searched with MS/MS data by Sequest and compared with the previous analysis (**Table 25**). Individual peptide scores and matched fragment ion percentage were systematically higher with *N. bombycis de novo* sequences than with false-positive hits, strengthening the identification obtained with the peptides in the "chimera" proteins and thus strengthening the MS/MS spectra interpretation by the *de novo* sequencing programs. The sequenced peptides shared no homology with known proteins in Blast analysis.

4. Discussion

Despite of the microsporidian *Nosema bombycis* historic and economical importance, very few data are available at the molecular level about this parasite physiology and its relationships with its main host *Bombyx mori*. Nevertheless, important information should soon be delivered by its

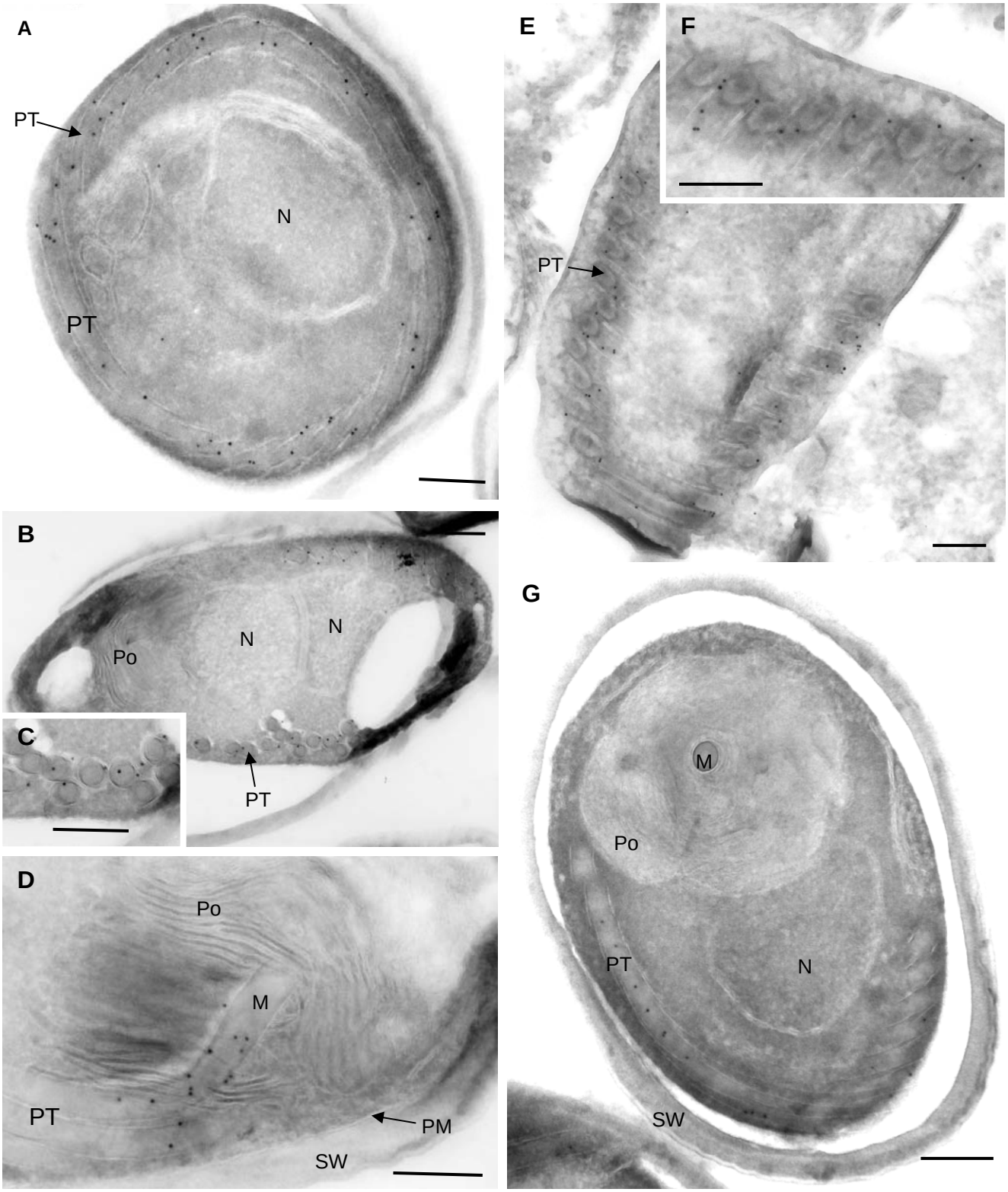

Figure 53. Reactivity of the anti-PEL1, anti-PEL2 and anti-PEL3 PAbs on cryosections of *N. bombycis* spores observed by TEM. Cryosections were incubated with anti-PEL1 (A-D, dilution 1:100), anti-PEL2 (E-F, dilution 1:30) and anti-PEL3 (G, dilution 1:100) PAbs. C and F are enlargements of B and E, respectively. Each antibody reacted with the polar tube. Bar = 200 nm. *SW: spore wall; M: manubrium (anterior part of the polar tube); N: nucleus; PM: plasma membrane; Po: polaroplast; PT: polar tube.*

complete genome sequence (project running at Chongqing, China; announced in [33]) and its comparison not only with the fully sequenced *E. cuniculi* nuclear genome sequence (mammalian parasite) [6], the partial *Antonospora locustae* one (insect parasite, http://jbpc.mbl.edu/Nosema /index.html) and the future *Brachiola algerae* one (mammalian and insect parasite, Génoscope, France), but also with *B. mori* genome sequence [42]. These genomics will open post-genomics studies and in particular proteomic ones. Since protein extraction is a critical step for these latter studies [43], this work thus constitutes an important preliminary step towards the proteomics of *N. bombycis*. The large-scale separation of different *N. bombycis* cell stages from highly infected silkworm larvae is still a difficult task, especially because this small-sized parasite (mean spore size: 3.1-4.2 x 1.9-2.6 µm) develops asynchronously inside the host tissues. As a result, the procedures available for the parasite purification from host debris only allow the recovery of mature spores. Their thick proteino-chitinous cell wall interferes with cell disruption and protein solubilization by making them highly resistant to different classical lyses treatments including osmotic shock or enzymatic degradation. We thus optimized *N. bombycis* protein extraction by combining not only different harsh disruption treatments but also sequential solubilization protocols to increase the analyzed protein repertoire, this step appearing as crucial to establish complementary and diversified 1- and 2-DE protein patterns.

While some unicellular parasites have been subjected to various proteomic studies [44], very little has been done for microsporidia. A previous study compared the three insect-infecting microsporidia *A. (Nosema) locustae*, *N. bombycis* and *Vairimorpha necatrix* to distinguish them on the basis of their 2-DE spore protein patterns after isoelectric focusing (IEF) and nonequilibrium isoelectric focusing (NIEF) [37]. *N. bombycis* spore proteins associated with insoluble material after spore breakage were solubilized in a PEL-like extract and 80 spots were observed in Coomassie blue-stained NIEF-2-DE gels. Our IEF-2-DE gels of PEL extract exhibited completely different patterns with 335 silver-stained spots (105 when Coomassie blue-stained), suggesting more efficient protein extraction and/or 2-DE resolution. Most of the proteomic works on microsporidia concern the *Encephalitozoon* genus. About 200 protein spots were separated by 2-DE from spores of the human pathogen *E. intestinalis* and 95 spots were shown to be immunogenic in the rabbit [45], while MALDI-TOF mass spectrometry analysis

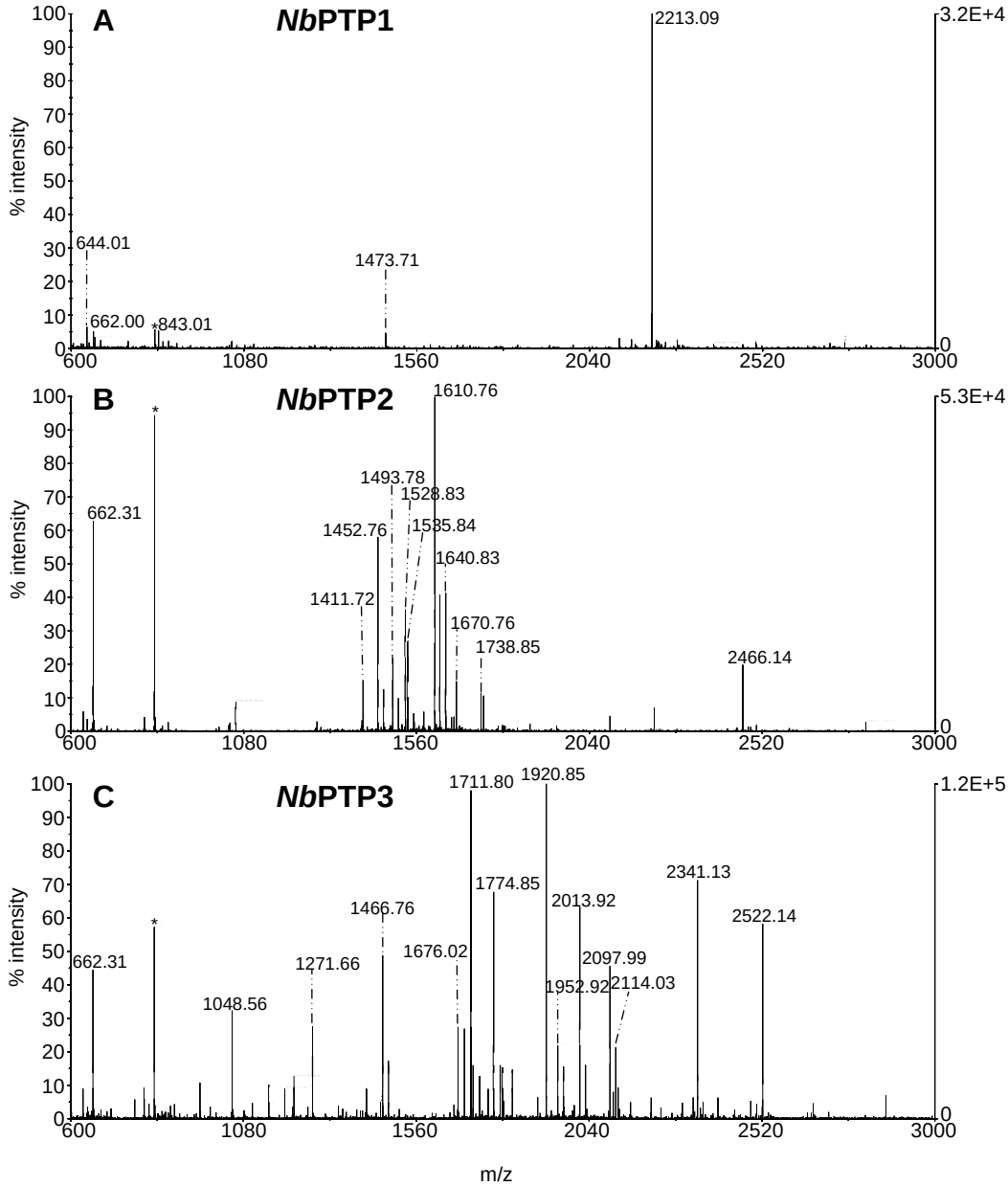

Figure 54. **MALDI-TOF mass spectrometry spectra of the three *N. bombycis* polar tube proteins.** The three 2-DE spots corresponding to PTPs, PEL1-*Nb*PTP1 (A), PEL2-*Nb*PTP2 (B) and PEL3-*Nb*PTP3 (C), were excised from a Coomassie blue-stained gel, digested by trypsin and submitted to MALDI-TOF-MS analysis. The star-labelled peaks correspond to a contaminant.

was evaluated for a rapid discrimination of microsporidian species on the basis of peptide biomarkers in the 2-8-kDa range [46]. The most achieved work concerns *E. cuniculi* late sporogonial stages (spores and late sporoblasts) which were subjected to a proteomic study combining 2-DE followed by mass spectrometry protein identification and LC-MS/MS for a 2-DE-free shotgun proteomic approach [24]. Reference 2-DE maps from a urea extract exhibited about 350 major spots with multiple isoforms, and a large set of unique proteins (177) was identified. Although *N. bombycis* and *E. cuniculi* were shown to belong to phylogenetically related but distinct microsporidian groups [47, 48], their 2-DE patterns of urea-extracted spore proteins share some common major features: the acidic 50-55-kDa and the basic 35-kDa regions, the mildly acidic 70-80-kDa window or the acidic 28-kDa spot which correspond in the *E. cuniculi* proteome to PTP1-SWP1, PTP2, HSP proteins and a Golgian protein of unknown function, respectively. Nevertheless the *N. bombycis* extract contains more spots, in particular more low-size proteins (<21 kDa), probably in relation with the methods used and the genome sizes (15.3 Mbp for *N. bombycis* [49] versus 2.9 Mbp for *E. cuniculi* [50]). NaOH- and Laemmli-extract patterns from both species also differ in the number and size of their major SDS-PAGE bands. While common points between the 2-DE maps from both organisms should refer to microsporidian specific proteins such as polar tube ones, the differences probably reflect biological adaptations to different host specificities (insect *versus* mammalian), host relationships (direct contact with the host cell cytoplasm *versus* a parasitophorous vacuole), host dependency because of specific metabolic requirement imposed by a more or less compact and restricted genome. The *N. bombycis* complementary proteomic patterns we have established thus constitute the basis for future isolate comparisons but also for physiology study of parasite stages when combined with high throughput protein identification.

In this work, we described for the first time three *N. bombycis* PTPs, the physico-chemical properties of which clearly matching the ones of the three PTP families previously reported from mammalian- [10-12, 16, 39] and insect- [13, 14] infecting microsporidia. While PTP1 and PTP3 are acidic or slightly acidic proteins with apparent molecular masses of 50-55 kDa and 150 kDa respectively, PTP2 are 35-kDa basic proteins that present a characteristic whole-pH smear migration on 2-D gels. In order to generate specific *Nb*PTP patterns, we performed a mass

Table 24. *De novo* MS/MS sequencing of some *Nb*PTPs trypsic peptides

Protein	Peptides			Peaks Online			DeNovoX				individual peptide score with Mascot (and Sequest)	
	m/z	Charge	MM_{obs} (Da)	Sequence	MM_{calc} (Da)	Score	Sequence	MM_{calc} (Da)	Absolute probability	Relative probability	Peaks sequence	DeNovoX sequence
*Nb*PTP1	575.04	2	1148.1	ARVEDELYR	1150.2	85.43	MPVEDELYR	1151.3	18.1%	28.9%	34 (3.1)*	34 (NA)
*Nb*PTP2	519.92	2	1037.8	GLQTLEHLK	1038.2	89.74	AVQTLEHLK	1038.2	21.2%	76.7%	48 (3.0)**	56 (3.0)**
	755.55	2	1509.1	QDPEYTVTGEENK	1509.5	62.79	RSPEYTVTGFQPK	1509.6	0.2%	15.8%	82 (4.4)**	88 (3.5)**
	820.83	2	1639.7	EAYVFNALGEVLSTK	1640.8	96.44	SEFVFNALGEAVQND	1639.7	0.1%	1.1%	89 (5.0)**	NA (NA)
*Nb*PTP3	462.62	2	923.2	VEDELYR	922.9	99.99	TENELYR	923.9	20.6%	53.3%	36 (2.8)*	12 (1.9)
	491.42	2	980.8	LADHLDAVK	981.1	99.92	LADHLDAVK	981.1	19.1%	84.9%	56 (3.5)**	56 (3.5)**
	1052.31	1	1051.3	EAAEDAVGYK	1052.1	99.99	EAALMAVGYK	1052.2	0.6%	9%	61 (2.9)**	59 (2.7)**
	633.91	2	1265.8	LALAHSVSNAVGK	1266.4	99.96	LANAHSGENAVGK	1267.3	7.6%	44.5%	64 (3.8)**	54 (3.7)**
	856.61	2	1711.2	YPTAVADEEFDSLVR	1711.8	99.99	YPTAVGFEEDAGSLVR	1710.8	0.1%	6.6%	93 (5.1)**	71 (3.8)**
							YPT		*25.7%*	*98.2%*	-	Not tested
							YPTAVGFEED		*27.8%*	*99.8%*	-	Not tested

Peaks and DeNovoX were run with the following parameters: standard amino acid table (no modification introduced) and m/z error tolerance for parent and fragment peptides of 0.4 for Peaks Online and 0.8 for DeNovoX. For a given peptide, identical sequences predicted by both algorithms are underlined. We obtained very few sequence differences when other parameters (variable AA modifications: acetylation, cysteine carbamidomethylation, oxidation; mass tolerance: 0.8) were tested for Peaks Online analysis (data not shown). The Peaks score or confidence level is a percentage number between 0 and 100% which indicates how likely the complete sequence is correct. While the absolute probability calculated by DeNovoX is the probability that a given sequence is the peptide of interest, the relative probability takes into account other conditions, such as the spectrum quality, charged ion pairs presence or enzymatic cleavage rules. With DeNovoX the longest is the deduced sequence, the lowest could be the probabilities as exemplified with sequence tags of the 1711-Da *Nb*PTP3 peptide (last lines). (Continues to next verso)

spectrometry analysis which is a highly efficient and convenient method to characterize proteins and identify them in a post-genomic context [51]. To complete our MS data that already fully characterize the *Nb*PTPs, we performed *de novo* sequencing to obtain specific peptide sequence tags. This sequencing method consists in interpreting MS/MS spectra without using any sequence database, and has been used in other organisms [40] or for the identification of a conserved STL2 rhamnose-binding lectin from the microsporidian *Loma salmonae*, a salmonid parasite [52]. In our work, four different algorithms were combined to delineate nine reliable sequences from the three *Nb*PTPs: (i) the *de novo* sequencing was realized with Peaks Online and DeNovoX, and (ii) the reliability of the deduced sequence tags was evaluated on the basis of the discrimination of MS/MS identification parameters between true- and false-positive hits by Mascot and Sequest. Our mass spectrometry data will be easily used to characterize *Nb*PTPs at the sequence level as soon as the *N. bombycis* genome sequence will be available, and will also help genome annotation. Moreover this *de novo* MS/MS sequencing strategy can also be used in a non-genomic context using the peptide sequence tags either to search databases or to obtain specific primers for gene amplification.

To date, the sequences of PTPs are only known for five species belonging to two phylogenetically distant microsporidian groups. While in the mammalian-infesting *Encephalitozoon* genus (*E. cuniculi*, *E. hellem*, *E. intestinalis*) PTP1 proteins share 48-49% identity and PTP2 58-80%, in the insect-infesting *Antonospora*-related genus (*A. locustae*, *P. grylli*) PTP1 exhibit 67% identity and PTP2 85%. When these two microsporidian groups are compared, the identity scores fail to ~20% for both PTPs with identical sequence stretches no longer than 3 aminoacids. Despite this inter-species high sequence divergence for PTP1 and PTP2, some cysteine residues are conserved [12, 13], suggesting an overall conservation of their respective structure to maintain the astonishing polar tube architecture and elasticity which allow diameter variations from 0.1-0.15 µm in the spore to 0.4 µm during the sporoplasm passage [9]. Even if *N. bombycis* belongs to a clade that appears as a sister-group of the *Encephalitozoon* one [47], this does not mean that *N. bombycis* and *Encephalitozoon* proteins necessarily share high identity scores because microsporidian genomes are paradoxically composed of rapidly evolving gene sequences harbored within a slowly evolving genome [47]. Thus, the inability to attribute

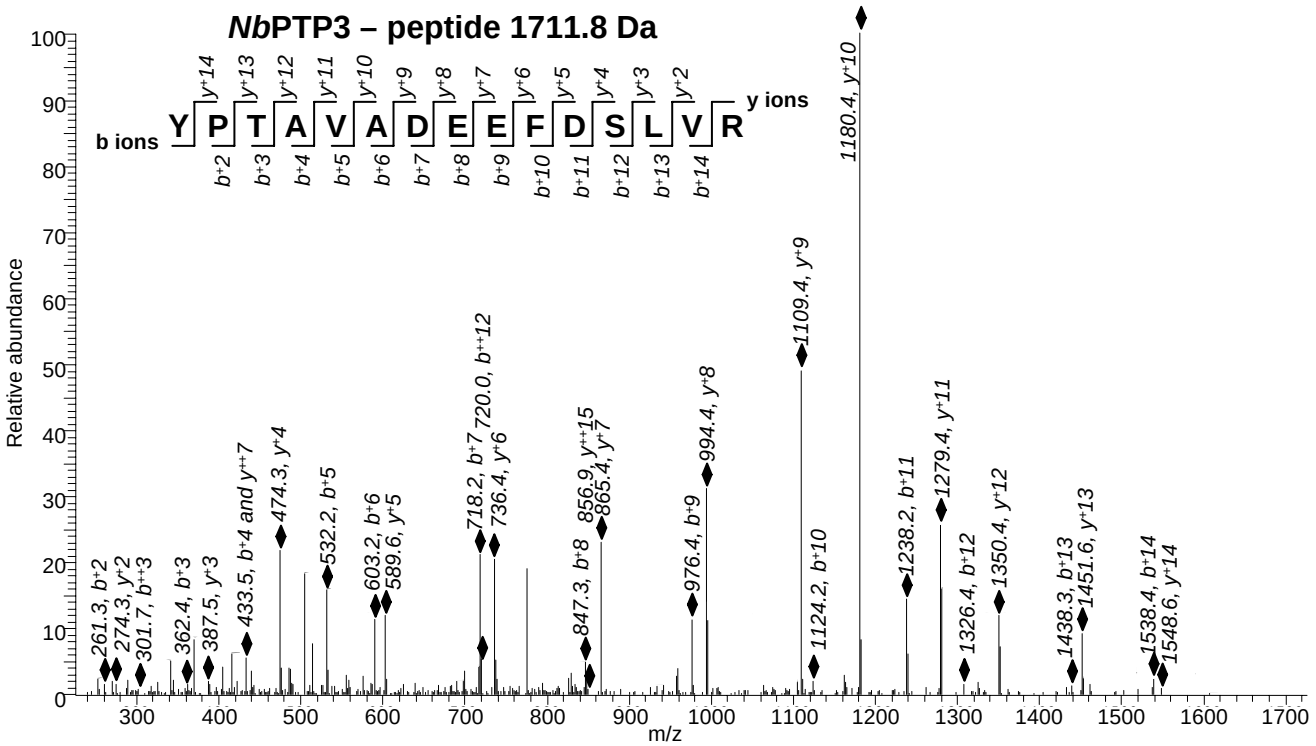

Figure 55. *De novo* sequencing of the trypsic 1711.8-Da *Nb*PTP3 peptide. Trypsic peptides from *N. bombycis* PTPs were submitted to MS/MS analysis. Spectra obtained after fragmentation, exemplified here by the 1711.8-Da *Nb*PTP3 peptide one, were used to perform *de novo* sequencing with the Peaks Online and DeNovoX algorithms. One-charge (b+ and y+ ions) and double-charged (b++ and y++ ions) fragments used for the sequencing are highlighted by diamonds. The mass difference between adjacent b-ions (or adjacent y-ions) is indicative of an amino-acid residue mass and allows the extraction of a specific sequence from the spectrum.

positive hits to *Nb*PTPS MALDI-TOF data and peptide sequence tags may not be the mark of new PTP families but strongly suggests that their sequences should present few homologies with the other PTPs.

In the *Encephalitozoon* genus, both structures involved in host invasion (PT and SW) were shown to be glycosylated [15, 23] and to directly interact with the host cell through carbohydrates components. The O-mannosylation of PTP1 from *E. hellem* is involved in some interactions with an unknown host cell mannose-binding molecule [15]. *E. intestinalis* specifically adheres to target cells by way of sulfated host cell surface glycosaminoglycans, this mechanism enhancing infectivity [20]. With both genomes being sequenced [33, 42] and with silkworm genetics tools being available [53], the *N. bombycis*/*B. mori* system constitutes an interesting biological *in vivo* model for host-microsporidia relationships. Further studies on *Nb*PTPs which are located at the polar tube periphery should focus on their glycosylation and on their interaction with host proteins and carbohydrates.

Acknowledgements

JianYang Wang was supported by a grant from "Conseil Régional d'Auvergne". We thank Damien Brosson, Frédéric Delbac and Emmanuel Cornillot for helpful discussions and critical reading of this manuscript, Gérard Prensier for his transmission electron microscopy expertise, and Qing GuangXin for *N. bombycis* cell culture and spore purification.

References

[1] Vavra, J., Larson, J., in: Wittner, M. (Ed), *The Microsporidia and Microsporidiosis*, ASM Press, Washington DC 1999, pp. 7-84.

[2] Keeling, P.J., Luker, M.A., Palmer, J.D., Mol. Biol. Evol. 2000, *17*, 23-31.

[3] Keeling, P.J, Fungal. Genet. Biol. 2003, *38*, 298-309.

[4] Peyretaillade, E., Biderre, C., Peyret, P., Duffieux, F. et al., Nucleic Acids Res.1998, *26*, 3513-3520.

[5] Fischer, W.M., Palmer, J.D., Mol. Phylog. Evol. 2005, *36*, 606-622.

[6] Katinka, M.D., Duprat, S., Cornillot, E., Méténier, G. et al., Nature 2001, *414*, 450-453.

Peptide *de novo* sequences of a given *Nb*PTP were incoporated in its *E. cuniculi* homologue sequence between trypsin proteolysis sites, and the "chimera" proteins were added in a large database for Mascot and Sequest searches with our MS/MS raw data. For Mascot, individual peptide ion scores >38 indicate identity or extensive homology ($p<0.05$). With Sequest, scores are significant when they are >2.0 and >2.5 for one- and double-charge peptides, respectively. * and ** label peptides the scores of which are significant for one algorithm and for both, respectively. *NA: not attributed.* MM_{obs}, MM_{calc} *: observed and calculated molecular masses*

Table 25. Comparison of MS/MS identification parameters between positive and false-positive hits

Protein	Peptides			Sequest search in a local database with microsporidian polar tube chimera proteins				Sequest search in the Swissprot database			
	m/z	Charge	MM_{obs} (Da)	Matched sequence	MM_{calc} (Da)	individual peptide score	No of matched fragment ions (%)	Matched sequence	MM_{calc} (Da)	individual peptide score	No of matched fragment ions (%)
*Nb*PTP1	575.04	2	1148.1	ARVEDELYR	1150.2	3.1*	14/16 (87.5%)	VKVKPNM*YR	1150.4	2.3	11/16 (68.8%)
*Nb*PTP2	519.92	2	1037.8	GLQTLEHLK	1038.2	3.0*	14/16 (87.5%)	AVKHQVDLK	1037.2	1.9	10/16 (62.5%)
	755.55	2	1509.1	QDPEYTVTGEENK	1509.5	4.4*	21/24 (87.5%)	EIPKFYVLEENK	1508.7	3.0*	17/22 (77.3%)
	820.83	2	1639.7	EAYVFNALGEVLSTK	1640.8	5.0*	22/28 (78.6%)	TYVVESQKNAGKSTK	1639.8	2.7*	14/28 (50.0%)
*Nb*PTP3	462.62	2	923.2	VEDELYR	922.9	2.8*	11/12 (91.7%)	IDDELYR	922.9	2.2	10/12 (83.3%)
	491.42	2	980.8	LADHLDAVK	981.1	3.5*	15/16 (93.8%)	ALYSDNLGK	980.0	2.3	10/16 (62.5%)
	1052.31	1	1051.3	EAAEDAVGYK	1052.1	2.9*	12/18 (66.7%)	KVTEKVGYK	1051.2	1.9	9/16 (56.3%)
	633.91	2	1265.8	LALAHSVSNAVGK	1266.4	3.8*	20/24 (83.3%)	ALLAYAFSLLGK	1266.5	2.1	11/22 (50.0%)
	856.61	2	1711.2	YPTAVADEEFDSLVR	1711.8	5.1*	25/28 (89.3%)	MEGWCQQMEREER	1711.9	2.7*	14/24 (58.3%)

Chimera proteins were constructed by incorporated, between trypsin proteolysis sites, peptide sequences of a given *Nb*PTP (Peaks sequences) in its *E. cuniculi* homologue sequence, then added in a large database (see text) which was searched by the Sequest software using our MS/MS raw data. In order to evaluate the level of false-positive hit scores, these raw data were also used to search the total Swissprot database (2006 July, 228630 entries, no *Nb*PTPs) with Sequest. Sequest scores are significant (*) when they are >2.0 and >2.5 for one- and double-charge peptides, respectively. Common sequence tags shared by *N. bombycis* and Swissprot proteins are underlined. M*: oxidised methionine

[7] Thomarat, F., Vivarès, C.P., Gouy, M., J. Mol. Evol. 2004, *59*, 780-791.

[8] Williams, B.A.P., Hirt, R.P., Lucocq, J.M., Embley, T.M., Nature 2002, *418*, 865-869.

[9] Xu, Y., Weiss, L.M., Int. J. Parasitol. 2005, *35*, 941-953.

[10] Delbac, F., Peyret, P., Méténier, G., David, D. et al., Mol. Microbiol. 1998, *29*, 825-834.

[11] Keohane, E.M., Orr, G.A., Zhang, H.S., Takvorian, P.M. et al., Mol. Biochem. Parasitol. 1998, *94*, 227-236.

[12] Delbac, F., Peuvel, I., Méténier, G., Peyretaillade, E., Vivarès, C.P., Infect Immun. 2001, *69*, 1016-1024.

[13] Polonais, V., Prensier, G., Méténier, G., Vivarès, C.P., Delbac, F., Fungal Genet. Biol. 2005, *42*, 791-803.

[14] Dolgikh, V.V., Semenov, P.B., Mironov, A.A., Beznoussenko, G.V., Protist 2005, *156*, 77-87.

[15] Xu, Y., Takvorian, P.M., Cali, A., Orr, G., Weiss, L.M., Infect. Immun. 2004, *72*, 6341-6350.

[16] Peuvel, I., Peyret, P., Méténier, G., Vivarès, C.P., Delbac, F., Mol. Biochem. Parasitol. 2002, *122*, 69-80.

[17] Couzinet, S., Cejas, E., Schittny, J., Deplazes, P. et al., Infect Immun. 2000, *68*, 6939-6945. **[18] Vivarès, C.P., Méténier, G.**, Bioessays 2001, *23*, 194-202.

[19] Franzen, C., Muller, A., Hartmann, P., Salzberger, B., Parasitology 2005, *130*, 285-292.

[20] Hayman, J.R., Southern, T.R., Nash, T.E., Infect. Immun. 2005, *73*, 841-848.

[21] Leitch, G.J., Ward, T.L., Shaw, A.P., Newman, G., Infect. Immun. 2005, *73*, 7697-7704.

[22] Bohne, W., Ferguson, D.J., Kohler, K., Gross, U., Infect. Immun. 2000, *68*, 2268-2275.

[23] Hayman, J.R., Hayes, S.F., Amon, J., Nash, T.E., Infect. Immun. 2001, *69*, 7057-7066.

[24] Brosson, D., Kuhn, L., Delbac, F., Garin, J. et al., Proteomics 2006, *6*, 3625-3635.

[25] Peuvel-Fanget, I., Polonais, V., Brosson, D., Texier, C. et al., Int. J. Parasitol. 2006, *36*, 309-318.

[26] Xu, Y., Takvorian, P., Cali, A., Wang, F. et al., Infect. Immun. 2006, *74*, 239-247.

[27] Brosson, D., Kuhn, L., Prensier, G., Vivarès, C.P., Texier, C., FEMS Microbiol Lett. 2005, *247*, 81-90.

[28] Iwano, H., Ishibara, R., J. Invertebr. Pathol. 1991, *57*, 211-219.

[29] Iwano, H., Ishibara, R., J. Seric. Sci. Jpn. 1991, *60*, 249-256.

[30] Cali, A., Takvorian, P.M., in: Wittner, M. (Ed), *The Microsporidia and Microsporidiosis*, ASM Press, Washington DC 1999, pp. 85-128.

[31] Becnel, J.J., Andreadis, T.G., in: Wittner, M. (Ed), *The Microsporidia and Microsporidiosis*, ASM Press, Washington DC 1999, pp. 447-501.

[32] Legay, J.-M., Chavancy, G., Natures Sciences Sociétés 2004, *12*, 413-417.

[33] Xu, J., Pan, G., Fang, L., Li, J., Int J Parasitol. 2006, *36*, 1049-1056.

[34] Wang, J.Y., Huang, K.W., Mao, X.C., Zhao, Y., Lu, C.D., Acta biochimica et biophysica Sinica 2001, *33*, 229-232.

[35] Fujiwara T., J. Sericult. Sci. Jpn 1979, *48*, 376-380.

[36] Pitarch, A., Sanchez, M., Nombela, C., Gil, C., Mol. Cell. Proteomics 2002, *1*, 967-982.

[37] Langley, R.C. Jr, Cali, A., Somberg, E.W., J Parasitol. 1987, *73*, 910-918.

[38] Sato, R., Kobayashi, M., Watanabe, H., J. Invertebr. Pathol. 1982, *40*, 260-265.

[39] Peuvel, I., Delbac, F., Méténier, G., Peyret, P., Vivarès, C.P., Parasitol. 2000, *121*, 581-587.

[40] Chao, C.-C., Wu, S.-L., Ching, W.-M., Biochim. Biophys. Acta 2004, *1702*, 145-152.

[41] Ma, B., Zhang, K., Hendrie, C., Liang, C. et al., Rapid Commun. Mass Spectrom. 2003, *17*, 2337-2342.

[42] Mita, K., Kasahara, M., Sasaki, S., Nagayasu, Y. *et al.*, DNA Res., 2004, *11*, 27-35.

[43] Molloy, M.P., Anal. Biochem. 2000, *280*, 1-10.

[44] Belli, S.I., Walker, R.A., Flowers, S.A., Proteomics 2005, *5*, 918-924.

[45] Moura, H., Visvesvara, G.S., J. Eukaryot. Microbiol. 2001, *48 suppl*. *s1*, 56S-59S.

[46] Moura, H., Ospina, M., Woolfitt, A.R., Barr, J.R., Visvesvara, G.S., J Eukaryot Microbiol. 2003, *50*, 156-163.

[49] Slamovits, C.H., Fast, N.M., Law, J.S., Keeling, P.J., Curr. Biol. 2004, *14*, 891-896.

[50] Rao, S.N., Nath, B.S., Saratchandra, B., Genome 2005, *48*, 355-366.

[49] Kawakami, Y., Inoue, T., Ito, K., Kitamizu, K. et al., Appl. Entomol. Zool. 1994, *29*, 120-123.

[50] Biderre, C., Pagès, M., Méténier, G., Canning, E.U., Vivarès, C.P., Mol. Biochem. Parasitol. 1995, *74*, 229-231.

[51] Patterson, S.D., Aebersold, R.H., Nat Genet 3003, *33 suppl*, 311-323.

[52] Booy, A., Haddow, J.D., Olafson, R.W., J. Fish Dis. 2005, *28*, 455-462.

[53] Tamura, T., Thibert, C., Royer, C., Kanda, T. *et al*., Nat. Biotechnol., 2000, *18*, 81-84.

General Discussion and Perspectives

1. *NOSEMA BOMBYCIS-BOMBYX MORI* INTERACTIONS *IN VIVO*:

In this study, we mainly characterized *Nosema bombycis-Bombyx mori* interactions *in vivo* including *N. bombycis* dissemination mechanism and *B. mori* immune response to *N. bombycis*

Since *N. bombycis* complete life cycle is the prerequisite to study its dissemination mechanism, we firstly characterized *N. bombycis* complete life cycle *in vivo* at the ultrastructural level, confirming the previous proposed *N. bombycis* life cycle model based on the sporogonial dimorphism and their binary fission mode both in merogony and in sporogony. Importantly, for the first time, we observed that the primary spores can form in nearly all tissues and organs. The primary spores are characterized with their spontaneous germination and known to spread infection within the host. Since they can develop in all tissues and organs, it means that they play a very important role in *N. bombycis* dissemination *in vivo*. However, it must be kept in mind that the primary spores are also characterized with their very short polar tubes, we wondered how the parasite infection can be spread to those spatially separated tissues and organs from *B. mori* anterior midgut epithelial wall which is often the first settle of *N. bombycis* and the producer of both environmental and primary spores, especially at the early stage of infection.

Considering that all insects including *B. mori* have an open circulating system with all interior tissues and organs immersed in the hemolymph, we proposed that *B. mori* hemolymph and hemocyte can disseminate the parasite infection to those distant tissues and organs by their continuously circulation. Then, we described *N. bombycis* interactions with *B. mori* hemolymph and hemocyte. Our results have shown that all five known types hemocytes and one of them being hypotrophic can support *N. bombycis* development. This finding is very important for us to further unravel *N. bombycis* dissemination mechanism *in vivo*. The following investigation on the time of *N. bombycis* presence in hemolymph and invasion of hemocyte further confirmed our proposition that the distant dissemination is mediated by *B. mori* hemolymph and hemocytes.

While phagocyotsis is often considered as a conventional host immune response to the invading pathogens, it has been utilized by highly adaptive microsporidian as their other invasion route through their unique “spore germination” from the phagolysosome. In the present study, the phagocytosis of *N. bombycis* spore by *B. mori* prohemocyte has been observed by phase

contrast. This finding is very important for the study of microsporidian invasion and dissemination mechanism *in vivo*. On one hand, it means phagocytosis can be induced by *N. bombycis* invasion and probably phagocytosis is also one invasion route of *N. bombycis* in *B. mori*, no matter which tissure or organ. On the other hand, if *N. bombycis* spore can still germinate from host cell phagolysosome by preventing the acidification of phagolysosome, this observation will further corroborated our proposition of hemolymph-hemocyte distant dissemination role.

Insect typical immune response to microsporidian, melanization of *B. mori* hemocytes and *N. bombycis* in hemocytes and hemolymph has also been observed. Melanization has been considered as an important insect innate immune response in host eliminating the foreign pathogens. Very recently, the deteriorating effects of melanization on the microsporidian spore sporogony and morphogenesis have been reported. We also founded the similar malformed spores *N. bombycis* at the sites of melanized tissue by phase contrast. It suggested that the derivatives or intermediates produced in the melanin synthesis pathway should be cytotoxic to the microsporidian parasites, especially those still in their early developmental stages in which the thick protective spore wall is still not or not completely formed.

However, no matter how intense are these immune responses, innate immune responses of insects including *B. mori* are so inefficient that the dissemination of parasite infection within the specific tissue or the whole body appears as an inevitable tendency.

Current investigation on *N. bombycis*-*B. mori* interactions *in vivo* is just an preliminary step for future comprehensive and profound understandings of microsporidian-insect relationships. The further characterization of *N. bombycis*-*B. mori* interactions *in vivo* can direct towards several aspects or fields:

1.1. *N. bombycis* invasion mechanism *in vivo*

On one hand, Microsporidia have been acknowledged with their unique “spore germination” invasion mode, which has been observed *in vitro*. However, as we know, in insect hostile digestive fluid and hemolymph, there are very different destructive enzymes which could attack and digest microsporidian invasion apparatus-polar tube. In our study, we observed a large number of germinated empty spores and sporoplasm in the hemolymph, particularly at the late

infection stage, but we can not found the everted polar tube by IFA (PAbs of polar tube proteins prepared as 5.2.). It may suggest that the everted polar tubes could have been quickly digested in the hemolymph. However, the spore germination has been shown to be a very quick outburst process (<2s), we can not discount the possibility that before the polar tube was attacked by distructive enzymes in digestive fluid and hemolymph, the polar tube has successfully deposited the infectious sporoplasm into the host cell.

On the other hand, recent *in vitro* studies showed that phagocytosis can be utilized by microsporidian to invade host cells (Franzen, 2004). Though *B. mori* hemocyte phagocytosis of *N. bombycis* has been observed in our study, the fate of phagocytosed parasite needs further study. Whether *N. bombycis* can block the acidification of phagolysosome they reside in and survive to spread infection by germinating from the phagolysosome as the case *in vitro* is worth of future investigation.

Additionally, we should also pay attention to other host-invasion mechanisms utilized by microsporidian phylogenetic related fungi and other protozoan parasites. Both protease and chitinase activities have been implicated as pathogenicity determinants involved in host invasion by entomopathogenic fungi (Charley and St. Leger 1991). Apicomplexa parasites such as *Plasmodium* ookinete can secrete chitinase(s) that punch an “enzymatic hole” and facilitate the movement of the ookinete across the peritrophic matrix (Shahabuddin *et al*., 1993; Langer and Vinetz, 2001; Vinetz *et al*., 1999, 2000). Some animal parasitic nematodes also secrete proteases to assist in cuticle and tissue penetration (Abuhatab *et al*., 1995). It has also been reported that many pathogenic Protozoa produce cytolytic proteins that disrupt target cell membranes by forming discrete channels in the lipid bilayer and these are thought to play a significant role in the pathogenesis of many protozoan infections (Horta, 1997). A 17kDa protein which may be glycosylated and distribute on *N. bombycis* exospore has been considered as an infection-specific metalloprotease. All these findings led us to wonder when microsporidian traverse the peritrophic matrix of intestine and invade different host cells, 1) whether there are different proteases, which are needed to drill a hole in the peritrophic matrix or host cell membrane, also present on the surface of microsporidian spore wall or at the tip of polar tube; 2) when these proteases are activated or if they are activated only at the time of the host-parasite recognition; 3) whether these proteases are absolutely necessary for the polar tube penetration into host cell

membrane; 4) when these proteases present on the spore wall and whether they also have an important role in another possible invasion route-phagocytosis.

Taken together, microsporidian invasion mechanisms *in vivo* may be far more complex than those observed *in vitro*.

1.2. Further characterization of *N. bombycis* dissemination mechanism *in vivo*

Our study has shown that it is *N. bombycis* primary spores and *B. mori* hemolymph-hemocytes that cooperatively disseminate parasite infection. These primary results can be further characterized and completed by future refined analyses.

In this study, the large larvae (from the 3rd to 5th instar) have been analysed by light and electron microscopy of resin embedded blocks. During analyzing these large larvae, there are several inconveniences. Firstly, for being embedded in resin, a large larva is often needed to cut into three or four parts which were further separately fixed and embedded. In this case, the number of resin blocks markedly increase while the number of sampled larvae is seriously affected and decreased. Secondly, the cuticle of large larva has become more thick with less fixative penetrability. The fixation failure occasionally occurred in our studies. Additionally, when the fixed larvae are so large that it is very difficult to simultaneously observe more tissues/organs in one section, which means more section-cutting will be performed.

In the future tissue analyses, 1) The time intervals of sampling should be optimized or shortened to further characterize the duration of *N. bombycis* complete life cycle and the primary spore formation time which is very important for the comprehensive understanding of *N. bombycis* dissemination kinetics. 2) Those young larvae still in the 1st or 2nd instar should be fully utilized. 3) It is better to combine the vivisection analyses (directly dissecting the infected larvae without any treatment) with the semithin section study. The vivisection analyses will perfectly meet the needs of statistics and can also allow the intercomparisons with semithin analyses and the corroboration of observations. 4) The tissues and hemolymph-hemocyte samplings should be synchronized to further characterize the parasite dissemination kinetics *in vivo*.

1.3. Further characterization of *N. bombycis* interactions with *B. mori* hemocytes and hemolymph

According to our observations, *N. bombycis* interactions with *B. mori* hemocytes and hemolymph seem too complex to give a relatively comprehensive description before future extensive studies are performed.

First, how the circulating hemocytes can be infected? There are two possibilities: a. Adjacent infection by primary spores. One case is that when the circulating hemocytes are very close to the infected tissues/organs, they are infected by the primary spores formed in these tissues/organs. Then the primary spores formed in hemocytes can further infect other hemocytes when they meet together. The other case is that the hemocyte stem cells in hemopoietic organ are infected by the primary spores formed in their surrounding tissues. After they entered the hemolymph, they became the infected circulating cells. b. Phagocytosis. Since *B. mori* highly immunoreactive hemocytes can phagocytose the invading pathogens including *N. bombycis* (in this study), they can also be passively infected by their active phagocytosis of *N. bombycis* cells.

Second, when are hemocytes firstly infected?. On one hand, since we occasionally observed the sporoplasm or the meront in the hemolymph before 54h (*N. bombycis* primary spores first appear in *B. mori* midgut epithelial cells at 54h, Iwano H and Ishihara R, 1991b), and since some researchers suggested that those environmental spores with long polar tube can directly inject their infectious sporoplasms into the haemocoel (Canning *et al*., 1986; Dyková, 1995), we then wonder if *B. mori* hemocytes are firstly infected by their phagocytosis of sporoplasms which are earliestly deposited into the hemolymph by those environmental spores in the digestive tube. This case is very unlikely: firstly, the probability of the polar tube penetration the whole digestive tube wall seems very low, then, even if this penetration exists, the number of sporoplasm is also very small and perhaps be quickly eliminated by host immune response. On the other hand, whether are they firstly infected by the first generation of primary spores formed in the midgut epithelial cells after 54h (as aboved-mentioned, the primary spores first appear at 54h)? When the circulating hemocytes get very close to midgut epithelium, they are then infected by these primary spores. This case possible occurred in *B. mori* since we observed the hemocytes were firstly infected utill 71h.

Finally, what are the fates of *N. bombycis* cells in *B. mori* hemolymph and in the

phagolysosome of hemocyte after they are phagocytosed? According to our studies, *N. bombycis* sporoplasms and meronts can be present in hemolymph at very early stage after infection. Are these sporoplasm or meronts lysed or killed directly in hemolymph, or are they phagocytosed by hemocytes and then be killed in the phagolysosome, or can they still infect the hemocytes? At the same time, at the very late stage after infection, we observed nearly every developmental stages of *N. bombycis* cells including the environmental spores. Can *B. mori* hemolymph with different destructive enzymes and antimicrobial peptides affect their viabilities? Can these environmental spores germinate in *B. mori* hemolymph?

1.4. Further characterization of *B. mori* immune responses to *N. bombycis in vivo*

In current study, insect innate immune responses such as the phagocytosis and melanization have been observed. Since insect innate immune responses to the invading micrsoorganisms are far more complex then we have observed in this study, it is also very interesting to further characterize *B. mori* immune responses to *N. bombycis in vivo* at both the cellular level and the molecular level.

We found that *B. mori* hemocytes can phagocytose *N. bombycis*. But, can other types of *B. mori* cells such as the midgut epithelial cells also phagocytose them? which factors trigger *B. mori* cells to phagocytose of *N. bombycis*? which molecules actively participate in the host cell phagocytosis of *N. bombycis*? What kinds of roles do these molecules play in phagocytosis?

Melanization is considered as an insect typical immune response to microsporidian invasion. In our study, the melanotic layers or capsules on the surface of infected tissues such as midgut can often be optically observed. But how can the melanization kill *N. bombycis*? Often it has considered that the derivatives and intermediates produced in the melanin synthesis pathway are cytotoxic to the foreign pathogens. If so, how can these intermediates affect *N. bombycis* cells viabilities and development? which intermediate can result in the deterioration effects or killing *N. bombycis* cells? can these cytotoxic intermediates be used for the future therapy?

Insect other immune responses to *N. bombycis* such as the induced synthesis of antimicrobial peptides, the generation of reactive intermediates of oxygen (ROIs) or nitrogen (RNIs), the release of stress responsive proteins, encapsulation and nodule formation are also worth of future investigation.

With the easiness of availability or breeding of *B. mori* silkworms and with the successful establishment of transponson-mediated germline transformation in *B. mori*, the study of *N. bombycis-B. mori* interactions *in vivo* can set a good example to microsporidia-insect interactions *in vivo* and are also promising for future therapy strategies.

2. CHARACTERIZATION OF *NOSEMA BOMBYCIS* THREE POLAR TUBE PROTEINS BY A PROTEOMIC-BASED APPROACH

As a highly specialised structure, the polar tube is the microsprodian unique invasion apparatus. It serves as a conduit to transfer the infectious sporoplasm to the host cell by pierceing host cell membrane. As polar tube main components, polar tube proteins (PTPs) are a set of microsporidia-specific proteins involved in the host cell membrane-polar tube recognition. The characterization of polar tube proteins (PTP) will have an important significance not only for the molecular architecture study of the microsporidian polar tube, but also for the investigation of host cell attachment/penetration mechanism of polar tube.

In the present study, by a proteomic-based approach we characterized three polar tube proteins (NbPTP1, NbPTP2, NbPTP3) of *N. bombycis*. Since in several microsporidian species, four or five PTPs have been identified, other proteins should also be present in *N. bombycis* polar tube and need to be further identified. Obviously, much remains to be further studied about these PTPs involved in host invasion. On one hand, our immunolabelling for *N. bombycis* PTP2 exhibit a characteristic whole-pH smear, the same case for *Encephalitozoon cuniculi* PTP2. It should be mainly due to post-translational modifications (PTM) resulting in different isoforms. Since *Encephalitozoon hellem* PTP1 have been demonstrated to be O-mannosylated (Xu *et al*., 2004), since PTMs are often important for the protein functions, PTMs in *N. bombycis* PTPs are worth our further investigations; on the other hand, while disulfide bridges formed in PTP1 and PTP2 and ionic interactions between PTP2 and PTP3 have been suggested to play an essential role in the assembly of the polar tube, the specific interactions between identified *N. bombycis* three PTPs are unclear. The interactions between NbPTP1-3 and other polar tube components and the role of these interactions in the formation and function of *N. bombycis* polar tube remain to be determined. The further characterization of NbPTP domains involved in these interactions would also be of interest to better understand the architecture and assembly of polar tube. Additionally, when the coiled polar tube everted as a straight tube during *N. bombycis* spore germination, great changes of polar tube molecular architecture should have occurred. So whether the polar tube architecture changes also result in the rearrangement of *N. bombycis* PTPs

specific interactions needs future study. After the characterization of *N. bombycis* polar tube proteins, the investigation of host cell attachment/penetration mechanism of *N. bombycis* polar tube is a great challenge. While O-mannosylated PTP1 of *E. hellem* has been shown to interact with an host cell mannose-binding molecule and *Encephalitozoon intestinalis* specifically adheres to target cells by way of sulfated host cell surface glycosaminoglycans *in vitro* (Hayman *et al*., 2005), the study of *N. bombycis* polar tube interactions with host cells, especial with host proteins and carbohydrates, may also begin with the similar *in vitro* system on the base of *N. bombycis* germination priming *in vitro*.

The proteomic approach in this study is an introduction to future comprehensive applications of proteomics in both *N. bombycis* studies and *N. bombycis*-*B. mori* interactions investigation. By combining the mass spectrometry, an efficient and convenient method to identify proteins, and with the availabilities of *N. bombycis* and *B. mori* genome sequences in the near future, the proteomic methods can be used in many aspects in *N. bombycis/B. mori* studies.

2.1. *N. bombycis* studies:

1). *N. bombycis* polar tube study. Firstly, it can be used to identify polar tube proteins in a large scale. Considering the DTT-soluble property of polar tube proteins, we can also specially characterize the polar tube proteins by proteomic analyses of the "DTT-solubilised polar tube extract" from spores. This may lead to the numerous polar tube components and their isoforms identification. Secondly, it can be used to study polar tube biogenesis. But this needs to specially enrich the different developmental stages of parasites such as the meronts, sporonts and sporoblasts or spores, in which the polar tube is not synthesized, is synthesizing or has completely established respectively. Additionally, the proteomic approaches can also used to compare the polar tube differences between the primary spores and environmental spores to better understand the spore germination mechanism.

2). *N. bombycis* spores surface proteins and other organelles such as the mitosome studies. These studies include their compositions or their biogenesis analyses.

3). *N. bombycis* biology and physiology studies. The proteomic approaches can be used to compare the different geographical isolates or *N. bombycis* species variations. By analysing /comparing the protein expression patterns of *N. bombycis* different developmental stages, we

can identify not only *N. bombycis* housekeeping proteins but also the stage-specific proteins required for cell cycle progression or for the anchoring disk, spore wall organisation. In addition, we can apply the proteomic methods to compare *N. bombycis* primary spores and environmental spores.

3). *N. bombycis* drug response studies. The proteomic approaches can also be used to analyse the drug-binding proteins, or *N. bombycis* protein expression patterns change in response to drug exposure.

4). Since the glycoproteins often have important role in host-parasite recognition and phosphorylation of proteins is critical to the cell cycle progress and numerous signal pathways, the large scale analyses of these proteins (also called “glycoproteome” and “phosphoproteome”) in *N. bombycis* by the proteomics approach will be very helpful to the characterization of its biology and interactions with host.

2.2. *N. bombycis*-*B. mori* interactions investigation:

1). Parasite-host interfaces study, such as *N. bombycis* interactions with *B. mori* intestine peritrophic membrane, *N. bombycis* interactions with the midgut epithelial microvilli, *N. bombycis* interactions with *B. mori* hemocyte-hemolymph.

2). *B. mori* immune responses to *N. bombycis* invasion and their deteriorating effects on *N. bombycis* development.

3). Comparison of the sensibilities of different *B. mori* strains to *N. bombycis.*

With the completion of *N. bombycis* and *B. mori* genome sequences, the proteomic methods can be used to validate of *N. bombycis* or *B. mori* genomic annotation data and analyse of transcript expression.

In a word, the proteomic approaches can open a high throughput way to study microsporidian and their interactions with host cells, which are very promising not only for the better understanding of microsporidian unique spore germination mechanism and their host cell invasion mechanisms but also the therapy strategies.

References

Abraham EG, Jacobs-Lorena M. Mosquito midgut barriers to malaria parasite development. *Insect Biochem Mol Biol.* 2004, 34(7): 667-671.

Abraham EG, Pinto SB, Ghosh A, Vanlandingham DL, Budd A, Higgs S, Kafatos FC, Jacobs-Lorena M, Michel K. An immune-responsive serpin, SRPN6, mediates mosquito defense against malaria parasites. *Proc Natl Acad Sci U S A.* 2005, 102 (45): 16327-16332.

Abuhatab M, Selvan S, Gaugler R. Role of proteases in penetration in insect gut by the entomopathogenic nematode *Steinernema glaseri* (*Nematoda: Steinernematidae*). *Journal of Invertebrate Pathology* 1995, 66: 125-130.

Aguilar R, Dong Y, Warr E, Dimopoulos G. *Anopheles* infection responses; laboratory models versus field malaria transmission systems. *Acta Trop*. 2005, 95(3): 285-291.

Akai H, Sato S. Ultrastructure of the larval hemocytes of the silkworm *Bombyx mori* L. *International Journal of Insect Morphology and Embryology* 1973, 2: 207-231.

Altincicek B, Vilcinskas A. Metamorphosis and collagen-IV-fragments stimulate innate immune response in the greater wax moth, *Galleria mellonella*. *Dev Comp Immunol.* 2006, 30 (12): 1108-1118.

Arakawa T, Kato Y, Hattori M, Yamakawa M. Lipophorin: a carrier for lipids in insects participates in superoxide production in the haemolymph plasma. *Insect Biochemistry and molecular Biology* 1996, 26 (4): 403-409.

Arakawa T. Possible involvement of an enzymatic system for superoxide generation in lepidopteran larval haemolymph. *Archives of Insect Biochemistry and Physiology* 1995b, 29: 281-291.

Arakawa T. Superoxide generative reaction in insect haemolymph and its mimic model system with surfactants *in vitro*. *Insect Biochemistry and Molecular Biology* 1995a, 25 (2): 247-253.

Asano T, Ashida M. Transepithelially transported pro-phenoloxidase in the cuticle of the silk worm, *Bombyx mori*. *J Biol Chem* 2001, 276: 11113-11125.

Ashida M, Brey PT. (1998) Recent advances on the research of the insect prophenoloxidase cascade. In: Molecular Mechanisms of Immune Responses in Insects (Brey, P.T. and Hultmark, D., eds), pp. 135-172. Chapman & Hall, London.

Ashida M, Ochiai M, Niki T. Immunolocalization of prophenoloxidase among hemocytes of the silkworm, *Bombyx mori*. *Tissue & Cell* 1988, 20: 599-610.

Ashida M. The prophenoloxidase cascade in insect immunity. *Res Immunol* 1990, 141: 908–910.

Axen A, Carlsson A, Engstrom A, Bennich H. Gloverin, an antibacterial protein from the immune hemolymph of Hyalophora pupae. *Eur. J. Biochem.* 1997, 247: 614-619.

Bacchi CJ, Weiss LM, Lane S, Frydman B, Valasinas A, Reddy V, Sun JS, Marton LJ, Khan I, Moretto M, Yarlett N, Wittner M. Novel synthetic polyamines are effective treatments for experimental microsporidiosis, an opportunistic AIDS associated infection. *Antimicrob. Agents Chemother.* 2002, 46: 55-61.

Balbiani G. Sur les microsporidies ou sporospermies des articules. *C. R. Acad. Sci.* 1882, 95: 1168-1178.

Baldauf SL, Roger AJ, Wenk-Siefert I, Doolittle WF. A kingdom-levelphylogeny of eukaryotes based on combined protein data. *Science* 2000, 290: 972-977.

Barillas-Mury C, Kumar S. *Plasmodium*-mosquito interactions: a tale of dangerous liaisons. *Cell Microbiol.* 2005, 7(11): 1539-1545.

Barnes AI, Siva-Jothy MT. Density-dependent prophylaxis in the mealworm beetle *Tenebrio molitor* L. (*Coleoptera: Tenebrionidae*): cuticular melanization is an indicator of investment in immunity. *Proc Biol Sci.* 2000, 267(1439): 177-182.

Barwig B. Isolation and characterization of plasma coagulation of the cockroach *Leocophaea maderae*. *J. Comp. Physiol.* 1985, 155: 135-143.

Baton LA, Ranford-Cartwright LC. How do malaria ookinetes cross the mosquito midgut wall? *Trends Parasitol.* 2005, 21(1): 22-28.

Baton LA, Ranford-Cartwright LC. *Plasmodium falciparum* ookinete invasion of the midgut epithelium of *Anopheles stephensi* is consistent with the time bomb model. *Parasitol* 2004, 129: 663-676.

Beaulaton J. Hemocytes and hemocytopoiesis in silkworms. *Biochimie* 1979, 61: 157-164

Becnel JJ, Andreadis TG. (1999). Microsporidia in insects. In: The Microsporidia and Microsporidiosis (ed. Wittner, M. and Weiss, L. M.), pp. 447-501. American Society for Microbiology Press, Washington, D.C.

BiderrE C, Pages M, Méténier G, David D, Bata J, Prensier G, Vivarès CP. On small genomes in eukaryotic organisms: molecular karyotypes of two microsporidian species (Protozoa) parasites of vertebrates. *C. R. Acad. Sci.* 1994, 317: 399-404.

Bigliardi E, Sacchi L. Cell biology and invasion of the microsporidia. *Microbes Infect.* 2001; 3 (5): 373-379.

Biron DG, Agnew P, Marche L, Renault L, Sidobre C, Michalakis Y. Proteome of *Aedes aegypti* larvae in response to infection by the intracellular parasite *Vavraia culicis*. *Int J Parasitol.* 2005a, 35(13): 1385-1397.

Biron DG, Moura H, Marche L, Hughes AL, Thomas F. Towards a new conceptual approach to "parasitoproteomics". *Trends Parasitol.* 2005b, 21(4): 162-168.

Blandin S, Levashina EA. Thioester-containing proteins and insect immunity. *Mol. Immunol.* 2004b, 40: 903-908.

Blandin S, Shiao SH, Moita LF, Janse CJ, Waters AP, Kafatos FC, Levashina EA. Complement-like protein TEP1 is a determinant of vectorial capacity in the malaria vector *Anopheles gambiae. Cell.* 2004a, 116(5): 661-670.

Boete C. Malaria parasites in mosquitoes: laboratory models, evolutionary temptation and the real world. *Trends Parasitol.* 2005, 21(10): 445-447.

Bohne W, Ferguson DJ, Kohler K, Gross U. Developmental expression of a tandemly repeated, glycine- and serine-rich spore wall protein in the microsporidian pathogen *Encephalitozoon cuniculi. Infect. Immun.* 2000, 68: 2268-2275.

Brey P, Lee W, Yamakawa M, Koizumi Y, Perrot S, Francois M, and Ashida M. Role of the integument in insect immunity: epicuticular abrasion and induction of cecropin synthesis in cuticular epithelial cells. *Proc. Natl. Acad. Sci. USA* 1993, 90: 6275-6279.

Brivio MF, Mastore M and Pagani M. Parasite–host relationship: a lesson from a professional killer. *Invertebr Surviv J.* 2005, 2: 41-53.

Brogden KA. Antimicrobial peptides: pore formers or metabolic inhibitors in bacteria? *Nat Rev Microbiol.* 2005, 3(3): 238-250.

Brooks WM. The inflammatory response of the tobacco hornworm, *Manduca sexta*, to infection by the microsporidian, *Nosema sphingidis. Journal of Invertebrate Pathology,* 1971, 17(1): 87-93.

Brosson D, Kuhn L, Delbac F, Garin J, P Vivares C, Texier C. Proteomic analysis of the eukaryotic parasite *Encephalitozoon cuniculi* (microsporidia): a reference map for proteins expressed in late sporogonial stages. *Proteomics.* 2006, 6(12): 3625-3635.

Brown JR, Doolittle WF. Gene descent, duplication, and horizontal transferin the evolution of glutamyl- and glutaminyl-tRNAsynthetases. *J. Mol. Evol.* 1999, 49: 485-495.

Brown JR, Doolittle WF. Root of the universal tree of life based on ancient aminoacyl-tRNA synthetase gene duplications. *Proc Natl Acad Sci U S A.* 1995, 92(7): 2441-2425.

Budd A, Blandin S, Levashina EA, Gibson TJ. Bacterial alpha2-macroglobulins: colonization factors acquired by horizontal gene transfer from the metazoan genome? *Genome Biol*. 2004, 5(6): R38.

Bulet P, Charlet M, Hetru C. Antimicrobial peptides in insect immunity. In: Ezekowitz AB, Hoffmann JA, editors. Infectious disease: Innate immunity. Totowa, NJ: Humana Press; 2003, p: 89-107.

Bulet P, Hetru C, Dimarcq JL, Hoffmann D. Antimicrobial peptides in insects; structure and function. *Dev Comp Immunol.* 1999, 23(4-5): 329-344.

Bulet P, Stocklin R, Menin L. Anti-microbial peptides: from invertebrates to vertebrates. *Immunol. Rev.* 2004, 198: 169-184.

Cali A, Takvorian PM, Lewin S, Rendel M, Sian CS, Wittner M, Tanowitz HB, Keohane E, Weiss LM. *Brachiola vesicularum*, n. g., n. sp., a new microsporidium associated with AIDS and myositis. *J. Eukaryot. Microbiol*. 1998, 45: 240-251.

Cali A, Takvorian PM. Developmental morphology and life cycles of the microsporidia. In: The Microsporidia and Microsporidiosis (ed. Wittner, M. and Weiss, L. M.), pp. 85-1284. 1999. American Society for Microbiology Press, Washington, D.C.

Cali A. Morphogenesis in the genus *Nosema*. 1971 Proceedings of the IVth international Colloquium on insect pathology, College Park, Md.

Canning E U, Lom J, Dykova I. 1986. The Microsporidia of vertebrates. Academic Press, Orlando, Florida, 289 p.

Canning EU. Microsporidia IV: host-parasite interaction. *Parasitic Protozoa*, 1993, 6:342-345.

Castro VM, Boman HG, Hammarstrrm S. Isolation and characterization of a group of isolectins with galactose/N-acetylgalactosamine specificity from hemolymph of the giant silk moth *Hyalophora cecropia*. *Insect Biochem.* 1987, 17: 513-523.

Cavalier-Smith T. Archamoebae: the ancestral eukaryotes? *Biosystems*. 1991, 25(1-2): 25-38.

Cerenius L, Söderhäll K. The prophenoloxidaseactivating system in invertebrates. *Immunol. Rev.* 2004, 198: 116-126.

Charnley AK, St. Leger RJ. The role of cuticle-degrading enzymes in fungal pathogenesis in insects. In The Fungal spore & Disease initiation in plants and Animals, ed. Cole, G.T & Hoch, H.C. 1991, pp. 267-286. Plenum, New York.

Chen C, Billingsley PF. Detection and characterization of a mannan-binding lectin from the mosquito, *Anopheles stephensi*. *Eur. J. Biochem.* 1999, 263: 360-366.

Chen K, Yao Q, Li M, Wang Y. Screening of RAPD markers for fluoride resistance in *Bombyx mori* L. *Int. J. Indust. Entomol.* 2003, 7: 11-14.

Christensen BM, Li J, Chen CC, Nappi AJ. Melanization immune responses in mosquito vectors. *Trends Parasitol.* 2005, 21(4): 192-199.

Christophides GK, Zdobnov E, Barillas-Mury C, Birney E, Blandin S, Blass C, Brey PT, Collins FH, Danielli A, Dimopoulos G, Hetru C, Hoa NT, Hoffmann JA, Kanzok SM, Letunic I, Levashina EA, Loukeris TG, Lycett G, Meister S, Michel K, Moita LF, Muller HM, Osta MA, Paskewitz SM, Reichhart JM, Rzhetsky A, Troxler L, Vernick KD, Vlachou D, Volz J, von Mering C, Xu J, Zheng L, Bork P, Kafatos FC. Immunity-related genes and gene families in *Anopheles gambiae*. *Science* 2002, 298: 159-165.

Clarkson J, Screen S, Bailey A, Cobb B, Charnley K. Fungal pathogenesis in insects. In: Molecular Variability of Fungal Pathogens (Bridge, P., Couteaudier, Y. and Clarkson, J., Eds.), 1998, pp. 83-93. CAB International (Chapter 6).

Colasanti, M. Gradoni L, Mattu M, Persichini T, Salvati L, Venturini G, Ascenzi P. Molecular bases for the anti-parasitic effect of NO. *Int. J. Mol. Med.* 2002, 9: 131-134.

Collins FH, Sakai RK, Vernick KD, Paskewitz S, Seeley DC, Miller LH, Collins WE, Campbell CC, Gwadz RW. Genetic selection of a *Plasmodium*-refractory strain of the malaria vector *Anopheles gambiae*. *Science.* 1986, 234(4776): 607-610.

Costa SF, Weiss LM. Drug treatment of microsporidiosis. *Drug Resist Updat.* 2000, 3(6): 384-399.

Couzinet S, Cejas E, Schittny J, Deplazes P, Weber R, Zimmerli S. Phagocytic uptake of *Encephalitozoon cuniculi* by nonprofessional phagocytes. *Infect. Immun*. 2000, 68: 6939-6945.

Cytrynska M, Zdybicka-Barabas A, Jakubowicz T. Studies on the role of protein kinase A in humoral immune response of *Galleria mellonella* larvae. *J Insect Physiol.* 2006, 52(7): 744-753.

De Gregorio E, Spellman PT, Tzou P, Rubin GM, Lemaitre B. The Toll and Imd pathways are the major regulators of the immune response in *Drosophila*. *EMBO J.* 2002, 21(11): 2568-2579.

Delbac F, Peuvel I, Metenier G, Peyretaillade E, Vivares CP. Microsporidian invasion apparatus: identification of a novel polar tube protein and evidence for clustering of ptp1 and ptp2 genes in three *Encephalitozoon* species. *Infect Immun.* 2001, 69(2): 1016-1024.

Delbac F, Peyret P, Metenier G, David D, Danchin A, Vivares CP. On proteins of the microsporidian invasive apparatus: complete sequence of a polar tube protein of *Encephalitozoon cuniculi*. *Mol Microbiol.* 1998, 29(3): 825-834.

Desportes I, Le Charpentier Y, Galian A, Bernard F, Cochand-Priollet B, Lavergne A, Ravisse P, Modigliani R. Occurrence of a new microsporidan: *Enterocytozoon bieneusi* n.g., n. sp., in the enterocytes of a human patient with AIDS. *J Protozool.* 1985, 32(2): 250-254.

Desportes-Livage I, Chilmonczyk S, Hedrick R, Ombrouck C, Monge D, Maiga I, Gentilini M. Comparative development of two microsporidian species: *Enterocytozoon bieneusi* and *Enterocytozoon salmonis*, reported in AIDS patients and salmonid fish, respectively. *J Eukaryot Microbiol*. 1996,43(1): 49-60

Dessens JT, Mendoza J, Claudianos C, Vinetz JM, Khater E, Hassard S, Ranawaka GR, Sinden RE. Knockout of the rodent malaria parasite chitinase pbCHT1 reduces infectivity to mosquitoes. *Infect. Immun*. 2001, 69, 4041-4047.

Dessens JT, Siden-Kiamos I, Mendoza J, Mahairaki V, Khater E, Vlachou D, Xu XJ, Kafatos FC, Louis C, Dimopoulos G, Sinden RE. SOAP, a novel malaria ookinete protein involved in mosquito midgut invasion and oocyst development. *Mol Microbiol.* 2003, 49(2): 319-329.

Didier ES, Didier PJ, Snowden KF, Shadduck JA. Microsporidiosis in mammals. *Microbes Infect.* 2000, 2(6): 709-720.

Didier ES, Martin AD, Stovall ME, Alvarez X, Mittleider D, Green LC, Bowers LC, Plauche AK, Didier PJ, Brindley PJ. Methionine aminopeptidase 2 expression in microsporidia. *J Eukaryot Microbiol.* 2003; 50 Suppl: 569-571.

Didier ES. Microsporidiosis: an emerging and opportunistic infection in humans and animals. *Acta Trop*. 2005, 94(1): 61-76.

Dimopoulos G, Seeley D, Wolf A, Kafatos FC. Malaria infection of the mosquito *Anopheles gambiae* activates immune-responsive genes during critical transition stages of the parasite life cycle. *EMBO J.* 1998, 17: 6115-6123.

Dimopoulos G. Insect immunity and its implication in mosquito-malaria interactions.*Cell Microbiol*. 2003, 5(1): 3-14.

Dolgikh VV, Semenov PB, Mironov AA, Beznoussenko GV. Immunocytochemical identification of the major exospore protein and three polar-tube proteins of the microsporidia *Paranosema grylli. Protist.* 2005, 156(1): 77-87.

Dunn PE, Dai W, Kanost M R, Geng C. Soluble peptidoglycan fragments stimulate antibacterial protein synthesis by fat body from larvae of *Manduca sexta*. *Dev. Comp. lmmunol.* 1985, (9): 559-568.

Duvic B, Brehélin M. Two major proteins from locust plasma are involved in coagulation and are specifically precipitated by laminarin, a beta-1,3-glucan. *Insect Biochem. Mol. Biol.* 1998, 28: 959-967.

Dyková I. 1995. Phylum microspora. In Fish diseases and disorders, Vol. 1, P. T. K. Woo and J. F. Leatherland (eds.). CAB International, Wallinford, U.K., p. 149-179.

Edlind TD, Li J, Visvesvara GS, Vodkin MH, McLaughlin GL, Katiyar SK. Phylogenetic analysis of β-tubulin sequences from amitochondrial protozoa. *Mol. Phylogenet. Evol.* 1996, 5: 359-367.

Fang FC. Antimicrobial reactive oxygen and nitrogen species: concepts and controversies. *Nature reviews in microbiology* 2004, 2: 820-832.

Fast NM, Keeling PJ. Alpha and beta subunits of pyruvate dehydrogenase E1 from the microsporidian *Nosema locustae*: mitochondrion-derived carbon metabolism in microsporidia. *Mol. Biochem. Parasitol.* 2001, 117: 201-209

Fast NM, Logsdon JM Jr, Doolittle WF. Phylogenetic analysis of the TATAbox binding protein (TBP) gene from *Nosema locustae*: evidence for a microsporidia-fungi relationship and spliceosomalintron loss. *Mol. Biol. Evol.* 1999, 16: 1415-1419.

Ferrandon D, Jung AC, Criqui M, Lemaitre B, Uttenweiler-Joseph S, Michaut L, Reichhart J, Hoffmann JA. A drosomycin-GFP reporter transgene reveals a local immune response in *Drosophila* that is not dependent on the Toll pathway. *EMBO J.* 1998, 17(5): 1217-1227.

Figueiredo MB, Castro DP, S Nogueira NF, Garcia ES, Azambuja P. Cellular immune response in Rhodnius prolixus: role of ecdysone in hemocyte phagocytosis. *J Insect Physiol.* 2006, 52(7): 711-716.

Findley AM, Weidner EH, Carman KR, Xu Z, Godbar JS. Role of the posterior vacuole in *Spraguea lophii* (Microsporidia) spore hatching. *Folia Parasitol.* 2005, 52: 111-117.

Finnerty CM, Karplus PA, Granados RR. The insect immune protein scolexin is a novel serine proteinase homolog. *Protein Sci.* 1999, 8: 242-248.

Franzen C, Hosl M, Salzberger B, Hartmann P. Uptake of *Encephalitozoon* spp. and *Vittaforma corneae* (Microsporidia) by different cells. *J Parasitol.* 2005, 91(4): 745-749.

Franzen C. Microsporidia: how can they invade other cells? *Trends Parasitol.* 2004, 20(6): 275-279.

Frixione E, Ruiz L, Cerbon J, Undeen AH. Germination of *Nosema algerae* (Microspora) spores: conditional inhibition by D_2O, ethanol and Hg^{2+} suggests dependence of water influx upon membrane hydration and specific transmembrane pathways. *J. Eukaryot. Microbiol.* 1997, 44: 109-116.

Fugiwara T. Microsporidia from silkworm moths in egg-production sericulture. *J. Seric. Sci. Jpn.* 1985, 54, 108-111

Fujii H. Genetical Stocks and Mutations of *Bombyx mori*: Important Genetic Resources. Fukuoka, Jpn. Kyushu Univ. 1998, 54 pp.

Furukawa S, Taniai K, Ishibashi J, Hara S, Shono T, Yamakawa M. A novel member of lebocin gene family from the silkworm *Bombyx mori*. *Biochem Biophys Res Comm* 1997, 238: 769-774.

Gadjeva M, Takahashi K, Thiel S. Mannan-binding lectin-a soluble pattern recognition molecule. *Mol. Immunol.* 2004, 41: 113-121.

Gao YZ, Huang KW, The ultrastructural studies of microsporidian pathogenic to the silkworm *Bombyx mori* (in Chinese). *Acta Sericologica Sinica*. 1999, 25(3): 163-168.

Garcia-del portillo F, Finlay BB. The varied lifestyles of intracellular pathogens within eukaryotic vacuolar compartments. *Trends in Microbiology* 1995, 3: 373-380.

Garcia-Lara J, Needham AJ, Foster SJ. Invertebrates as animal models for *Staphylococcus aureus* pathogenesis: a window into host-pathogen interaction. *FEMS Immunol Med Microbiol.* 2005, 43(3): 311-323.

Geng C, Dunn PE. Hemostasis in larvae of *Manduca sexta*: formation of a fibrous coagulum by hemolymph proteins. *Biochem. Biophys. Res. Com.* 1988, 155: 1060-1065.

Germot A, Philippe H, Le Guyader H. Evidence for loss of mitochondriain Microsporidia from a mitochondrial type HSP70 in *Nosema locustae*. *Mol. Biochem. Parasitol.* 1997, 87: 159-168.

Gill EE, Fast NM. Assessing the microsporidia-fungi relationship: Combined phylogenetic analysis of eight genes. *Gene.* 2006, 375: 103-109.

Gillespie JP, Kanost MR, Trenczek T. Biological mediators of insect immunity. *Annu Rev Entomol* 1997, 42: 611-643.

Goldsmith MR, Shimada T, Abe H. The genetics and genomics of the silkworm, *Bombyx mori*. *Annu Rev Entomol.* 2005, 50: 71-100.

Gorman MJ, Andreeva OV, Paskewitz SM. SP22D: a multidomain serine protease with a

putative role in insect immunity. *Gene* 2000, 251: 9-17.

Govind S, Nehm RH. Innate immunity in fruit flies: a textbook example of genomic recycling. *PLoS Biol.* 2004, 2(8): E276.

Gupta L, Kumar S, Han YS, Pimenta PF, Barillas-Mury C. Midgut epithelial responses of different mosquito-*Plasmodium* combinations: the actin cone zipper repair mechanism in *Aedes aegypti*. *Proc Natl Acad Sci U S A.* 2005, 15; 102(11): 4010-4015.

Hahn UK, Bender RC, Bayne CJ. Involvement of nitric oxide in killing of *Schistosoma mansoni* sporocysts by hemocytes from resistant *Biomphalaria glabrata*. *J. Parasitol.* 2001, 87: 778-785.

Hajek AE, Leger RJ St. Interactions between fungal pathogens and insect hosts. *Annu. Rev. Entomol.* 1994. 39: 293-322.

Han SS, Lee MH, Kim WK, Wago H, Yoe SM. Hemocytic differentiation in hemopoietic organ of *Bombyx mori* larvae. *Zool Sci* 1998,15: 371–379

Han YS, Thompson J, Kafatos FC, Barillas-Mury C. Molecular interactions between *Anopheles stephensi* midgut cells and *Plasmodium berghei*: the time bomb theory of ookinete invasion of mosquitoes. *EMBO J.* 2000, 19(22): 6030-6040.

Hancock RE, Scott MG. The role of antimicrobial peptides in animal defenses. *Proc Natl Acad Sci.* 2000, 97(16): 8856-8861.

Hara S, Taniai K, Kato Y, Yamakawa M. Isolation and a-amidation of the non-amidated form of cecropin D from larvae of *Bombyx mori*. *Comp Biochem Physiol* 1994, 108B: 303-308.

Hara S, Yamakawa M. A novel antibacterial peptide family isolated from the silkworm, *Bombyx mori*. *Biochem. J.* 1995a, 310: 651-656.

Hara S, Yamakawa M. Moricin, a novel type of antibacterial peptide isolated from the silkworm, *Bombyx mori*. *J. Biol. Chem.* 1995b, 270: 29923-29927.

Hayman JR, Hayes SF., Amon J, Nash TE. Developmental expression of two spore wall proteins during maturation of the microsporidian *Encephalitozoon intestinalis. Infect. Immun.* 2001, 69: 7057-7066.

Hayman JR, Southern TR, Nash TE. Role of sulfated glycans in adherence of the microsporidian *Encephalitozoon intestinalis* to host cells *in vitro*. *Infect Immun.* 2005, 73(2): 841-848.

He N-J, Lu C, Li B, Zhou Z-y, Xiang ZH. Construction of a linkage map in the silkworm, *Bombyx mori*, based on SADF and RAPD markers. In: The Third Youth Symposium of the Association of Sericulture of China. Chongqing, China: Southwest Agric. Univ. 269 pp., Southwest Agricultural University. 2001.

Hetru C, Troxler L, Hoffmann JA. *Drosophila melanogaster* antimicrobial defense. *J Infect Dis* 2003, 187(Suppl. 2): S327-S334.

Hillyer JF, Schmidt SL, Christensen BM. Hemocyte-mediated phagocytosis and melanization in the mosquito *Armigeres subalbatus* following immune challenge by bacteria. *Cell Tissue Res* 2003b, 313:117-127

Hillyer JF, Schmidt SL, Christensen BM. Rapid phagocytosis and melanization of bacteria and *Plasmodium* sporozoites by hemocytes of the mosquito *Aedes aegypti*. *J. Parasitol.* 2003a, 89: 62-69.

Hinkle G, Morrison HG, Sogin ML. Genes coding for reverse transcriptase, DNA-directed

RNA polymerase, and chitin synthase from the microsporidian *Spraguea lophii*. *Biol. Bull.* 1997, 193: 250-251.

Hirt RP, Healy B, Vossbrinck CR, CanningEU, Embley TM. A mitochondrial Hsp70 orthologue in *Vairimorpha necatrix*: molecular evidence thatmicrosporidia once contained mitochondria. *Curr. Biol.* 1997, 7: 995-998.

Hirt RP, Logsdon JM Jr, Healy B, DoreyMW, Doolittle WF, Embley TM. Microsporidia are related to Fungi: evidencefrom the largest subunit of RNA polymerase II and other proteins. *Proc.Natl. Acad. Sci. USA* 1999, 96: 580-585.

Hoch G, Solter LF, Schopf A. Hemolymph melanization and alterations in hemocyte numbers in *Lymantria dispar* larvae following infections with different entomopathogenic microsporidia. *Entomologia Experimentalis et Applicata* 2004, 113: 77-86

Hoffmann JA, Kafatos FC, Janeway CA, Ezekowitz RAB. Phylogenetic perspectives in innate immunity. *Science*, 1999, 284: 1313-1318.

Hoffmann JA, Reichhart JM, Hetru C. Innate immunity in higher insects. *Curr Opin Immunol* 1996, 8: 8-13.

Hoffmann JA, Reichhart JM. *Drosophila* innate immunity: an evolutionary perspective. *Nat Immunol* 2002, 3(2): 121-126.

Hoffmann JA. The immune response of *Drosophila. Nature.* 2003, 426(6962): 33-38.

Horn C, Schmid BG, Pogoda FS, Wimmer EA. Fluorescent transformation markers for insect transgenesis. *Insect Biochem. Mol. Biol.* 2002, 32: 1221-1235.

Horn C, Wimmer EA. Highly sensitive, fluorescent transformation marker for *Drosophila* transgenesis. *Dev. Genes Evol.* 2000, 210: 623-629.

Horta MF. Pore-forming proteins in pathogenic protozoan parasites. *Trends in Microbiology* 1997, 5: 363-366.

Hortsch M. The L1 family of neural cell adhesion molecules: old proteins performing new tricks. *Neuron.* 1996, 17: 587-593.

Huang HW. Molecular mechanism of antimicrobial peptides: The origin of cooperativity. *Biochimica et Biophysica Acta*, 2006, 1758(9): 1292-1302.

Huang Q, Deveraux QL, Maeda S, Stennicke HR, Hammock BD, Reed JC. Cloning and characterization of an inhibitor of apoptosis protein (IAP) from *Bombyx mori*. *Biochim. Biophys. Acta* 2001, 1499: 191-198.

Huber M, Cabib E, Miller LH. Malaria parasite chitinase and penetration of the mosquito peritrophic membrane. *Proc Natl Acad Sci U S A.* 1991, 88(7): 2807-2810.

Hurlbert RE, Karlinsey JE, Spence KD. Differential synthesis of bacteria-induced proteins of *Manduca sexta* larvae and pupae. *J. Insect Physiol.* 1985, 31: 205-215.

Iguchi T, Iwano H, Hatakeyama Y, Kawakami Y, Onoda K, Hayasaka S, Inoue T, Ishihara, R. Sporogony of microsporidium, *Nosema* sp. NIS-M11 (Microspora: *Nosematidae*) in larvae of the silkworm *Bombyx mori* raised under two distinct levels of temprature. *J. Sericult. Sci.Jpn.* 1997, 66: 445-452.

Imamura M, Yang J, Yamakawa M. cDNA cloning, characterization and gene expression of nitric oxide synthase from the silkworm, *Bombyx mori*. *Insect Mol Biol.* 2002, 11(3): 257-265.

Imler JL, Bulet P. Antimicrobial peptides in *Drosophila*: structures, activities and gene regulation. *Chem Immunol Allergy*. 2005, 86: 1-21.

Ishihara R, Hayashi T. Some properties of ribosomes from the sporoplasm of *Nosema*

bombycis. *J.Invert. Path.*1968, 11: 377-385.

Ishihara R, Sohi S. Infection of ovarian tissue culture of *Bombyx mori* by *Nosema bombycis* spores. *J. Invert. Path.* 1966, 8: 538-540.

Ishihara R. Researches in pebrine for the past twenty years. *J. Seric. Sci. Jpn.* 1985, 54, 347-353

Ishihara R. Some observations on the fine structure of sporoplasm discharged from spores of a microsporidian, *Nosema bombycis*. *J. Invert. Path.* 1968, 11: 377-385.

Ishihara R. The life cycle of *Nosema bombycis* as revealed in tissue culture cells of Bombyx. *J Invertebr Pathol.* 1969, 14(3): 316-320.

Ishino T, Orito Y, Chinzei Y, Yuda M. A calcium-dependent protein kinase regulates *Plasmodium* ookinete access to the midgut epithelial cell. *Molecular Microbiology* 2006, 59 (4): 1175-1184.

Itoh A, Iizuka K, Natori S. Antitumor effect of *Sarcophaga* lectin on murine transplanted tumors. *Jpn J Cancer Res.* 1985, 76(10): 1027-1033.

Iwanaga S, Lee BL. Recent advances in the innate immunity of invertebrate animals. *J Biochem Mol Biol.* 2005, 38(2): 128-150.

Iwano H, Ishihara R. Dimorphic development of *Nosema bombycis* spore in the gut epithelium of larvae of the silkworm, *Bombyx mori*. *J. Seric. Sci. Jpn.,* 1991b, 60: 249-256.

Iwano H, Ishihara R. Dimorphism of spores of *Nosema* spp. in cultured cell. *Journal of Invertebrate Pathology,* 1991a, 57 (2): 211-219.

Iwano H, Ishihara R. Intracellular germination of spores of a *Nosema* sp. immediately after their formation in cultured cell. *Journal of Invertebrate Pathology,* 1989, 54(1): 125-127.

Jack DL, Turner MW. Anti-microbial activities of mannosebinding lectin. *Biochem. Soc.* 2003, 31: 753-757.

Janeway CA, Medzhitov R. Innate immune recognition. *Annu Rev Immunol* 2002, 20: 197-216.

Janeway CA. The immune system evolved to discriminate infectious nonself from noninfectious self. *Immunol Today* 1992, 13: 11-16.

Jin Y, Chen Y, Jiang Y, Xu M. Proteome analysis of the silkworm (*Bombyx mori*. L) colleterial gland during different development stages. *Arch Insect Biochem Physiol.* 2006, 61(1): 42-50.

Jiravanichpaisala P, Leeb BL, Söderhälla K. Cell-mediated immunity in arthropods: Hematopoiesis, coagulation, melanization and opsonization. *Immunobiology.* 2006, 211: 213-236.

Johnson MA, Becnel JJ, Undeen AH. A New Sporulation Sequence in *Edhazardia aedis* (Microsporidia: Culicosporidae), a Parasite of the Mosquito *Aedes aegypti* (Diptera: Culicidae). *Journal of Invertebrate Pathology.* 1997, 70 (1): 69-75

Johny S, Kanginakudru S, Muralirangan MC, Nagaraju J. Morphological and molecular characterization of a new microsporidian (Protozoa: Microsporidia) isolated from *Spodoptera litura* (Fabricius) (*Lepidoptera: Noctuidae*). *Parasitology*. 2006, 132(Pt 6): 803-814.

Jomori T, Natori S. Function of the lipopolysaccharide-binding protein of *Periplaneta americana* as an opsonin. *FEBS Lett.* 1992, 296: 283-286.

Kadono-Okuda K, Kosegawa E, Mase K, Hara W. Linkage analysis of maternal EST cDNA clones covering all twenty-eight chromosomes in the silkworm, *Bombyx mori*. *Insect*

Mol. Biol. 2002, 11: 443-451.

Kadota K, Ishino T, Matsuyama T, Chinzei Y, Yuda M. Essential role of membrane-attack protein in malarial transmission to mosquito host. *Proc Natl Acad Sci U S A.* 2004, 101(46): 16310-16315.

Kaito C, Akimitsu N, Watanabe H, Sekimizu K. Silkworm larvae as an animal model of bacterial infection pathogenic to humans. *Microb Pathog.* 2002, 32(4): 183-190.

Kaito C, Kurokawa K, Matsumoto Y, Terao Y, Kawabata S, Hamada S, Sekimizu K. Silkworm pathogenic bacteria infection model for identification of novel virulence genes. *Mol Microbiol.* 2005, 56(4): 934-944.

Kamaishi T, Hashimoto T, Nakamura Y, Masuda Y, Nakamura F, Okamoto K, Shimizu M, Hasegawa M. Complete nucleotide sequences of the genes encoding translation elongation factors 1alpha and 2 from a microsporidian parasite, *Glugea plecoglossi*: implications for the deepest branching of eukaryotes. *J. Biochem.* 1996a, 120: 1095-1103.

Kamaishi T, Hashimoto T, Nakamura Y,Nakamura F, Murata S, Okada N, Okamoto K, Shimizu M, Hasegawa M. Protein phylogeny of translation elongation factor EF-1α suggests Microsporidians are extremely ancient eukaryotes. *J. Mol. Evol*. 1996b, 42: 257-263.

Kanost MR, Jiang H, Yu XQ. Innate immune responses of a lepidopteran insect, *Manduca sexta*. *Immunol Rev* 2004, 198: 97-105.

Kappe SH, Buscaglia CA, Nussenzweig V. *Plasmodium* sporozoite molecular cell biology. *Annu Rev Cell Dev Biol* 2004, 20: 29-59.

Kashkarova LF, Khakhanov AI. Range of the hosts of the causative agent of pebrine (*Nosema bombycis*) in the mulberry silkworm. *Parazitologiia.* 1980, 14(2): 164-167.

Katinka MD, Duprat S, Cornillot E, Metenier G, Thomarat F, Prensier G, Barbe V, Peyretaillade E, Brottier P, Wincker P, Delbac F, El Alaoui H, Peyret P, Saurin W, Gouy M, Weissenbach J, Vivares CP. Genome sequence and gene compaction of the eukaryote parasite *Encephalitozoon cuniculi. Nature.* 2001, 414 (6862): 450-453.

Katsumi Y, Kihara H, Ochiai M, Ashida M. A serine protease zymogen in insect plasma. Purification and activation by microbial cell wall components. *Eur J Biochem.* 1995, 228(3): 870-877.

Kavanagh K, Reeves EP. Exploiting the potential of insects for *in vivo* pathogenicity testing of microbial pathogens. *FEMS Microbiol Rev.* 2004, 28(1): 101-112.

Kawabata T, Yasuhara Y, Ochiai M, Matsuura S, Ashida M. Molecular cloning of insect pro-phenol oxidase: a copper-containing protein homologous to arthropod hemocyanin. *Proc Natl Acad Sci U S A.* 1995, 92(17): 7774-7778.

Kawakami Y, Inoue T, **Ito K, Kikuchi M, Takayanagi M, Sunairi M, Ando T, Ishihara R.** Comparison of chromosomal DNA from microsporidia pathogenic to the silkworm, *Bombyx mori*. *Appl Entomol Zool* 1994, 29(1): 120-123.

Kawarabata T, Hayasaka S. An enzyme-linked immunosorbent assay to detect alkali-soluble spore surface antigens of strains of *Nosema bombycis* (Microspora: Nosematidae). *Journal of Invertebrate Pathology.* 1987, 50 (2): 118-123

Kawarabata T, Ishihara R. Infection and development of *Nosema bombycis* (Microsporidia: Protozoa) in a cell line of *Antheraea euealypti*. *J Invertebr Pathol* 1984, 44: 52-62.

Kawarabata T. Biology of microsporidians infecting the silkworm, *Bombyx mori*, in Japan. *Journal of insect Biotechnology and Sericology*, 2003, 72: 1-32.

Ke Zhaoxi, Weidong Xie, Xunzhang Wang, Qingxing Long and Zhelong Pu. A monoclonal antibody to *Nosema bombycis* and its use for identification of microsporidian spores. *Journal of Invertebrate Pathology* 1990, 56 (3): 395-400

Keeling PJ, Doolittle WF. Alpha tubulin from early-diverging eukaryoticlineages and the evolution of the tubulinfamily. *Mol. Biol. Evol.* 1996, 13: 1297-305.

Keeling PJ, Fast NM. Microsporidia: biology and evolution of highly reduced intracellular parasites. *Annu Rev Microbiol.* 2002, 56: 93-116.

Keeling PJ, Luker MA, Palmer JD. Evidence from beta-tubulin phylogeny that microsporidia evolved from within the fungi. *Mol Biol Evol*. 2000, 17(1): 23-31.

Keeling PJ, Slamovits CH. Simplicity and complexity of microsporidian genomes. *Eukaryot Cell*. 2004, 3(6): 1363-1369.

Keeling PJ. Congruent evidence from alpha-tubulin and beta-tubulin gene phylogenies for a zygomycete origin of microsporidia. *Fungal Genet. Biol.* 2003, 38, 298-309.

Keohane EM, Weiss LM. Characterization and function of the microsporidianpolar tube: a review. *Folia Parasitol.* 1998, 45: 117-127.

Keohane EM, Weiss LM. The structure, function, and composition of the microsporidian polar tube. In: The Microsporidia and Microsporidiosis (ed. Wittner, M. and Weiss, L. M.), pp. 196-224. 1999. American Society for Microbiology Press, Washington, D.C.

Koizumi N, Imai Y, Morozumi A, Imamura M, Kadotani T, Yaoi K, Iwahana H, Sato R. Lipopolysaccharide-binding protein of *Bombyx mori* participates in a hemocyte-mediated defense reaction against gram-negative bacteria. *J Insect Physiol* 1999, 45: 853-859.

Koizumi N, Morozumi A, Imamura M, Tanaka E, Iwahana H, Sato R. Lipopolysaccharide -binding proteins and their involvement in the bacterial clearance from the hemolymph of the silkworm *Bombyx mori*. *Eur J Biochem* 1997, 248: 217-224.

Komano H, Mizuno D, Natori S. Purification of lectin induced in the hemolymph of *Sarcophaga peregrina* larvae on injury. *J. Biol. Chem.* 1980, 255: 2919-2924.

Komoto N, Yukuhiro K, Tamura T. Structure and expression of tandemly duplicated xanthine dehydrogenase genes of the silkworm (*Bombyx mori*). *Insect Mol. Biol.* 1999, 8:73-83.

Korayem AM, Fabbri M, Takahashi K, Scherfer C, Lindgren M, Schmidt O. A *Drosophila* salivary gland mucin is also expressed in immune tissues: evidence for a function in coagulation and the entrapment of bacteria. *Insect Biochem Mol Biol* 2004, 34(12): 1297-1304.

Kotani E, Yamakawa M, Iwamoto S, Tashiro M, Mori H, Sumida M, Matsubara F, Taniai K, Kadono-Okuda K, Kato Y. Cloning and expression of the gene of hemocytin, an insect humoral lectin which is homologous with the mammalian von Willebrand factor. *Biochim. Biophys. Acta.* 1995, 1260: 245-258.

Krishnan N, Sehnal F. Compartmentalization of oxidative stress and antioxidant defense in the larval gut of *Spodoptera littoralis. Arch Insect Biochem Physiol*. 2006, 63(1): 1-10.

Kudo R. Experiments on the extrusion of polar filaments of cnidosporidian spores. *J. Parasitol.* 1918, 4: 141-147

Kumar S, Christophides GK, Cantera R, Charles B, Han YS, Meister S, Dimopoulos G, Kafatos FC, Barillas-Mury C. The role of reactive oxygen species on *Plasmodium* melanotic encapsulation in *Anopheles gambiae*. *Proc Natl Acad Sci U S A*. 2003, 100(24):14139-14144.

Kurtz J, Nahif AA, Sauer KP. Phagocytosis of *vairimorpha* sp. (Microsporida, Nosematidae) spores by *Plutella xylostella* and *Panorpa vulgaris* hemocytes. *J Invertebr Pathol.* 2000, 75(3): 237-239.

Kyriakides TR, McKillip J, Spence KD. Biochemical characterization, developmental expression, and induction of the immune protein scolexin from *Manduca sexta*. *Arch. Insect Biochem. Physiol.* 1995, 29: 269-280.

Kyriakides TR, McKillip JL, Spence KD. *In vivo* distribution of immune protein scolexin in bacteria injected *Manduca sexta* larvae. *Tissue Cell* 1993, 25: 423-434.

Lagueux M, Perrodou E, Levashina EA, Capovilla M, Hoffmann JA. Constitutive expression of a complement-like protein in Toll and JAK gain-of-function mutants of *Drosophila*. *Proc. Natl. Acad. Sci. USA.* 2000, 97(21): 11427-11432.

Lamberty M, Caille A, Landon C, Tassin-Moindrot S, Hetru C, Bulet P, Vovelle F. Solution structures of the antifungal heliomicin and a selected variant with both antibacterial and antifungal activities. *Biochemistry* 2001, 40: 11995-12003.

Lamberty M, Zachary D, Lanot R, Bordereau C, Robert A, Hoffmann JA, Bulet P. Insect immunity: Constitutive expression of a cysteine-rich antifungal and a linear antibacterial peptide in a termite insect. *J Biol Chem.* 2001, 276(6): 4085-4092.

Langer RC, Li F, Popov V, Kurosky A, Vinetz JM. Monoclonal antibody against the *Plasmodium falciparum* chitinase, PfCHT1, recognizes a malaria transmission-blocking epitope in *Plasmodium gallinaceum* ookinetes unrelated to the chitinase PgCHT1. *Infect Immun.* 2002, 70(3):1581-1590.

Langer RC, Vinetz JM. *Plasmodium* ookinete-secreted chitinase and parasite penetration of the mosquito peritrophic matrix. *Trends Parasitol.* 2001, 17(6): 269-272.

Langley RC Jr, Cali A, Somberg EW. Two-dimensional electrophoretic analysis of spore proteins of the Microsporida. *J Parasitol.* 1987, 73: 910-918.

Larsson JI. Fixation of microsporidian spores for electron microscopy *J. Invertebr Pathol*. 2005, 90: 47-50

Lavine MD, Strand MR. Insect hemocytes and their role in immunity *Insect Biochemistry and Molecular Biology* 2002, 32: 1295-1309.

Lee WJ, Brey PT. Isolation and characterization of the lysozyme-encoding gene from the silkworm *Bombyx mori*. *Gene* 1995, 161: 199-203.

Legay J M, Chavancy G. La phase pastorienne de la sériciculture: La crise de la pebrine et ses consequences. *Natures Sciences Sociétés* 2004, 12, 413-417.

Levashina EA, Moita LF, Blandin S., Vriend G, Lagueux M, Kafatos FC. Conserved role of a complement-like protein in phagocytosis revealed by dsRNA knockout in cultured cells of the mosquito, *Anopheles gambiae*. *Cell* 2001, 104: 709-718.

Levashina EA. Immune responses in *Anopheles gambiae*. *Insect Biochem Mol Biol.* 2004 , 34(7): 673-678.

Levin D, Breuer LN, Zhuang S, Anderson SA, Nardi JB, Kanost MR. A hemocyte-specific integrin required for hemocytic encapsulation in the tobacco hornworm, Manduc sexta. *Insect Biochemistry and Molecular Biology* 2005, 35(5): 369-380.

Levy F, Bulet P, Ehret-Sabatier L. Proteomic analysis of the systemic immune response of *Drosophila*. *Mol. Cell. Proteomics* 2004, 3: 156-166.

Levy JA. The importance of the innate immune system in controlling HIV infection and disease. *TRENDS Immunol*. 2001, 22: 312-316.

Li D, Scherfer C, Korayem AM, Zhao Z, Schmidt O, Theopold U. Insect hemolymph clotting: evidence for interaction between the coagulation system and the prophenoloxidase activating cascade. *Insect Biochem Mol Biol.* 2002, 32(8): 919-928.

Li M, Guo Q, Hou C, Miao X, Xu A, Guo X, Huang Y. Linkage and mapping analyses of the densonucleosis non-susceptible gene nsd-Z in the silkworm *Bombyx mori* using SSR markers. *Genome*. 2006, 49(4): 397-402.

Li M, Yao Q, Hou C, Cheng L, Chen K. Studies on RAPD markers linked to the densonucleosis refractoriness gene, nsd-Z, in the silkworm, *Bombyx mori*. *Sericologia* 2001, 41: 409-415.

Ling E, Shirai K, Kanehatsu R, Kiguchi K. Reexamination of phenoloxidase in larval circulating hemocytes of the silkworm, *Bombyx mori*. *Tissue Cell.* 2005b, 37(2):101-107

Ling E, Shirai K, Kanekatsu R, Kiguchi K. Classification of larval circulating hemocytes of the silkworm, *Bombyx mori*, by acridine orange and propidium iodide staining. *Histochem Cell Biol* 2003, 120: 505-511.

Ling E, Shirai K, Kanekatsu R, Kiguchi K. Hemocyte differentiation in the hematopoietic organs of the silkworm, *Bombyx mori*: prohemocytes have the function of phagocytosis. *Cell Tissue Res*. 2005a, 320(3): 535-543.

Ling E, Yu XQ. Cellular encapsulation and melanization are enhanced by immulectins, pattern recognition receptors from the tobacco hornworm *Manduca sexta*. *Dev Comp Immunol*. 2006a, 30(3): 289-299.

Ling E, Yu XQ. Hemocytes from the tobacco hornworm Manduca sexta have distinct functions in phagocytosis of foreign particles and self dead cells. *Dev Comp Immunol*. 2006b, 30(3): 301-309.

Lowman PM, Takvorian PM, Cali A. The effects of elevated temperature and various time-temperature combinations on the development of *Brachiola* (*Nosema*) *algerae* n. comb. in mammalian cell culture. *J. Eukaryot. Microbiol.*, 2000, 47: 221-234.

Lu C, Dai F-Y Xiang Z-H. Studies on the mutant strains of the *Bombyx mori* gene bank. In: The Third Youth Symposium of the Association of Sericulture of China. Chongqing, China: Southwest Agric. Univ. 269 pp., Southwest Agricultural University. 2001. pp. 43-48.

Luckhart S, Vodovotz Y, Cui L, Rosenberg R. The mosquito *Anopheles stephensi* limits malaria parasite development with inducible synthesis of nitric oxide. *Proc. Natl. Acad. Sci. U. S. A.* 1998, 95: 5700-5705.

Ludtke SJ, He K, Heller WT, Harroun TA, Yang L, Huang HW. Membrane pores induced by magainin. *Biochemistry* 1996, 35: 13723-13728.

Luque T, Okano K, O'Reilly DR. Characterization of a novel silkworm (*Bombyx mori*) phenol UDP-glucosyltransferase. *Eur. J. Biochem.* 2002, 269: 819-825.

Ma G, Roberts H, Sarjan M, Featherstone N, Lahnstein J, Akhurst R, Schmidt O. Is the mature endotoxin Cry1Ac from *Bacillus thuringiensis* inactivated by a coagulation reaction in the gut lumen of resistant *Helicoverpa armigera* larvae? *Insect Biochemistry and Molecular Biology*, 2005, 35(7): 729-739.

Martinelli C, Reichhart JM. Evolution and integration of innate immune systems from fruit flies to man: lessons and questions. *J Endotoxin Res*. 2005, 11(4): 243-248.

Matsuzaki K, Murase O, Tokuda H, Fujii N, Miyajima K. An antimicrobial peptide, magainin 2, induced rapid flip-flop of phospholipids coupled with pore formation and peptide translocation. *Biochemistry* 1996, 35: 11361-11368.

Medzhitov R, Janeway CA Jr. Decoding the patterns of self and nonself by the innate immune system. *Science.* 2002, 296(5566): 298-300.

Medzhitov R. Toll-like receptors and innate immunity. *Nat Rev Immunol*. 2001, 1(2): 135-145.

Meis JF, Pool G, van Gemert GJ, Lensen AH, Ponnudurai T, Meuwissen JH. *Plasmodium falciparum* ookinetes migrate intercellularly through Anopheles stephensi midgut epithelium. *Parasitol. Res.* 1989, 76: 13-19.

Meister S, Kanzok SM, Zheng XL, Luna C, Li TR, Hoa NT, Hoa NT, Clayton JR, White KP, Kafatos FC, Christophides GK, Zheng L. Immune signaling pathways regulating bacterial and malaria parasite infection of the mosquito *Anopheles gambiae*. *Proc Natl Acad Sci USA* 2005, 102(32): 11420-11425.

Mello CB, Nigam Y, Garcia ES, Azambuja P, Newton RP, Ratcliffe NA. Studies on a haemolymph lectin isolated from *Rhodnius prolixus* and its interaction with *Trypanosoma rangeli. Exp Parasitol* 1999, 91(4): 289-296.

Méténier G, Vivarès CP. Molecular characteristics and physiology of microsporidia. *Microbes Infect.* 2001, 3: 407-415.

Michel K, Kafatos FC. Mosquito immunity against *Plasmodium*. *Insect Biochem Mol Biol.* 2005, 35(7): 677-689.

Minnick MF, Rupp RA, Spence KD. A bacterial-induced lectin which triggers hemocyte coagulation in *Manduca sexta*. *Biochem. Biophys. Res. Commun.* 1986, 137: 729-735.

Mita K, Kasahara M, Sasaki S, Nagayasu Y, Yamada T, Kanamori H, Namiki N, Kitagawa M, Yamashita H, Yasukochi Y, Kadono-Okuda K, Yamamoto K, Ajimura M, Ravikumar G, Shimomura M, Nagamura Y, Shin-I T, Abe H, Shimada T, Morishita S, Sasaki T. The genome sequence of the silkworm, *Bombyx mori*. *DNA Res*. 2004, 11: 27-35.

Mita K, Morimyo M, Okano K, Koike Y, Nohata J, Kawasaki H, Kadono-Okuda K, Yamamoto K, Suzuki MG, Shimada T, Goldsmith MR, Maeda S. The construction of an EST database for *Bombyx mori* and its application. *Proc. Natl. Acad. Sci. USA* 2003, 100: 14121-14126.

Mittleider D, Green LC, Mann VH, Michael SF, Didier ES, Brindley PJ. Sequence survey of the genome of the opportunistic microsporidian pathogen, *Vittaforma corneae*. *J. Eukaryot. Microbiol.* 2002, 49: 393-401.

Moita LF, Wang-Sattler R, Michel K, Zimmermann T, Blandin S, Levashina EA, Kafatos FC. *In vivo* identification of novel regulators and conserved pathways of phagocytosis in *A. gambiae*. *Immunity* 2005, 23: 65-73.

Moret Y, Siva-Jothy MT. Adaptive innate immunity? Responsive-modd prophylaxis in the

mealworm beetle, *Tenebrio moditor*. *Proc Biol Sci.* 2003, 270(1532): 2475-2480.

Moret Y. "Trans-eenerational immune priming": specific enhancement of the antimicrobial immune response in the mealworm beetle, *Tenebrio molitor*. *Proc Biol Sci.* 2006, 273(1592): 1399-1405.

Mori H, Tsukada M. New silk protein: modification of silk protein by gene engineering for production of biomaterials. *J. Biotechnol.* 2000, 74: 95-103.

Morishima I, Suginaka S, Ueno T, Hirano H. Isolation and structure of cecropins, inducible antibacterial peptides, from the silkworm *Bombyx mori*. *Comp Biochem Physiol* B 1990, 95: 551-554.

Moura H, Ospina M, Woolfit AR, Barr JR, Visvesvara GS. Analysis of four human microsporidian isolates by MALDI-TOF mass spectrometry. 2003. *J Eukaryot Microbiol.* 50, 156-163.

Moura H, Visvesvara GS. A proteome approach to the host-parasite interaction of the microsporidian *Encephalitozoon intestinalis*. *J. Eukaryot. Microbiol.* 2001. 48 *suppl*. s1, 56S-59S.

Mylonakis E, Aballay A. Worms and flies as genetically tractable animal models to study host-pathogen interactions. *Infect Immun*. 2005, 73(7): 3833-3841.

Myung JM, Marshall P, Sinnis P. The *Plasmodium* circumsporozoite protein is involved in mosquito salivary gland invasion by sporozoites. *Mol. Biochem. Parasitol.* 2004, 133: 53-59.

Nagaraju J, Goldsmith MR. Silkworm genomics—progress and prospects. *Curr. Sci.* 2002, 83: 415-425.

Nägeli K. Über die neue Krankheit der Seidenraupe und verwandte Organismen. *Bot. Ztg.* 1857, 15: 760-761.

Nappi AJ, Christensen BM. Melanogenesis and associated cytotoxic reactions: Applications to insect innate immunity. *Insect Biochem Mol Biol.* 2005, 35(5): 443-459.

Nappi AJ, Kohler L, Mastore M. Signaling pathways implicated in the cellular innate immune responses of *Drosophila*. *Inv. Surv. J.* 2004, 1: 5-33.

Nappi AJ, Vass E. Cytotoxic reactions associated with insect immunity. *Adv Exp Med Biol.* 2001, 484: 329-348.

Nappi AJ, Vass E. Melanogenesis and the generation of cytotoxic molecules during insect cellular immune reactions. *Pigment Cell Res* 1993, 6: 117-126.

Nardi JB, Pilas B, Ujhelyi E, Garsha K, Kanost MR. Hematopoietic organs of *Manduca sexta* and hemocyte lineages. *Development Genes and Evolution* 2003, 213: 477-491.

Nardia JB, Zhuangb S, Pilasc B, Beed CM, Kanost MR. Clustering of adhesion receptors following exposure of insect blood cells to foreign surfaces. *Journal of Insect Physiology* 2005, 51: 555-564.

Nassonova ES, Tokarev YS, Trammer T, Entzeroth R, Sokolova YY. Phagocytosis of *Nosema grylli* (Microsporida, *Nosematidae*) spores *in vivo* and *in vitro*. *J Eukaryot Microbiol.* 2001, Suppl: 83S-84S.

Natori S, Shiraishi H, Hori S, Kobayashi A. The roles of *Sarcophaga* defense molecules in immunity and metamorphosis. *Dev Comp Immunol.* 1999, 23(4-5): 317-328.

Ochiai M, Ashida M. A pattern recognition protein for peptidoglycan. Cloning the cDNA and the gene of the silkworm, *Bombyx mori*. *J Biol Chem.* 1999, 274(17): 11854-11858.

Ochiai M, Ashida M. A pattern-recognition protein for beta-1,3-glucan. The binding domain and the cDNA cloning of beta-1,3-glucan recognition protein from the silkworm, *Bombyx mori*. *J Biol Chem.* 2000, 275(7): 4995-5002.

Ochiai M, Ashida M. Purification of a beta-1,3-glucan recognition protein in the prophenol -oxidase activating system from hemolymph of the silkworm, *Bombyx mori*. *J Biol Chem.* 1988, 263(24): 12056-12062.

Oduol F, Xu J, Niare O, Natarajan R, Vernick KD. Genes identified by an expression screen of the vector mosquito *Anopheles gambiae* display differential molecular immune response to malaria parasites and bacteria. *Proc. Natl. Acad. Sci. USA* 2000, 97: 11397-11402.

Ohshima K. On the autogamy of nuclei and the spore formation of *Nosema bombycis* Nageli. *Annot. Zool. Jpn.* 1973, 46: 30-44

Ohta M, Watanabe A, Mikami T, Nakajima Y, Kitami M, Tabunoki H, Ueda K, Sato R. Mechanism by which *Bombyx mori* hemocytes recognize microorganisms: direct and indirect recognition systems for PAMPs. *Dev Comp Immunol.* 2006, 30(10): 867-877.

Oshima K. A preliminary note on the structure of the polar filament of *Nosema bombycis* and its functional significance. *Annot. Zool. Jpn.* 1927, 11: 235-243.

Oshima K. Effect of potassium ion on filament evagination of spores of *Nosema bombycis* as studied by the neutralization method. *Annot. Zool. Jpn.* 1964, 37: 102-102.

Oshima K. Emergence mechanism of sporoplasm from the spore of *Nosema bombycis* and the action of filament during evagination. *Jpn. J. Zool.* 1966, 15: 203-220.

Oshima K. On the function of the polar filament of *Nosema bombycis*. *Parasitology* 1937, 29: 220-224.

Otvos LJr, O I, Rogers ME, Consolvo PJ, Condie BA, Lovas S, Bulet P, Blaszczyk-Thurin M. Interaction between heat shock proteins and antimicrobial peptides. *Biochemistry* 2000, 39: 14150-14159.

Ourth DD, Narra MB, Chung KT. Isolation of mannose-binding C-type lectin from *Heliothis virescens* pupae. *Biochem Biophys Res Commun.* 2005, 335(4): 1085-1089.

Park CB, Kim HS, Kim SC. Mechanism of action of the antimicrobial peptide buforin II: buforin II kills microorganisms by penetrating the cell membrane and inhibiting cellular functions. *Biochem. Biophys. Res. Commun.* 1998, 244, 253-257.

Pasteur L. 1870, Etudes sur la ver à soi, Paris, France.

Patil CS, Jyothi NB, Dass CMS. Role of *Nosema bombycis* infected male silk moths in the venereal transmission of pebrine disease in *Bombyx mori* (Lep., *Bombycidae*) *J. Appl. Ent.* 2002, 126: 563-566.

Pearson AM, Baksa K, Ramet M, Protas M, McKee M, Brown D, Ezekowitz RA. Identification of cytoskeletal regulatory proteins required for efficient phagocytosis in *Drosophila*. *Microbes Infect*. 2003, 5(10): 815-824.

Peek R, Delbac F, Speijer D, Polonais V, Greve S, Wentink-Bonnema E, Ringrose J, van Gool T. Carbohydrate moieties of microsporidian polar tube proteins are targeted by immunoglobulin G in immunocompetent individuals. *Infect Immun.* 2005, 73(12): 7906-7913.

Pereira MEA, Andrade AFB, Ribeiro JMC. Lectins of distinct specificity in *Rhodniusp rolixus* interact selectively with *Trypanosomcar uzi. Science* 1981, 211: 597-600.

Peterson TM, Luckhart S. A mosquito 2-Cys peroxiredoxin protects against nitrosative and

oxidative stresses associated with malaria parasite infection. *Free Radical Biology and Medicine*, 2006, 40(6): 1067-1082.

Peuvel I, Peyret P, Metenier G, Vivares CP, Delbac F. The microsporidian polar tube: evidence for a third polar tube protein (PTP3) in *Encephalitozoon cuniculi*. *Mol. Biochem. Parasitol.* 2002, 122: 69-80.

Peuvel I, Polonais V, Brosson D, Texier C, Kuhn L, Peyret P, Vivares C P, Delbac F. EnP1 and EnP2, two proteins associated with the *Encephalitozoon cuniculi* endospore, the chitin-rich inner layer of the microsporidian spore wall. *Int J Parasitol.* 2006, 36(3): 309-318.

Peyretaillade E, Broussolle V, Peyret P, Méténier G, Gouy M, Vivarès CP. Microsporidia, amitochondrial protists, possess a 70-kDa heat shock protein gene of mitochondrial evolutionary origin. *Mol. Biol. Evol.* 1998, 15: 683-689

Pierro DJ, Myles KM, Foy BD, Beaty BJ, Olson KE. Development of an orally infectious Sindbis virus transducing system that efficiently disseminates and expresses green fluorescent protein in *Aedes aegypti*. *Insect Mol. Biol.* 2003, 12: 107-116.

Polonais V, Prensier G, Metenier G, Vivares CP, Delbac F. Microsporidian polar tube proteins: highly divergent but closely linked genes encode PTP1 and PTP2 in members of the evolutionarily distant *Antonospora* and *Encephalitozoon* groups. *Fungal Genet Biol.* 2005, 42(9): 791-803.

Promboon A, Shimada T, Fujiwara H, Kobayashi M. Linkage map of random amplified DNAs (RAPDs) in the silkworm, *Bombyx mori*. *Genet. Res.* 1995, 66: 1-7.

Quan GX, Kanda T, Tamura T. Induction of the white egg 3 mutant phenotype by injection of the double-stranded RNA of the silkworm white gene. *Insect Mol. Biol.* 2002, 11: 217-222.

Rämet M, Pearson A, Manfruelli P, Li X, Koziel H, Gobel V, Chung E, Krieger M, Ezekowitz RAB. *Drosophila* scavenger receptor CI is a pattern recognition receptor for bacteria. *Immunity* 2001, 15: 1027-1038.

Rao SN, Muthulakshmi M, Kanginakudru S, Nagaraju J. Phylogenetic relationships of three new microsporidian isolates from the silkworm, *Bombyx mori*. *J Invertebr Pathol.* 2004, 86(3): 87-95.

Rao SN, Nath BS, Saratchandra B. Characterization and phylogenetic relationships among microsporidia infecting silkworm, *Bombyx mori*, using inter simple sequence repeat (ISSR) and smallsubunit rRNA (SSU-rRNA) sequence analysis. *Genome* 2005, 48(3): 355-366.

Reddy KD, Abraham EG, Nagaraju J. Microsatellites in the silkworm, *Bombyx mori*: abundance, polymorphism, and strain characterization. *Genome* 1999, 42: 1057-1065.

Ribeiro C, Brehelin M. Insect haemocytes: What type of cell is that? *Journal of Insect Physiology* 2006, 52417-52429.

Rivero A. Nitric oxide: an antiparasitic molecule of invertebrates. *Trends in Parasitology* 2006, 22(5): 219-225.

Romani L. Immunity to *Candida albicans*: Th1, Th2 cells and beyond. *Curr. Opin. Microbiol.* 1999, 2: 363-367.

Sadd BM, Siva-Jothy MT. Self-harm caused by an insect's innate immunity. *Proc Biol Sci.* 2006, 273(1600): 2571-2574.

Salzet M. Vertebrate innate immunity resembles a mosaic of invertebrate immune responses. *Trends Immunol*. 2001, 22: 285-288.

Sato H, Feix JB. Peptide-membrane interactions and mechanisms of membrane destruction by amphipathic α-helical antimicrobial peptides *Biochimica et Biophysica Acta*, 2006, 1758(9): 1245-1256.

Sato R, Kobayashi M, Watanabe H. Internal ultrastructure of spores of microsporidians isolated from silkworm, *Bombyx mori*. *J Invertebr Pathol* 1982, 40: 260-265.

Sato R, Watanabe H. Sporogonial sequence in microsporideae pathogenic to silkworm, *Bombyx mori*. *J. Sericult. Sci.Jpn.* 1986, 55: 10-16.

Satoh D, Horii A, Ochiai M, Ashida M. Prophenoloxidase-activating enzyme of the silkworm, *Bombyx mori*: Purification, characterization, and cDNA cloning. *J Biol Chem.* 1999, 274(11): 7441-7453.

Scanlon M, Shaw AP, Zhou CJ, Visvesvara GS. Infection by microsporidia disrupts the host cell cycle. *J. Eukaryot. Microbiol.* 2000, 47: 525-531.

Scherfer C, Karlsson C, Loseva O, Bidla G, Goto A, Havemann J, Dushay MS, Theopold U. Isolation and characterization of hemolymph clotting factors in *Drosophila melanogaster* by a pullout method. *Curr Biol.* 2004, 14(7): 625-629.

Scherfer C, Qazi MR, Takahashi K, Ueda R, Dushay MS, Theopold U, Lemaitre B. The Toll immune-regulated *Drosophila* protein Fondue is involved in hemolymph clotting and puparium formation. *Dev Biol.* 2006, 295(1): 156-163.

Schmidt O, Theopold U, Strand MR. Innate immunity and evasion by insect parasitoids. *BioEssays* 2001, 23: 344-351.

Shahabuddin M, Toyoshima T, Aikawa M, Kaslow DC. Transmission-blocking activity of a chitinase inhibitor and activation of malarial parasite chitinase by mosquito protease. *Proc Natl Acad Sci U S A.* 1993, 90(9): 4266-4270.

Shaw RW, Kent ML. Fish microsporidia. In: The Microsporidia and Microsporidiosis (ed. Wittner, M. and Weiss, L. M.), pp. 418-446. 1999. American Society for Microbiology Press, Washington, D.C.

Shi J, Heckel DG, Goldsmith MR. A genetic linkage map for the domesticated silkworm, *Bombyx mori*, based on restriction fragment length polymorphisms. *Genet. Res.* 1995, 66: 109-126.

Sieber KP, HuberM, KaslowD, Banks SM, ToriiM, AikawaM, Miller L. The peritrophic membrane as a barrier: its penetrationby *Plasmodium gallinaceum* and the effect of a monoclonal antibody to ookinetes. *Exp Parasitol.* 1991, 72(2): 145-156.

Silveira H, Canning EU. *Vittaforma corneae* N. Comb. for the human microsporidium *Nosema corneum* Shadduck, Meccoli, Davis & Font, 1990, based on its ultrastructure in the liver of experimentally infected athymic mice. *J Euk Microbiol* 1995, 42: 158-165.

Sinden RE, Billingsley PF. *Plasmodium* invasion of mosquito cells: hawk or dove? *Trends Parasitol.* 2001, 17(5): 209-212.

Sironmani TA. Immunological characterization of spore proteins of the microsporidian *Nosema bombycis. World J. Microbiol. Biotechnol.* 1999, 15: 607-613.

Siva-Jothya MT, Moretb Y, Rolffa J. Insect Immunity: An Evolutionary Ecology Perspective Advances in *Insect Physiology*. 2005, 32: 1-48

Slamovits CH, Fast NM, Law JS, Keeling PJ. Genome compaction and stability in

microsporidian intracellular parasites. *Curr. Biol.* 2004, 14: 891-896.

Söderhäll K, Cerenius L. Role of the prophenoloxidase-activating system in invertebrate immunity. *Curr. Opin. Immunol.* 1998, 10: 23-28.

Sokolova YY, Dolgikh VV, Morzhina EV, Nassonova ES, Issi IV, Terry RS, Ironside JE, Smith JE, Vossbrinck CR. Establishment of the new genus *Paranosema* based on the ultrastructure and molecular phylogeny of the type species *Paranosema grylli* Gen. Nov., Comb. Nov. (Sokolova, Selezniov, Dolgikh, Issi 1994), from the cricket *Gryllus bimaculatus* Deg. *J. Invertebr. Pathol.* 2003, 84: 159-172.

Solter LF and Becnel JJ. (2000). Entomopathogenic microsporidia. In Field Manual of Techniques for the Evaluation of Entomopathogens (ed. Lacey, L. A. and Kaya, H.), pp. 231-254. Kluwer Academic Publishers, Dordrecht, The Netherlands.

Song KH, Jung SJ, Seo YR, Kang SW, Han SS. Identification of up-regulated proteins in the hemolymph of immunized *Bombyx mori* larvae. *Comparative Biochemistry and Physiology*, Part D 1 2006: 260-266.

Sprague V, Becnel JJ, Hazard EI. Taxonomy of phylum microspora. *Crit.Rev. Microbiol.* 1992, 18: 285-395.

Sprague V, Becnel JJ. 1999. Check list of available generic names for microsporidia with type species and type hosts. In: The Microsporidia and Microsporidiosis (ed. Wittner, M. and Weiss, L. M.), pp. 517-530. 1999. American Society for Microbiology Press, Washington, D.C.

Sprague V, Becnel JJ. Note on the name-author-date combination for the taxon MICRO-SPORIDIES Balbiani, 1882, when ranked as a Phylum. *J Invertebr Pathol.* 1998, 71(1): 91-94.

Sprague V, Vávra J. 1977. Systematics of the Microsporidia. In: Bulla, L.A., Cheng, T.C. (Eds.), Comparative Pathobiology. Plenum, New York.

Stebbins MR, Hapner KD. Preparation and properties of haemagglutinin from haemolymph of *Acrididae* (grasshoppers). *Insect Biochem.* 1985, 15: 451-462.

Steiner H, Hultmark D, EngstroÈ m A, Bennich H, Boman HG. Sequence and specificity of two antibacterial proteins involved in insect immunity. *Nature* 1981, 292: 246-2488.

Streett DA Analysis of *Nosema locustae* (Microsporidia: *Nosematidae*) chromosomal DNA with pulsed field gel electrophoresis. *J. Invertebr. Pathol.* 1994, 63: 301-303.

Sugiyama M, Kuniyoshi H, Kotani E, Taniai K, Kadono-Okuda K, Kato Y, Yamamoto M, Shimabukuro M, Chowdhury S, Xu J, Choi SK, Kataoka H, Suzuki A, Yamakawa M. Characterization of a *Bombyx mori* cDNA encoding a novel member of the attacin family of insect antibacterial proteins. *Insect Biochem Mol Biol* 1995, 25: 385-392.

Takahashi H, Komano H, Kawaguchi N, Kitamura N, Nakanishi S, Natori S. Cloning and sequencing of cDNA of *Sarcophaga peregrina* humoral lectin induced on injury of the body wall. *J. Biol. Chem*. 1985, 260: 12228-12233.

Takizawa H, Vivier E, Petitprez A. Développement intranucléaire de la microsporidie *Nosema bombycis* dans les cellules de vers à soie après infestation experimentale. *C. R. Acad. Sci.* 1973, 277: 1769-1772.

Tamura T, Thibert C, Royer C, Kanda T, Abraham E, Kamba M, Komoto N, Thomas JL, Mauchamp B, Chavancy G, Shirk P, Fraser M, Prudhomme JC, Couble P. Germline transformation of the silkworm *Bombyx mori* L. using a *piggyBac* transposon-derived vector.

Nat. Biotechnol. 2000, 18: 81-84.

Tan YD, Wan C, Zhu Y, Lu C, Xiang Z, Deng HW. An amplified fragment length polymorphism map of the silkworm. *Genetics* 2001, 157: 1277-1284.

Tanaka H, Yamamoto M, Moriyama Y, Yamao M, Furukawa S, Sagisaka A, Nakazawa H, Mori H, Yamakawa M. A novel Rel protein and shortened isoform that differentially regulate antibacterial peptide genes in the silkworm *Bombyx mori*. *Biochim Biophys Acta.* 2005, 1730(1): 10-21.

Taniai K, Lee JH, Lee IH. *Bombyx mori* cell line as a model of immune-system organs. *Insect Mol Biol.* 2006, 15(3): 269-279.

Taupin V, Garenaux E, Mazet M, Maes E, Denise H, Prensier G, Vivares CP, Guerardel Y, Metenier G. Major O-glycans in the spores of two microsporidian parasites are represented by unbranched manno-oligosaccharides containing alpha-1,2 linkages. *Glycobiology.* 2007, 17(1): 56-67.

Templeton TJ, Kaslow DC, Fidock DA. Developmental arrest of the human malaria parasite *Plasmodium falciparum* within the mosquito midgut via CTRP gene disruption. *Mol Microbiol.* 2000, 36(1): 1-9.

Texier C, Brosson D, El Alaoui H, Metenier G, Vivares CP. Post-genomics of microsporidia, with emphasis on a model of minimal eukaryotic proteome: a review. *Folia Parasitol* (Praha). 2005, 52(1-2): 15-22.

Theopold U, Li D, Fabbri M, Scherfer C, Schmidt O. The coagulation of insect hemolymph. *Cell Mol. Life Sci.* 2002, 59: 363-372.

Theopold U, Schmidt O, Söderhäll K, Dushay MS. Coagulation in arthropods: defence, wound closure and healing. *Trends Immunol.* 2004, 25(6): 289-294.

Theopold U, Schmidt O. *Helix pomatia* lectin and annexin V, two molecular probes for insect microparticles: possible involvement in hemolymph coagulation. *J. Insect Physiol.* 1997, 43: 667-674.

Thomarat F, Vivares CP, Gouy M. Phylogenetic analysis of the complete genome sequence of *Encephalitozoon cuniculi* supports the fungal origin of microsporidia and reveals a high frequency of fast-evolving genes. *J Mol Evol.* 2004, 59(6): 780-791.

Thomas JL, Da Rocha M, Besse A, Mauchamp B, Chavancy G. 3XP3-EGFP marker facilitates screening for transgenic silkworm *Bombyx mori* L. from the embryonic stage onwards. *Insect Biochem. Mol. Biol.* 2002, 32: 247-253.

Tokarev YS, Sokolova YY, Entzeroth R. A primary culture of haemocytes isolated from *Gryllus bimaculatus* (*Orthoptera, Gryllidae*) and their interactions with two intracellular parasites-*Paranosema grylli* (Microsporidia) and *Adelina grylli* (*Coccidia*). *Tsitologiia.* 2005, 47(6): 478-486.

Tokarev YS, Sokolova YY, Entzeroth R. Microsporidia-insect host interactions: Teratoid sporogony at the sites of host tissue melanization. *J Invertebr Pathol.* 2007, 94(1):70-73.

Tomas AM, Margos G, Dimopoulos G, van Lin LH, de Koning-Ward TF, Sinha R, Lupetti P, Beetsma AL, Rodriguez MC, Karras M, Hager A, Mendoza J, Butcher GA, Kafatos F, Janse CJ, Waters AP, Sinden RE. P25 and P28 proteins of the malaria ookinete surface have multiple and partially redundant functions. *EMBO J.* 2001, 20(15): 3975-3983.

Tomita M, Munetsuna H, Sato T, Adachi T, Hino R, Hayashi M, Shimizu K, Nakamura N, Tamura T, Yoshizato K. Transgenic silkworms produce recombinant human type III procollagen in cocoons. *Nat Biotechnol.* 2003, 21(1): 52-56.

Torii M, Nakamura K, Sieber KP, Miller LH, Aikawa M. Penetration of the mosquito (*Aedes aegypti*) midgut wall by the ookinetes of *Plasmodium gallinaceum*. *J Protozool.* 1992, 39(4): 449-454.

Tossi A, Sandri L. Molecular diversity of ribosomially synthesized cationic antimicrobial polypeptides. *Curr. Pharm. Design,* 2002, 8: 743-761.

Trager W. The hatching of the spores of *Nosema bombycis* Nageli and the partial development of the organism in tissue cultures. *J. Parasitol.* 1937, 23: 226-227

Tsai YL, Hayward RE, Langer RC, Fidock DA, Vinetz JM. Disruption of *Plasmodium falciparum* chitinase markedly impairs parasite invasion of mosquito midgut. *Infect Immun.* 2001, 69(6): 4048-4054.

Tzou P, De Gregorio E, Lemaitre B. How *Drosophila* combats microbial infection: a model to study innate immunity and host-pathogen interactions. *Curr. Opin. Microbiol*. 2002, 5: 102-110.

Tzou P, Ohresser S, Ferrandon D, Capovilla M, Reichhart JM, Lemaitre B, Hoffmann JA, Imler JL. Tissue-specific inducible expression of antimicrobial peptide genes in *Drosophila* surface epithelia. *Immunity* 2000, 13: 737-748.

Uhlirova M, Asahina M, Riddiford LM, Jindra M. Heat-inducible transgenic expression in the silkmoth *Bombyx mori*. *Dev. Genes Evol.* 2002, 212: 145-151.

Uhlirova M, Foy BD, Beaty BJ, Olson KE, Riddiford LM, Jindra M. Use of Sindbis virus-mediated RNA interference to demonstrate a conserved role of Broad-Complex in insect metamorphosis. *Proc. Natl. Acad. Sci. USA* 2003, 100: 15607-15612.

Undeen AH, Frixione E. The role of osmotic pressure in the germination of *Nosema algerae* spores. *J. Protozool.* 1990, 37: 561-567.

Undeen AH, Vander Meer RK. Conversion of intrasporal trehalose into reducing sugars during germination of *Nosema algerae* (Protista: Microspora) spores: A quantitative study. *J. Eukaryotic Microbiol.* 1994, 41: 129-132.

Undeen AH. A proposed mechanism for the germination of microsporidian (Protozoa: Microspora) spores. *J. Theoret. Biol.* 1990, 142: 223-235.

Ursic-Bedoya RJ. and Lowenberger CA. *Rhodnius prolixus*: Identification of immune-related genes up-regulated in response to pathogens and parasites using suppressive subtractive hybridization. *Developmental & Comparative Immunology* 2007, 31(2): 109-120.

Vass E, Nappi AJ. Fruit fly immunity. *BioEssays*. 2001, 51: 529-535.

Vávra J "Polar vesicles" of microsporidia are mitochondrial remnants ("mitosomes")? *Folia Parasitol (Praha)*. 2005, 52(1-2): 193-195.

Vávra J, Larsson JI. Structure of the microsporidia. In: The Microsporidia and Microsporidiosis (ed. Wittner, M. and Weiss, L. M.), pp. 7-84. 1999. American Society for Microbiology Press, Washington, D.C.

Vávra J. Etude au microscope électronique de la morphologie et du développement de quelques microsporidies *C. R. Acad. Sci.* (Paris) 1965, 261: 3467-3470.

Vávra J. Structure of microsporidia, 1976, p.1-86. In L.A. Bulla and T.C. Cheng (ed.),

Comparative Pathobiology, vol. 1. Plenum Press, New York.

Vernick KD, Fujioka H, Aikawa M. *Plasmodium gallinaceum*: a novel morphology of malaria ookinetes in the midgut of the mosquito vector. *Exp Parasitol.* 1999, 91(4): 362-366.

Vernick KD, Fujioka H, Seeley DC, Tandler B, Aikawa M, Miller LH. *Plasmodium gallinaceum*: a refractory mechanism of ookinete killing in the mosquito, *Anopheles gambiae*. *Exp. Parasitol*. 1995, 80: 583-595.

Villalon JM, Ghosh A, Jacobs-Lorena M. The peritrophic matrix limits the rate of digestion in adult *Anopheles stephensi* and *Aedes aegypti* mosquitoes. *J Insect Physiol.* 2003, 49(10): 891-895.

Vilmos P, Kurucz E. Insect immunity: evolutionary roots of the mammalian innate immune system. *Immunol. Lett.* 1998, 62: 59-66.

Vinetz JM, Dave SK, Specht CA, Brameld KA, Xu B, Hayward R, Fidock DA. The chitinase PfCHT1 from the human malaria parasite *Plasmodium falciparum* lacks proenzyme and chitin-binding domains and displays unique substrate preferences. *Proc Natl Acad Sci U S A.* 1999, 96(24):14061-14066.

Vinetz JM, Valenzuela JG, Specht CA, Aravind L, Langer RC, Ribeiro JM, Kaslow DC. Chitinases of the avian malaria parasite *Plasmodium gallinaceum*, a class of enzymes necessary for parasite invasion of the mosquito midgut. *J Biol Che.* 2000, 275(14):10331-10341.

Vinetz JM. *Plasmodium* Ookinete Invasion of the Mosquito Midgut, *CTMI* 2005, 295: 357-382.

Vizioli J, Bulet P, Hoffmann JA, Kafatos FC, Muller HM, Dimopoulos G. Gambicin: a novel immune responsive antimicrobial peptide from the malaria vector *Anopheles gambiae*. *Proc. Natl Acad. Sci. U.S.A.* 2001, 98: 12630-12635.

Vizioli J, Salzet M. Antimicrobial peptides from animals: focus on invertebrates. *Trends Pharmacol Sci* 2002, 23: 494-496.

Vlachou D, Schlegelmilch T, Runn E, Mendes A, Kafatos FC. The developmental migration of *Plasmodium* in mosquitoes. *Curr Opin Genet Dev.* 2006, 16(4): 384-391.

Vlachou D, Zimmermann T, Cantera R, Janse CJ, Waters AP, Kafatos FC. Real-time, *in vivo* analysis of malaria ookinete locomotion and mosquito midgut invasion. *Cell Microbiol.* 2004, 6(7): 671-685.

Vossbrinck C R, Maddox J V, Friedman S, Debrunner-Vossbrinck BA, Woese C R. Ribosomal RNA sequence suggests microsporidia are extremely ancient eukaryotes. *Nature* 1987, 326: 411-1497.

Vossbrinck CR, Woese CR. Eukaryotic ribosomes that lack a 5.8S RNA. *Nature* 1986, 320: 287-288.

Wago H. Phagocytic recognition in *Bombyx mori.* In: Gupta AP (ed) Immunology of insects and other arthropods. CRC Press, Boca Raton, 1991, pp 215-235

Wang J, Xia Q, He X, Dai M, Ruan J, Chen J, Yu G, Yuan H, Hu Y, Li R, Feng T, Ye C, Lu C, Wang J, Li S, Wong GK, Yang H, Wang J, Xiang Z, Zhou Z, Yu J. SilkDB: a knowledgebase for silkworm biology and genomics. *Nucleic Acids Res.* 2005, 33(Database issue): D399-402.

Wang JY, Huang KW, Mao XC, Zhao Y, Lu CD. Small subunit ribosomal RNA genes of microsporidia. *Acta biochimica et biophysica Sinica* (*Sheng Wu Hua Xue Yu Sheng Wu Wu Li Xue Bao,* Shanghai) 2001, 33: 229-232.

Wang Y, Zhang P, Fujii H, Banno Y, Yamamoto K, Aso Y. Proteomic studies of lipopolysaccharide induced polypeptides in the silkworm, *Bombyx mori*. *Biosci Biotechnol Biochem.* 2004, 68(8): 1821-1823.

Wasson K, Peper RL. Mammalian microsporidiosis. *Vet. Pathol.* 2000, 37: 113-128.

Weber R, Schwartz DA, Deplazes P. Laboratory diagnosis of microsporidiosis. In: The Microsporidia and Microsporidiosis (ed. Wittner, M. and Weiss, L. M.), pp. 315-362. 1999. American Society for Microbiology Press, Washington, D.C.

Weidner E, Byrd W, Scarborough A, Pleshinger J, Sibley LD. Microsporidian spore discharge and the transfer of polaroplast organelle into plasma membrane *J. Protozool.* 1984, 31: 195-198.

Weidner E, Halonen SK. Microsporidian spore envelope keratins phosphorylate and disassemble during spore activation. *J. Eukaryot. Microbiol.* 1993, 40: 783-788.

Weidner E, Sibley LD. Phagocytized intracellular microsporidian blocks phagosome acidification and phagosome-lysosome fusion. *J. Protozool.* 1985, 32: 311-317.

Weidner E. Cytoskeletal proteins expressed by microsporidian parasites. *Subcell. Biochem.* 1992, 18: 3 85-399.

Whitten MMA, Mello CB, Gomes SAO, Nigam Y, Azambuja P, Garcia E S, Ratcliffe NA. Role of superoxide and reactive nitrogen intermediates in *Rhodnius prolixus* (*Reduviidae*)/*Trypanosoma rangeli* interactions. *Experimental Parasitology*, 2001, 98(1): 44-57.

Whitten MMA., Shiao SH, Levashina EA. Mosquito midguts and malaria: cell biology, compartmentalization and immunology. *Parasite Immunology*. 2006, 28: 121-130.

Wiegand C, Levin D, Gillespie JP, Willott E, Kanost MR, Trenczek T. Monoclonal antibody MS13 identifies a plasmatocyte membrane protein and inhibits encapsulation and spreading reactions of *Manduca sexta* hemocytes. *Archives of Insect Biochemistry and Physiology* 2000, 45: 95-108.

Williams BA, Hirt RP, Lucocq JM, Embley TM. A mitochondrial remnant in the microsporidian *Trachipleistophora hominis*. *Nature.* 2002, 418(6900): 865-869.

Williams BA, Keeling PJ. Microsporidian mitochondrial proteins: expression in *Antonospora locustae* spores and identification of genes coding for two further proteins. *J Eukaryot Microbiol.* 2005, 52(3): 271-276.

Williams MJ. Regulation of antibacterial and antifungal innate immunity in fruitflies and humans. *Adv Immunol.* 2001, 79: 225-259.

Wittner M, Weiss LM. (1999). The Microsporidia and Microsporidiosis. American Society for Microbiology Press, Washington, D.C. 533pp.

Wittner M. Historic perspective on the microsporidia: expanding horizons, In: The Microsporidia and Microsporidiosis (ed. Wittner, M. and Weiss, L. M.), pp. 1-4. 1999. American Society for Microbiology Press, Washington, D.C.

Xia Q, Zhou Z, Lu C, Cheng D, Dai F, Li B, Zhao P, Zha X, Cheng T, Chai C, Pan G, Xu J, Liu C, Lin Y, Qian J, Hou Y, Wu Z, Li G, Pan M, Li C, Shen Y, Lan X, Yuan L, Li T, Xu H, Yang G, Wan Y, Zhu Y, Yu M, Shen W, Wu D, Xiang Z, Yu J, Wang J, Li R, Shi J, Li H, Li G, Su J, Wang X, Li G, Zhang Z, Wu Q, Li J, Zhang Q, Wei N, Xu J, Sun H, Dong L, Liu D, Zhao S, Zhao X, Meng Q, Lan F, Huang X, Li Y, Fang L, Li C, Li D, Sun Y, Zhang Z, Yang Z, Huang Y, Xi Y, Qi Q, He D, Huang H,

Zhang X, Wang Z, Li W, Cao Y, Yu Y, Yu H, Li J, Ye J, Chen H, Zhou Y, Liu B, Wang J, Ye J, Ji H, Li S, Ni P, Zhang J, Zhang Y, Zheng H, Mao B, Wang W, Ye C, Li S, Wang J, Wong GK, Yang H. A draft sequence for the genome of the domesticated silkworm (*Bombyx mori*). *Science*. 2004, 306(5703): 1937-1940.

Xu J, Pan G, Fang L, Li J, Tian X, Li T, Zhou Z, Xiang Z. The varying microsporidian genome: existence of long-terminal repeat retrotransposonin domesticated silkworm parasite *Nosema bombycis*. *Int J Parasitol* 2006, 36(9): 1049-1056.

Xu Y, Peter Takvorian, Ann Cali, Fang Wang, Hong Zhang, George Orr, and Louis M. Weiss. Identification of a new spore wall protein from *Encephalitozoon cuniculi. Infect. Immun*. 2006, 74: 239-247.

Xu Y, Takvorian PM, Cali A, Orr G, Weiss LM. Glycosylation of the major polar tube protein of *Encephalitozoon hellem*, a microsporidian parasite that infects humans. *Infect. Immun.* 2004, 72, 6341-6350.

Xu Y, Weiss LM. The microsporidian polar tube: a highly specialised invasion organelle. *Int J Parasitol.* 2005, 35(9): 941-953.

Yamakawa M, Tanaka H. Immune proteins and their gene expression in the silkworm, *Bombyx mori. Dev Comp Immunol.* 1999, 23(4-5): 281-289.

Yamao M, Katayama N, Nakazawa H, Yamakawa M, Hayashi Y, Hara S, Kamei K, Mori H. Gene targeting in the silkworm by use of a baculovirus. *Genes Dev.* 1999, 13(5): 511-516.

Yamashita M, Iwabuchi K. *Bombyx mori* prohemocyte division and differentiation in individual microcultures. *J Insect Physiol* 2001, 47: 325-331

Yao Q, Li MW, WangY, Wang WB, Lu J. Screening of molecular markers for NPV resistance in *Bombyx mori* L. (Lep., *Bombycidae*). *J. Appl. Entomol.* 2003, 127: 134-136.

Yasukochi Y. A dense genetic map of the silkworm, *Bombyx mori*, covering all chromosomes based on 1018 molecular markers. *Genetics* 1998, 150:1513-1525.

Yoshida H, Ochiai M, Ashida M. Beta-1,3-glucan receptor and peptidoglycan receptor are present as separate entities within insect prophenoloxidase activating system. *Biochem Biophys Res Commun.* 1986,141(3): 1177-1184.

Yu HS, Chen XC, Zhu ZC, Zhuang DH, Liu ZY, Jiang XL, Jia JF. The sericultural sciences in China, 1994.

Yu XQ, Gan H, Kanost MR. Immulectin, an inducible C-type lectin from an insect, *Manduca sexta*, stimulates activation of plasma prophenol oxidase. *Insect Biochem Mol Biol.* 1999, 29(7): 585-597.

Yu XQ, Kanost MR. Immulectin-2, a lipopolysaccharide-specific lectin from an insect, *Manduca sexta*, is induced in response to gram-negative bacteria. *J Biol Chem.* 2000a, 275(48): 37373-37381.

Yu XQ, Kanost, M.R. A family of C-type lectins in *Manduca sexta*. *Adv. Exp. Med. Biol.* 2000b, 484: 191-194.

Yu XQ, Ling E, Tracy ME, Zhu Y. Immulectin-4 from the tobacco hornworm *Manduca sexta* binds to lipopolysaccharide and lipoteichoic acid. *Insect Mol Biol.* 2006, 15(2): 119-128.

Yu XQ, Zhu YF, Ma C, Fabrick JA, Kanost MR. Pattern recognition proteins in *Manduca sexta* plasma. *Insect Biochem. Mol. Biol.* 2002, 32: 1287-1293.

Yuda M, Sakaida H, Chinzei Y. Targeted disruption of the plasmodium berghei CTRP gene reveals its essential role in malaria infection of the vector mosquito. *J Exp Med.* 1999, 190(11):1711-1716.

Zhang P, Aso Y, Yamamoto K, Banno Y, Wang Y, Tsuchida K, Kawaguchi Y, Fujii H. Proteome analysis of silk gland proteins from the silkworm, *Bombyx mori*. *Proteomics.* 2006, 6(8): 2586-2599.

Zhang P, Yamamoto K, Aso Y, Banno Y, Sakano D, Wang Y, Fujii H. Proteomic studies of isoforms of the P25 component of *Bombyx mori* fibroin. *Biosci Biotechnol Biochem.* 2005, 69(11): 2086-2093.

Zieler H, Dvorak JA. Invasion in vitro of mosquito midgut cells by the malaria parasite proceeds by a conserved mechanism and results in death of the invaded midgut cells. *Proc. Natl. Acad. Sci. USA*. 2000, 97: 11516-11521.

Zieler H, Garon CF, Fischer ER, Shahabuddin M. Adhesion of *Plasmodium gallinaceum* ookinetes to the *Aedes aegypti* midgut: sites of parasite attachment and morphological changes in the ookinete. *J Eukaryot Microbiol.* 1998, 45(5): 512-520.

Abstract

Nosema bombycis is a spore-forming obligate intracellular parasite which belongs to the fungi-related Microsporidia phylum. It is the causative agent of the silkworm *Bombyx mori* pebrine disease which inflicts severe worldwide economical losses in sericulture. Little is known about *N. bombycis in vivo* dissemination mechanism and its interactions with its natural host *B. mori* at the cellular or molecular level, despite the ongoing genome sequencing projects of both organisms.

In this study, we investigate *N. bombycis* (Zhenjiang isolate ISC-ZJ) dissemination in *per os* infected *B. mori* larvae (Nistari). At different times post-infestation, larvae were harvested and *B. mori* larva tissues, hemocytes and hemolymph were analysed by histochemistry and immunocytochemistry microscopy (optic and transmission electron microscopy). This allowed us to document not only *N. bombycis* ISC-ZJ *in vivo* life cycle at the ultrastructural level, but also the hitherto unreported *N. bombycis* dissemination route in silkworm larvae. *N. bombycis* infestation first settles in the anterior epithelial midgut. The infection spreads to the muscles and tracheae closely surrounding the anterior midgut. Distant tissues and organs are then infected concomitantly with the apparition of the parasite in the hemolymph or internalized in hemocytes, before the systemic infestation with all tissues parasitized. Our results strongly suggest that hemolymph and hemocytes are vectors for the parasite dissemination in its host. Moreover the silkworm innate immune response, although existing -we identified *N. bombycis* melanization and its phagocytosis by *B. mori* hemocytes – seem to be strongly overtaken by the microsporidian development with underlying mechanisms still unknown.

To further study the *N. bombycis/B. mori* interactions at the molecular level, we focused on major microsporidian structural proteins from the spore wall and the polar tube which are known to be involved in host invasion. We developed a proteomic-based approach to identify few *N. bombycis* proteins belonging to these cell structures. Protein extraction protocols were optimized and four *N. bombycis* spore protein extracts were compared by mono- and bi-dimensionnal electrophoresis to establish complementary proteomic profiles. Three proteins (71, 48 and 30 kDa) were shown to be located at the parasite spore wall using a polyclonal antibody raised against formaldehyde-fixed spores. Moreover seventeen polyclonal antibodies were raised against major *N. bombycis* proteins from all extracts, and three spots, spot PEL1 (54 kDa, pI 5.4), spot PEL2 (36 kDa, pI 10) and spot PEL3 (150 kDa, pI 7.1), were shown to correspond to polar tube proteins (PTPs) by IFA and transmission electron microscopy immunocytochemistry on cryosections. These PTPs were respectively named *Nb*PTP1, *Nb*PTP2 and *Nb*PTP3 according to their global physio-chemical properties. Specific patterns for each PTP were obtained by MALDI-TOF-MS and MS/MS mass spectrometry. Peptide sequence tags were deduced by d*e novo* sequencing using Peaks Online and DeNovoX, then evaluated by Mascot and Sequest searches. Identification parameters were higher than false-positive hits, strengthening our strategy that could be enlarged to a non-genomic context.

Keyword: Microsporidia, *Nosema bombycis*, *Bombyx mori*, *in vivo* dissemination, hemolymph and hemocyte, 2-DE proteomic maps, MS/MS *de novo* sequencing, polar tube proteins

Résumé

Nosema bombycis est un parasite intracellulaire obligatoire dont le cycle de développement passe par des spores et qui appartient au phylum Microsporidia apparenté aux champignons. Cette microsporidie est l'agent responsable de la pébrine, maladie du ver à soie *Bombyx mori* qui inflige de sévères pertes économiques à la sériciculture mondiale. Cependant, peu de choses sont connues en ce qui concerne les mécanismes de dissémination *in vivo* de *N. bombycis* et ses interactions cellulaires et moléculaires avec son hôte naturel, et ce, malgré les projets en cours de réalisation de séquençage du génome des deux organismes.

Dans ce travail, nous avons étudié la dissémination de *N. bombycis* (isolat Zhenjiang ISC-ZJ) dans des larves de *B. mori* (Nistari) infestées par voie orale. A différents temps après l'infestation, les larves ont été récoltées et leurs tissus, y compris l'hémolymphe et les hémocytes, ont été analysés par microscopies optique et électronique à transmission après marquage histologique ou immunocyto- chimique. Cela nous a permis de documenter non seulement le cycle de *N. bombycis* ISC-ZJ au niveau ultrastructural, mais aussi la progression de sa dissémination dans le ver à soie. L'infestation par *N. bombycis* démarre au niveau de l'épithélium intestinal antérieur, puis s'étend aux muscles et trachées adjacents. Les tissus plus distants sont ensuite infectés de façon concomitante avec l'apparition du parasite libre dans l'hémolymphe ou internalisé dans les hémocytes, prélude à l'infestation systématique de tous les tissus. Nos résultats suggèrent fortement que l'hémolymphe et les hémocytes sont les vecteurs de la dissémination de la microsporidie dans son hôte. De plus, la réponse immune innée de la chenille, bien qu'existante comme le montre la mise en évidence de mélanisation du parasite et de sa phagocytose par des hémocytes, semble fortement dépassée par le développement microsporidien selon un mécanisme inconnu.

Pour étudier les interactions *N. bombycis/B. mori* au niveau moléculaire, nous nous sommes intéressés aux protéines microsporidiennes de la paroi et du tube polaire, deux structures impliquées dans l'invasion de la cellule-hôte. Nous avons développé une approche protéomique pour identifier certaines de ces protéines chez la spore mature de *N. bombycis*. Nous avons donc optimisé les protocoles d'extraction protéique et obtenu quatre extraits qui ont été comparés par électrophorèses mono- et bi-dimensionnelles afin d'établir des profils protéomiques complémentaires. Un anticorps polyclonal dirigé contre des spores fixées au formaldéhyde et décorant la paroi sporale réagit avec trois protéines à 71, 48 et 30 kDa. De plus, des anticorps polyclonaux spécifiques de dix-sept protéines majeures du parasite ont été produits et analysés. Trois spots, PEL1 (54 kDa, pI 5,4), PEL2 (36 kDa, pI 10) et PEL3 (150 kDa, pI 7,1), correspondent à des protéines de tube polaire (PTP) comme montré par IFA et immunocytochimie sur cryocoupes observées par microscopie électronique à transmission. Ces PTP ont été nommées *Nb*PTP1, *Nb*PTP2 et *Nb*PTP3 en raison de leurs propriétés physico-chimiques globales. Des profils spécifiques de chaque PTP ont été obtenus par spectrométrie de masse MALDI-TOF et MS/MS. Des motifs de séquence peptidique ont pu en être déduits par les programmes Peaks Online et DeNovoX, puis évalués par algorithmes Mascot et Sequest. Les paramètres d'identification plus élevés de ces séquences par rapport aux faux positifs renforcent la pertinence de notre stratégie qui peut être étendue à des contextes non génomiques.

Mots-clés: Microsporidia, *Nosema bombycis*, *Bombyx mori*, dissémination *in vivo*, hémolymphe et hémocytes, profils protéomiques bidimensionnels, séquençage MS/MS *de novo*, protéines de tube polaire